

UCSF

UC San Francisco Electronic Theses and Dissertations

Title

Glucocorticoid Receptor Signaling in the Mammalian Germline

Permalink

<https://escholarship.org/uc/item/5pn2g409>

Author

Cincotta, Steven Anthony

Publication Date

2022

Peer reviewed|Thesis/dissertation

Glucocorticoid Receptor Signaling in the Mammalian Germline

by
Steven Cincotta

DISSERTATION

Submitted in partial satisfaction of the requirements for degree of
DOCTOR OF PHILOSOPHY

in

Developmental and Stem Cell Biology

in the

GRADUATE DIVISION

of the

UNIVERSITY OF CALIFORNIA, SAN FRANCISCO

Approved:

DocuSigned by:

Barbara Panning

Barbara Panning

B18F20197C95417...

Chair

DocuSigned by:

Diana Laird

Diana Laird

DocuSigned by:

Kaveh Ashrafi

Kaveh Ashrafi

DocuSigned by:

Brian Feldman

Brian Feldman

C17A9F5C654444B...

Committee Members

Dedicated to my parents, for their constant support and love,
without which none of this would have been possible.

And to my Aunt Jody, for all her help in starting my scientific career.
I miss you dearly and wish you could have been here to see this day.

Acknowledgements

Firstly, to my thesis mentor, Diana. Thank you for taking a chance on the young and confused graduate student who showed up to your office. Thank you for welcoming me into your lab with open arms at a time when I was doubting my scientific career. Your constant encouragement and reassurance when I first joined the lab restored my confidence in my ability to become a successful scientist. Your devotion to scientific innovation and pushing the boundaries of our knowledge has been inspirational when thinking of my own project over the years, and has helped me to think creatively, both in a technical and conceptual sense. I greatly admire your unending passion for science, and your boundless optimism has been truly inspirational at times in my project when I felt the most lost. During my time in the lab, you have given me the freedom I needed to explore my interests and passions, while simultaneously helping me to develop into the independent and critical-thinking scientist that I am today. I am truly grateful for all of your help, guidance, and encouragement these past years, and for having the opportunity to work as part of the wonderful team that you have built.

To my thesis chair, Barbara, thank you for your very valuable mentorship throughout the course of my PhD. From my first classes at UCSF to my final thesis committee meeting, you have been with me every step of the way. Thank you for leadership as both a member of my qualifying exam committee and as the chair of my thesis committee, and for constantly working to ensure my successful graduation. On a personal note, you have helped me through some of my darkest moments during my PhD, and for that I will always be grateful. To Kaveh, I am so grateful for the perspective you provided during my committee meetings. Your insightful questions and suggestions over the past few years have pushed me to think deeply and critically about my project, and have greatly improved the quality of my work and my critical thinking skills as a scientist. To Brian, your expertise in GR biology has proved invaluable for my thesis work. I am

extremely grateful for the many, many occasions that you took time out of your busy schedule to meet with me one on one to talk all things glucocorticoids, which truly helped to push my project forward these past few years.

To my first ever PI, Laertis, thank you for taking a chance on a fledgling young scientist who knew virtually nothing about research. I will never forget our first few months of setting up your lab, and I am so happy that I was able to be a part of it. You taught me so many of the core lab techniques I still use to this day, from culturing my first stem cells to qPCR, to FACS, to IF and so much more. You taught me about the core principles of stem cell biology, and inspired me to pursue my passion and continue exploring biology as a graduate student. But most of all you taught me how to think like a scientist, how to ask the right questions, how to design an experiment and how to interpret and present my data. You played such a foundational role in my scientific training, and for that I am eternally grateful.

To all of my colleagues back at Boston University. To my developmental biology teacher, Cynthia Bradham. Never have I been more inspired by a single class or single subject in my life. I looked forward to your class *every single day*. Your zeal for teaching was truly unmatched, and you ignited within me a passion for developmental biology that I never knew existed. You were instrumental in my decision to pursue a degree in developmental biology, and for that I am truly grateful. To Darrell Kotton, my former mentor at the CReM, thank you for taking a chance on me. For answering my email the first week of undergrad and giving me the interview that ended up shaping my entire career. Thank you for leading by example and teaching me the true meaning of scientific integrity. I will always be grateful for your mentorship during my time at the CReM. And to my CReM friends, Reeti, Keri, Billy, Bess, Anjali, George, Katie, Derek, and Geordie. To Reeti, Keri, Billy and Bess especially, thank you all so much for making my first lab home an incredible one. You all taught me so much when I still knew so little, and I appreciate you all more

than you could know. Reeti, you were a constant source of support (and wonderfully witty sarcasm) every day. You constantly listened to me when I needed someone most, and you helped me through my most challenging times during undergrad, even if you didn't realize it at the time. I miss you terribly, and I am so so proud of all you have accomplished in grad school Dr. Sanghrajka! Anjali, it has been wonderful having you now join my Bay Area family, and our evenings of wine and venting these past few months have been more helpful than you could imagine. To George, thank you so much for all of your help in transitioning into the world industry this past year. I am so happy to have gotten the chance to work with you a second time, and I can only hope to be lucky enough to work with you again in the future.

To my Laird Lab family, both past and present, I am honored to have been able to work alongside such incredible colleagues. Being surrounded by such intelligent and passionate people constantly inspired me to be the best scientist that I could be. To Boris, my first Laird Lab mentor, thank you for taking me under your wing and teaching me the ropes after joining the lab at a difficult point in my life. You taught me so many new skills, from dissections, to how to scruff my first mouse, to staining, imaging, and so much more. You made me feel welcomed into my new home, and I am so happy to have gotten the chance to work with you on our paper together. You are an amazing teacher, scientist, and friend, and I can only hope that I get the chance to work with you again in the future. To Dan and Rebecca, my original grad student buddies, thank you for all of our insightful science conversations during the early stage of my project, as well as the equally important late night hangout sessions in RMB that kept us all sane. To our wonderful lab manager Lina, thank you for your constant help over our years working together. I could *always* count on you to lend a helping hand when I needed it the most. Even when you had a million other fires to put out, you always asked me if I needed any help, and that truly means the world to me. I am so excited to see what the next chapter of your life as a grad student holds in store for you, and I wish you the best of luck as you embark on this exciting new journey. Lastly, I think I can

confidently say that your wonderful friendship over the years has finally earned your forgiveness for your heinous murder of Arthur (the duck embryo, nobody panic). To Lauren, our genotyping fairy, I am so grateful for your technical support over the years. But most of all thank you for reiterating to me the important life lesson that the gym can always wait when there is free beer in the break room. To my bench buddy Suping, thank you for always putting a smile on my face each day. Thank you for all your help in getting Westerns and protein work set up for my project, and for all your critical scientific feedback during the early years of my project. And of course thank you for the amazing lessons on how to make the perfect traditional dumplings. To my incredible rotation student and now even more amazing labmate, Mariko. Since day one, it has been an absolute delight getting to work with you. It has been wonderful welcoming you into the Laird lab and seeing how much excitement and passion for science that you have brought into the lab. Thank you for all of your help on my project over the past year, from huge things such as full-scale experiments and managing my colony while I was away, to things as small as lending a hand in the mouse house. You have always been ready to spring into action to help me when I've needed it the most, and I can't possibly explain how much I appreciate you for it. It has been so wonderful to see how much you've grown since joining the lab. I'm excited to see where your graduate school journey leads, and I'm confident that you will do an *incredible* job. To Eliza, quite possibly the most cheerful person I know, for bringing a wonderful and joyful energy into the lab. It has been a delight getting to teach you, while simultaneously getting taught by you in the process. Our near *constant* back and forth exchange of the best ways to wrangle mice has just gone to show me that there is always room to learn new things from your colleagues, no matter your experience level. To both Mariko and Eliza, I will forever be grateful for all of our project brainstorming sessions together and all the insight you have given me on my project. To all of my other labmates, Brandon, Caroline, Eman, Ernesto, Estelle, Jing, Jocelyn, Jonathan, Noa and Thanh - your critical scientific feedback and insight have proven invaluable during our time working together. Thank you all so much for the many laughs together, our crazy lab shenanigans,

and all the fun over the years. But most of all, thank you for not only your patience in putting up with me when I was at my worst, but also your support in getting me through the inevitable challenges of graduate school. And of course, to the often unacknowledged, yet crucial piece of my work and the work of many generations of graduate students before me: to the many, *many* mice that were sacrificed over the course of my graduate work. I will *always* value the crucial role that they played in my work in helping to expand the bounds of scientific knowledge.

To my roommates Sean and Andrew. Thank you both for giving me a wonderful apartment to come home to. Thank you for all of the late night science brainstorming sessions, and perhaps equally important science venting sessions when the mice just would not cooperate. Thank you for all the help over the years during our late night group coding trying to get just one simple R program to work. I know it was often the last thing we wanted to do, but I am so appreciative for all of your help. And of course, our many late night video game battle royales kept me far more sane than you could know. I feel very fortunate to have lived with such wonderful people.

To all of my Gladstone friends and colleagues, of which there are far too many to name, thank you so much for all of your support and lasting friendships. Thank you especially to Elphège for taking me under your wing and training me during my early years of graduate school. I can't even begin to explain how much I learned from you, and I will always be extremely grateful for it.

To all of my DSCB friends, past and present. To my original cohort, Arpana, Nate, Melissa, Lauren, Jacob and Sung - thank you for helping me to survive our first year of classes, and for making the transition to graduate school a fun and slightly less stressful experience. To Arpana and Nate especially, thank you for the seemingly endless nights of quals prep sessions together that inspired and motivated me to think critically about my work, while also being a wonderful excuse to get together and chat over some wine. Thank you to Ryan B. and Lauren for all your

help in getting CUT&RUN up and running in our lab, from sharing reagents to troubleshooting sample prep and discussing data analysis strategies. To Ryan S for your tremendous help with the early bioinformatics analysis of my single cell RNA-seq dataset and confirming GR wasn't doing anything (and that I was, in fact, not going insane). To all the rest of my wonderful DSCB friends, thank you for the years of laughs and support. I truly wouldn't have made it through without you all.

To Dimitris, my pen pal turned invaluable friend, thank you for your wonderful friendship over the years. Our talks together have helped me through some of my most difficult moments of graduate school. Thank you for being someone I can always confide in. Although I wish we lived a bit closer, our fleeting vacations together have taught me two very important things. Firstly, you've reminded me just how much fun I can have if I take a moment to step away from my work and experience the world around me. And secondly, you've shown me how important it is to spend time with the people that bring a smile to your face. I miss you terribly buddy, and I hope that I can see you soon.

To my wonderful cousin Salvo, thank you for your endless support and encouragement as I've fought my way through the past eleven years of my academic career. Thank you for all of our late night chats during undergrad, motivating me to fight my way through even the most difficult times. I will never forget your impromptu "I'm coming to Boston tomorrow" trip, which was my favorite moment of undergrad by far. It has been so challenging not having you around more often, and I wish the distance between us wasn't so great. I miss you more than you could know, and I hope that we will be able to see each other again soon.

To Robbie, thank you for all of your unwavering support these past few years of graduate school. Thank you for teaching me how to stand up for myself and advocate for the things I needed at a

time when I struggled so much to do so. But most of all thank you for helping me to embrace who I truly am, and not worry about what anyone else thinks. We have been through so much together these past few years, and I truly appreciate everything you have done for me.

To my parents and sister for their constant and unending support and love. Everything I have achieved is all thanks to you, and not a day goes by where I don't miss you all dearly. To my mom, my all time number one cheerleader. I honestly don't even know where to begin thanking you. You have been an unlimited fountain of support and encouragement for as long as I can remember. You always know what to say to pick me up when I'm feeling down, and have coached me through every stage of my career. Thank you for your optimism in the times I struggled most, for always helping me to see the positive in a situation and realize that maybe things happen for a reason. For always reassuring me in my moments of self doubt, of which graduate school has provided plenty. For giving up your entire career to raise Mel and I, and for devoting your life to us and your family. For supporting me in my decisions to move away for undergrad and grad school and do what was best for my career, even if it meant we wouldn't be able to see each other as often. For showing that not even a car / boat / train / subway ride back to Boston could stop you from feeding me, and always ensuring that I was the only person on Amtrak with an entire duffel bag full of frozen ravioli. For your unconditional love, going *above and beyond* every time I come home to make sure that I never forget where my true home is. To my dad, I think it's finally safe to say that I'm going to pass on joining the family business. Although the All Systems offer was *VERY* tempting at times during the PhD, I think I'm going to see where the whole science thing takes me. Thank you for always being my voice of reason, and for constantly reminding me that I am yes, *yet again*, overthinking everything. I can always count on you to give me the best advice, both in my career and in my personal life, especially when my emotions have gotten the best of me and I can't think clearly. Thank you for coaching me through all the challenging points of my PhD, both big and small, and for *a/ways* supporting me in the decisions that I make. For

always reminding me to stand up for myself, and also reminding me to not let life pass me by. For saving all the best wine for me when I come home. And of course, for always listening to (or at the very least faking interest in) my biology rants on our car rides home from the ferry - not that you had much of a choice. To my sister Melanie, thank you for always being there to chat when I needed someone to talk to. For always making me laugh with ridiculous pictures and videos of Rio and Benny, and for always lifting my spirits when I'm feeling down. I love you all so SO much. Thank you for everything.

And lastly, to Bikiem, aka G., aka Boygur, aka the incredible Dr. Gül Kaya, (aka *actually* Dr. Soygur so she doesn't get mad at me). To my comrade in arms, my partner in crime, my Turkish teacher extraordinaire, my on-call emergency c-section partner, my weekend imaging buddy, my ex-finacé, my baklava supplier, my tiramisu and lentil ball chef, and a çok important person in my life. Firstly, I cannot begin to thank you enough for your technical help on my project, from teaching me embryo dissections when I first started, to all the quirks of Imaris, to how to troubleshoot basically *every possible problem* a confocal microscope can have, to teaching me how to make meiotic spreads, and teaching me basically everything I know about meiosis. For all of your help in the mouse room, for coming in at 6pm on Saturdays to help with c-sections, for helping me with weans and injections and dissections when my life was just too much to handle at times. For the probably 2 liters of digest solution I collectively "borrowed" from you over the years. For helping me with the nightmare single cell experiment prep at 6am without hesitation. For the months and months on end of troubleshooting tamoxifen dosing for my project when you had so much else on your plate. For *always* dropping *everything* you were doing, without hesitation, to help me when I needed it the most. For all your insight and critical thinking, and allowing me to borrow your two functional brain cells to brainstorm on my project at times when everything seemed to be failing. I cannot even begin to put into words how grateful I am to have met you. In those moments when I am constantly questioning whether the stress of graduate school was truly all worth it, I remind

myself that I would do it *all over again* just to meet you. I would have *never* survived the last few years without your constant help, guidance, reassurance, support and love, and there really are no words to express to you how grateful I am to have had you as a lab member and as my best friend. *Çok seni seviyorum kanka, ve her şey için çok teşekkür ederim.*

Contributions

All work performed in this dissertation was performed in the lab of, and under the direct supervision of Dr. Diana J. Laird. Additional conceptual and technical guidance was provided by thesis committee members Dr. Barbara Panning, PhD (chair), Dr. Kaveh Ashrafi, PhD, and Dr. Brian Feldman, MD, PhD.

Chapter 1 of this thesis consists of a literature review performed by **Steven A. Cincotta**.

Chapter 2 of this thesis contains text and figures for a manuscript currently in preparation:

“Glucocorticoid Receptor Signaling in the Mammalian Germline.” **Steven A. Cincotta**, Mariko Foecke, Diana J. Laird.

Conceptualization: **SAC**, DJL; Experimentation: **SAC**; Imaging and Image Analysis: **SAC**, MF; Bioinformatics and Data Analysis: **SAC**; Writing - Original Draft: **SAC**, DJL; Funding Acquisition: **SAC**, DJL

Chapter 3 of this thesis contains text and figures heavily adapted from a previously published review article:

“Heterogeneity of Transposon Expression and Activation of the Repressive Network in Human Fetal Germ Cells.” Boris Reznik, **Steven A. Cincotta**, Rebecca G. Jaszczak, Leslie J. Mateo, Joel Shen, Mei Cao, Laurence Baskin, Ping Ye, Wenfeng An, Diana J. Laird. *Development* (2019), 146(12). doi: 10.1242/dev.171157

Conceptualization: BR, DJL; Methodology: BR, **SAC**, RGJ, LJM, PY, WA; Software: **SAC**, RGJ, PY; Validation: PY, DJL; Formal analysis: BR, **SAC**, RGJ; Investigation: BR, JS, MC, WA, DJL; Resources: JS, MC, LB, DJL; Data curation: **SAC**, RGJ; Writing - original draft:

BR, **SAC**, DJL; Writing - review & editing: BR, **SAC**, RGJ, LJM, PY, WA, DJL; Supervision:
LB, DJL; Project administration: DJL; Funding acquisition: LB, DJL

Chapter 4 of this thesis contains concluding remarks and future directions written by **Steven A. Cincotta**.

Glucocorticoid Receptor Signaling in the Mammalian Germline

Steven Anthony Cincotta

Abstract

While physiologic stress has long been known to impair mammalian reproductive capacity through hormonal dysregulation, mounting evidence now suggests that stress experienced prior to or during gestation may also negatively impact the health of future offspring. A growing body of work in recent years has clearly demonstrated that rodent models of physiologic stress can induce a variety of neurologic and behavioral phenotypes that are able to persist for up to three generations, suggesting that stress signals can induce lasting epigenetic changes in the germline. Any perturbations to the proper transmission of genetic information through the germ cells can be detrimental, and thus understanding the mechanism by which stress can lead to epigenetic alterations in the germline remains a crucial unanswered question in the field. Interestingly, treatment with glucocorticoid stress hormones is sufficient to recapitulate the transgenerational phenotypic inheritance seen in physiologic stress models. These hormones are known to bind and activate the glucocorticoid receptor (GR), a ligand-inducible transcription factor, thus implicating GR-mediated signaling as a potential contributor to the transgenerational inheritance of stress-induced phenotypes. It remains unclear, however, whether the heritability of stress-induced phenotypes following glucocorticoid treatment results from direct actions of glucocorticoids on the germ cells of the gonad, or from indirect effects of glucocorticoids elsewhere in the body. Moreover, evidence for the expression of GR in the developing and adult germ cells of both the male and female remains controversial, making it difficult to assess any potential cell-autonomous roles of GR in modulating the epigenome of the germline in response to stress. We therefore set out to definitively characterize the expression of GR in the germline of

the developing and adult gonads, and to determine what cell-intrinsic role GR plays in normal germline formation and function. We discovered that GR is expressed in the female germline specifically during fetal development (peaking at approximately E13.5 - E14.5), yet is absent from the adult oocyte. We found that the female germline is, surprisingly, resistant to changes in GR signaling. Both genetic deletion of GR as well as GR agonism with dexamethasone revealed minimal transcriptional changes in the female germ cells, as well as no significant changes in meiotic progression, suggesting the female germline is intrinsically buffered against changes in GR signaling. In contrast we found that GR is expressed in the male germline during the final days of development, with expression maintained in pro-spermatogonia during early postnatal development. This expression becomes restricted to the spermatogonia of the adult, and transcriptomic analysis of germ cells from dexamethasone treated males revealed a potential role of GR in regulating RNA splicing. Together our data confirm the dynamic spatiotemporal expression of GR in both the male and female germ cells of the mouse, and suggest a sexually dimorphic function for this receptor in the mammalian germline.

Table of Contents

Chapter 1 - Introduction	1
1.1 - Stress and Reproductive Function: An Overview	1
1.2 - Effects of Physiologic Stress Models on the Gonad and Reproductive Function ...	5
Effects of physiologic stress on the rodent testis	6
Effects of physiologic stress on the rodent ovary	11
1.3 - Effects Of Natural And Synthetic Glucocorticoids On The Gonad	16
Effects of glucocorticoids on the testis	16
Effects of glucocorticoids on the ovary	27
1.4 - Transgenerational Inheritance Of Stress-Induced Phenotypes	35
1.5 - GR Expression in the Testis	42
1.6 - GR Expression in the Ovary	45
1.7 - Genetic Deletion Of GR In The Gonad	48
 Chapter 2 - Sexually Dimorphic Roles of Glucocorticoid Receptor Signaling in the Mammalian Germline	 53
2.1 - Introduction	53
2.2 - Spatiotemporal expression of the glucocorticoid receptor in the female germline	 56
2.3 - Germ cells and somatic cells of the fetal ovary use alternative first exons of <i>Nr3c1</i>	 60

2.4 - Genetic deletion of GR leads to minimal transcriptional changes in the female germline	62
2.5 - Meiosis in the female proceeds normally in the absence of GR	65
2.6 - Developing ovarian somatic cells, but not germ cells, show GR transcriptional activation following exogenous glucocorticoid treatment	67
2.7 - Subcellular localization of GR in the female germline is dynamically regulated in response to ligand	70
2.8 - Fetal ovarian germ and somatic cells show no evidence for the use of inhibitory translational isoforms	71
2.9 - Fetal ovarian germ and somatic cells have no detectable GR β transcriptional isoform	71
2.10 - Spatiotemporal expression GR in the male germline	73
2.11 - Germ cells and somatic cells of the postnatal testis also use alternative first exons of <i>Nr3c1</i>	76
2.12 - Germ cells of the perinatal testis show GR transcriptional activation following exogenous glucocorticoid treatment	79
2.13 - Regulation of mRNA splicing in the early postnatal testis	82
2.14 - Dexamethasone does not alter splicing of genes known to be differentially spliced during meiotic progression	85
2.15 - Discussion	90
<i>Glucocorticoid receptor immunofluorescence in the ovary and testis:</i>	
<i>discrepancies and similarities with the literature</i>	<i>90</i>

<i>Discovery of novel germ cell-specific exon 1 isoform(s) in the 5' UTR of</i>	
<i>Nr3c1</i>	92
<i>The female germline is resistant to changes in GR-mediated signaling</i>	93
<i>GR in the regulation of RNA splicing</i>	95
<i>Difficulties in generating adult GR knockout mice</i>	97
2.16 - Materials and Methods	100
Chapter 3 - Heterogeneity of transposon expression and activation of the	
repressive network in human fetal germ cells	121
3.1 - Introduction	121
3.2 - Dynamic expression and subcellular localization of PIWI homologs in male	
fetal germ cells	124
3.3 - Evidence of transposon-derived primary and secondary piRNAs in fetal testis ...	129
3.4 - L1 transposons are expressed in AGCs coordinately with the transposon	
repression network at the single cell level	135
3.5 - Dynamic relationships between L1 and the repression pathway at transcript	
and protein level	140
3.6 - Declining L1 expression and increasing H3K9me3 during fetal development	145
3.7 - Discussion	156
3.8 - Materials and Methods	162
Chapter 4 - Future Directions and Concluding Remarks	169
4.1 - Fertility studies in GR conditional knockout mice	169
4.2 - Mechanistic analysis of GR signaling resistance in female germ cells	170

4.3 - Further analysis to confirm GR regulation of RNA splicing in spermatogonia	172
4.4 - Concluding remarks	174
References	175

List of Figures

Figure 2.1 - Expression of the glucocorticoid receptor in the developing female germline	57
Figure 2.2 - Expression of the glucocorticoid receptor in the postnatal female germline	59
Figure 2.3 - Germ cells and somatic cells of the fetal ovary use alternative first exons of Nr3c1	61
Figure 2.4 - Genetic deletion of GR leads to minimal transcriptional changes in the female germline	64
Figure 2.5 - Meiosis proceeds normally in the absence of GR	66
Figure 2.6 - Developing ovarian somatic cells, but not germ cells, show GR transcriptional activation following exogenous glucocorticoid treatment	69
Figure 2.7 - Fetal ovarian germ and somatic cells show no evidence for the use of inhibitory transcriptional or translational isoforms	72
Figure 2.8 - Expression of the glucocorticoid receptor in the developing male germline	74
Figure 2.9 - Expression of the glucocorticoid receptor in the postnatal male germline	75
Figure 2.10 - Expression of the glucocorticoid receptor in the adult male germline	76
Figure 2.11 - Germ cells and somatic cells of the early postnatal testis use alternative first exons of Nr3c1	78
Figure 2.12 - Both germ and somatic cells of the early postnatal testis show GR transcriptional activation following exogenous glucocorticoid treatment	81
Figure 2.13 - Dexamethasone-dependent changes in RNA splicing in the early postnatal testis	84
Figure 2.14 - Dexamethasone does not alter splicing of genes known to be differentially spliced during meiotic progression	88

Figure 3.1 - Expression of PIWI proteins in human fetal testis across development	126
Figure 3.2 - Expression of PIWI proteins in human and mouse fetal testis	128
Figure 3.3 - Identification of transposon derived piRNAs in the human fetal testis	131
Figure 3.4 - Schematic of small RNA-seq data analysis pipeline	132
Figure 3.5 - Small RNA-seq analysis of human fetal testis	134
Figure 3.6 - Single cell sequencing reveals dramatic upregulation of L1 family retrotransposons in advanced germ cells.....	137
Figure 3.7 - Schematic of single cell RNA-seq data analysis pipeline	138
Figure 3.8 - Validation of cluster identities in analysis of human fetal testis single cell RNA-seq	139
Figure 3.9 - L1 expression in advanced germ cells	141
Figure 3.10 - Developmental time course of L1 expression in human fetal testis	143
Figure 3.11 - Decrease in L1 transcript levels as development progresses	146
Figure 3.12 - Single cell sequencing of GW25 human fetal germ cells	147
Figure 3.13 - Evidence for PIWI-piRNA pathway activity in fetal testis	149
Figure 3.14 - Evidence for PIWI-piRNA pathway activity in fetal testis (Supplemental)	151
Figure 3.15 - No evidence for global DNA remethylation in AGCs	153
Figure 3.16 - PRMT5 expression in human fetal testis	155
Figure 3.17 - Coordinated transposon repression in GCs of the human fetal testis	160

List of Tables

Table 2.1 - Mouse lines used, genotyping primers, and genotyping reactions	101
Table 2.2 - Tissue fixation parameters	102
Table 2.3 - Antibodies used	118
Table 2.4 - RT-PCR Primers Used	119
Table 2.5 - Splice Junction Primers Used (qRT-PCR)	119
Table 2.6 - qRT-PCR Primers Used	120
Table 3.1 - Relative percentage of all RNA subtypes across all samples	133
Table 3.2 - Top ten transposable elements mapped to by Repbase-mapping reads across all samples	135
Table 3.3 - L1 transcript expression from the single cell dataset in Figure 3.11	145
Table 3.4 - Samples used for small RNA analysis	157
Table 3.5 - Antibodies used	164

List of Abbreviations

ACTH - adrenocorticotropin releasing hormone

AGC - advanced germ cells

AGD - anogenital distance

AMH - anti-müllerian hormone

BDNF - brain derived neurotrophic factor

BSA - bovine serum albumin

CAT - catalase

cDNA - complementary DNA

cKO - conditional knockout

CL - corpus luteum

CRH - corticotropin releasing hormone

CUT&RUN - cleavage under targets & release using nuclease

DEG - differentially expressed gene

dex - dexamethasone

ECM - extracellular matrix

EV - extracellular vesicles

FACS - fluorescence activated cell sorting

FDR - false discovery rate

FSH - follicle stimulating hormone

GD - gestational day

GFP - green fluorescent protein

GnRH - gonadotropin-releasing hormone

GO - gene ontology

GPX - glutathione peroxidase

GR - glucocorticoid receptor

GSH - glutathione

GST - glutathione S-transferase

GV - germinal vesicle

GVBD - germinal vesicle breakdown

GW - gestational week

hCG - human chorionic gonadotropin

HPA - hypothalamic-pituitary-adrenal axis

HPG - hypothalamic-pituitary-gonadal axis

HSP90 α - heat shock protein 90 α

IF - immunofluorescence

IHC - immunohistochemistry

IL-1 β - interleukin 1 beta

IP - intraperitoneal injection

KO - knockout

L1 - LINE1, long interspersed element type 1

LH - luteinizing hormone

MAPK - mitogen-activated protein kinase

MDA - malondialdehyde

miRNA - micro RNA

mRNA - messenger RNA

MSUS - maternal separation and unpredictable maternal stress

mTOR - mammalian target of rapamycin

NF- κ B - nuclear factor kappa B

PBS - phosphate buffered saline

PFA - paraformaldehyde

PGC - primordial germ cell

PI3K - phosphoinositide 3-kinase

piRNA - PIWI-interacting RNA

PIWI - P-element induced wimpy testis in Drosophila

PN - postnatal day

PR - progesterone receptor

PTM - peritubular myoid cells

PTM - post translational modification

PVN - paraventricular nucleus

qPCR - quantitative polymerase chain reaction

qRT-PCR - quantitative reverse transcription polymerase chain reaction

ROS - reactive oxygen species

RA - retinoic acid

RT - room temperature

RT-PCR - reverse transcription polymerase chain reaction

snoRNA - short nucleolar RNA

SOD - superoxide dismutase

Sycp3 - synaptonemal complex protein 3

TE - transposable element

TNF- α - tumor necrosis factor alpha

tRNA - transfer RNA

TUNEL - Terminal deoxynucleotidyl transferase dUTP nick end labeling

UTR - untranslated region

WGA - wheat germ agglutinin

WT - wildtype

Chapter 1 - Introduction

1.1 - Stress and Reproductive Function: An Overview

The production of stress hormones by the hypothalamic-pituitary-adrenal (HPA) axis is a natural and involuntary response of the mammalian body to one of many possible external stressors that perturb organismal homeostasis. When an organism detects an external stressor, the hypothalamic neurons of the paraventricular nucleus (PVN) trigger the production and release of corticotropin releasing hormone (CRH), which then signals to cells of the anterior pituitary gland to secrete adrenocorticotropin releasing hormone (ACTH). ACTH travels through the bloodstream to the adrenal glands, where it signals for the production stress hormones known as glucocorticoids (cortisol in humans and corticosterone in rodents). These glucocorticoids can then act on tissues throughout the body by binding to their cellular receptor, the glucocorticoid receptor (GR), to elicit rapid cellular changes in an attempt to restore homeostatic conditions and thus preserve survival of the individual.

Animals have evolved to shut down non-essential processes in times of stress or imminent danger in order to reallocate energy and ensure survival of the individual. Perhaps the best example of this phenomenon is the inhibition of the reproductive system, given the energetic demands of producing gametes. The predominant mechanism by which stress inhibits the reproductive system is by provoking global hormonal changes in the hypothalamic-pituitary-gonadal (HPG) signaling axis, which collectively act to shut down both male and female reproductive function at multiple levels. As a brief review, HPG axis activity begins in the hypothalamus with the pulsatile production of gonadotropin-releasing hormone (GnRH), an important regulator of reproductive hormone production in both males and females.

GnRH passes into the anterior pituitary where it triggers the production and secretion of luteinizing hormone (LH) and follicle-stimulating hormone (FSH) by gonadotropic neurons into the bloodstream. LH and FSH then go on to trigger testosterone production in the male, and estrogen/progesterone production in the female, which collectively act to regulate sex-specific roles in gametogenesis and sexual maturation/function (Geraghty and Kaufer, 2015; Whirledge and Cidlowski, 2010). Stress hormones have been shown to interfere with each stage of the HPG axis, as reviewed below.

It is now well-accepted that glucocorticoids can directly inhibit the production of GnRH by the neurons of the hypothalamus. Direct incubation of rat hypothalamic explants in culture with either corticosterone or the synthetic glucocorticoid dexamethasone (dex) lead to a dose-dependent decrease in the release of GnRH from neurons (Calogero et al., 1999). Additional *in vitro* studies using immortalized GnRH-secreting hypothalamic neurons have shown that dex treatment directly inhibits the transcription of GnRH by signaling through GR (Chandran et al., 1994). More recent studies have also confirmed this phenomenon in sheep *in vivo*, in which direct measurements of GnRH levels in pituitary portal blood demonstrated that chronic cortisol treatment was able to directly inhibit the release of GnRH from the hypothalamus (Oakley et al., 2009). While glucocorticoids have also been shown to interfere with hormone activity in the pituitary, particularly the production and secretion of LH by gonadotropic neurons, their effects are highly variable and dependent on the type and duration of stress, as well as the interplay with various gonadally-derived sex hormones (Geraghty and Kaufer, 2015; Whirledge and Cidlowski, 2010). This remains a contested and highly active area of investigation, as removing the confounding influence of alternative hormones has proven challenging.

In the gonad, glucocorticoids act to regulate testosterone and estrogen/progesterone biosynthesis in a sex-specific manner. In the rodent testis, both restraint stress models (Marić et al., 1996; Orr and Mann, 1990; Orr and Mann, 1992) and direct injection of glucocorticoids (Kavitha et al., 2006; SAEZ et al., 1977; Sankar et al., 2000) have been shown to directly inhibit the production and release of testosterone. It has also been demonstrated that co-injection of the potent pharmacologic antagonist of the glucocorticoid receptor RU486 into stressed mice is able to rescue testosterone production, suggesting that this phenomenon is dependent on intact GR signaling. It has been confirmed through both *in vivo* and *in vitro* studies that stress-induced glucocorticoids specifically act on the hormone-producing Leydig cells of the testis directly through GR in order to inhibit the transcription of enzymes required for testosterone biosynthesis (Bambino and Hsueh, 1981; Hales and Payne, 1989; Kavitha et al., 2006; Orr and Mann, 1990; Orr and Mann, 1992; Rengarajan and Balasubramanian, 2007; Rengarajan and Balasubramanian, 2008; SAEZ et al., 1977; Sankar et al., 2000). Furthermore, this mechanism of glucocorticoid-induced suppression of testosterone has also been found to extend to humans (CUMMING et al., 1983). The hormonal influence on the ovary has traditionally been more challenging to study due to the cyclical nature of the menstrual cycle. Nevertheless, studies of both rat (ADASHI et al., 1981; Hsueh and Erickson, 1978; Kashino et al., 2021; Schoonmaker and Erickson, 1983; Yuan et al., 2016) and human (Michael et al., 1993) *in vitro* cultured granulosa cells have been able to provide insight into the hormonal dysregulation in the ovary in response to glucocorticoids. These studies have collectively concluded that glucocorticoids act to inhibit estrogen/estradiol biosynthesis by directly inhibiting expression of P450 aromatase (Hsueh and Erickson, 1978; Kashino et al., 2021; Michael et al., 1993; Schoonmaker and Erickson, 1983), an enzyme essential for the conversion of androgens into estrogens. Conversely, glucocorticoids also induce the production and release of progesterone by directly increasing expression of a variety of enzymes required for progesterone biosynthesis (ADASHI

et al., 1981; Hsueh and Erickson, 1978; Kashino et al., 2021; Schoonmaker and Erickson, 1983; Yuan et al., 2016).

Aside from hormonal dysregulation, glucocorticoids have been shown to have many other widespread effects in the different cell types of the gonads. In the next sections, I will highlight key examples of how both *in vivo* models of physiologic stress and *in vivo* / *in vitro* models of direct glucocorticoid exposure can have profound impacts on the testis and ovary - both in adulthood and during development *in utero*.

1.2 - Effects of Physiologic Stress Models on the Gonad and Reproductive Function

Below I will summarize key examples from the literature of how physiologic stress in rodent models can have profound effects on gonad morphology and function, highlighting examples of how the germline and somatic cells of the gonad are impacted at the molecular level. It is important to note that while there are some phenotypic outcomes that are overwhelmingly consistent across studies, a relatively recent surge in this research area has shown that some phenotypes can vary considerably between studies depending on the model of stress that is used.

Important factors to consider when comparing results of stress models include the type of stress induced (i.e. psychological stress, physical/pain stress, etc.), the duration of stress (i.e. chronic treatment over weeks/months, or single acute stressors), the severity of the stress (i.e. ten minutes a day or six hours a day), as well as the predictability of the stress (i.e. varied, unpredictable stress, or habituation with a consistent stressor). For the purpose of this review, I will focus almost entirely on psychological/physiological stress, as the vast majority of research thus far has been in this area.

Most work outlined below uses either a restraint stress or “immobilization” model (in which the animal is physically restrained in one of various setups for a defined period of time), or a model of unpredictable, non-habituating stress (in which the animal is given a novel and non-repeating stressor daily, such as changes to light/dark cycle, soaked bedding, disruptive noise, cold shock, heat shock, predator odor, forced swimming, food/water deprivation, and others). The latter model has come under criticism for impairing animal welfare, and more “mild” forms of stress

that do not impair animal food/water intake are currently being explored. Where differences in phenotypes arise between studies, I will do my best to highlight the differences in stress models utilized that likely account for these discrepancies.

Effects of physiologic stress on the rodent testis

Morphological alterations

It is well accepted that both restraint stress and chronic unpredictable stress lead to changes in the gross morphology of the testis. In all cases where measured, the body weight of stressed male rodents was significantly lower than unstressed controls, regardless of the stress model employed (Fahim et al., 2019; Guo et al., 2017a; Mehfooz et al., 2018; Nirupama et al., 2013; Ribeiro et al., 2018; Sakr et al., 2015; Zou et al., 2019). In most instances, stress led to decreases in the weight of both testis and epididymis (Guo et al., 2017a; Mehfooz et al., 2018; Nirupama et al., 2013), which was also accompanied by decreases in the diameter and the thickness of the seminiferous tubules (Hou et al., 2014; Kolbasi et al., 2021; Ribeiro et al., 2018). Some studies have shown that stress can lead to a thinning of the basement membrane surrounding the tubules (Hou et al., 2014; Kolbasi et al., 2021), as well as a decrease in the surface area of the interstitial compartment between tubules (Hou et al., 2014). Kolbasi and colleagues further demonstrated that impaired expression of the tight junction proteins ZO-1 and CLDN11 in the basal lamina in response to stress can also lead to disruptions in the blood-testis barrier (Kolbasi et al., 2021), the integrity of which is crucial for maintaining proper spermatogenesis.

Disruption of testosterone biosynthesis

Another highly consistent and well-established impact of stress on the testis is the dysregulation of hormone production by the interstitial Leydig cells. Chronic restraint stress and unpredictable stress regimens of almost any severity or duration have been shown to cause a dramatic decrease in the levels of testosterone in both the serum and the testis (Almeida et al., 1998; Charpenet et al., 1981; Fahim et al., 2019; Guo et al., 2020; Kolbasi et al., 2021; Lin et al., 2014; Marić et al., 1996; Mehfooz et al., 2018; Orr and Mann, 1990; Orr and Mann, 1992; Sakr et al., 2015; Yazawa et al., 1999; Zou et al., 2019). Even a single session of three hour restraint stress is sufficient to drop plasma testosterone levels, highlighting the robustness of this effect (Orr and Mann, 1990). *In vitro* studies have confirmed that this decrease in testosterone production is a result of actions of glucocorticoids on the Leydig cells of the interstitium, in which corticosterone can directly inhibit the production of testosterone in a dose-dependent manner (Charpenet et al., 1981; Marić et al., 1996; Orr and Mann, 1990). This effect is mediated by direct action of corticosterone on GR, as co-treatment both *in vitro* and *in vivo* with the potent GR inhibitor RU486 has been shown to be sufficient to rescue the production of testosterone (Lin et al., 2014; Orr and Mann, 1992). GR in the Leydig cells directly suppresses the expression of enzymes involved in testosterone biosynthesis, including StAR, P450_{scc}, Cyp17a1, Cyp11a1, Hsd3b1, Hsd17b3, and others (Fahim et al., 2019; Guo et al., 2020; Lin et al., 2014; Sakr et al., 2015). Stress has also been found to induce apoptosis in the Leydig cells in a GR-dependent manner, which could further contribute to the loss of testosterone production seen (Chen et al., 2011; Mehfooz et al., 2018). While testosterone production is consistently decreased in response to stress, changes in serum levels of gonadotropin hormones (LH and FSH) produced in the pituitary seem to vary between studies. One study did show that stress led to a decreased sensitivity to artificial gonadotropin treatment, where a higher amount of

gonadotropin (in this case hCG) was required in order to induce testosterone production in mice that received restraint stress (Charpenet et al., 1981).

Decreased sperm number and quality

There are also a multitude of studies demonstrating the detrimental effects of stress on sperm quantity, motility, and differentiation/maturation. Both restraint stress and chronic unpredictable stress models in adult male rodents have been found to decrease total epididymal sperm count, as well as the number of mature spermatids in the testis (Almeida et al., 1998; Guo et al., 2017a; Guo et al., 2020; Hou et al., 2014; Mehfooz et al., 2018; Nirupama et al., 2013; Sakr et al., 2015; Zou et al., 2019). In the majority of studies, this decrease in sperm concentration was accompanied by a decrease in sperm motility (Kolbasi et al., 2021; Mehfooz et al., 2018; Ribeiro et al., 2018; Sakr et al., 2015) and viability (Mehfooz et al., 2018; Ribeiro et al., 2018), along with an increase in the number of morphologically abnormal sperm observed (Guo et al., 2020; Kolbasi et al., 2021; Mehfooz et al., 2018; Nirupama et al., 2013; Sakr et al., 2015). Many groups have demonstrated that this decrease in the number of mature sperm is likely due to elevated apoptosis at multiple stages of germline development in response to stress (Guo et al., 2017a; Hou et al., 2014; Mehfooz et al., 2018; Nirupama et al., 2013; Yazawa et al., 1999; Zou et al., 2019), as stress-induced apoptosis of the spermatogonia, spermatocytes, and spermatids alike has been documented. Zou and colleagues have also shown that chronic unpredictable stress is also able to induce a G_0/G_1 cell cycle arrest in spermatogonia, which may also contribute to the observed decrease in mature spermatids/spermatozoa (Zou et al., 2019).

Altered non-coding RNA content in sperm

Two research groups in particular have conducted extensive research into the effects of physiologic stress on sperm RNA content in an effort to understand how the transfer of small non-coding RNAs to offspring via sperm can lead to lasting stress-induced phenotypes across generations. The transgenerational effects of stress will be reviewed in more detail below. Rodgers and colleagues first demonstrated that in a six week chronic unpredictable stress model, the offspring of stressed male mice showed a blunted HPA axis-induced production of corticosterone in response to an acute 15 min restraint stress in comparison to offspring from unstressed males (Rodgers et al., 2013). This memory of paternal stress led the authors to hypothesize that something was being passed from the sperm of stressed males into the offspring. After performing small RNA-sequencing on sperm from stressed and unstressed males, they found robust changes in miRNA content, particularly of miRNAs with predicted target genes involved in chromatin regulation, DNA methylation, and miRNA processing (Rodgers et al., 2013). Very impressively, Rodgers et al. then went on to show that injection of nine stress-enriched miRNAs into control zygotes was sufficient to phenocopy the blunted HPA axis phenotype in offspring (Rodgers et al., 2015). Furthermore, they also demonstrated that extracellular vesicles (EVs) produced by the epididymal epithelial cells also showed highly altered miRNA content in response to stress, and when control sperm were incubated with EVs isolated from stressed mice, this was also sufficient to phenocopy their previous work (Chan et al., 2020). Collectively this work suggests a mechanism by which stress induces changes in the miRNA content of epididymal EVs, which can be transferred to spermatozoa during migration through the epididymis, ultimately altering sperm miRNA content that leads to lasting epigenetic effects in the somatic cells of offspring. Gapp and colleagues also showed a very similar phenomenon, in which they utilized a model of unpredictable maternal separation to induce stress in pre-weaning-age mouse pups. They found that stressed F1 males had a variety of

behavioral phenotypes that could be transmitted to the F2 progeny, along with elevated levels of multiple miRNAs in the sperm (Gapp et al., 2014), similar to that observed by Rodgers and colleagues. They were able to show that injection of these select miRNAs from stressed sperm into control fertilized oocytes was sufficient to transfer the behavioral phenotypes seen in the F1 to the resulting progeny (Gapp et al., 2014). More recently, the same group showed that the long non-coding RNA content of sperm is also altered in response to stress (Gapp et al., 2020). Intriguingly, oocyte injection with long non-coding RNAs vs miRNAs led to different phenotypic effects, suggesting that different RNA classes can transmit different phenotypes across generations (Gapp et al., 2020). The work from these two groups represents a very exciting new area of research, and will likely be the subject of much further investigation.

Oxidative damage and inflammation

Although still a very novel research area, there have been a few documented examples of chronic models of physiologic stress leading to both altered oxidative stress within the testis, as well as the activation of inflammatory cell signaling pathways. Various independent studies of chronic stress models (all greater than four weeks of treatment) have shown a significant increase in the levels of malondialdehyde (MDA), a natural biomarker for oxidative stress, in the testis in response to stress (Fahim et al., 2019; Guo et al., 2017a; Guo et al., 2020; Kolbasi et al., 2021; Nirupama et al., 2013; Sakr et al., 2015). This increase in oxidative stress is likely due to the stress-induced decreases in expression of various oxidoreductase enzymes in the testis, including superoxide dismutase (SOD), catalase (CAT), glutathione (GSH), glutathione S-transferase (GST), and glutathione peroxidase (GPX) (Fahim et al., 2019; Guo et al., 2017a; Guo et al., 2020; Nirupama et al., 2013; Sakr et al., 2015). Very interestingly, multiple groups were able to show that treatment with a variety of antioxidant reagents (including melatonin, resveratrol, dimethyl fumarate and even probiotics) was actually sufficient to rescue the majority

of stress-induced testicular phenotypes seen (Fahim et al., 2019; Guo et al., 2017a; Guo et al., 2020). However, Nirupama and colleagues showed that a four month “recovery” period (following a 60 day mixed stress model) without any type of antioxidant intervention was insufficient to reverse the oxidative stress phenotypes seen (Nirupama et al., 2013). This suggests that induction of oxidative stress in the testis may play a much greater role in the etiology of testicular stress-induced phenotypes than previously thought. Many of these studies also found an induction in inflammatory cytokine production in the testis following stress, including activation of NF- κ B, TNF- α and IL-1 β signaling pathways (Fahim et al., 2019; Guo et al., 2017a; Guo et al., 2020). The exact function of these signaling pathways in the stress response is yet to be determined, and remains an ongoing area of investigation.

Effects of physiologic stress on the rodent ovary

Morphologic/physiologic alterations

Despite the considerable variability in some stress-induced phenotypes between different studies, a few key changes were consistent across almost all studies. Regardless of the type of stress model used, chronic stress led invariably to a decrease in overall body weight (Gao et al., 2016; Gao et al., 2019; Natale et al., 2019; Sun et al., 2018; Xu et al., 2018; Xu et al., 2020; Zhang et al., 2011) as well as the weight of the ovary (Gao et al., 2019; Xu et al., 2018). Another consistent effect of stress was severe disruption in estrous cycling in every case in which it was quantified, including irregular cyclicity, general lengthening of cycle, or pause in diestrus (Casillas et al., 2021; Fu et al., 2018; Natale et al., 2019; Xu et al., 2018).

Decreased number of follicles and oocytes

Multiple research groups also seem to agree that stress, in general, leads to changes in the number of oocytes and follicles - although there are some discrepancies over the exact follicular stage(s) affected. Many studies have shown a decrease specifically in the number of primordial follicles following chronic restraint stress (Xu et al., 2018), chronic unpredictable stress (Gao et al., 2019), and predator stress (Natale et al., 2019). Xu and colleagues suggest that this depletion of the primordial follicle pool is actually due to activation of these follicles to differentiate into primary follicles in response to high circulating levels of CRH, a phenomenon which could be recapitulated by dosing neonatal ovaries *ex vivo* with CRH (Xu et al., 2018). While Gao and colleagues show decreases in the number of preantral follicles and corpora lutea in response to an eight week mouse model of chronic unpredictable stress (Gao et al., 2019), another group using a four week rat model of chronic unpredictable stress showed no change in preantral follicle number, but instead a decrease in antral follicles (Xu et al., 2020). It is unclear whether this difference in preantral vs antral follicle response to stress is due to differences in the duration of stress, or is actually a species-specific difference between mice and rats. It was also shown that chronic restraint stress could impair rates of ovulation (Zhang et al., 2011), and that the number of oocytes retrieved following stimulated ovulation of unpredictably stressed mice was significantly decreased (Wu et al., 2012a). Furthermore, a few groups have also suggested that stress may lead to premature follicular atresia (apoptosis) (Li et al., 2018a; Liang et al., 2013; Wu et al., 2012b; Xu et al., 2020; Zhao et al., 2020), particularly in secondary and antral stage follicles (Wu et al., 2012b; Xu et al., 2020). One group has proposed that this restraint stress-induced apoptotic phenotype may be due to hormonal disruptions that trigger activation of the Fas/FasL and TNF- α pathways in the ovary (Li et al., 2018a; Liang et al., 2013; Zhao et al., 2020). An isolated example of a predator stress model, however, measured no

changes in apoptotic rates, suggesting that apoptotic activity may be stressor-dependent (Natale et al., 2019).

Impaired oocyte developmental potential

Another phenotype that seems to be generally consistent across different stress models is a stress-induced impairment of the developmental potential of oocytes, although exactly how this phenotype manifests varies slightly from study to study. In studies across all stress models, oocytes subjected to *in vitro* maturation assays showed defects or delays in blastocyst formation (Lian et al., 2013; Liang et al., 2013; Wu et al., 2012a; Zhang et al., 2011). Stress appears to increase the relative number of oocytes in the germinal vesicle (GV) stage (Casillas et al., 2021), and also appears to decrease the rate and percentage of oocytes that undergo germinal vesicle breakdown (GVBD) (Sun et al., 2018) - an important step in the resumption of meiosis. This stress-induced delay in GVBD is concomitant with a delay in the rate of, and decrease in the total number of oocytes that undergo meiotic resumption (Casillas et al., 2021; Sun et al., 2018). Moreover, this is accompanied by an increase in the number of abnormal oocytes, which include defects including increases in zona pellucida malformations, cytoplasmic blebbing, GV mis-positioning, meiotic spindle abnormalities, and rates of aneuploidy (Casillas et al., 2021; Lian et al., 2013; Xu et al., 2018). The combination of these oocyte defects in response to stress provides a plausible explanation for the pronounced defects in blastocyst formation seen.

Disruption of ovarian hormone production

A slightly more contentious area of study is the effect that physiologic stress has on the production of sex hormones by the ovary. There seems to be some consistency across studies that both restraint and unpredictable stress models suppress ovarian production of estradiol and

testosterone (Fu et al., 2018; Gao et al., 2019; Liang et al., 2013; Xu et al., 2020), and that these effects are occurring at the level of the hormone producing granulosa and theca cells. The effect of stress on the levels of other hormones, particularly AMH produced by the ovary and FSH and LH produced by the pituitary, is highly variable depending on the stress model employed, and remains an area of active study (Fu et al., 2018; Gao et al., 2019; Natale et al., 2019; Xu et al., 2018; Xu et al., 2020).

Additional signaling pathways induced by stress

Lastly, there are a handful of specific signaling pathways that seem to be disrupted in response to chronic stress. The first is activation of PI3K/Akt/mTOR signaling through the growth factor brain derived neurotrophic factor (BDNF). Wu and colleagues demonstrated that 30 days of chronic unpredictable stress led to a dramatic decrease in BDNF levels specifically in antral follicles, along with severe defects in blastocyst formation as described above (Wu et al., 2012a). Surprisingly, administration of BDNF alone to stressed mice was sufficient to completely rescue the stress-induced phenotypes seen. Two other groups independently showed dampening of BDNF/PI3K/Akt/mTOR signaling in follicles in response to different stress models (Xu et al., 2018; Xu et al., 2020), strongly suggesting that this may be a primary pathway through which stress hormones are interfering with oocyte developmental competence. Two independent studies have also highlighted an increase in oxidative damage in response to either restraint or chronic unpredictable stress (Lian et al., 2013; Sun et al., 2021). Sun and colleagues showed that granulosa cells of stressed ovaries experience a decrease in gene expression for genes with oxidoreductase activity (e.g. IDH1), and that this increase in oxidative damage leads to a decrease in proliferation and increase in granulosa cell senescence *in vivo* (Sun et al., 2021). They further confirmed that increased reactive oxygen species (ROS) in response to IDH1 knockdown in cultured granulosa cells specifically induced MAPK activity and

downstream signaling pathways (Sun et al., 2021), suggesting MAPK activity may be important for ovarian sensitivity to oxidative damage. Lian et al. also showed a similar induction of oxidative damage and impairment of oocyte maturation, which was rescued by co-administration of antioxidants to stressed animals (Lian et al., 2013).

1.3 - Effects Of Natural And Synthetic Glucocorticoids On The Gonad

Given that models of non-habituating and chronic stress directly induce the production of glucocorticoid stress hormones, many studies have attempted to study the effects of direct treatment with these hormones on the function of the gonad. While this literature is expansive, I have done my best to highlight the key known effects of glucocorticoids on the male and female gonads, and have broken down the effects by cell type. The majority of studies utilize either naturally occurring glucocorticoids (e.g. corticosterone) or synthetic analogs (e.g. dexamethasone or betamethasone), which all have high affinity for, and ability to activate downstream signaling of, the glucocorticoid receptor (GR). For the scope of this thesis, I have limited this review to the effects of glucocorticoids on rodent and human systems specifically, although some additional data exists for a variety of other species. While the majority of work to date has been studying the effects of these glucocorticoids on adult gonad function, I will also highlight an increasing number of recent studies that have begun to demonstrate the powerful effects that glucocorticoids can elicit on the developing fetal gonads following *in utero* exposure.

Effect of glucocorticoids on the testis

Spermatogenic cells

Multiple independent studies have shown that both natural and synthetic glucocorticoid treatment can lead to morphological defects within the seminiferous tubules of the testis, with fairly consistent results across studies. Orazizadeh and colleagues utilized a seven day daily dexamethasone dosing regimen in adult mice, and observed dex dose-dependent decreases in both the thickness of the spermatogenic epithelial layer, as well as seminiferous tubule diameter

(Orazizadeh et al., 2010). They demonstrated a dex dose-dependent increase in the number of germ cells that were detached or sloughed off of the spermatogenic epithelium, and an increase in the number of deformities within the epithelium, including vacuole formation and the presence of multinucleated giant cells (implying aberrant meiosis) (Orazizadeh et al., 2010). Ren et al. showed a strikingly similar response after four week administration of the natural glucocorticoid corticosterone in mice. Dex-treated mice showed decreased sperm counts along with higher rates of sperm morphological abnormalities and multinucleated giant cells (Ren et al., 2021). In addition, they also observed a decrease in Sycp3 protein expression by Western blot, further implying a defect in proper meiotic progression (Ren et al., 2021). Taken together these results show that glucocorticoid signaling clearly leads to defects within the spermatogenic epithelium, although it is still not entirely clear whether these phenotypes are a result of direct action of glucocorticoids on the cells of the testis, or if they may be the result of broader metabolic/hormonal disruption in the body. Interestingly, there is also one study in human that observed many similar phenotypes after the administration of prednisolone (another synthetic glucocorticoid) to adult male patients. The authors found 30 mg daily of prednisolone over four weeks led to decreases in sperm counts and motility, and this effect was not reversed upon hormone withdrawal until approximately six months later (Mancini et al., 1966). Testicular biopsies from the same patients revealed spermatogenic arrest, decreased number of spermatogonia and spermatozoa, as well as sloughing of germinal cells into the chord lumen (Mancini et al., 1966). These results strongly suggest that the negative effects of glucocorticoids on spermatogenesis may be conserved across mammals more broadly.

Glucocorticoid treatment has also been implicated in germ cell apoptosis of the testis. Yazawa et al. were the first to show that one week of daily dosing with dex was sufficient to induce a ten-fold increase in the number of apoptotic germ cells of the rat testis, as assessed by TUNEL staining (Yazawa et al., 2000). Furthermore, they were able to demonstrate that this effect could

be completely abrogated by co-administration with the potent GR antagonist RU486 (also known as mifepristone), strongly suggesting that this effect was glucocorticoid receptor mediated (Yazawa et al., 2000). Apoptosis seemed to occur predominantly in the outer spermatogonia of the testis cords, and a similar induction of apoptosis predominantly in the spermatogonia was recapitulated by another group in a four week corticosterone dosing mouse model (Ren et al., 2021). As outlined in a later section of this introduction, GR expression has been seen in the spermatogonia (Biagini and Pich, 2002; Stalker et al., 1989) (also personal data, see Chapter 2), which could suggest direct induction of apoptosis in the spermatogonia as a result of high doses of dex. Another group independently replicated these results in the mouse testis using a similar dex dosing strategy, where they saw a dose-dependent increase in TUNEL staining in all spermatogenic cell types of the testis (Orazizadeh et al., 2010). The authors hypothesize that as germ cells of both androgen-dependent *and* androgen-independent stages are affected by dex treatment, it is unlikely that the sole cause of this phenotype is a potential disruption in testosterone production. The same group went on to show by IHC that dex treatment induced expression of the pro-apoptotic protein Bax in spermatogenic cells, implicating it as a potential mediator of dex-induced apoptosis (Mahmoud et al., 2009).

One very important point to note is that while there are clear effects of glucocorticoid treatment on the spermatogenic cells of the testis, it is almost impossible to rule out whether these effects are due to direct actions of glucocorticoids on the germline, or if hormonal imbalances produced in the hypothalamus, pituitary, adrenals, or somatic cells of the gonad in response to glucocorticoid treatment are having indirect effects on the germline. Given that proper testosterone production is crucial for spermatogenesis (Smith and Walker, 2014), any hormonal imbalance could indirectly impair spermatogenesis (see Leydig cell section below for more details). While many other cell types of the testis can be easily cultured with glucocorticoids *ex vivo* (e.g. peritubular myoid cells and Leydig cells (see below)), it is very difficult to culture germ

cells without their somatic niche, making it difficult to tease out the direct effect of glucocorticoids on the germline without somatic cell influences. The most efficient way to test the germ cell intrinsic role of GR would be to generate a germ cell conditional knockout for GR.

Another important area of study worth noting is the effect of glucocorticoid treatment on the epigenetic and non-coding RNA landscape of spermatogenic cells within the testis. This area is gaining increasing attention in recent years as more groups try to understand the potential epigenetic mechanisms within the germline underlying stress-induced transgenerational effects (see above for details). While DNA methylation was initially proposed as an enticing method of non-genetic transmission, multiple studies have demonstrated that glucocorticoid treatment does not appear to lead to sustained changes in DNA methylation across generations. Petropoulos et al. demonstrated that adult male mice treated with dex had no significant changes in global CpG methylation of the sperm by 35 or 60 days after treatment, and only a minor increase in non-CpG methylation by 60 days (Petropoulos et al., 2014). Furthermore, they showed that these methylation changes were not maintained in the sperm of the F1 offspring. This is likely due to the global erasure of DNA methylation that occurs during fetal germline development, implying that direct glucocorticoid-dependent changes in DNA methylation of the sperm are unlikely to be the cause of any heritable dex-dependent phenotypes. Another group assessed changes in global DNA methylation of adult sperm of F1 rats following *in utero* dex administration, and found no significant differences (Cartier et al., 2018). The same study also saw no significant changes in other putative epigenetic marks, including histone modifications (H3K4me1, H3K4me3, H3K9me3, and H3K27me3) and small RNA profiles (Cartier et al., 2018). The results of this study, however, may not be entirely accurate based on data accumulated during my thesis work. Cartier and colleagues utilized a very low dose of dexamethasone (0.1 mg/kg), which may have been insufficient to provoke significant changes. Furthermore, while the authors dosed rats with dex during E15-E19 of fetal development, I have shown that GR

expression in the developing mouse male germline does not appear until approximately the final 24 hours before birth, after their window of treatment. Thus, this dosing regimen may have been insufficient to elicit any direct effects on the germline through GR.

While glucocorticoids appear to have a minimal effect on DNA methylation, they do appear to alter small RNA profiles of spermatogenic cells. Short et al. showed that four week chronic treatment of male mice with corticosterone led to altered expression of many miRNAs in the sperm of treated males (Short et al., 2016). They also were able to show that two hippocampal growth factors (*Igf2* and *Bdnf*) whose expression was perturbed in F1 hippocampi contain binding sites for these differentially expressed miRNAs (Short et al., 2016). While the authors imply that differential expression of these miRNAs in the sperm could be one potential explanation for the altered expression of *Igf2* and *Bdnf* in the F1 hippocampi, they also point out that many further functional studies would be needed to confirm this hypothesis. More recently, Gapp and colleagues demonstrated that a single dose of dexamethasone in adult male mice was sufficient to dramatically alter the RNA payload of the sperm within fourteen days after treatment (Gapp et al., 2021). Dex administration resulted in significant changes in the expression of certain miRNAs, circular RNAs, and tsRNAs (small RNA fragments derived from tRNAs), and a small subset of these changes could even be seen in IVF-generated zygotes using sperm from treated males (Gapp et al., 2021). While these studies collectively show that sperm RNA content can clearly be perturbed by glucocorticoid treatment, the field is still lacking any clear functional studies that directly link altered sperm RNA content to heritable, transgenerational phenotypic outcomes.

Leydig cells

The Leydig cells of the testis are the primary hormone producing cells of the testis, and are found within the interstitial space between the seminiferous tubules. There is a large body of evidence to support the glucocorticoid-mediated disruption of testosterone biosynthesis in the Leydig cells. The direct effect of dexamethasone and/or corticosterone on testosterone production in rodent Leydig cells has been shown by a variety of groups after glucocorticoid administration both *in vivo* (Kavitha et al., 2006; SAEZ et al., 1977; Sankar et al., 2000) and in primary Leydig cells cultured *in vitro* (Bambino and Hsueh, 1981; Hales and Payne, 1989; Orr and Mann, 1992; Rengarajan and Balasubramanian, 2007; Rengarajan and Balasubramanian, 2008; SAEZ et al., 1977; Sankar et al., 2000). The collective research of various groups has shown that glucocorticoids impair multiple components of the testosterone biosynthetic pathway. First, glucocorticoids have been shown to directly repress the transcription of various enzymes required for testosterone production, including the cholesterol side-chain cleavage enzyme P450_{scc} (Hales and Payne, 1989; Rengarajan and Balasubramanian, 2008), the cholesterol mitochondrial transport protein StAR (Rengarajan and Balasubramanian, 2008), and the cholesterol dehydrogenases 11 β HSD (Rengarajan and Balasubramanian, 2007), 3 β HSD (Badrinarayanan et al., 2006; Rengarajan and Balasubramanian, 2008), and 17 β HSD (Badrinarayanan et al., 2006; Rengarajan and Balasubramanian, 2008). In addition to repressing expression of these enzymes, glucocorticoids also result in a net decrease in enzymatic activity for P450_{scc}, 11 β HSD, 3 β HSD and 17 β HSD (Rengarajan and Balasubramanian, 2007; Rengarajan and Balasubramanian, 2008; Sankar et al., 2000). Dexamethasone and corticosterone have been shown both *in vivo* (Bambino and Hsueh, 1981) and *in vitro* (Rengarajan and Balasubramanian, 2007) to decrease expression of the luteinizing hormone (LH) receptor on the surface of Leydig cells, which is normally required for gonadotropin-dependent induction of testosterone production. Corticosterone is also able to

disrupt the metabolic profile of Leydig cells both *in vivo* and *in vitro*, inhibiting glucose oxidation and NADPH production which is a critical rate-limiting step of the biosynthetic pathway (Kavitha et al., 2006; Rengarajan and Balasubramanian, 2007). Lastly, it has also been shown that high levels of corticosterone are sufficient to induce apoptosis of Leydig cells following both *in vivo* administration as well as in primary cell cultures *ex vivo* (Gao et al., 2002; Gao et al., 2003). Homeostatic maintenance of testosterone levels by the Leydig cells is crucial for regulating various aspects of spermatogenesis, including the maintenance of the blood-testis barrier, proper meiotic progression, adhesion between Sertoli cells and spermatids, and sperm release (Smith and Walker, 2014). Therefore, this robust and reproducible decline in testosterone production following glucocorticoid treatment is likely to also impair various aspects of spermatogenesis.

Peritubular myoid cells

Peritubular myoid cells (PTMs) are a smooth muscle-like cell that line the outer layer of the seminiferous tubules and perform multiple functions, including providing structure to the seminiferous tubules, contracting to allow for the passage of spermatozoa through the cords, as well as maintaining the spermatogonia stem cell niche (Chen et al., 2014; MAEKAWA et al., 1996; Zhou et al., 2019). Very little is known about the effect of glucocorticoid administration on PTMs, with only two studies addressing this question. Weber and colleagues utilized an immortalized rat PTM cell line, in which they found that treatment with dexamethasone led to a dose-dependent decrease in fibronectin production and a decrease in proliferation (Weber et al., 2000). However, a similar study using primary cultures of human PTMs demonstrated the opposite effect, in which dex treatment led to an increase in expression of extracellular matrix (ECM) genes, including *ELN* and *FBLN5* (Welter et al., 2020). This study also showed that dex led to an increase in actin stress fiber formation and subsequent increase in contractility (Welter

et al., 2020). It is possible that this differing response in ECM production could be species dependent (as architectural differences in the PTM layer are known to exist between rodents and humans (MAEKAWA et al., 1996)), although further studies will be needed to validate this. While the exact effect of glucocorticoid treatment on PTMs clearly requires further study, special care should be given to studying this population as they are one of the highest GR-expressing cells of the testis (Biagini and Pich, 2002; Hazra et al., 2014; Schultz et al., 1993; Weber et al., 2000) (and personal data), and therefore highly susceptible to glucocorticoid treatment.

Sertoli cells

Sertoli cells are located within the seminiferous tubules, and represent one of the primary support cells of the differentiating spermatogenic cells. Despite their close ties to and very important role in maintaining spermatogenesis, very little is known about the effect of glucocorticoids on this cell type. Only two studies could be found in which the effect of dexamethasone treatment on Sertoli cells was assessed. Levy and colleagues treated primary cell cultures of rat Sertoli cells with dexamethasone and saw a dose-dependent increase in two particular genes, the androgen binding protein (*Abp*) and the cAMP-dependent protein kinase regulatory subunit type II beta (*Prkar2b*), although failed to show any further functional result of these gene expression changes (LEVY et al., 1989). Ren et al. demonstrated that long term corticosterone exposure in mice led to an altered metabolic profile in Sertoli cells, in which total lactate content was decreased along with a concomitant decrease in expression of genes required for lactate metabolism (Ren et al., 2021). They were able to repeat this result in Sertoli cell cultures *in vitro*, along demonstrating impaired phagocytosis following corticosterone treatment (Ren et al., 2021). As proper lactate metabolism and phagocytic activity are required for proper Sertoli cell function, the authors postulate that this Sertoli cell impairment could have contributed to the spermatogenic impairment they saw in corticosterone treated animals. As the

expression of GR in the Sertoli cell is still debated and seems to vary with developmental stage (Hazra et al., 2014) (see GR expression section of introduction below), it is very possible that the responses seen in both studies above may be the result of indirect changes due to altered signaling between Sertoli cells and other more GR-responsive cell types.

Gestational glucocorticoid treatment and effects on male fertility

Aside from the detrimental effects of glucocorticoid treatment on adult testis function as outlined above, a mounting number of recent studies have begun to demonstrate that exposure of the fetus to excessive levels of glucocorticoids during development can lead to defects in spermatogenesis that can span multiple generations. In a set of two complementary studies, Jeje and colleagues treated lactating rats and pregnant rats with dexamethasone in order to assess the effect on the fertility of male F1 pups when they reached adulthood. When lactating mothers were treated daily for three weeks with dexamethasone and the nursing pups were subsequently allowed to reach twelve weeks of age, they noticed a significant decrease in sperm count and motility, along with a concomitant increase in the number of morphologically abnormal sperm (Jeje et al., 2016). The authors also observed a decrease in serum hormone levels, including testosterone, LH and FSH, which could have been a major contributor to the spermatogenic defects seen (Jeje et al., 2016). In their second study, the authors dosed pregnant females with dexamethasone during different windows of gestation, including early (gestational day (GD) 1-7), mid (GD 8-14), late (GD 15-21) or all of gestation (GD 1-21). They observed that dex during late or the entirety of gestation led to a variety of phenotypic effects in young pups, including decreased viability, decreased birth weight, decreased weight at weaning, decreased anogenital distance (AGD) at birth, and a delay in the onset of puberty as measured by preputial separation (Jeje and Raji, 2017). When these F1 offspring reached twelve weeks of age, the animals having received dex during late/all of gestation had significantly decreased

sperm motility as well as increased morphologically abnormal sperm (Jeje and Raji, 2017). Similar to the effect seen during dex treatment during lactation, they also observed that gestational dex led to a broad hormonal dysregulation in F1 adults, including decreased levels of testosterone and LH, and increased levels of GnRH and corticosterone (Jeje and Raji, 2017). Furthermore, when these dex-dosed F1 males were mated to control females, the majority of the F1 phenotypes were strikingly maintained in the F2 progeny, including decreased birth and weaning weight, decreased AGD, delayed puberty, decreased sperm counts, motility and quality, and broad hormonal dysregulation (Jeje and Raji, 2017). An independent study by Liu et al. dosing rats with dex from GD 9-20 confirmed many of these phenotypes, including dex-dependent decreases in testosterone and sperm count in both fetal and adult F1 males (Liu et al., 2018). They also saw decreased expression of many testosterone biosynthetic enzymes, which is likely due to the direct action of dex on the Leydig cells (Liu et al., 2018). This disruption of testosterone production in both pubertal and adult rats in response to gestational dex has also been confirmed elsewhere (PAGE et al., 2001), and is highly consistent with the known role of dex in inhibiting testosterone production in the adult testis (Bambino and Hsueh, 1981; Hales and Payne, 1989; Kavitha et al., 2006; Rengarajan and Balasubramanian, 2007; Rengarajan and Balasubramanian, 2008; SAEZ et al., 1977; Sankar et al., 2000).

Another group studying the effect of gestational betamethasone (another potent synthetic glucocorticoid agonist with high clinical relevance, similar to dex) in rats came to similar conclusions to Jeje and colleagues. In each of the following studies, a consistent dosing regimen was used: 0.1 mg/kg betamethasone delivered on GD 12, 13, 18, and 19. The effects of gestational betamethasone are evident immediately at birth, with pups from treated mothers showing a significant decrease in body weight that persists through early postnatal development (Barros et al., 2018; Borges et al., 2016). These pups show a delayed onset of puberty, as well as various testicular aberrations at puberty, including disruptions in hormone production

(increased LH and decreased testosterone) and defects in tubular morphology (Borges et al., 2016). These phenotypes are maintained into adulthood, at which point they display decreased sperm number (in both the testis and cauda epididymis), decreased motility, and increases in morphologically abnormal sperm (Borges et al., 2016; Borges et al., 2017a; Piffer et al., 2009). When these adult males from betamethasone-treated dams are used for natural mating as adults, they show decreased fertility, which the authors hypothesize is due to the higher rates of pre-implantation embryo loss and drop in fetal viability observed (Borges et al., 2016; Piffer et al., 2009). Quite strikingly, when F1 males from treated dams are mated to control females, many of these phenotypes are maintained into males of the F2 generation, including decreases in sperm number and motility, increased DNA damage, increases in sperm morphological defects, hormonal disruptions, and ultimately fertility impairment (Borges et al., 2017b). Furthermore, after seeing betamethasone-dependent decreases in testosterone production, the authors went on to assess whether gestational betamethasone impairs epididymal development, as testosterone is known to play an important role in regulating this process. They found that betamethasone treatment led to a delay in the differentiation of the epithelium of the cauda epididymis, and that this phenotype was maintained into the F2 generation (Kempinas et al., 2019).

Collectively, these two sets of studies show the rather dramatic effects of *in utero* exposure to synthetic glucocorticoids on fetal health, reproductive development, and future fertility across generations. These studies are of extreme relevance to human health, as both dexamethasone and betamethasone are commonly administered to pregnant women at risk of preterm birth in order to induce rapid lung maturation of the fetus. While this has been a life-saving intervention for many, it is imperative that we continue to study the adverse effects that these drugs may have on the reproductive system, especially as these effects may persist across many generations. Future fertility studies in adults that were subject to glucocorticoid exposure in the

womb will hopefully be able to give insight into the effects these drugs may have had, while also providing insights on relevant doses to minimize these effects in the future.

Effect of glucocorticoids on the ovary

Oocytes

Although various studies have attempted to elucidate the effects of glucocorticoid treatment on oocyte development and maturation, the results to date have been very contradictory. González et al. cultured *in vitro* fertilized mouse oocytes in varying concentrations of dex or corticosterone and saw that high levels of corticosterone resulted in significant decreases in fertilization rate and embryo cleavage, and a complete failure of embryos to mature to the blastocyst stage (González et al., 2010a). Surprisingly, however, dexamethasone did not show any of the same effects (González et al., 2010a). Tohei et al., however, suggested that dexamethasone had a stimulatory effect on follicle development, claiming that *in vivo* dex administration led to increases in the total number of oocytes ovulated in response to hCG treatment (Tohei et al., 2001). Wei and colleagues obtained directly contradictory results, in which they showed that 3-4 week old mice injected with corticosterone showed decreases in ovulation rates, along with decreases in ovarian weight, secondary and mature follicle number, estrogen and progesterone production, and expression of steroid biosynthesis genes (Wei et al., 2019). While Li and colleagues also showed detrimental effects of corticosterone treatment on fertility and implantation rates during pregnancy, they demonstrate that this is instead due to placental defects in the dam following corticosterone exposure, and not actually due to a defect in developmental competence of cort-dosed blastocysts. While it seems that the general consensus amongst the literature is that glucocorticoids are negatively impacting oocyte maturation, the underlying mechanisms by which this is occurring are still a mystery. To further

complicate things, there is very little (and highly conflicting) evidence for whether GR is expressed in the oocyte itself, making it even more difficult to untangle whether any of the effects seen are a result of direct action of glucocorticoids on the oocyte, indirect effects due to perturbations to surrounding somatic cells, or even more likely a combination thereof.

One phenotype that appears to be relatively consistent across studies is the ability of glucocorticoids to induce apoptosis in the oocyte. Yuan et al. demonstrated that a single dose of corticosterone to adult females was sufficient to increase expression of the pro-apoptotic Fas receptor in oocytes (Yuan et al., 2016), to activate TNF- α signaling in oocytes, as well as increase levels of reactive oxygen species (Yuan et al., 2020). The authors also showed that when GV-staged oocytes from corticosterone injected females were isolated and subjected to an *in vitro* maturation assay, the resulting embryos showed a significant decrease in their ability to reach the blastocyst stage, which the authors hypothesize is likely due to the increase in ROS and pro-apoptotic proteins (as well as influences from the surrounding ovarian somatic cells) (Yuan et al., 2020). In a similar *in vitro* maturation assay, Čikoš and colleagues showed that while both corticosterone and dex significantly and dose-dependently inhibit embryo maturation to the blastocyst stage, only dex-treated embryos, and not cort-treated embryos showed an increase in number of apoptotic cells. Similar experiments across many other species have yielded highly conflicting results with regards to the effects of dexamethasone and corticosterone on oocyte/embryo maturation (Andersen, 2003; Gong et al., 2017; González et al., 2010a; González et al., 2010b; Merris et al., 2007; Scarlet et al., 2017; Yang et al., 1999; Zhang et al., 2011), emphasizing the need for future studies analyzing the species-specific differences in response to glucocorticoid exposure. Lastly, while studies on human oocytes and early embryos are critically lacking, one study by Poulain et al. assessed the effect of glucocorticoid treatment on fetal ovarian samples. Human fetal ovaries ranging from GW 7.3 to 10.8 cultured for two weeks in the presence of dexamethasone showed a dose-dependent

increase in the number of cleaved-Caspase3⁺ germ cells (Poulain et al., 2012). As the number of total human oocytes does not expand after birth, it is crucial to understand how chemicals such as glucocorticoid that are commonly administered during gestation could potentially regulate processes such as apoptosis. Future studies examining how type, timing, and dose of difference glucocorticoids can influence fetal oocyte apoptosis, and thus lead to lasting effects on the ovarian reserve and reproductive longevity of the female, will be imperative moving forward.

Granulosa cells

Granulosa cells are one of the predominant somatic cell types of the ovary that provide growth factors and hormones (e.g. estrogen) which function to support oocytes during each stage of follicular development. There is considerably more consensus in the literature regarding the effect of glucocorticoid treatment on the granulosa cells. Both dexamethasone and corticosterone have been shown in a variety of studies to induce progesterone production in *in vitro* cultures of primary rat granulosa cells (ADASHI et al., 1981; Hsueh and Erickson, 1978; Kashino et al., 2021; Schoonmaker and Erickson, 1983; Yuan et al., 2014) as well as human granulosa cells (Sasson et al., 2001). This is likely due to glucocorticoid-induced increases in mRNA expression of enzymes required for progesterone production, including StAR, Cyp11a, and Hsd3b (Kashino et al., 2021; Yuan et al., 2014). Along with this increase in progesterone biosynthesis, many studies have also shown a simultaneous decrease in estrogen biosynthesis, which is likely due to repression of expression of the estrogen biosynthesis enzyme aromatase (Cyp19a1, P450arom) (Kashino et al., 2021; Schoonmaker and Erickson, 1983). Furthermore, dex seems to be able to act synergistically with FSH in order to induce the expression of progesterone (ADASHI et al., 1981) and tissue-type plasminogen activator (Xiao-Chi et al., 1990) in rat granulosa cells, emphasizing the importance in further exploring the combinatorial

effects that glucocorticoids may have with other gonadal and non-gonadal hormones. Additionally, Sasson et al. have demonstrated that glucocorticoid treatment also exerts an anti-apoptotic effect on granulosa cells through the regulation of Bcl-2 levels in cultured human granulosa cells. This is true for various apoptotic triggers, including serum deprivation, cAMP-induction, TNF- α activation, and p53 activation (Sasson and Amsterdam, 2003; Sasson et al., 2001). Moreover, this effect can be entirely reversed by co-administration with the GR antagonist RU486, suggesting that this effect is mediated by direct activity of GR in the granulosa cells (Sasson et al., 2001).

Corpus luteum

The corpus luteum (CL) is a structure that forms from both the granulosa and theca cells of a ruptured follicle following ovulation of the oocyte, and is a crucial structure for the production of the high levels of progesterone needed to maintain pregnancy (Stocco et al., 2007). Only a few studies to date have looked at the effects of glucocorticoids on the CL. Sugino et al. showed that when primary cultures of rat CL cells were cultured with corticosterone, there was a dose-dependent decrease in progesterone production in as little as six hours (Sugino et al., 1991). In an alternate study, Towns and colleagues performed *in vivo* injections of dex into female rats for four days, followed by dissection of ovaries and corpora lutea. They found that while dex had no effect on progesterone levels in the CL, dex did induce production of 20 α -dihydroprogesterone, a major progesterone metabolite produced by the CL (Towns et al., 1999). It is unclear whether the difference between these two studies could be due to the different glucocorticoids used, or whether something about the *in vivo* environment could have altered the response of the CL to glucocorticoid treatment.

Theca cells

Theca cells are one of the less well studied somatic cell types of the ovary, with their main function being to produce androgens as a substrate for estrogen biosynthesis in granulosa cells (Young and McNeilly, 2010). Only one paper could be found looking at the effect of dexamethasone treatment on primary theca cell cultures. While the authors claimed that dex treatment led to increased testosterone production (which they hypothesized was due to increases in Cyp17a1 and Cyp11a1 expression), the purity of their primary theca cell isolates was questionable (Ong et al., 2019). My personal data has shown that GR is robustly expressed in the theca cell layer of the adult mouse ovary (see Chapter 2), making this cell type a prime target for glucocorticoid activity, and thus an open area for future study.

Gestational glucocorticoid treatment and effects on female fertility

As already described for the male, gestational exposure to glucocorticoids has also been documented to have multiple detrimental effects on both ovarian development and reproductive function as an adult. Borges et al. demonstrated very clearly that administration of betamethasone to pregnant rats at GD 12, 13, 18 and 19 resulted in obvious phenotypic effects as early as postnatal day (PN) 1, showing a decrease in body weight and increase in anogenital distance of pups born to betamethasone-dosed dams (Borges et al., 2017c). These female pups displayed a delay in the onset of puberty, as measured by the day of vaginal opening and day of first estrous (Borges et al., 2017c). As adults, these mice showed increases in serum LH levels and disrupted estrous cycling, with increased cycle length and decreased number of cycles (Borges et al., 2017c). Furthermore, mating behavior and subsequent fertility tests showed decreased lordosis quotient, increased percentages of post-implantation embryo loss and resorption, and decreased fetal weight, further demonstrating the long term effects of

betamethasone exposure during crucial windows of development (Borges et al., 2017c).

Borges et al. also quantified the percentages of ovarian follicle subtypes in the ovary, and came to the conclusion that there was no change in the relative percentages of different follicles (Borges et al., 2017c). There appears to be considerable confusion amongst the literature as to whether glucocorticoid treatment influences the number and subtype distribution of different follicles, as many conflicting results have recently been published. Ristić and colleagues initially showed a decrease in follicle number when rats were dosed with dexamethasone from GD16-18 (RISTIĆ et al., 2008). However, they also observed a reduction in total ovarian volume (RISTIĆ et al., 2008; Ristić et al., 2019); when follicle numbers were normalized to volume estimates, this change was no longer significant (RISTIĆ et al., 2008), suggesting that the effect of dex on ovarian growth may indirectly lead to fewer germ cells. The authors do demonstrate an increase in apoptosis of oocytes by PN21 which may account for some of this decrease (Ristić et al., 2019). Hułas-Stasiak and colleagues published two seemingly conflicting papers in the spiny mouse *Acomys cahirinus*, using a model of fetal dex administration from GD20 to parturition. They first demonstrated that fetal dex exposure led to a decrease in folliculogenesis and a reduction in the total pool of healthy follicles (Hułas-Stasiak et al., 2015), although they later published a contradictory paper showing that dex treatment during the same window increased the total number of ovarian follicles (Hułas-Stasiak et al., 2017). Lastly, Gong and colleagues showed that prenatal dexamethasone in rats from GD 9 - 20 led to a decrease in the number of primordial follicles and an increase in the number of atretic follicles in ovaries of dex-exposed rats at eight weeks of age (Gong et al., 2021a; Gong et al., 2021b). Very impressively, when these F1 females were mated to control males, this phenotype of diminished ovarian reserve was maintained through to the unexposed F3 generation (Gong et al., 2021b; Gong et al., 2021a), showing that *in utero* exposure to dex can program the ovarian reserve for generations to come. The ambiguity of these studies is likely due to a multitude of factors,

including differences in dexamethasone dose, timing/duration of administration, and species to species variability. However, the striking results of Gong et al. showing the potential for lasting, transgenerational effects of gestational glucocorticoid exposure highlight the importance for more systematic studies to parse out timing and degree of susceptibility of ovarian folliculogenesis and follicular reserve number to glucocorticoid exposure.

Gong, Lv, and colleagues also uncovered many other phenotypes in addition to a decrease in follicle number. They observed that fetal exposure to dex led to decreased serum estradiol levels when the F1 progeny reached adulthood, and that this decrease was maintained transgenerationally through to the F3 generation (Gong et al., 2021b; Lv et al., 2018). This decrease in estradiol levels was likely due to decreased levels of ovarian cytochrome P450 aromatase, one of the key enzymes in estrogen biosynthesis, which was also observed to be lower in F3 progeny of fetally-exposed F1 females (Gong et al., 2021b; Lv et al., 2018). Expression of many other genes were altered in F1, F2, and F3 progeny consistently, including various steroidogenic enzymes, *Foxl2*, *Cdkn1b*, *Igf1*, *Runx2*, and a few miRNA genes (Gong et al., 2021a; Gong et al., 2021b; Lv et al., 2018). Many of the gene expression changes detected *in vivo* were recapitulated when human ovarian granulosa cells were dosed with dex *in vitro*, where the authors also confirmed these effects were dependent on GR signaling based on the ability of the GR antagonist RU486 to counteract these changes (Gong et al., 2021a; Gong et al., 2021b). These results collectively suggest that fetal dex exposure can lead to dynamic changes in gene expression and hormone production of the developing granulosa cells, indirectly decrease follicle number and the future ovarian reserve, and that these effects can be passed on to future unexposed generations.

Lastly, treatment with glucocorticoids during pregnancy not only affects the developing fetus as outlined above, but can also lead to complications in pregnancy due to alterations in maternal

uterine function. Li et al. showed that continued administration of corticosterone throughout mouse gestation led to pregnancy failure, with decreased implantation rates, and low survival of embryos past E13.5 (Li et al., 2018b). The authors hypothesize that this could be due to cort-induced impairments in the uterus of the dam, rather than an effect of corticosterone on the oocytes/blastocysts themselves. In a set of elegant cross-implantation experiments, the authors confirmed this by showing that blastocysts from corticosterone-treated moms could develop normally when transplanted to control mice, but control embryos could *not* develop when transplanted into the uterus of cort-treated females. This study provided a reminder for future studies of *in utero* glucocorticoid exposure that maternal effect of glucocorticoid administration cannot be ignored, and all potential effects on both maternal and fetal health should be carefully considered when assessing phenotypic outcomes.

1.4 - Transgenerational Inheritance Of Stress-Induced Phenotypes

A growing body of work has demonstrated that stress can lead to lasting effects across multiple generations, even in generations unexposed to the initial stressor. When phenotypic effects are passed on to the direct offspring (F1) of stressed parents (F0), this is known as multi- or intergenerational inheritance; when phenotypes persist to additional unexposed generations, this is defined as transgenerational inheritance. For males and *non-pregnant* females, characterization of the F2 generation is thus sufficient to confirm transgenerational transmission. However, in cases where pregnant females are exposed to stress, transgenerational inheritance can only be confirmed in the F3 generation, due to the fact that the developing fetus (F1) and its developing germline (F2) are all exposed to the stressor. There is now an abundance of research showing that environmental exposure to a wide range of chemicals, environmental toxicants, dietary abnormalities, smoking, alcohol, psychological stress, drought, and heat stress can lead to transgenerational inheritance of diseases from humans to plants to many animals in between. This work has been reviewed extensively elsewhere (Nilsson et al., 2018), and I will thus focus on examples from the literature highlighting transgenerational effects of physiologic/traumatic stress in rodent models.

The past decade of research studying the transgenerational heritability of stress-induced phenotypic outcomes has revealed a propensity for behavioral and neurologic impairments in the offspring of stressed animals. These studies have collectively produced considerable variability in results, and have therefore highlighted that stress-induced phenotypic inheritance can vary considerably between (a) sex of the offspring, (b) the lineage through which the stress phenotype is passed (i.e. paternal vs maternal transmission), and (c) the type of stress regimen that is employed, including duration/chronicity of stress and the type of stress employed (i.e.

social vs non-social). In a comparative experiment, He and colleagues demonstrated that while models of restraint stress and social instability stress both lead to transgenerational transmission of anxiety-like phenotypes to the F2 offspring, restraint stress led to a heritable reduction in anxiety whereas social stress led to a heritable increase in offspring anxiety (He et al., 2016). These seemingly contradictory results emphasize that caution should be taken when comparing phenotypic effects across studies utilizing entirely different models of stress.

Changes in depression- and anxiety-like behaviors are a common phenotype observed in F1 and downstream offspring of stressed parents. Multiple independent studies have concluded that stress induces depressive-like symptoms in F1 and F2 offspring as measured by forced swim, tail suspension, and sucrose consumption tests (Franklin et al., 2010; Gapp et al., 2014; Wu et al., 2017). These studies encompassed various stress paradigms, including a model of chronic unpredictable maternal separation combined with maternal restraint or forced swim stress (collectively referred to as the MSUS stress model) (Franklin et al., 2010; Gapp et al., 2014; Wu et al., 2017), and a model of chronic stress that included alternating restraint and bright illumination stress (Wu et al., 2017). These converging results obtained using different stress models bolsters the idea that stress can broadly induce depression-like symptoms across generations. Furthermore, the fact that phenotypic transmission was limited to the paternal line in all three of these studies supports an involvement in epigenetic transmission of information through the sperm, which will be discussed more below. While the ability of stress to induce anxiety-like behaviors across generations has been clearly demonstrated across multiple studies, differing stress models have shown considerable variation in how these symptoms are manifested. In models of MSUS, F1 males that were exposed to stress during early postnatal development sire F2 and F3 offspring that show increased social anxiety as measured by time spent investigating novel mice (Franklin et al., 2011). Surprisingly, while these MSUS offspring mice show increased *social* anxiety, they conversely show reduced anxiety in terms of risk

aversion and risk assessment, with reduced rates of novel environment fear/avoidance (Gapp et al., 2014; Weiss et al., 2011). Other studies have also demonstrated that social anxiety and impaired socialization behaviors are not limited to MSUS stress models. Using a chronic social instability stress model, Saavedra-Rodríguez and colleagues demonstrated a heritable increase in social anxiety and loss of preference for novel social interactions that persisted across two generations (Saavedra-Rodríguez and Feig, 2013). While this effect of chronic *social* stress has been confirmed by other groups to lead to a transgenerationally heritable decrease in socialization behavior (Babb et al., 2014), other studies of chronic *non-social* stress have shown a converse reduction in anxiety in F2 mice (Manners et al., 2019). These examples collectively emphasize that the type of stress experienced has a large impact on the presentation of behavioral phenotypes and their heritability.

In addition to behavioral changes, stress has also been linked to changes in brain function that can be inherited across generations. Memory impairments have been documented in studies of offspring sired from F1 mice stressed with the MSUS stress model described above. F2 and F3 females have shown impaired social, yet not olfactory, memory that is accompanied by impaired serotonergic signaling in the brain (Franklin et al., 2011). F2 offspring also demonstrated impaired fear memory and object recognition memory, and microarray analysis on the hippocampi of F2 mice revealed downregulation of genes required for maintaining synaptic plasticity as a potential causative factor (Bohacek et al., 2015). Furthermore, offspring from MSUS-stressed mice have shown altered brain metabolism in the prefrontal cortex, with stress-induced reductions in metabolites required for neurotransmitter biosynthesis (Gapp et al., 2016), as well as a decline in functional neural connectivity across generations as measured by functional MRI (Razoux et al., 2017). These heritable alterations to brain function are also accompanied by changes to gene expression and epigenetic marks, including altered F2 hippocampal miRNA expression (Gapp et al., 2014) and select gene promoter DNA methylation

(Bohacek et al., 2015; Franklin et al., 2010). Heritable deficiencies in Notch and Akt/mTOR signaling have also been found in the amygdala and hippocampus, respectively, in models of chronic unpredictable stress (Manners et al., 2019; Wu et al., 2017).

Some of these behavioral and neurologic phenotypes have also been recapitulated by other groups through the direct administration of synthetic glucocorticoids to create an artificially exacerbated state of stress. Short and colleagues administered corticosterone to mice for four weeks and demonstrated that corticosterone dosed fathers showed an increase in both anxiety and depressive behaviors that were passed on to F2 offspring (Short et al., 2016). They further showed that sperm from corticosterone treated males had altered miRNA content, which they suggested could be a potential mechanism for the transmission of this phenotype. Moisiadis and colleagues also observed an anxiety-like phenotype in guinea pigs dosed with the synthetic glucocorticoid, betamethasone. They found enhanced HPA axis activation and hyperactivity in response to stress that could be passed strictly through the paternal lineage to F1 through F3 females (Moisiadis et al., 2017). This was accompanied by changes in gene expression in the PVN, prefrontal cortex, and hippocampus that were consistently inherited in female offspring of betamethasone dosed males (Constantinof et al., 2019a; Constantinof et al., 2019b; Moisiadis et al., 2017). These studies have suggested that elevated levels of glucocorticoids alone may be sufficient to lead to heritable behavioral and neurological phenotypes.

As the germ cells of the male and female gonad are the cells responsible for carrying genetic information across generations, it is safe to assume that some type of epigenetic alterations must be occurring within the germ cells in response to stress in order for these phenotypic outcomes to persist transgenerationally. The more pronounced transmission of stress-induced phenotypes through the paternal lineage in many of the studies highlighted above has led to the hypothesis that epigenetic changes to the sperm are a likely causative factor in

transgenerational transmission of these stress-induced effects. Some studies have shown that stress can induce changes in DNA methylation at the promoters of select genes within sperm, and these methylation changes can be passed on and similarly altered in the brains of offspring (Bohacek et al., 2015; Franklin et al., 2010). While these limited examples of stress-induced changes in DNA methylation do exist, the field is shifting away from DNA methylation as a causative factor in transgenerational inheritance, particularly due to the fact that the mammalian germline undergoes global DNA demethylation during primordial germ cell development, which wipes away the majority of genomic methylation between generations (with the exception of a few key imprinted regions). Similarly, while post-translational modification of histone proteins is another canonical form of epigenetic regulation, the replacement of the vast majority of histones with protamines during spermatogenesis likely precludes histone modifications from being a major driver of transgenerational inheritance.

There is now a growing body of evidence, however, that stress-induced regulation of small non-coding RNA expression within the sperm is potentially a major mechanism through which the stress-induced phenotypes described above can be transmitted across generations. Two groups in particular have now demonstrated a causal link between miRNA disruption and transgenerational inheritance following stress. Rodgers and colleagues demonstrated that six weeks of chronic unpredictable stress experienced during either puberty or adulthood yielded male mice with significantly altered sperm miRNA content (Rodgers et al., 2013). The predicted targets of these miRNAs included genes with known roles in the regulation of chromatin, DNA methylation and miRNA processing, suggesting that these stress-induced miRNAs may play key roles in regulating the epigenetic landscape of the developing embryo following fertilization. Strikingly, when a combination of nine of these stress-induced miRNAs was injected into a control fertilized zygote, this miRNA cocktail alone was sufficient to recapitulate the HPA axis dysregulation phenotype they observed in their stress model (Rodgers et al., 2015). Gapp and

colleagues came to a very similar set of results using their MSUS stress model. They detected disrupted miRNA expression in the sperm of F1 stressed males, and these miRNAs were similarly disrupted in the brains of their F2 progeny (Gapp et al., 2014). When they isolated miRNAs directly from sperm of F1 stressed males and injected them into control fertilized oocytes, they found this was sufficient to phenocopy the behavioral and molecular effects of their MSUS stress model (Gapp et al., 2014). The same group also showed that stress could induce changes in long non-coding RNA content in addition to miRNAs (Gapp et al., 2020). When RNA from the sperm of stressed males was isolated, fractionated based on size, and injected into fertilized oocytes, the authors uncovered that different sized RNA molecules were able to induce different subsets of the overall stress phenotype (Gapp et al., 2020). The authors went on to recently show that a single administration of glucocorticoids (in this case dexamethasone) was sufficient to alter non-coding RNA production in sperm, and also implicated tRNA fragments and circular RNA molecules as potential novel RNA subtypes that may mediate downstream phenotypic effects of stress (Gapp et al., 2021). Taken together these studies suggest that various subtypes of non-coding RNAs may be altered in sperm in response to stress, and that they may act together to produce phenotypic outcomes that can persist across generations.

Given that glucocorticoid treatment is sufficient to phenocopy the transgenerational inheritance of stress induced behavioral changes (Moisiadis et al., 2017; Short et al., 2016), as well as alter the non-coding RNA content of the sperm (Gapp et al., 2021), it is not a stretch to imagine that these effects may be mediated by the glucocorticoid receptor. It is still unclear whether the effects seen could be due to (a) actions of glucocorticoids on GR in the somatic cells of the gonad, leading to indirect regulation of the germline, (b) direct actions of glucocorticoids on GR expressed by the germ cells, or (c) broad disruption of hormonal regulation in the body leading to indirect influences on the germline. A central question of my thesis has been to determine

whether GR is expressed in the mammalian germ cells during development or adulthood, and if so, what function it may be having to regulate the germline's response to stress. The following sections of this introduction will highlight what is known about expression of the glucocorticoid receptor within both the testis and the ovary, as well as attempts to understand its functional role within the cells of the gonad using genetic knockout models.

1.5 - GR Expression in the Testis

Expression of the glucocorticoid receptor in the rodent testis was first reported as early as 1974 (BALLARD et al., 1974) based on the ability of whole rat testis lysate to bind radioactive dexamethasone. Shortly after, similar radioactive binding assays revealed GR binding activity in both cytoplasmic and nuclear fractions of both seminiferous tubule cells and interstitial cells, with more robust binding by GR in the interstitial compartment (Evain et al., 1976). It was not until 1987 that the GR transcript was first definitively detected by northern blot analysis of whole testis lysate (Kalinyak et al., 1987). Further analysis of GR transcript revealed cell type specific expression in both the Sertoli cells and peritubular myoid cells of the rat testis, as well as an age-related decline in GR transcript over the first 60 days of postnatal development (LEVY et al., 1989). When cultured in the presence of dexamethasone, these Sertoli cells exhibited a dose-dependent change in select gene expression, suggesting active GR signaling in the testis for the first time (LEVY et al., 1989).

Since then, various studies attempting to characterize the cell type-specific expression of GR in the testis have led to conflicting results. The first immunocytochemistry stain for GR in rat testis revealed strong GR expression in the Leydig cells of the interstitium, as well as weaker staining in the seminiferous tubules (Stalker et al., 1989). *In vivo* administration of radiolabeled dex followed by quantitative radiography confirmed highest label retention (i.e. highest GR expression) in the Leydig cell compartment, and to a lesser extent within the seminiferous tubules (Stalker et al., 1989). Schultz et al. detected a strong nuclear localization of GR in Leydig cells, some peritubular myoid cells, some endothelial cells, and primary spermatocytes – yet notably not in Sertoli cells (Schultz et al., 1993). Biagini et al. confirmed staining in Leydig cells, peritubular cells, and some primary spermatocytes, but also saw staining in Sertoli cells

and spermatogonia (Biagini and Pich, 2002). Weber et al. assessed GR staining in postnatal, rather than adult testes, and saw very weak staining in Leydig cells, peritubular cells, primary spermatocytes, spermatogonia, and a few Sertoli cells (Weber et al., 2000). The differences seen are likely due to differences in epitopes recognized by the different antibodies used, and/or differences in tissue preparation. Furthermore, work by Hazra et al. demonstrated that GR expression in each cell type may vary as a function of developmental time. While GR expression in the Leydig and peritubular myoid cells seemed consistent between postnatal day 20 (PN20) and adult testes, expression in the Sertoli cells seen at PN20 was completely absent by adulthood, which might explain the conflicting results on Sertoli cell GR expression in the literature (Hazra et al., 2014). It is entirely possible that GR expression in the spermatogenic cell types of the testis might also vary with developmental time or spermatogenic tubule stage, which could also explain conflicting results in the literature thus far. My thesis work, as described below, will attempt to clarify this ambiguity.

A handful of studies have also attempted to characterize GR expression in the human testis. Nordkap and colleagues performed IHC for GR in adult human testis, and saw strong staining in the somatic compartment of the testis, including Leydig and peritubular myoid cells, as well as endothelial and smooth muscle cells of blood vessels (Nordkap et al., 2017). Within the seminiferous tubules, the authors noticed very heterogeneous expression of GR amongst the germ cells, with very high expression in the type B and A pale (A_p) differentiating spermatogonia, very low expression in pachytene spermatocytes, and virtually no expression in spermatids, spermatozoa, and the most undifferentiated type A dark (A_d) spermatogonia (Nordkap et al., 2017). The authors also performed IHC for GR on fetal human testis tissue, in which they saw staining in the undifferentiated interstitial compartment at gestational week (GW) 10 and GW14 and subsequent fetal Leydig cells by GW20. GR expression was not seen in the germ cells until the pre-spermatogonia stage of GW20, although staining was sporadic. Very

interestingly, GR expression in the Sertoli cells of the human showed a developmental stage-dependent change very similar to that seen in the mouse testis by Hazra et al. (Hazra et al., 2014). GR expression could be seen in Sertoli cells starting at GW20, although was absent from the adult Sertoli cells, suggesting a similar perinatal window of expression for GR in the human Sertoli cell (Nordkap et al., 2017). In another study, Welter et al. performed IHC for GR on biopsies of human testicular tissue from patients with obstructive azoospermia (but normal spermatogenesis) and found a strikingly similar pattern of GR expression to Nordkap and colleagues, with the only notable exception being positive staining for GR in the adult Sertoli cells (Welter et al., 2020). Lastly the Human Protein Atlas ([proteinatlas.org](https://www.proteinatlas.org)) also has publicly available IHC data for GR in various ages of adult testis (Uhlén et al., 2015). This data strongly corroborates the result of Nordkap et al. for all ages, with again the only exception being positive staining in the Sertoli cells. Taken together, it is clear that GR is expressed in the Leydig cells, peritubular cells, and differentiating spermatogonia of the human testis, and is markedly lower or absent from the spermatocytes and spermatids. Further studies, perhaps with a much larger cohort of human samples, will be needed to confirm or refute the presence of GR in the Sertoli cells.

1.6 - GR Expression in the Ovary

While a fair amount of data exists showing GR expression in the male - particularly IHC showing cell type specific localization of GR - there is considerably less literature regarding GR expression in the different cell types of the ovary.

The first evidence for GR expression in the rodent ovary was reported in 1982 by Schreiber and colleagues using a traditional biochemical receptor-binding assay approach (Schreiber et al., 1982). Similar to early studies in the male (BALLARD et al., 1974), a radioactive, synthetic, GR-specific ligand - in this case ^3H -dexamethasone - was shown to bind to cytosolic lysate of total rat ovary, strongly suggesting the presence of GR in at least one cell type of the ovary (Schreiber et al., 1982). It was not until almost seventeen years later that GR transcript was confirmed to be expressed in the rat ovary. Using an RNase protection assay, Tetsuka et al. demonstrated that GR transcript was present in isolated granulosa cells, isolated corpora lutea, as well as residual ovarian cells post isolation of other cell types (Tetsuka et al., 1999). They further showed that GR transcript was highest in corpus luteum cells in comparison to the other populations observed (Tetsuka et al., 1999). At the same time, Towns et al. independently confirmed this result, showing by Western blot that GR protein was present in both rat corpus luteum cytosol, as well as non-luteal ovarian cytosol (Towns et al., 1999). More recently, single cell RNA-sequencing of the fetal mouse ovary has revealed that GR is expressed in the developing mouse germline, and steadily increases in expression from E12.5 to E14.5 (Ge et al., 2021). The same group also confirmed GR protein expression between E12.5 and E14.5 in dissociated and plated fetal germ cells, although information about staining in the fetal somatic cells was not provided (Ge et al., 2021).

To the best of our knowledge, the only examples of IHC for GR in whole ovarian sections have been in non-rodent mammalian systems. In bovine ovaries, Amweg et al. showed by both qPCR and IHC that GR is present in both the granulosa cell and theca interna layer of all ovarian follicle stages observed (Amweg et al., 2016). This result was consistent with an earlier study in bovine ovaries that showed by qPCR that GR was expressed in both granulosa and theca cells, although to a much higher extent in the theca cell layer (TETSUKA et al., 2010). Pontes and colleagues performed IHC for GR in caprine ovarian tissue, with results that differed from rodent and bovine models. While GR was seen relatively consistently in the granulosa cells irrespective of follicular stage, expression in the theca interna seemed to vary by stage - with high expression in theca cells surrounding antral follicles, but low to absent expression in more immature follicle stages (Pontes et al., 2019). Surprisingly, they also saw GR expression in the oocyte of primordial and antral follicles, which had not been seen in any other study (Pontes et al., 2019). It is unclear whether these differences seen are due to species specific differences in GR expression or due to differences in sample preparation and/or quality.

In particular, there is very little evidence in the literature directly confirming the expression of GR in the human ovary. One study by Poulain et al. performed qPCR for GR in bulk human fetal ovary samples ranging from GW6 to GW22 and found that GR was expressed at all stages observed, with a peak in expression at GW14.5 (Poulain et al., 2012). The authors confirmed that the GR transcript expressed was exclusively the active GR α isoform, and not the GR β inhibitory isoform (Poulain et al., 2012). They also performed IHC in a GW9.2 ovary and saw GR expression in both the fetal germ and somatic cells, although they noted that expression was quite heterogeneous across the tissue (Poulain et al., 2012). Additional work is needed to confirm whether this fetal expression of GR is maintained into adulthood, particularly whether GR expression is maintained in the oocyte of the adult. Based on conserved expression in the

granulosa, theca and corpus luteum cells across species, it is likely that a similar pattern of expression will be seen in the human ovary.

1.7 - Genetic Deletion of GR in the Gonad

A considerable amount of research over the past 20 years has gone into understanding the widespread, pleiotropic effects of GR in differing cell types across the body. The first ever targeted genetic deletion of GR in 1995 revealed an essential role for GR in fetal and perinatal development of multiple organ systems (Cole et al., 1995). Homozygous deletion of GR resulted in lethality at birth, due predominantly to severe defects in alveolar maturation, with defects in the lung seen as early as E15.5 (Cole et al., 1995). In addition, knockout embryos showed defects in multiple additional organs, including impaired activation of many gluconeogenic enzymes in the liver, severe hypertrophy of the adrenal cortex, complete failure of the adrenal medulla to produce catecholamines at birth, and broad disruption of the HPA axis, with highly elevated levels of cortisol and ACTH at birth (Cole et al., 1995). While one group attempted to circumvent this lethality by generating a mouse line with transgenic overexpression of GR in the distal alveolar lung epithelium (in the background of a GR null mouse), they were ultimately unable to fully prevent respiratory failure, which they postulate was likely due to a lack of GR in all other cell types of the proximal airway and mesenchyme (Gagnon et al., 2006). The multi-systemic effects of loss of GR have therefore made it impossible to study the effects of full body deletion of GR into adulthood, including whether loss of GR has any effect on fertility and reproduction.

To circumvent the widespread phenotypic consequences of full body GR deletion and therefore study the role of GR in adulthood, various conditional genetic deletion models of GR have been created (reviewed extensively in Whirlledge et al. (Whirlledge and DeFranco, 2018)). In all cases, mice containing Cre recombinase driven by a tissue specific promoter have been crossed to one of four floxed conditional GR alleles (Brewer et al., 2003; Jeanneteau et al.,

2012; Oakley et al., 2013; Tronche et al., 1999). The most commonly utilized floxed allele (including in our own work below) has become the allele generated in Tronche et al. (Tronche et al., 1999), in which exon 3 (encoding a large portion of the GR DNA binding domain) is flanked by loxP sites. Comparative studies using the same Sim1-Cre model to delete GR specifically from the paraventricular nucleus (PVN) of the hypothalamus demonstrated that exon 3 deletion was sufficient to reduce GR expression by 90% and elicit robust metabolic phenotypes, whereas exon 1C/2 deletion using a different floxed allele was unable to recapitulate this phenotype (Jeanneteau et al., 2012; Laryea et al., 2013; Tronche et al., 1999). One possible explanation for this difference could be that GR has many alternative translation start sites throughout the exon 2 encoded N-terminal domain of GR, which can result in truncated proteins outside of the deletion region that retain some function (Lu and Cidlowski, 2005).

In the context of the reproductive system, only a few studies to date have employed conditional knockout models to study the role of GR in the reproductive tissues of the adult. In the female, deletion of GR from the uterus using a progesterone receptor (PR)-driven Cre led to subfertility, with reduced litter size, impaired uterine implantation, and impaired decidualization of the endometrial stroma (Whirledge et al., 2015). However, to the best of our knowledge, there have been no studies to date deleting GR from any of the cell types of the ovary.

In the male, only one study currently exists examining the conditional deletion of GR from the testis. Hazra and colleagues utilized an Amh-Cre mouse model to delete GR specifically from early postnatal Sertoli cells (Hazra et al., 2014). They found that while GR is only expressed in the Sertoli cells for a brief period of postnatal development, deletion of GR during this window led to lasting phenotypic consequences in the adult testis. Conditional knockout mice demonstrated decreased expression of canonical GR response genes, impaired seminiferous tubule lumen morphology, Leydig cell hypertrophy and lipid accumulation, as well as decreased

levels of serum gonadotropins and decreased testicular hormone synthesis (Hazra et al., 2014). This study highlights both an importance for GR specific in Sertoli cells for proper steroidogenesis in the adult, as well as an example of a developmental role for GR that can have prolonged consequences in adult testicular homeostasis.

There is still a considerable gap in the field in understanding the cell-intrinsic roles of GR in the additional cell types of both the ovary and the testis. In the testis, there is considerable consensus amongst the literature across many species that GR is highly expressed in the Leydig cells and peritubular myoid cells of the adult testis. Although there is a wealth of data supporting that high levels of glucocorticoids can directly inhibit testosterone production in Leydig cells (reviewed extensively elsewhere (Hu et al., 2008; Whirledge and Cidlowski, 2010)), conditional deletion of GR from the Leydig cell to assess the role of GR under physiologic (non-stressed) conditions has yet to be performed. The function of GR in the peritubular myoid cell is also unclear, also lacking any functional deletion studies. However, one recent study on human peritubular cells cultured *in vitro* with and without dexamethasone demonstrated a dex-dependent increase in extracellular matrix production and cellular contractility (Welter et al., 2020). The authors suggest that normal GR activity in the peritubular myoid compartment may promote the proper contractility of the seminiferous tubules and subsequent migration of spermatozoa through the testis, although further *in vivo* validation would be needed to confirm this hypothesis. Lastly, the question of whether GR plays any functional role in the germ cells of either the ovary or testis remains completely unexplored. As described above, the expression of GR in the adult oocyte remains very unclear, and has been limited to a sole study in caprine ovaries (Pontes et al., 2019). The expression of GR in the spermatogenic lineage of the mouse has varied considerably between studies. My work, as explained below, has aimed to address these questions of whether GR is expressed in the mammalian germ cells of both the ovary and testis, and whether GR may play any role in the proper formation and function of the germline.

While the lethality of global GR knockout has prevented fertility studies in rodent models, two independent groups have produced viable zebrafish with a genetic deletion of GR, which have proven to be an exciting novel model for studying the role of GR in fertility (Facchinello et al., 2017; Faught and Vijayan, 2018). Facchinello and colleagues demonstrated that while GR knockout fish were viable and fertile during early life, their reproductive capacity dropped by approximately 10 months of age (Facchinello et al., 2017). This group further went on to show that while ovarian morphology of GR knockout fish appeared normal, they displayed a subfertility phenotype characterized by decreased number of eggs laid and decreased egg fertilization rate (Maradonna et al., 2020). Faught and colleagues independently came to very similar results, in which they identified an age-dependent decline in female fertility between 9 and 12 months of age (Faught et al., 2020). Aged GR knockout fish showed a variety of reproductive defects, including decreased spawning frequency, decreased fecundity, and a decrease in the number of embryos fertilized per clutch (Faught et al., 2020). Furthermore, the embryos produced from these GR knockout fish demonstrated pronounced developmental defects including delayed somitogenesis and a mere 20% survival rate in the first 24 hours post fertilization (Faught et al., 2020).

While these zebrafish models have revealed important insight into a role for GR in regulating vertebrate fertility, it is difficult to untangle the exact mechanism by which loss of GR leads to subfertility in the fish. Global deletion of GR in the mouse embryo has been shown to lead to broad disruptions in the HPA axis, including elevated serum glucocorticoid levels (Cole et al., 1995), which was also seen in both GR knockout fish models (Facchinello et al., 2017; Faught and Vijayan, 2018). It is possible that loss of GR from the neurons of the hypothalamus and pituitary could lead to more broad disruptions in the production of other non-glucocorticoid hormones, especially gonadotropin hormones, which could indirectly influence fertility. Faught

and colleagues also point out that in GR knockout fish with high levels of circulating cortisol, intact mineralocorticoid receptor (a highly similar hormone receptor with cortisol-binding activity) may lead to functional glucocorticoid-dependent signaling even in the absence of GR. Altogether while these two studies have clearly shown a role for GR in regulating fertility and ovarian aging, additional functional studies will be needed in order to carefully dissect the tissue specific roles of GR in regulating the complex process of reproduction.

Chapter 2 - Sexually Dimorphic Roles of Glucocorticoid Receptor Signaling in the Mammalian Germline

2.1 - Introduction

The negative effects of stress on mammalian reproductive capacity have long been appreciated. The hypothesis that stress not only influences an adult's ability to conceive, but may also impact the health of their offspring has gained considerable attention amongst the scientific community in recent years. A growing body of work in recent years has very clearly demonstrated that rodent models of stress can induce a variety of neurologic and behavioral phenotypes that are able to persist across generations (reviewed extensively in Chapter 1). The persistence of such phenotypes for up to three generations suggests that stress signals can induce lasting epigenetic changes in the germline. As the committed precursors of eggs and sperm established during early embryogenesis, fetal germ cells are responsible for transmitting genetic information across generations. Any perturbations to the proper transmission of this genetic information can be detrimental, and thus understanding the mechanism by which stress can lead to epigenetic alterations in the germline remains a crucial unanswered question.

Interestingly, the results of some research groups have found that treatment of rodents with natural or synthetic glucocorticoid stress hormones is sufficient to recapitulate the transgenerational phenotypic inheritance seen in stress models. These hormones are known to bind and activate receptors such as the glucocorticoid receptor (GR), thus implicating GR-mediated signaling as an important piece in transgenerational inheritance of stress.

GR is a member of the nuclear hormone receptor family, and is encoded by the *Nr3c1* gene. Binding of GR to its ligand in the cytoplasm promotes receptor translocation into the nucleus where it then binds response elements and recruits transcriptional cofactors to modulate target

gene expression. As such, GR functions as a ligand-inducible transcription factor, allowing for robust changes to gene expression in response to stress hormones. While GR was shown to be a potent transcriptional regulator in a wide variety of cell types, its function in the cells of the gonad remains less clear. We were particularly interested in the question of whether GR is expressed within the germ cells of the developing or adult gonads, and whether it may therefore render the germline susceptible to direct cell-intrinsic actions of glucocorticoid hormones. As GR is known to interact with many epigenetic modifying enzymes, we hypothesized that glucocorticoid hormones could act directly on germ cells to activate GR-signaling, thereby triggering epigenetic modifications that could explain the heritable stress-induced phenotypes observed.

At the onset of this study, evidence for GR expression in the germ cells was fairly sparse. In the mouse testis, one study suggested GR expression was limited to primary spermatocytes (Schultz et al., 1993), while others suggested that GR is expressed in both spermatogonia as well as spermatocytes (Biagini and Pich, 2002; Weber et al., 2000). In humans, multiple studies have shown that GR is highly expressed in differentiating spermatogonia, as well as lowly expressed in primary spermatocytes (Nordkap et al., 2017; Welter et al., 2020), consistent with some of the mouse studies. In the female, however, considerably less is known. To the best of our knowledge, there is no immunohistochemical evidence for GR expression in the oocytes of adult rodent or human ovaries. A single study of the human fetal ovary found evidence for GR expression by IHC in the oocytes of a nine week old embryo (Poulain et al., 2012), although the authors noted that expression was quite heterogeneous across the tissue. A more recent study of mouse fetal oocyte development using single cell RNA-sequencing revealed increasing expression of GR in the oocytes between E12.5 to E14.5 (Ge et al., 2021). Taken together this data suggested that GR may be expressed in the rodent / human germline, but in limited developmental windows.

Furthermore, no studies to date have directly assessed the cell-intrinsic role of GR in the germ cells using standard conditional knockout genetic models. While there are many studies showing a variety of defects to the male and female germline in response to glucocorticoid treatment (reviewed extensively in Chapter 1), it is unclear whether the phenotypes observed are due to the direct action of glucocorticoids on germ cells, or the indirect effects of systemic glucocorticoid treatment on gonadal somatic cells and/or hormone producing cells of the hypothalamus and pituitary.

We therefore set out to definitively characterize the expression of GR in the germline of the developing and adult gonads, and to determine what is the cell-intrinsic role of GR in normal germline formation and function. We discovered that GR is expressed in the female germline during fetal development, yet is absent from the adult oocyte. We demonstrated that the female germline is, surprisingly, resistant to changes in GR signaling. Both genetic deletion of GR, as well as GR agonism with dexamethasone (dex), revealed minimal transcriptional changes in the female germline, as well as no significant changes in meiotic progression, suggesting the female germline is intrinsically buffered from changes in GR signaling. In contrast we find that GR is expressed in the male germline during the final days of development, with expression maintained in pro-spermatogonia during early postnatal development. This expression becomes restricted to the spermatogonia of the adult, and transcriptomic analysis of germ cells from dex-treated males reveals a potential role of GR in regulating RNA splicing. Together our data confirm GR expression in both the male and female, and suggest a sexually dimorphic action for this receptor in the mammalian germline.

2.2 - Spatiotemporal expression of the glucocorticoid receptor in the female germline

To first assess whether GR is expressed in the developing female germline, we performed immunofluorescent staining on mouse fetal ovaries ranging from E12.5 through E18.5. Female germ cells, marked by either Oct4-GFP (*Pou5f1-ΔPE-eGFP* transgene) or Tra98, showed robust expression of GR starting at E13.5, which waned as development progressed (**Figure 2.1A**). The majority of GR-expressing germ cells showed nuclear localization, irrespective of developmental stage, suggesting that GR may be functioning as a transcription factor within the female germline. (**Figure 2.1B**). To quantify GR expression dynamics more carefully, we utilized the Imaris Image Analysis Software to obtain DAPI-normalized GR expression levels at the individual cell level. Sections were stained with wheat germ agglutinin (WGA) to mark cellular membranes, individual cells segmented using the Imaris's Cell module, and then germ cells were computationally distinguished based on relative expression of the germ cell markers Oct4-GFP or Tra98 (**Figure 2.1C**). These studies confirmed that GR expression in the germline decreased from E13.5 to E18.5 (**Figure 2.1D**).

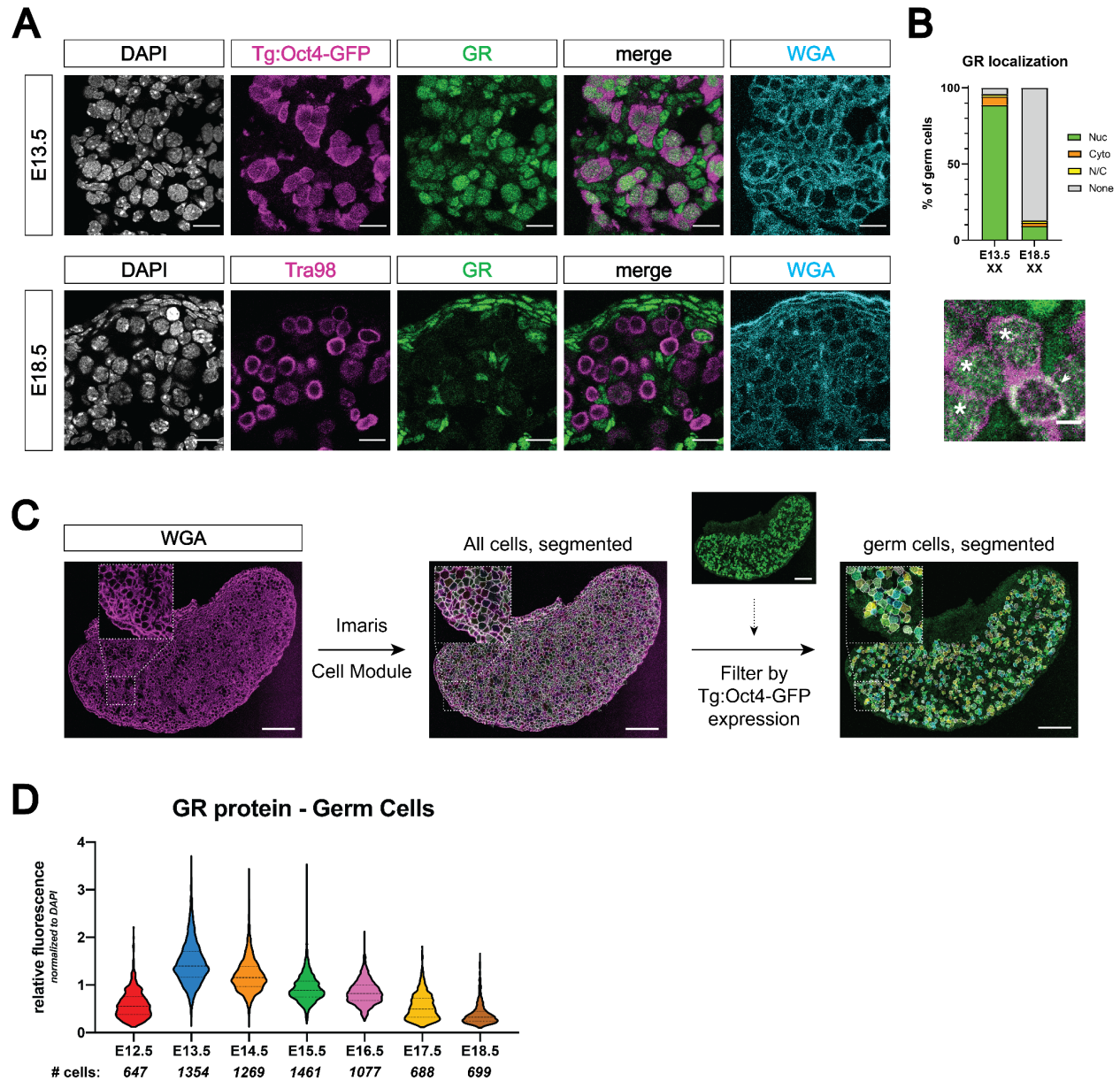


Figure 2.1 - Expression of the glucocorticoid receptor in the developing female germline

(A) IF staining showing expression of GR in mouse fetal ovary sections at E13.5 (top) and E18.5 (bottom), counterstained with DAPI. Germ cells are marked by either transgenic Oct4-GFP or Tra98. Cellular membranes were stained with wheat germ agglutinin (WGA) to facilitate computational segmentation of individual cells. Scale bars: 15 μ m.

(B) Quantification of GR subcellular localization within germ cells, scored manually (top). Zoomed in image showing examples of both nuclear (asterisk) and cytoplasmic (arrowhead) GR staining (bottom). Scale bar: 5 μ m.

(C) Representative images of computational cell segmentation using Imaris's Cell module. WGA was used to stain all cellular membranes, and expression of a germ cell marker (here Oct4-GFP) was used in order to filter out germ cells from somatic cells. Scale bars: 100 μ m.

(D) Quantitative IF analysis of relative GR protein expression in the germ cells across developmental time. Individual cells were computationally segmented using WGA, and GR protein levels were normalized to DAPI on an individual cell basis. Images and total cell numbers counted were obtained from a minimum of three ovaries from independent biological replicates at each developmental stage.

We next performed IF during the early postnatal window to assess if any germline expression of GR is maintained after birth. Staining at PN0 revealed a very small number of oocytes at the cortex of the ovary with nuclear GR, although by PN2 GR expression was virtually absent (apart from a few sporadic cortical oocytes with cytoplasmic GR) (**Figure 2.2A**). By PN5, GR expression was absent from all oocytes, which remained true through PN21. In the adult, GR expression was absent from oocytes of all follicular stages (**Figure 2.2B**). In the somatic compartment, GR was virtually absent from Foxl2⁺ granulosa cells, but was strongly expressed in the theca cell layer (marked by α -SMA) from as early as PN7 through adulthood (**Figure 2.2C**).

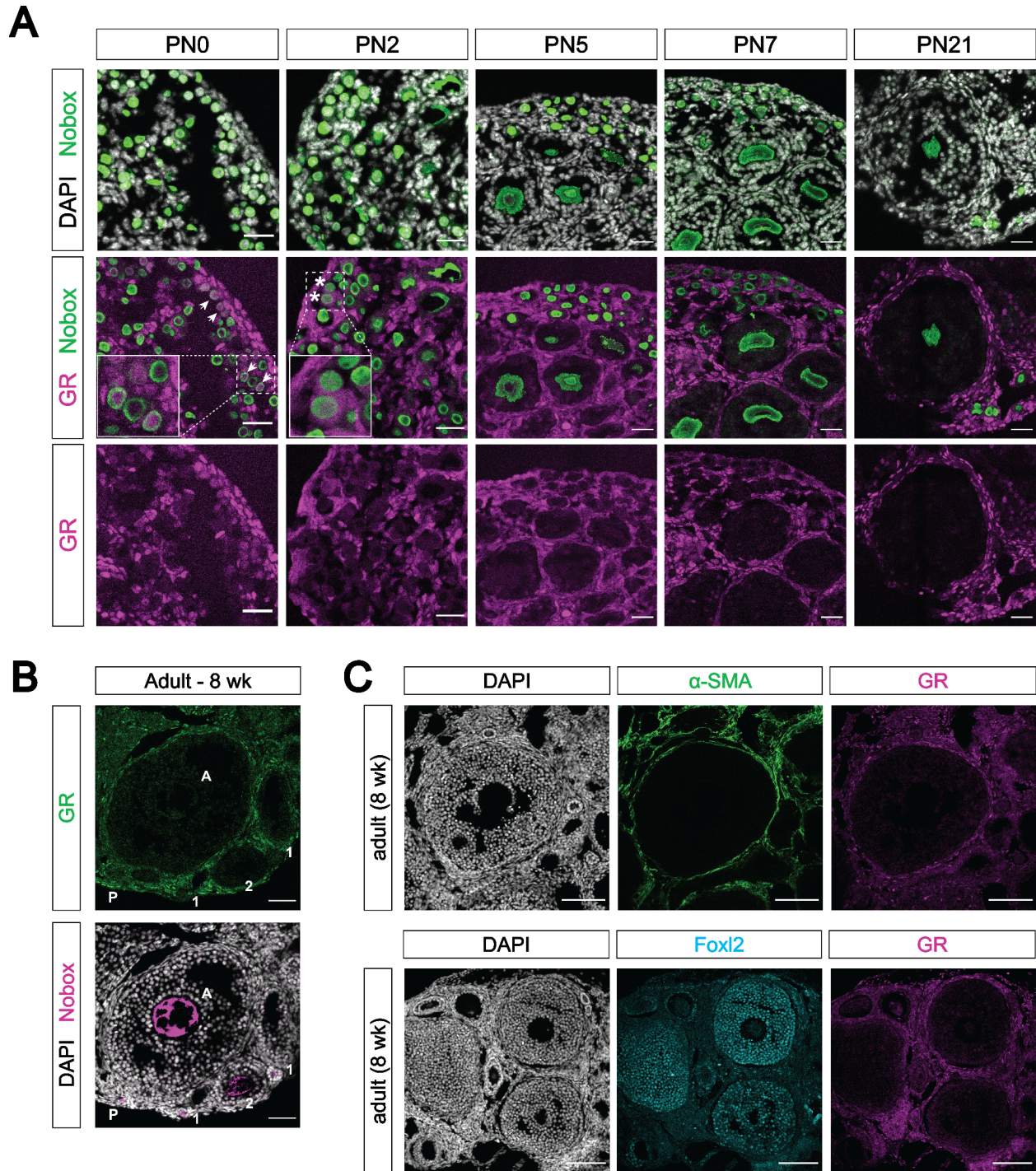


Figure 2.2 - Expression of the glucocorticoid receptor in the postnatal female germline

(A) IF staining showing expression of GR in mouse postnatal ovary sections at PN0, PN2, PN5, PN7 and PN21. Oocytes are marked by Nobox, and all nuclei are stained with DAPI. Cortical oocytes with remaining GR expression at PN0 are marked by arrowheads, and few remaining oocytes with cytoplasmic GR at PN2 are marked by asterisks. Scale bars: 30 μ m.

(B) IF staining showing GR expression in the adult mouse ovary at 8 weeks of age. Different follicular stages were determined based on classic morphological features, and are abbreviated

as follows: P - primordial follicle; 1 - primary follicle; 2 - secondary follicle; A - antral follicle. Oocytes are marked with Nobox, and nuclei are stained with DAPI. Scale bars: 50 μ m.

(C) IF staining showing co-expression of GR and somatic cell markers in the adult ovary. The theca interna layer is broadly marked by smooth muscle actin (α -SMA; top), and the granulosa cells are marked by Foxl2 (bottom). Scale bars: 100 μ m.

2.3 - Germ cells and somatic cells of the fetal ovary use alternative first exons of *Nr3c1*

It was suggested that one explanation for the spatiotemporal differences in GR expression across the body is the use of alternative, non-coding *Nr3c1* exon 1 splice isoforms in different cell types (Turner et al., 2006). To explore this possibility, we looked for evidence of exon 1 alternative splicing in our paired-end RNA-seq data of E15.5 sorted Oct4-GFP⁺ germ cells and GFP⁻ somatic cells (see Figure 2.6B for details). To identify the repertoire of isoforms used in each cell type, we took advantage of the paired-end sequencing reads that, once aligned to the genome, spanned a junction between exon 2 and one of the multiple known exon 1 variants (**Figure 2.3A**). Sashimi plots generated to visualize these junctions demonstrated that while somatic cells appear to use exclusively exon 1B, 1D and 1F, germ cells use a much wider range of known exon 1 variants, including 1A, 1B, 1C, 1D and 1F. Surprisingly, we also found evidence for the use of three novel splice isoforms exclusively in the germ cells, labeled here as predicted exons 1 α , 1 β , and 1 γ (**Figure 2.3A**, blue lines). To validate these differences in exon 1 isoform usage between the germ and somatic populations, we performed RT-PCR on bulk and sorted populations using primers designed specifically to amplify each of the known and predicted exon 1-2 junctions (**Figure 2.3B**). This wider diversity of *Nr3c1* exon 1 variants in the germline suggests that various promoter sequences at each of these exons may be active. As transcription factor binding at regulatory elements such as promoters and enhancers is known to regulate the spatiotemporal regulation of gene expression over development, this may

explain the more dynamic temporal regulation of GR in comparison to the soma. However, future functional studies would be needed to confirm.

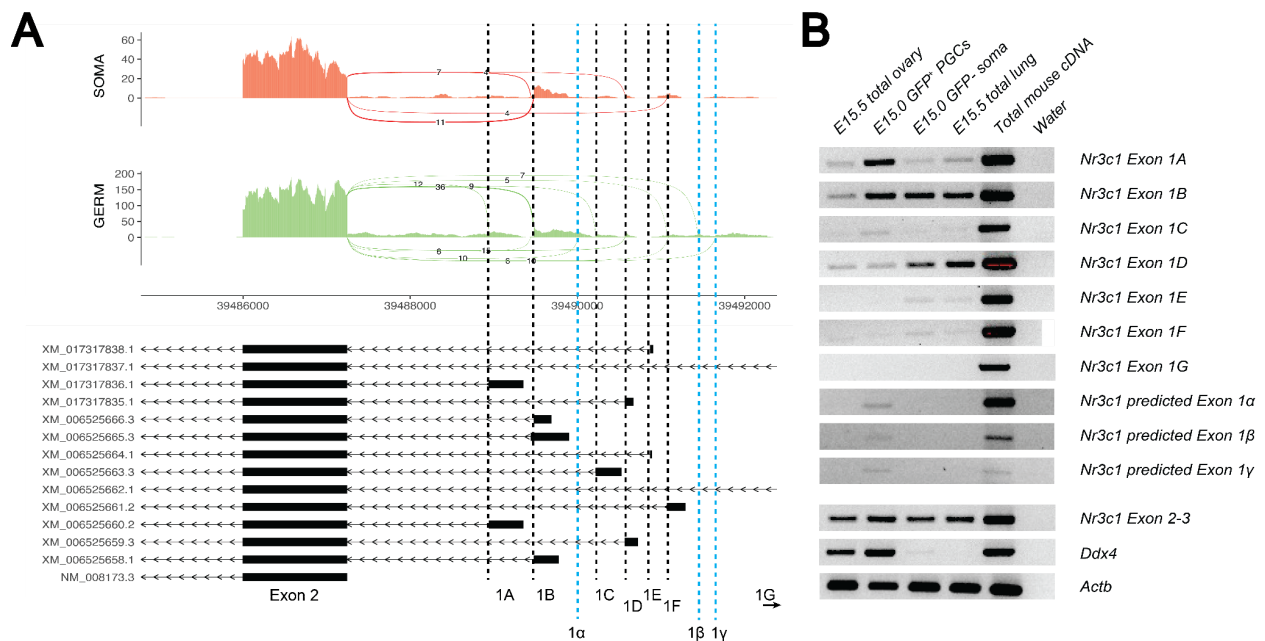


Figure 2.3 - Germ cells and somatic cells of the fetal ovary use alternative first exons of *Nr3c1*

(A) Sashimi plots showing differences in alternative exon 1 splicing events at the *Nr3c1* locus between ovarian germ and somatic cells. Plots were generated from paired-end RNA-seq data of E15.5 germ and somatic cells (saline control; Figure 2.6B). Previously annotated exon 1 variants have been arbitrarily labeled as exons 1A through 1G (with exon 1A being closest to exon 2). Three novel exon 1 splice sites identified in this study have been labeled as predicted exons 1α, 1β, and 1γ (marked by the dotted blue lines).

(B) RT-PCR validation of exon 1 variant usage in bulk E15.5 ovary, as well as sorted populations of germ and somatic cells at E15.0. Total mouse cDNA and water serve as positive and negative controls for all reactions, respectively. Primer set spanning *Nr3c1* exon 2-3 junction (present in all isoforms) was used as a positive control.

2.4 - Genetic deletion of GR leads to minimal transcriptional changes in the female germline

The strong, nuclear expression of GR seen in the female germline during a narrow window of development led us to hypothesize that GR may be selectively functioning as a transcriptional regulator of early oocyte development. To identify the putative transcriptional targets of GR in the female germline as well as any downstream cellular pathways that might be regulated by GR signaling, we utilized two orthogonal transcriptomic approaches in a mouse model with a genetic deletion for GR. Briefly, *Nr3c1* exon 3 floxed mice were crossed to a constitutive β -actin cre mouse line to generate a constitutive null allele of GR (henceforth referred to as “KO”). *Nr3c1* exon 3 deletion has previously been shown to result in efficient loss of functional GR protein (reviewed extensively elsewhere (Whirledge and DeFranco, 2018)), which we confirmed by IF at E17.5 (**Figure 2.4A**), immunoblot at E13.5 (**Figure 2.4B**), and qRT-PCR at E15.5 (**Figure 2.4C**). Because full body deletion of GR results in lethality at birth (due to defects in lung maturation (Cole et al., 1995)), mice were maintained as heterozygotes, and homozygous KO embryos were collected for experiments prior to birth. We first performed a low-input RNA-seq on FACS-sorted Oct4-GFP⁺ germ cells from individual WT and KO embryos at E17.5. While our differential gene expression analysis pipeline revealed robust expression differences between WT female and WT male germ cells (**Figure 2.4D'**), we surprisingly saw no statistically significant differentially expressed genes between female WT and KO germ cells (**Figure 2.4D''**). Conditional deletion of GR specifically in the germ cells using Oct4-CreERT2 yielded the same result (**Figure 2.4D'''**). In tandem, we performed 10X single cell RNA-seq on E15.5 WT and KO germ cells. After dissecting and removing mesonephroi, ovaries were dissociated and FACS sorted for Oct4-GFP to enrich for the smaller germ cell compartment. GFP⁻ soma were re-combined with the purified germ cells at a ratio of 60:40 germ to soma, and then

captured using the Chromium 10X platform. All expected cell types of the fetal ovary were detected in both WT and KO embryos (**Figure 2.4E'**), and total *Nr3c1* transcript was depleted in all cell types of the ovary (**Figure 2.4E''**). Differential gene expression analysis performed between WT and KO cells within the germ cell cluster revealed an extremely low number of differentially expressed genes with minor fold changes (**Figure 2.4E'''**), corroborating our bulk RNA-seq results that the loss of GR has little effect on the transcriptional landscape of the germline. Similar differential gene expression analysis on the somatic cell clusters also showed minimal transcriptional changes (**Figure 2.4E''''**).

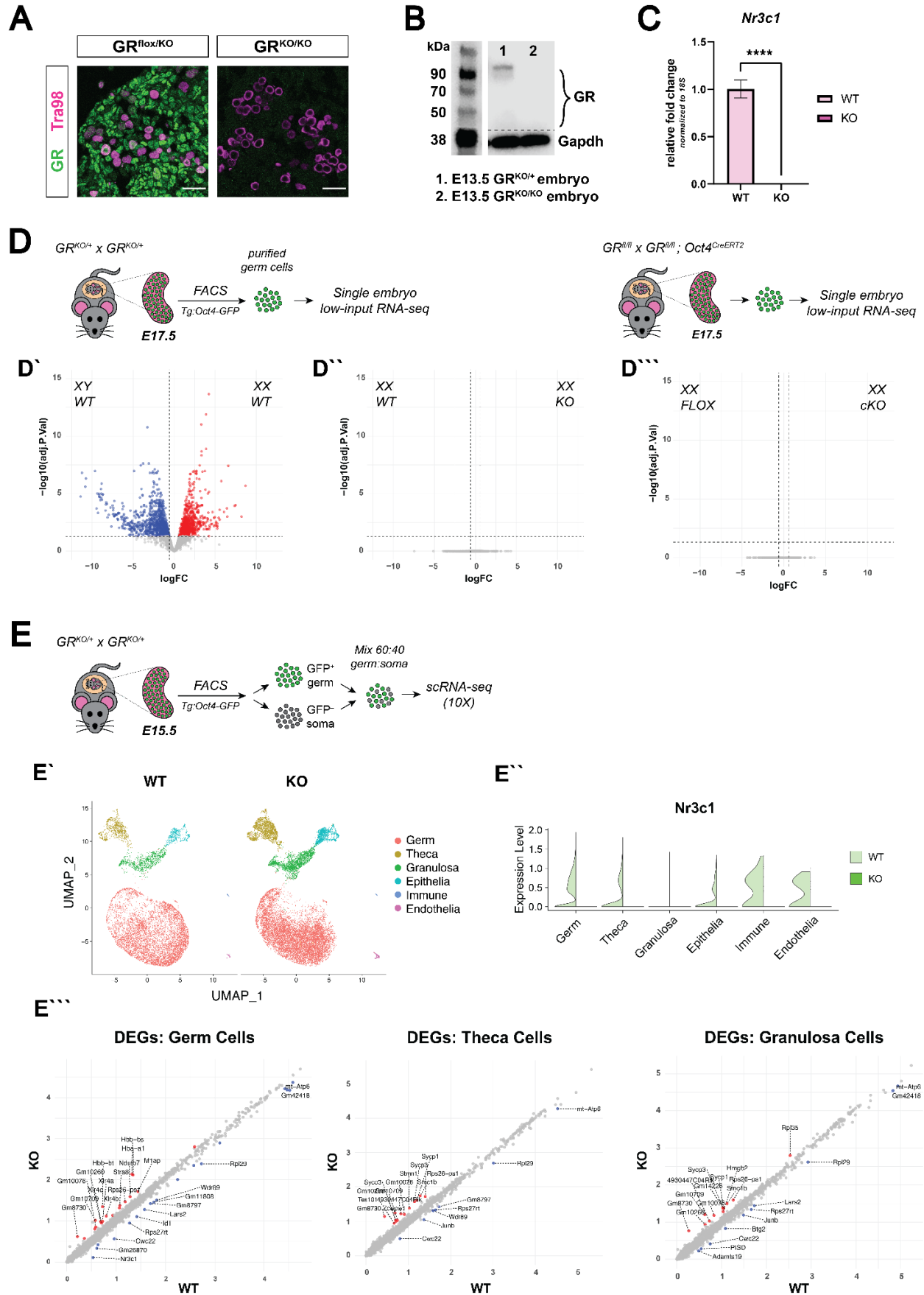


Figure 2.4 - Genetic deletion of GR leads to minimal transcriptional changes in the female germline

(A) IF staining for GR in E17.5 ovaries. GR^{flox/KO} ovaries, which contain one functional floxed allele of GR show robust GR expression, whereas GR^{KO/KO} ovaries homozygous for the deletion allele show complete loss of GR. Scale bars: 30 μ m.

(B) Western blot performed on whole cell lysate prepared from entire E13.5 embryos of different genotypes. Membranes were blotted with a GR antibody that recognizes all known GR isoforms, as well as Gapdh as a loading control.

(C) qRT-PCR on bulk E15.5 WT (n=3) and KO (n=5) ovaries for *Nr3c1*, normalized to 18S ribosomal RNA housekeeping gene using $2^{-\Delta\Delta Ct}$ quantification method. Data are mean \pm s.d., and p-values were calculated for each gene using a two-tailed, unpaired t-test, where ****: $p \leq 0.0001$.

(D) Bulk RNA-seq performed on Tg:Oct4-GFP⁺ sorted germ cells from E17.5 gonads. For each genotype, 4-5 single-embryo biological replicates were used for low-input library prep followed by 3' Tag-Seq. Volcano plots show differentially expressed genes ($\log_{2}FC \geq 0.6$; adjusted p-value ≤ 0.05) between: (D') WT male and WT female germ cells, (D'') WT and GR KO female germ cells, and (D''') Oct4-CreERT2⁺ GR conditional knockout (cKO) female germ cells and floxed cre-negative controls.

(E) 10X Single cell RNA-sequencing performed on E15.5 WT and GR KO ovaries. A total of n=4 WT ovaries and n=2 KO ovaries were each pooled prior to sorting to enrich for Oct4-GFP⁺ germ cells. (E') UMAP clustering on WT and KO cells, colored by cell type. (E'') Violin plot showing *Nr3c1* transcript expression in WT vs KO cells across each cell type, confirming GR deletion. (E''') Comparison of average gene expression between WT and KO cells within the germ cell, theca cell, and granulosa cell clusters. Differentially expressed genes ($\log_{2}FC \geq 0.25$; adjusted p-value ≤ 0.05) are labeled in blue or red for genes enriched in WT or KO cells, respectively.

2.5 - Meiosis in the female proceeds normally in the absence of GR

While preparing our transcriptomics samples, dynamic expression of *Nr3c1* expression observed in a scRNAseq study of WT fetal germ cells by Ge et al raised the possibility that GR may play a role as a transcriptional regulator during female meiotic progression (Ge et al., 2021). To test this, we first performed qRT-PCR on E15.5 WT and KO bulk ovary tissue for a panel of meiotic genes known to have important roles in meiotic progression (**Figure 2.5A**). While we were able to detect robust knockdown of *Nr3c1* transcript, we saw no significant changes in meiotic gene expression. To functionally test whether meiotic progression was either

delayed or disrupted following loss of GR, we prepared meiotic spreads for E15.5 WT and KO ovaries. Nuclei were stained for Sycp3, Sycp1 and γ H2AX to discern the different stages of meiotic prophase I (**Figure 2.5B**). After manual scoring, no significant changes in substage distribution could be detected between WT and KO nuclei, further suggesting that loss of GR does not disrupt meiotic progression. In contrast, we also asked whether pharmacological stimulation of GR during this window was sufficient to perturb meiotic progression. E14.5 ovaries were dissected and cultured for 48 hours *ex vivo* with dex, a potent synthetic agonist of GR. No significant changes in meiotic substage distribution were seen between dex and control nuclei, suggesting GR activation is not sufficient to disrupt meiotic progression (**Figure 2.5B**).

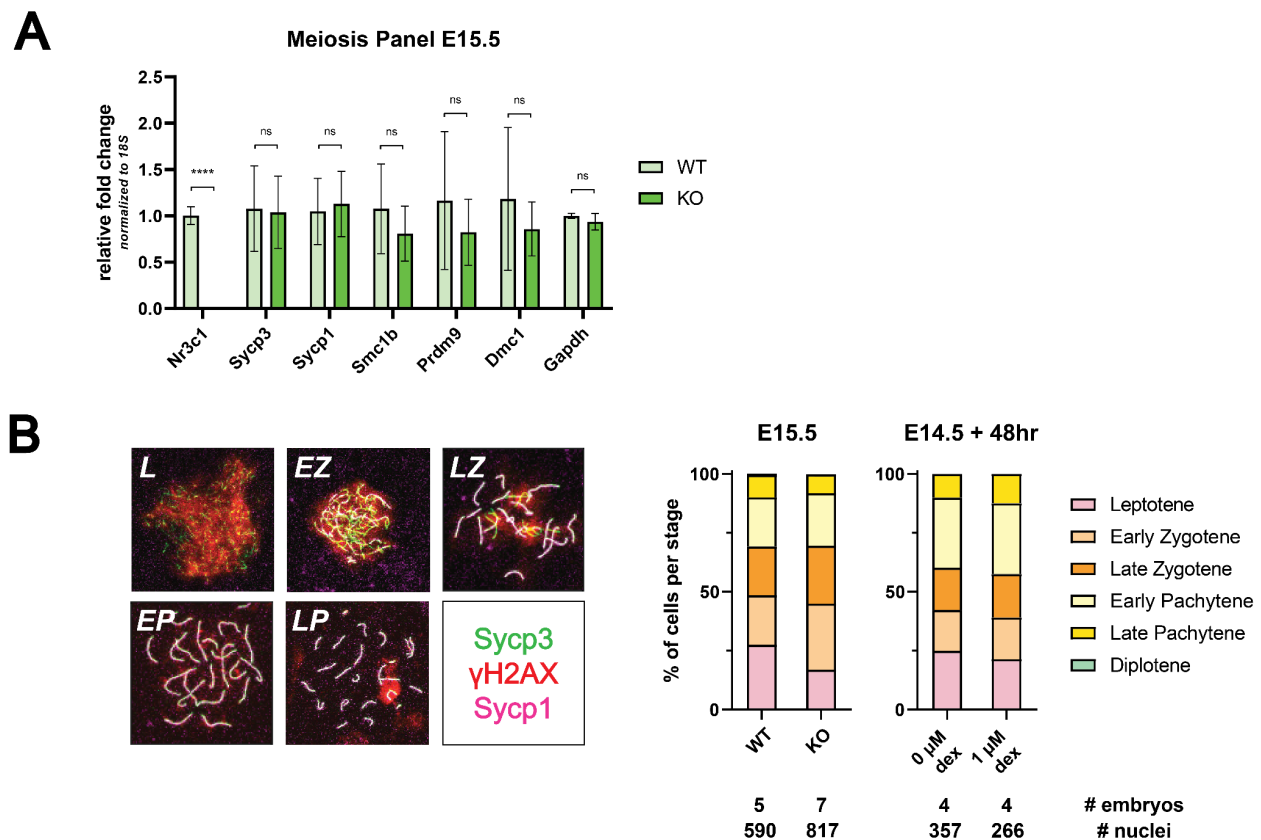


Figure 2.5 - Meiosis proceeds normally in the absence of GR

(A) qRT-PCR on bulk E15.5 WT (n=3) and KO (n=5) ovaries for a panel of meiotic genes, normalized to 18S ribosomal RNA housekeeping gene using $2^{-\Delta\Delta C_t}$ quantification method. *Nr3c1* serves as a positive control to confirm complete GR knockout, and *Gapdh* serves as an unchanged negative control. Data are mean \pm s.d., and p-values were calculated for each gene

using a two-tailed, unpaired t-test, where *: $p \leq 0.05$; **: $p \leq 0.01$; ***: $p \leq 0.001$; ****: $p \leq 0.0001$, n.s.: not significant.

(B) Meiotic spreads performed on germ cell nuclei from E15.5 WT and GR KO ovaries, as well as germ cell nuclei from E14.5 ovaries cultured for 48 hours *ex vivo* with or without 1 μ M dex. Top: representative images of meiotic prophase I staging of spreads co-stained with Sycp3 (green), Sycp1 (magenta), and γ H2AX (red). Bottom: Quantification of relative substages based on manual scoring. L: Leptotene; EZ: Early Zygotene; LZ: Late Zygotene; EP: Early Pachytene; LP: Late Pachytene.

2.6 - Developing ovarian somatic cells, but not germ cells, show GR transcriptional activation following exogenous glucocorticoid treatment

While our transcriptomic analysis of GR knockout oocytes suggests that endogenous GR (under basal conditions) does not regulate oocyte gene expression or meiotic progression, we next sought to determine whether administration with dex was sufficient to elicit a transcriptional response in the female germline. Pregnant dams were administered either saline vehicle or 10 μ g dex / g by IP injection daily from E12.5 to E15.5, coinciding with the window of highest GR expression in the female germline. We first validated that this dosing regimen was sufficient to elicit a robust induction of the canonical GR response gene *Fkbp5* in bulk ovary, testis, and lung tissue of E15.5 embryos (**Figure 2.6A**), confirming dex was able to transit the placenta from the dam to the embryos. Embryos of saline and dex-treated dams were dissected at E15.5, and mesonephroi removed from ovaries prior to pooling each litter. Both Oct4-GFP⁺ germ cells and total GFP⁻ somatic cells were FACS sorted and submitted for bulk RNA-seq. The resulting differential gene expression analysis on both the somatic and germ cell compartments revealed a striking difference in their response to dex (**Figure 2.6B**). While the somatic cells showed a robust transcriptional response following dex treatment (1477 total differential genes with adjusted $p\text{-val} \leq 0.05$), by comparison, the germ cells showed a severely dampened response (156 total differential genes with adjusted $p\text{-val} \leq 0.05$). GO term analysis of differentially

expressed genes from the somatic cells showed low fold enrichment across a wide range of unrelated categories, likely due to the heterogeneity of the total GFP⁻ population (**Figure 2.6C**). The few downregulated germ cell genes showed a strong enrichment for ribosomal assembly and translation (**Figure 2.6C**). This seems likely to be an artifact due to a combination of the very few differential genes used for GO analysis, as well as the extremely high levels of expression of ribosomal genes, where even very small differences in expression lead to a significant p-value. The set of upregulated (i.e. dex-induced) genes in the germ cells did not show any significant GO term enrichment. We also validated that the transcriptional changes induced by dex in the soma also led to changes at the protein level in a parallel *ex vivo* culture system. Fetal ovaries were dissected at E14.5 and cultured in hormone-depleted medium for 48 hours with and without 1 μ M dex. IF staining for PLZF (gene name *Zbtb16*), the most highly upregulated gene in the somatic cells by RNA-seq, confirmed a robust upregulation specifically in the Tg:Oct4-GFP⁻ soma and not the GFP⁺ germ cells (**Figure 2.6D**).

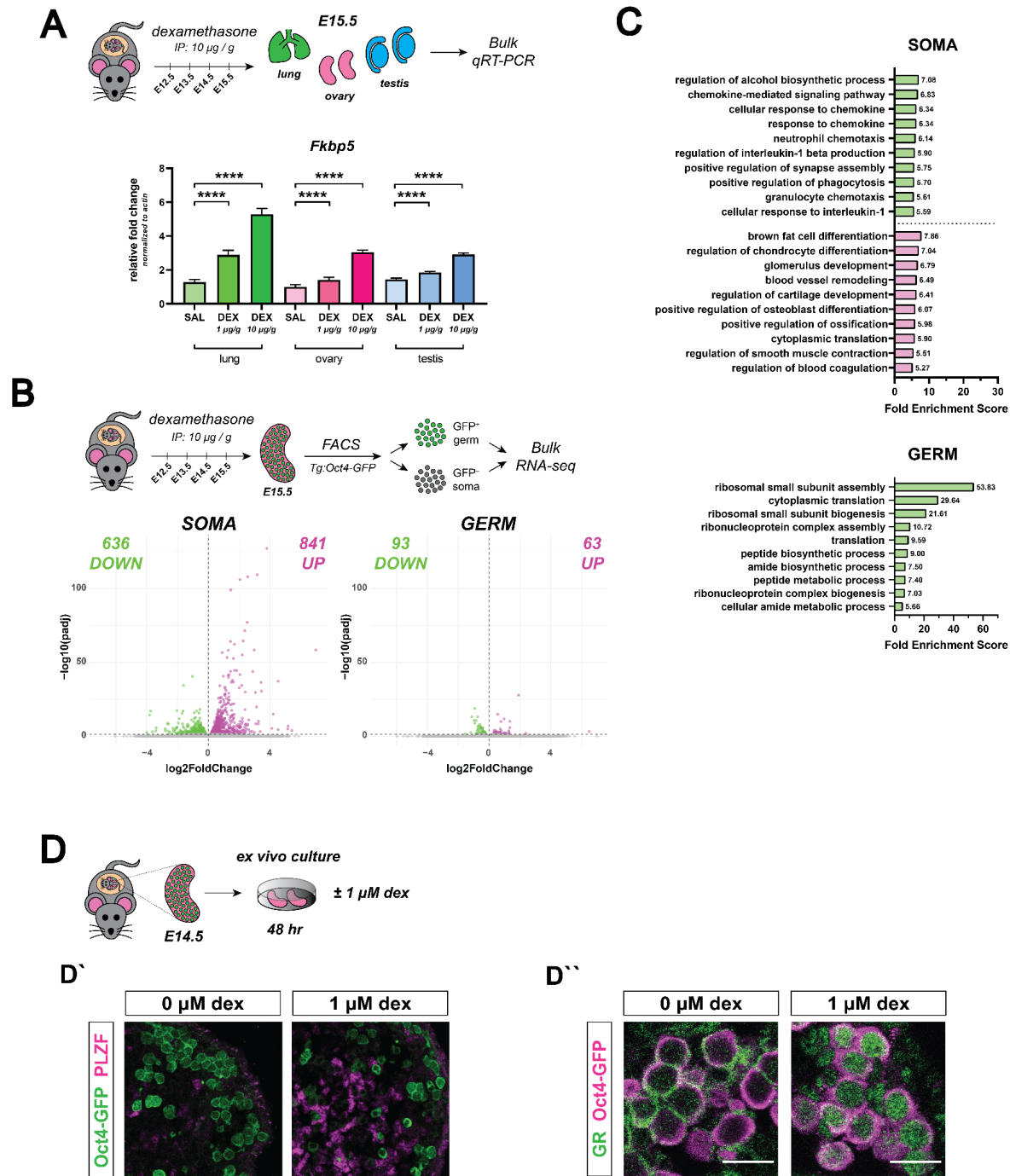


Figure 2.6 - Developing ovarian somatic cells, but not germ cells, show GR transcriptional activation following exogenous glucocorticoid treatment

(A) qRT-PCR on bulk E15.5 lung, ovary and testis tissue from *in vivo* dex-dosed embryos. Expression of *Fkbp5*, a known canonical GR-responsive gene, is shown following administration with 1 µg / g dex, 10 µg / g dex, or saline vehicle control (n=3 embryos per dose) to verify that maternal administration of dex from E12.5 – E15.5 is able to elicit a transcriptional response in the fetus. Lung serves as a positive control. Data are mean ± s.d., normalized to β-actin

housekeeping gene using $2^{-\Delta\Delta Ct}$ quantification method, and p-values were calculated for each dose comparison using a two-tailed, unpaired t-test, where ****: $p \leq 0.0001$.

(B) Bulk RNA-seq performed on sorted Tg:Oct4-GFP⁺ germ cells and GFP⁻ somatic cells from fetal ovaries dosed *in vivo* with dex. Pregnant dams were injected via IP with either 10 $\mu\text{g} / \text{g}$ dex or a saline vehicle control at E12.5, E13.5, E14.5 and E15.5, and ovaries were collected for sorting at E15.5. Three biological replicates were used per condition, each consisting of sorted cells from ovaries pooled together from a minimum of two entire independently dosed litters. Volcano plots show dex-induced differentially expressed genes (adjusted p-value ≤ 0.05) either upregulated (magenta) or downregulated (green) in comparison to vehicle controls for both germ cells, as well as total somatic cell population.

(C) GO term enrichment analysis using differentially expressed genes from *in vivo* dex-dosed RNA-seq data. The top 10 significant biological processes for upregulated (magenta) and downregulated (green) genes are shown, ranked by fold enrichment score, for both somatic cells and germ cells. Note that no statistically significant enrichment of GO terms was found for the germ cell dex-upregulated gene list.

(D) IF staining for select genes in E14.5 ovaries cultured for 48 hr *ex vivo* with and without 1 μM dex. (D') PLZF is induced specifically in the Tg:Oct4-GFP⁻ soma. (D'') GR shows dynamic subcellular localization in response to ligand, Scale bars: 15 μm .

2.7 - Subcellular localization of GR in the female germline is dynamically regulated in response to ligand

This lack of a transcriptional response in the germ cells, yet not the somatic cells, following both deletion of GR and dex treatment led us to hypothesize that the female germline may be resistant to GR signaling. As nuclear localization is important for the function of GR as a transcription factor, we tested whether its subcellular localization is altered in response to its ligand. In ovaries cultured *ex vivo* in hormone-depleted medium without dex, GR translocated to the cytoplasm of virtually all germ cells; in contrast, dex-treated controls retained nuclear localization (**Figure 2.6D''**). As GR localization still dynamically responded to the presence or absence of ligand, despite not robustly altering transcription, this suggests that some other modification to the GR protein specifically in the germ cells could be accounting for this lack of activity.

2.8 - Fetal ovarian germ and somatic cells show no evidence for the use of inhibitory translational isoforms

GR is a highly modified protein, with a wide range of transcriptional isoforms, translational isoforms, and post-translational modifications that have been characterized to date (Weikum et al., 2017). GR has multiple translation initiation sites that lead to a variety of protein isoforms with varying truncations in the regulatory N-terminal domain of the protein (Lu and Cidlowski, 2005). The most truncated forms of GR (the “GR-D” isoforms) have been suggested to exert an inhibitory dominant negative effect (Lu and Cidlowski, 2005). As the relative expression of these different isoforms varies across different tissues in the body (Lu and Cidlowski, 2005), we sought to address whether the lack of GR response in the germline could be due to the presence of these inhibitory translational isoforms. We performed a Western blot on E13.5 whole ovary lysate and control tissue, using an antibody designed specifically to recognize all known GR isoforms. Although GR-D isoforms could be detected within adult control tissue, we did not detect any GR-D isoforms (~50 kDa or less) in the ovary or the PN0 testis (**Figure 2.7A**).

2.9 - Fetal ovarian germ and somatic cells have no detectable GR β transcriptional isoform

Humans harbor two predominant transcriptional isoforms of GR: the GR α isoform, which encodes the full-length GR protein, and the GR β isoform, which is generated by an alternative splicing event leading to a truncated form of the protein (Encío and Detera-Wadleigh, 1991; Hollenberg et al., 1985). In the GR α isoform, exon 8 is spliced directly to the beginning of exon 9, thus creating the full-length transcript, whereas in the GR β isoform, exon 8 is spliced to an alternate splice acceptor site in the middle of exon 9. The resulting GR β isoform has been

shown to function as a dominant negative inhibitor of GR α due to a truncation in the ligand binding domain of the resulting protein (Bamberger et al., 1995; Oakley et al., 1996). Although it was previously believed that the GR β isoform does not exist in mice due to an evolutionary mutation in the exon 9 β splice acceptor site (Otto et al., 1997), one group recently demonstrated the existence of a mouse GR β protein; rather than alternative exon 9 splicing as in human, the mouse version is formed by intron 8 retention (Hinds et al., 2010). This murine GR β was highly similar in structure and function to human GR β , expressed in various mouse tissues, and appeared to function as a putative dominant negative regulator of murine GR α . To assess whether the lack of transcriptional response in dex-dosed female germ cells could be due to the presence of the GR β isoform, we looked for evidence of this intron 8 retention in our paired-end RNA-seq reads of both germ and somatic cells. Generation of Sashimi plots to visualize and quantify splicing events showed no evidence for intron 8 retention in either the germ or somatic compartment (**Figure 2.7B**). This result suggests that there is no appreciable expression of the mouse GR β isoform within the fetal ovary, and therefore this is not the likely cause of attenuated GR activity in the germline.

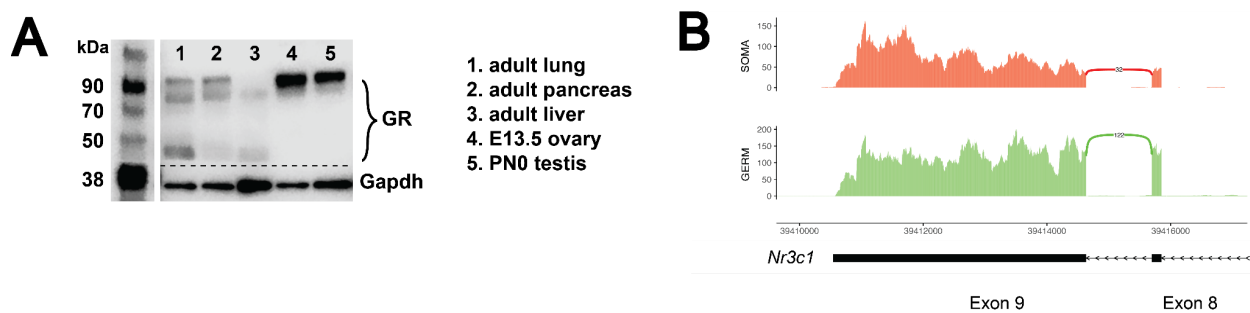


Figure 2.7 - Fetal ovarian germ and somatic cells show no evidence for the use of inhibitory transcriptional or translational isoforms

(A) Western blot performed on whole cell lysate prepared from adult lung, adult pancreas, adult liver, E13.5 whole ovary, and PN0 whole testis. Membranes were blotted with a GR antibody that recognizes all known GR isoforms, as well as Gapdh as a loading control. The full-length GR protein can be seen at just above 90 kDa.

(B) Sashimi plots showing lack of evidence for the alternatively spliced inhibitory GR β transcriptional isoform in both ovarian germ and somatic cells. Plots were generated from paired-end RNA-seq data of E15.5 germ and somatic cells (saline control; Figure 2.6B).

2.10 - Spatiotemporal expression GR in the male germline

The lack of GR transcriptional activity that we observed in the female germline was puzzling given that GR is such a potent transcription factor in the vast majority of other cell types studied thus far (Weikum et al., 2017; Whirledge and DeFranco, 2018). Furthermore we were curious as to whether this insensitivity to GR signaling was unique to the female germline, or whether the same phenomenon could be observed in the male germline. We first characterized the expression pattern of GR in the testis by IF from E12.5 through E18.5. In stark contrast to the female, germ cells of the fetal testis (marked by Tg:Oct4-GFP) showed no GR expression during early development (**Figure 2.8A**). It was not until E17.5 that male germ cells began to express GR, and by E18.5, over 90% of all germ cells expressed nuclear GR (**Figure 2.8A, 2.8B**). We employed a similar quantitative imaging analysis as in the female to confirm that GR expression peaked at E18.5 (**Figure 2.8C**).

As GR expression appeared to be increasing between E17.5 and the end of fetal development, we next asked whether this expression was maintained into the early postnatal window. Staining between PN0 (not shown) and PN2 revealed that strong nuclear GR expression was maintained in the Tra98⁺ germ cells shortly after birth (**Figure 2.9A**). Extending this analysis to PN7, PN10 and PN14, we observed that GR expression was maintained in both PLZF⁺ and c-kit⁺ spermatogonia, although at lower levels than PN2 (**Figure 2.9A, 2.9B**). As anticipated based on the literature, GR expression appeared high in the surrounding peritubular myoid cells and Leydig cells of the interstitium at all timepoints observed. By PN21, the first wave of

spermatogenesis has been completed, with tubules containing spermatocytes (currently undergoing meiosis) and spermatids (completed meiosis) can be easily identified. Quite strikingly, GR expression at PN21 became highly restricted to the undifferentiated (PLZF⁺) and differentiating (c-kit⁺) spermatogonia, yet was absent from more mature spermatocytes or spermatids (**Figure 2.9A, 2.9B**). Furthermore, this spermatogonia-restricted expression pattern was maintained into adulthood (**Figure 2.10A**), suggesting a potential stage specific role for GR in the male germline.

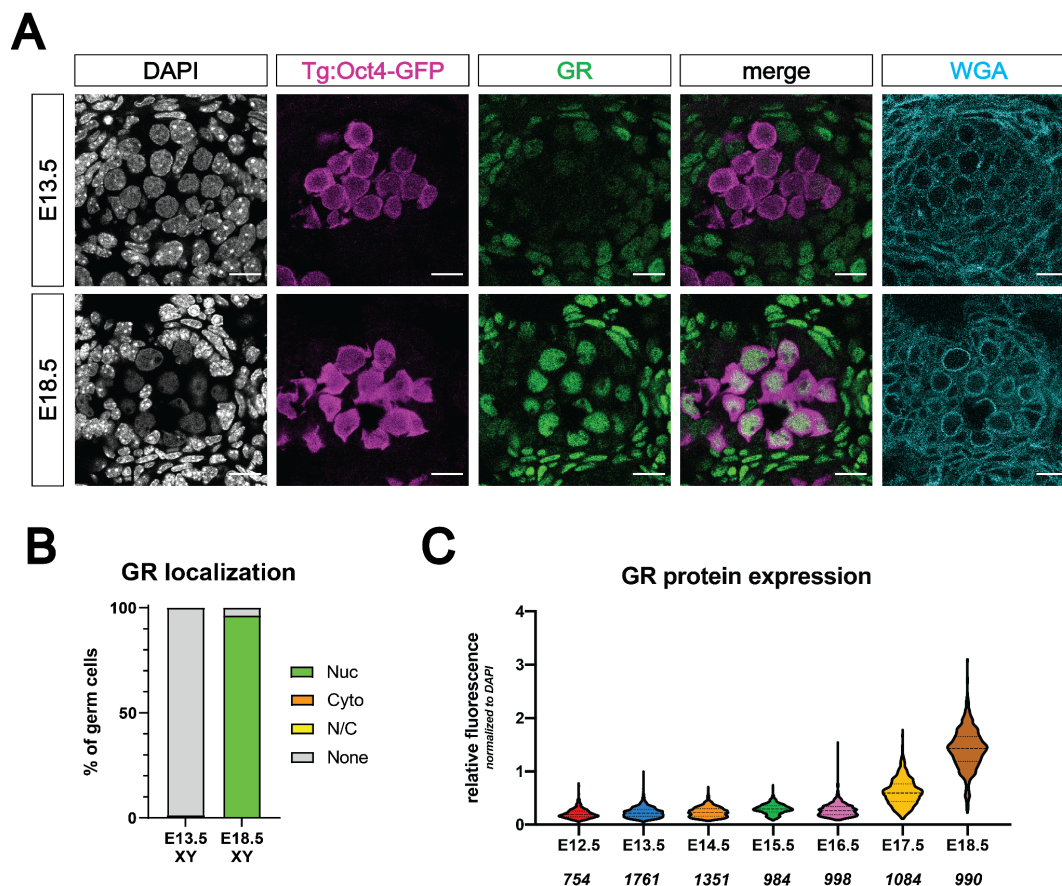


Figure 2.8 - Expression of the glucocorticoid receptor in the developing male germline

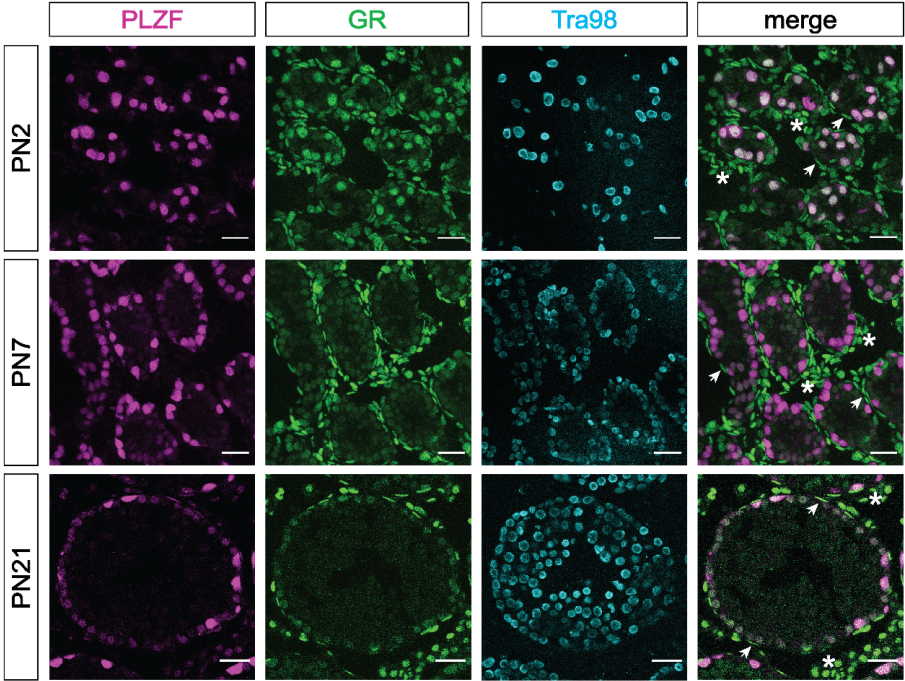
(A) IF staining showing expression of GR in mouse fetal testis sections at E13.5 (top) and E18.5 (bottom), counterstained with DAPI. Germ cells are marked by transgenic Oct4-GFP. Cellular membranes were stained with wheat germ agglutinin (WGA) to facilitate computational segmentation of individual cells. Scale bars: 15 μ m.

(B) Quantification of GR subcellular localization within germ cells, scored manually (top).

(C) Quantitative IF analysis of relative GR protein expression across developmental time in germ cells. Individual cells were computationally segmented using WGA, and GR protein levels

were normalized to DAPI on an individual cell basis. Images and total cell numbers counted were obtained from a minimum of three testes from independent biological replicates at each developmental stage.

A



B

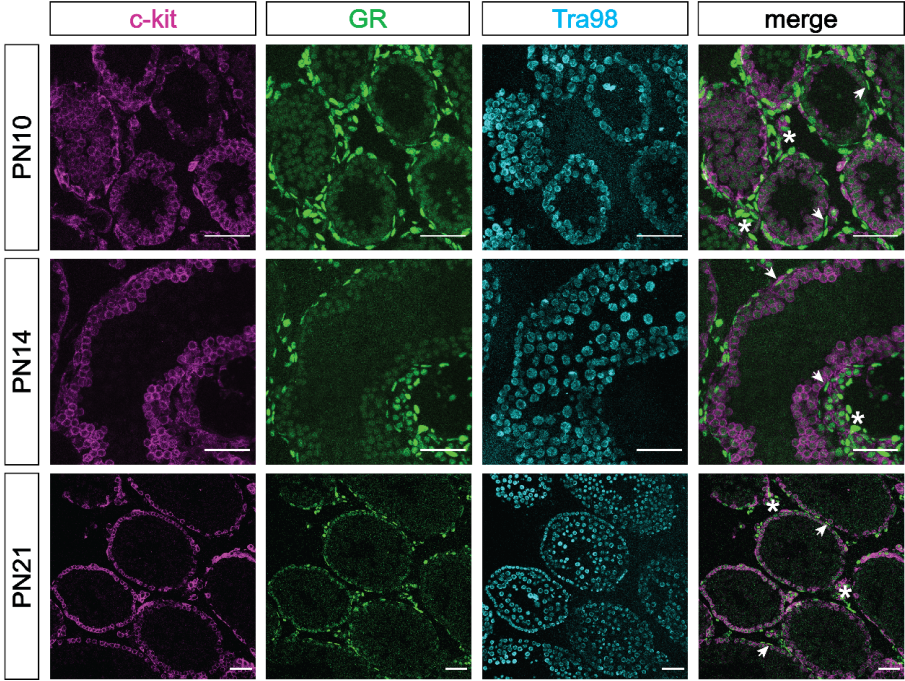


Figure 2.9 - Expression of the glucocorticoid receptor in the postnatal male germline

(A) IF staining showing expression of GR in mouse postnatal testis sections at PN2 (top), PN7 (middle) and PN21 (bottom). Spermatogonia are marked by PLZF, and total germ cells are marked by Tra98. Arrowheads show GR⁺ peritubular myoid cells, and asterisks show GR⁺ interstitial cells. Scale bars: 30 μ m.

(B) IF staining showing expression of GR in additional mouse postnatal testis timepoints. sections at PN10 (top), PN14 (middle), and PN21 (bottom). Differentiating spermatogonia are marked by c-kit, and total germ cells are marked by Tra98. Arrowheads show GR⁺ peritubular myoid cells, and asterisks show GR⁺ interstitial cells. Scale bars: 50 μ m.

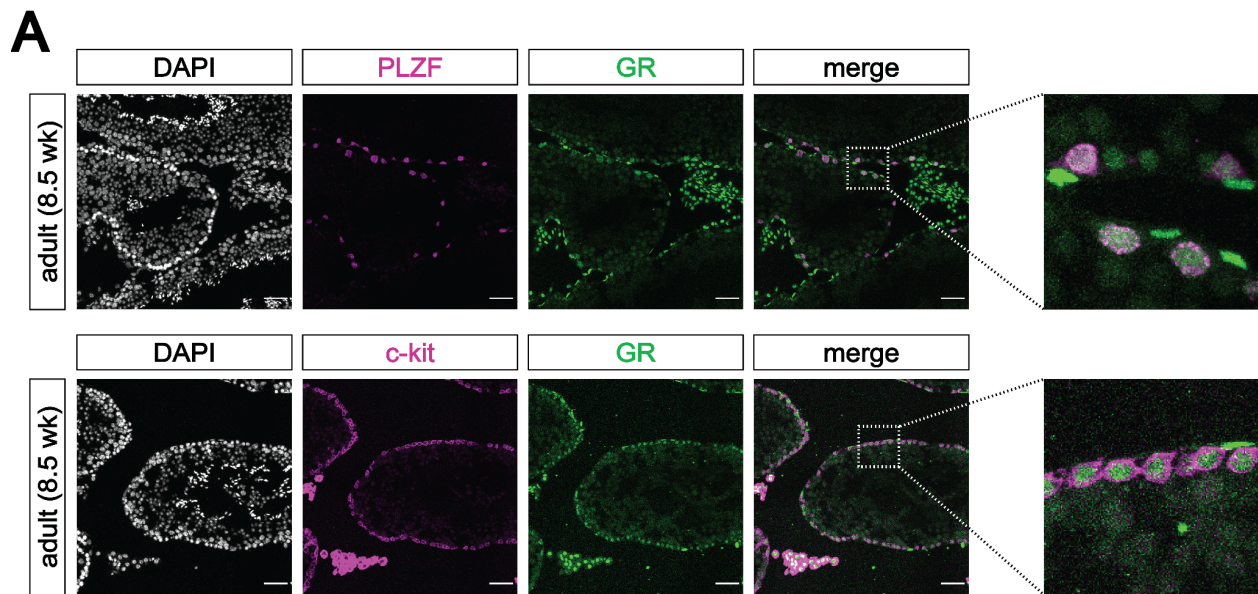


Figure 2.10 - Expression of the glucocorticoid receptor in the adult male germline

(A) IF staining showing expression of GR in mouse adult testis sections. GR expression overlaps with PLZF⁺ undifferentiated spermatogonia (top) and c-kit⁺ differentiating spermatogonia (bottom), zoomed images to highlight overlapping expression. Scale bars: 50 μ m.

2.11 - Germ cells and somatic cells of the postnatal testis use an alternative first exons of *Nr3c1*

As we discovered a difference in alternative exon 1 usage between germ and somatic cells of the fetal ovary, we checked whether this extended to the testis using our paired-end RNA-seq data of PN1 sorted Oct4-GFP⁺ germ cells and GFP⁻ somatic cells (see Figure 2.12A for details).

Analogous to what we found in the females, the germ cells of the testis appeared to display a wider repertoire of exon 1 alternative splicing in comparison to their somatic counterparts (**Figure 2.11A**). When considering previously annotated exons, somatic cells utilized exons 1A, 1B and 1E, whereas germ cells utilized exons 1A, 1B, 1D and 1F (**Figure 2.11A**). We also looked to see if any of the newly predicted exons identified in the female germ cells were present in the male, but only found evidence of exon 1 α and not 1 β or 1 γ (**Figure 2.11A**). This combination of germ cell exons is similar between male and female, although with less diversity in the male germline in comparison to the female, which may account for some of the differences in the spatiotemporal dynamics of GR observed between the sexes.

A

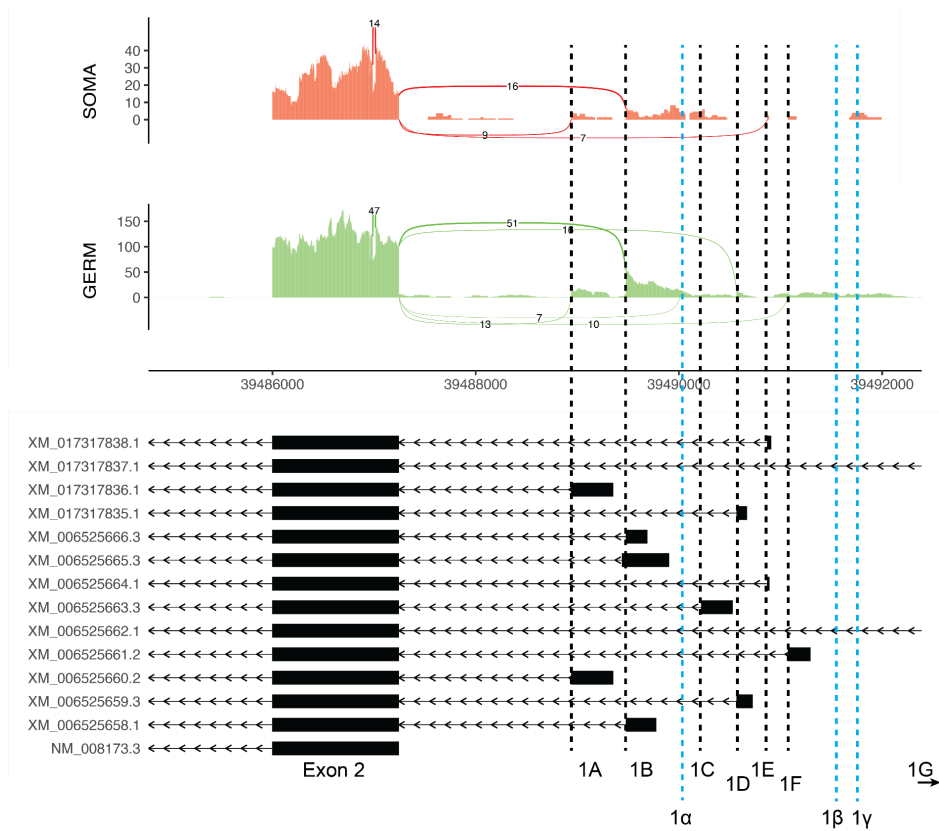


Figure 2.11 - Germ cells and somatic cells of the early postnatal testis use alternative first exons of *Nr3c1* (Supplemental)

(A) Sashimi plots showing differences in alternative exon 1 splicing events at the *Nr3c1* locus between germ and somatic cells from PN1 testes. Plots were generated from paired-end RNA-seq data of PN1 germ and somatic cells (saline control; Fig 2.12A). Previously annotated exon 1 variants have been arbitrarily labeled as exons 1A through 1G (with exon 1A being closest to exon 2). The three novel exon 1 splice sites identified in the female in Figure 2.3A have been labeled as predicted exons 1α, 1β, and 1γ (marked by the dotted blue lines).

2.12 - Germ cells of the perinatal testis show GR transcriptional activation following exogenous glucocorticoid treatment

As the transcriptional landscape of fetal ovarian germ cells appeared to be resistant to both loss and overactivation of GR signaling, we next wanted to ascertain whether this phenomenon was specific to the female germline, or if this resistance to changes in GR was preserved in the germline across sexes. We chose to dose with dex at the onset of GR expression in the male, which also allowed us to utilize our Tg:Oct4-GFP reporter to isolate early pro-spermatogonia by FACS before they downregulated Oct4 expression. Pregnant dams were injected with either 10 μg / g dex or saline vehicle by IP injection at E17.5 and E18.5, and pups were given the same dose of dex by subcutaneous injection at PN0. In a small pilot cohort, an additional subcutaneous injection at PN1 resulted in high mortality rates (data not shown), and thus we limited our injections to E17.5, E18.5 and PN0. Pups were dissected at PN1, and the epididymis and tunica were removed from each testis prior to pooling each litter. Oct4-GFP⁺ germ cells as well as GFP⁻ somatic cells were FACS sorted and subjected to bulk RNA-seq. In contrast to the female, differential expression analysis revealed a pronounced transcriptional response in male germ cells following dex treatment, within the same order of magnitude as the GFP⁻ somatic cells (**Figure 2.12A**). We next performed GO term analysis on differentially expressed genes in both the germ and somatic cells (**Figure 2.12B**). Very interestingly, the genes significantly downregulated in the germ cells in response to dex showed a strong enrichment for genes related to the regulation of mRNA splicing. The regulation of RNA splicing in germline cells is crucial for the proper progression of meiosis and spermatogenesis (Ehrmann et al., 2019; Horiuchi et al., 2018; Kuroda et al., 2000; Legrand et al., 2019; Li et al., 2007; Liu et al., 2017; Naro et al., 2017; O'Bryan et al., 2013; Schmid et al., 2013; Wu et al., 2021; Xu et al., 2017; Yuan et al., 2021; Zagore et al., 2015), and is conserved across species (Chen et al., 2019;

Mattox and Baker, 1991; Wu et al., 2016). Downregulated genes also showed an enrichment for mitotic cell cycle progression, which is of interest at this time point given that the mitotically-inactive germ cells will begin to re-enter mitosis at ~PN3-PN5. GO term analysis of differentially expressed genes in treated somatic cells showed a wider variety of terms, which is likely due to the heterogeneity of GFP⁻ cells collected. Downregulated genes were broadly enriched for ECM organization and cellular adhesion, whereas upregulated genes showed enrichment for canonical glucocorticoid response genes.

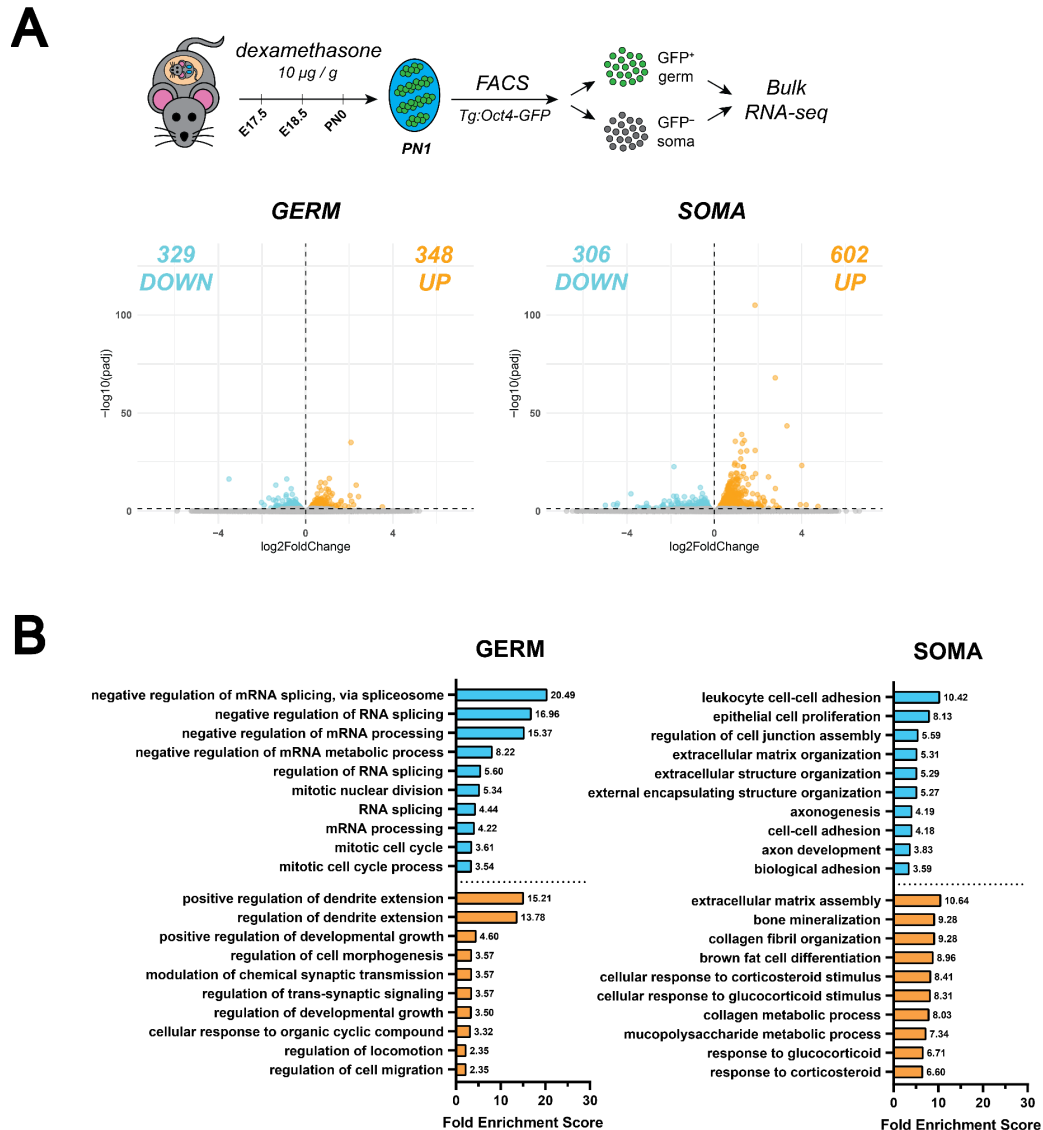


Figure 2.12 - Both germ and somatic cells of the early postnatal testis show GR transcriptional activation following exogenous glucocorticoid treatment

(A) Bulk RNA-seq performed on sorted Tg:Oct4-GFP⁺ germ cells and GFP⁻ somatic cells from postnatal testes dosed *in vivo* with dex. Pregnant dams were injected via IP with either 10 µg / g dex or a saline vehicle control at E17.5 and E18.5. Pups were then dosed with either dex or saline via subcutaneous injection at PN0, and testes were collected for sorting at PN1. Three biological replicates were used per condition, each consisting of sorted cells from testes pooled together from a minimum of two entire independently dosed litters. Volcano plots show dex-induced differentially expressed genes (adjusted p-value ≤ 0.05) either upregulated (orange) or downregulated (cyan) in comparison to vehicle controls for both germ cells, as well as total somatic cell population.

(B) GO term enrichment analysis using differentially expressed genes from *in vivo* dex-dosed RNA-seq data. The top 10 significant biological processes for upregulated (orange) and

downregulated (cyan) genes are shown, ranked by fold enrichment score, for both somatic cells and germ cells.

2.13 - Regulation of mRNA splicing in the early postnatal testis

Given the crucial role transcript splicing in spermatogenesis, we first validated this potential link between GR and splicing. To the best of our knowledge, no prior studies have identified GR in the regulation of mRNA splicing. To quantify any dose-dependent changes in splice factor gene expression, we performed qRT-PCR on bulk PN2 testis tissue from mice treated with three different doses of dex (0, 1, and 10 $\mu\text{g} / \text{g}$). Both *Tra2b* (a regulator of exon inclusion/skipping known to be expressed in the testis (Grellscheid et al., 2011)) and *Srsf7* (a member of the SR-rich family of pre-mRNA splicing factors) showed a significant and dose-dependent decrease in expression in response to dex, confirming our RNA-seq results (**Figure 2.13A**). *Prpf31* and *Hnrnph3* showed significant decreases only at the higher and lower doses of dex, respectively, whereas *Hnrnpa2b1* showed no change. To test whether this dex-dependent decrease in a subset of splicing factors resulted in any changes in transcript isoforms within the germ cells, we utilized the rMATS program (Shen et al., 2012) to specifically quantify differential splicing events from our paired-end RNA-seq data. This analysis revealed a small set of splicing events that were significantly altered in response to dex (**Figure 2.13B**), with the majority of events categorized as skipped exon events. We selected a small subset of these events to attempt to validate by qRT-PCR, in which split primers were designed spanning these novel exon junctions (**Figure 2.13C**, blue arrows). qRT-PCR on cDNA from sorted germ cells for splicing events within *Plag1* and *Usp14* (both genes with known functions in spermatogenesis (Juma et al., 2017; Kovács et al., 2020)) showed no change (**Figure 2.13D**) in expression of the predicted isoform. However, one gene with no known role in spermatogenesis, *Epb41l4b*, showed a very robust induction of novel isoform expression, suggesting that a subset of

dex-dependent splicing changes may exist (**Figure 2.13D`**). Control primers designed against a region in all known isoforms confirmed that the dex-dependent switch in *Epb41/4b* isoform usage was not simply due to an increase in the total gene expression following dex treatment (**Figure 2.13D``**). All together these results confirmed a dex-dependent decrease in splice factor expression that may lead to a small subset of exon skipping events.

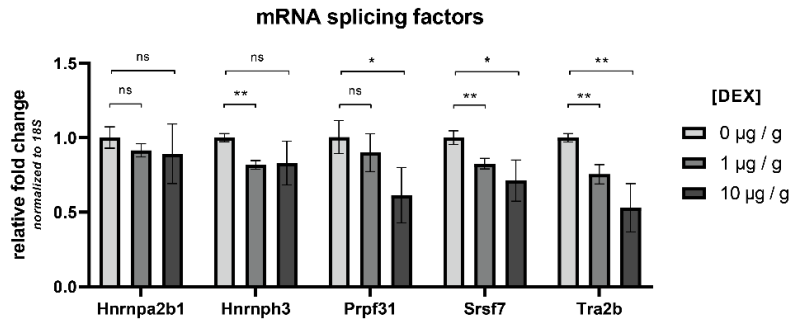
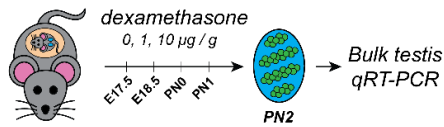
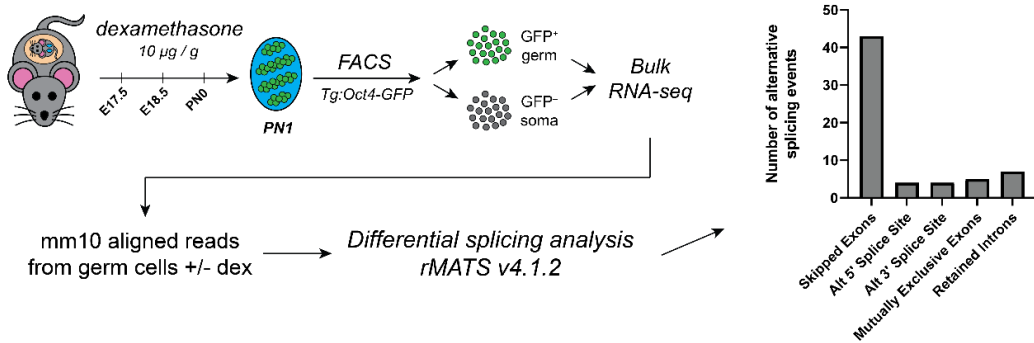
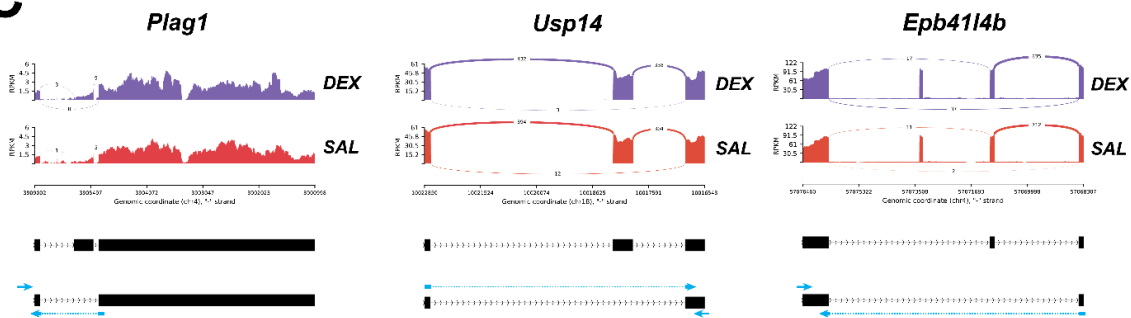
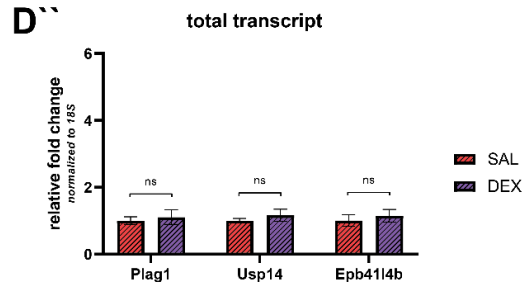
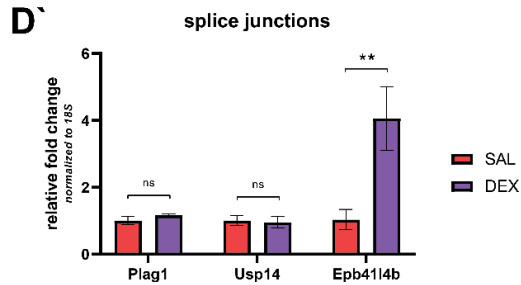
A**B****C****D**

Figure 2.13 - Dex-dependent changes in RNA splicing in the early postnatal testis

(A) qRT-PCR performed on bulk PN2 testis tissue from mice dosed with dex. Pregnant dams were injected via IP with either 1 µg / g dex, 10 µg / g dex, or a saline vehicle control at E17.5 and E18.5, and then pups were dosed with the equivalent condition via subcutaneous injection at PN0 and PN1. Genes queried were for RNA splicing factors found to be differentially downregulated in germ cells in the RNA-seq data (Figure 2.12A). Data are mean ± s.d., normalized to 18S ribosomal RNA housekeeping gene using $2^{-\Delta\Delta Ct}$ quantification method, and p-values were calculated for each dose comparison using a two-tailed, unpaired t-test, where *: $p \leq 0.05$; **: $p \leq 0.01$; n.s.: not significant.

(B) Schematic of differential transcript splicing analysis performed on sequencing reads derived from PN1 dex-dosed germ cells (Figure 2.12A). Paired-end RNA-seq results were analyzed using rMATS to detect significant differences in alternative splicing events between saline- and dex-treated germ cells. The bar graph (right) shows raw numbers of significant ($FDR \leq 0.05$) alternative splicing events, broken down by category.

(C) Representative sashimi plots highlighting select examples of “skipped exons” events that are differentially regulated in germ cells in response to dex treatment. Blue arrows represent locations of qRT-PCR primers below used in (D), with dotted lines indicating that the primer is split across the two exons indicated to allow for junction-specific amplification.

(D) qRT-PCR validation of differentially expressed isoforms performed on sorted germ cells that were treated with dex as described in (B). Primers were designed for *Plag1*, *Usp14*, and *Ebp41l4b* to specifically detect (D') the differentially spliced transcript isoforms identified in (B), or (D'') the total transcript as a control.

2.14 - Dexamethasone does not alter splicing of genes known to be differentially spliced during meiotic progression

We next sought to address whether dex treatment could alter RNA splicing at a slightly later developmental time point, specifically during the first wave of meiosis. It was previously shown, by RNA-seq analysis comparing pre-meiotic (PN6) and post-meiotic (PN21) testes, that there is a large change in the alternative splicing landscape during this transition from mitosis to meiosis (Schmid et al., 2013). In this study, Schmid and colleagues characterized a specific subset of genes that undergo meiotic-dependent switches in isoform usage, some of which were predicted to be regulated by the splicing factor Tra2β (encoded by *Tra2b*). As dex treatment resulted in a dose-dependent decrease in *Tra2b* (**Figure 2.13A**), we next wanted to address

whether dex-dependent activation of GR was sufficient to perturb these previously characterized meiosis-dependent splicing changes. Pups were treated with 2.5 µg / g of dex at PN0, PN2, PN4 and PN6, and bulk testis samples were collected for qRT-PCR at PN7 and PN21. A lower dose than the RNA-seq dosing regimen was necessary during this extended time period due to increased lethality with cumulative dosing of dex. Very surprisingly, qRT-PCR for splicing factors at PN7 revealed almost no significant changes in response to dex treatment, with the lone exception of a very small decrease in *Tra2b* expression (**Figure 2.14A`**). We confirmed dex-dependent changes in expression of the control genes *Map3k6*, *Slc25a34*, and *Zbtb16* (which were all highly upregulated in PN1 RNA-seq), suggesting that the lack of change in splice factor expression was not due to insufficient dex dosing (**Figure 2.14A``**). To further confirm that pups were responding to dex, we checked for a decrease in body weight in response to dex, as this is a known phenotype following dex or glucocorticoid treatment (Barros et al., 2018; Borges et al., 2016; Fahim et al., 2019; Gao et al., 2016; Gao et al., 2019; Guo et al., 2017a; Mehfooz et al., 2018; Natale et al., 2019; Nirupama et al., 2013; Ribeiro et al., 2018; Sakr et al., 2015; Sun et al., 2018; Xu et al., 2018; Xu et al., 2020; Zhang et al., 2011; Zou et al., 2019). As expected, pups at PN7, PN14, and PN21 all showed significant decreases in body weight and testis weight in response to dex (**Figure 2.14B**).

We next designed primers for some of the top differentially spliced genes detected by Schmid and colleagues, and validated these primers by qRT-PCR in a time course of wildtype testis tissue (**Figure 2.14C**). As expected, we were able to quantify exon loss (*Ezh2*) and exon gain (*Ralgps2*, *Vapa*) between PN7 and PN21. However, qRT-PCR on PN7 and PN21 testes from saline and dex treated pups, did not reveal any significant changes in splicing of *Ezh2*, *Ralgps2* or *Vapa* in response to dex (**Figure 2.14D**). To rule out the possibility that dex administration during the PN0 - PN6 window was too early to perturb meiotic splicing, we repeated the experiment, instead dosing at PN6, PN9, PN12, PN15, and PN18. Again, no significant

differences in alternative splicing of *Ezh2*, *Ralgps2*, or *Vapa* were detected at PN21 (**Figure 2.14E**), suggesting that GR does not play a role in the regulation of alternative splicing of these particular genes during meiotic progression.

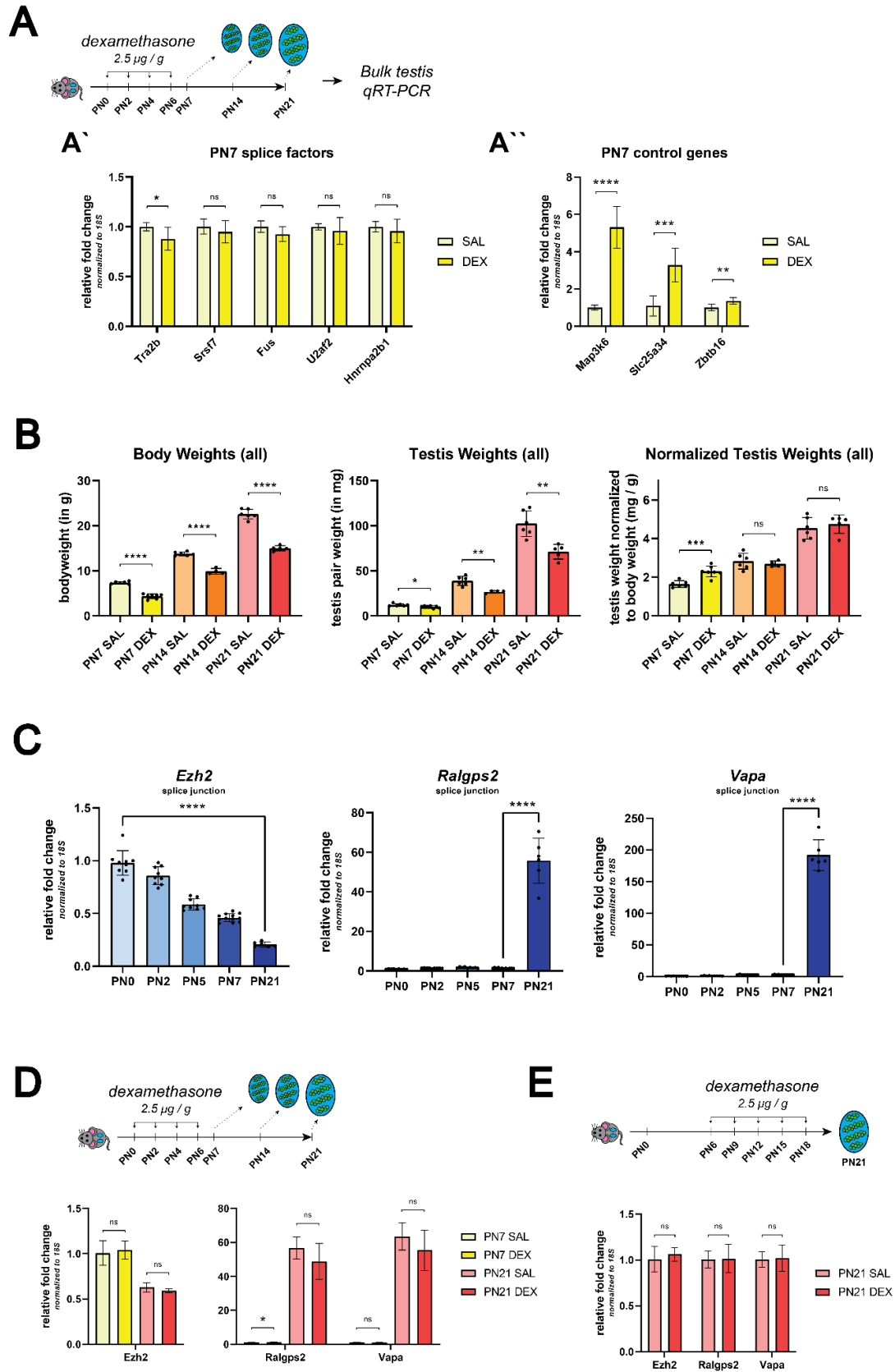


Figure 2.14 - Dex does not alter splicing of genes known to be differentially spliced during meiotic progression.

(A) qRT-PCR performed on bulk PN7 testis tissue from mice dosed subcutaneously with 2.5 µg /g dex at PN0, PN2, PN4 and PN6. Gene queried included a subset of genes for RNA splicing factors (A') as well as control genes (A'') that were differentially expressed in either germ or somatic cells of RNA-seq (Figure 2.12A). Data are mean ± s.d., normalized to 18S ribosomal RNA housekeeping gene using $2^{-\Delta\Delta Ct}$ quantification method, and p-values were calculated for each dose comparison using a two-tailed, unpaired t-test, where *: $p \leq 0.05$; **: $p \leq 0.01$; ***: $p \leq 0.001$; ****: $p \leq 0.0001$, n.s.: not significant.

(B) Body weight, testis weight, and testis weight normalized to body weight following perinatal dex administration. Pups were dosed via subcutaneous injection with saline or 2.5 µg / g dex at PN0, PN2, PN4, and PN6. Body weight was recorded immediately following euthanasia, and testis pair weight was recorded following dissection and removal of the epididymis and tunica vaginalis. Data are mean ± s.d., with each experimental group being composed of a minimum of n=6 individuals from two independent litters. P-values were calculated using a two-tailed, unpaired t-test, where *: $p \leq 0.05$; **: $p \leq 0.01$; ***: $p \leq 0.001$; ****: $p \leq 0.0001$, n.s.: not significant.

(C) qRT-PCR validating primers designed to track loss (*Ezh2*) or gain (*Ralgps2*, *Vapa*) of exons known to be differentially spliced during meiotic progression between PN6 and PN21 (Schmid et al., 2013). Data are mean ± s.d., normalized to 18S ribosomal RNA housekeeping gene, with each experimental group being composed of n=3 WT individuals. P-values were calculated for select comparisons using a two-tailed, unpaired t-test, where ****: $p \leq 0.0001$.

(D) qRT-PCR on bulk PN7 and PN21 testes showing lack of effect of dex on known meiotic splicing events. Pups were dosed via subcutaneous injection with 2.5 µg / g dex at PN0, PN2, PN4, and PN6, and pups were collected on PN7 and PN21. Data are mean ± s.d., normalized to 18S ribosomal RNA housekeeping gene using $2^{-\Delta\Delta Ct}$ quantification method, and p-values were calculated for each dose comparison using a two-tailed, unpaired t-test, where *: $p \leq 0.05$; n.s.: not significant.

(E) qRT-PCR on bulk PN21 testes showing lack of effect of dex on known meiotic splicing events following a prolonged dex dosing regimen throughout the first wave of meiotic initiation. Pups were dosed via subcutaneous injection with 2.5 µg / g dex at PN6, PN9, PN12, PN15 and PN18, and pups were collected on PN21. Data are mean ± s.d., normalized to 18S ribosomal RNA housekeeping gene using $2^{-\Delta\Delta Ct}$ quantification method, and p-values were calculated for each dose comparison using a two-tailed, unpaired t-test, where n.s.: not significant.

2.15 - Discussion

Glucocorticoid receptor immunofluorescence in the ovary and testis: discrepancies and similarities with the literature

At the onset of this project, our study was the first to have characterized the expression of GR during fetal ovary development in the mouse. Shortly after we discovered a peak in GR expression in the E13.5/E14.5 female germ cells (**Figure 2.1D**), a single cell RNA-sequencing study published by Ge and colleagues corroborated this result (Ge et al., 2021), showing that GR was expressed in the developing oocytes (at both the transcript and protein level) and steadily increased from E12.5 to E14.5. To the best of our knowledge, there are no published examples of IHC/IF for GR in the adult rodent ovary to date. We were unable to detect any appreciable levels of GR by IF in the adult oocytes of any follicular stage (**Figure 2.2B**), which contrasts with the result of Pontes et al in caprine ovaries, where the authors detected expression in primordial and antral oocytes (Pontes et al., 2019). It is unclear whether this discrepancy is due to genuine species-specific differences, or due to differences in sample preparation or antibodies used. We have rigorously validated the specificity of our GR antibody (Cell Signaling Tech #12041) in GR knockout tissue (**Figure 2.4A**) and GR knockout embryo lysate (**Figure 2.4B**). We have also validated our GR staining using mice containing an endogenous GR-GFP knockin reporter, and have observed almost perfect overlap with our antibody (data not shown). Thus, we are confident in the staining pattern observed. In the future, we would like to confirm this lack of expression by Western blot in isolated oocytes. Additionally, GR staining in the human ovary has been limited to one study in fetal tissue (Poulain et al., 2012), and thus the expression of GR in the adult ovary remains an open question. In the somatic cell compartment, we observed a strong staining in the theca cell layer

(**Figure 2.2C**), which is consistent with previous studies (Amweg et al., 2016; TETSUKA et al., 2010). Surprisingly, however, we observed very little expression of GR in the Foxl2⁺ granulosa cells. This is in contrast to IHC studies in bovine (Amweg et al., 2016) and caprine (Pontes et al., 2019) ovaries where it appears to be expressed in granulosa cells of all follicular stages. It has also been shown in a variety of studies that primary rat and human granulosa cells in culture respond very robustly to glucocorticoid treatment (ADASHI et al., 1981; Hsueh and Erickson, 1978; Kashino et al., 2021; Schoonmaker and Erickson, 1983; Yuan et al., 2014), and that this response is GR dependent (Sasson et al., 2001). The basis for this difference in our data is unclear; it is possible that GR levels in the granulosa cells are much lower than the theca cell layer (as has been suggested by one study (TETSUKA et al., 2010)) and cannot be detected by IF. It is entirely possible that GR expression could be induced during *ex vivo* culture of primary granulosa cells, thus leading to an appreciable response to glucocorticoid treatment. Future work will be needed to resolve this discrepancy.

Spatiotemporal localization of GR in the male, however, is highly consistent with the literature. In the somatic compartment, we have observed strong and reproducible staining for GR in the peritubular myoid cells and interstitial Leydig cells of the fetal, postnatal and adult testis (**Figures 2.8, 2.9, 2.10**), consistent with many other groups (Biagini and Pich, 2002; Hazra et al., 2014; Schultz et al., 1993; Stalker et al., 1989; Weber et al., 2000). In the late postnatal and adult testis, we observed a highly specific pattern of GR expression in the germline, where GR was strictly limited to undifferentiated (PLZF⁺) spermatogonia and differentiating (c-kit⁺) spermatogonia (**Figures 2.9, 2.10**). This result is consistent with multiple rodent studies showing staining in the spermatogonia (Biagini and Pich, 2002; Weber et al., 2000), as well as human studies (Nordkap et al., 2017; Welter et al., 2020). This highly restricted stage of expression suggested to us an important role in either the maintenance of spermatogonial stem cell fate, or in the induction of differentiation of the spermatogonia. Unfortunately, significant challenges with

creating a postnatal/adult deletion of GR in the germline (see below) has hindered further functional validation of this hypothesis up to this point. Lastly, we found it curious that in both the male and female germline, cells appear to express GR at the onset of meiotic initiation. In the stereotypic differentiation of the male germline, this occurs during the onset of spermatogonia differentiation (the cells with highest GR expression, **Figure 2.10A**); in the ovary, this occurs in the majority of germ cells by E13.5 (Soygur et al., 2021), which overlaps with the highest point of GR expression in the female (**Figure 2.1D**). Ge and colleagues also hypothesized that GR may be regulating the onset of female meiosis based on its highly restricted window of expression (Ge et al., 2021). Although we did not see any discernible disruptions to meiosis in the female at E15.5 (**Figure 2.5**), our difficulties in generating adults with GR deletion in the germline have prevented us from assessing whether GR plays any role in later stage of female meiosis or any role in meiosis in the male. In the future, it would be of interest to resolve this question if a functional conditional knockout model can be generated.

Discovery of novel germ cell-specific exon 1 isoform(s) in the 5' UTR of Nr3c1

GR expression varies across different cell types and tissues, and one hypothesis to explain its dynamic spatiotemporal regulation across the body is the use of alternative promoters and accompanying exon 1 variants in the 5' UTR of the gene (McCormick et al., 2000; Turner et al., 2006). By analyzing our saline control, paired-end RNA-seq data from both the E15.5 ovary (**Figure 2.6B**) and the PN1 testis (**Figure 2.12A**), we found that germ cells and somatic cells each utilize a diverse array of alternative exon 1 variants. In both the male and the female, the germ cells use a wider combination of different exon 1 variants than their corresponding somatic cells. This was a bit surprising given that the GFP⁻ cells consisted of a heterogeneous population of somatic cells. However, this could explain why GR expression in the soma is fairly consistent across development, whereas GR expression in the germ cells is highly temporally regulated.

While we observed that the majority of exon 1 / exon 2 splice junctions spanned by our paired-end sequencing reads were in previously annotated variants of exon 1, we also observed an appreciable number of reads mapping to novel exon 1 variants. One of these predicted novel exon 1 sites, which we termed exon 1 α , was found to be utilized by both male and female germ cells, yet not by the soma. We hypothesize that this could be a novel germ cell exon 1 variant, which could potentially explain the coinciding expression of GR at the onset of meiosis in both male and female (as described above). While the precise locations of the exon 1 / exon 2 splice junctions can be easily determined by mapping paired-end reads to the genome, the exact location of the promoter sequence driving expression from this novel exon can not be as easily determined. It would be interesting, perhaps using CUT&RUN or similar histone profiling method for H3K27ac, to map potential regulatory element activity around this novel exon and determine if there are any potential sites for germ cell transcription factor binding. In particular, we are curious to see whether any binding sites for the retinoic acid (RA) receptor family of transcription factors are present near this exon, due to the known role of RA in the initiation of meiosis.

The female germline is insulated from changes in GR-mediated signaling

Perhaps the most striking finding of our work was that both complete genetic deletion of GR and strong pharmacologic activation of GR led to almost no changes in the transcriptional landscape of the female germline (**Figures 2.4D, 2.4E, 2.6B**). This was an extremely surprising result given that GR is a potent transcription factor with a wide variety of functions in almost all cell types studied to date (Whirledge and DeFranco, 2018). Furthermore, the robust response of the ovarian soma, yet not the germ cells, to dex between E12.5 - E15.5 led us to hypothesize that this was not a technical artifact, but instead something inherent about the GR in the germline that resulted in minimal transcriptional response to changes in GR signaling. This is an interesting premise, as evolutionarily it would be advantageous for the germ cells to have

evolved some method to protect themselves from rampant GR-induced transcriptional changes that could result from any spikes in stress hormones experienced during gestation. What is puzzling, however, is why the germline would have evolved to retain expression of GR (in a highly spatiotemporally specific manner), given that we have thus far not seen any functional role of GR during female germline development.

Regardless of why GR is expressed in the germline, we have developed various hypotheses as to why GR in the germline may not be functional. The first hypothesis, which we have ruled out, is that the predominant isoform of GR in the female germline is either an inhibitory transcriptional or translational isoform. We have shown that there is no evidence for truncated protein isoforms (**Figure 2.7A**), and no evidence for expression of the GR β transcriptional isoform (**Figure 2.7B**). We did however observe that GR is able to change its subcellular localization in response to ligand (**Figure 2.6D''**), suggesting to us that ligand binding to GR and nuclear translocation ability remain intact. The second hypothesis is that post-translational modifications (PTMs) to GR may be interfering with its ability to either bind DNA, interact with other transcription factors, or recruit other cofactors required for its transcriptional activity. While a wide variety of PTMs to GR have been documented (Weikum et al., 2017), the limiting numbers of germ cells that can be obtained from the fetal ovary has made the detection of these PTMs via biochemical methods (particularly mass spectrometry) extremely difficult. One particular PTM of interest is acetylation of GR by the circadian histone acetyltransferase protein, Clock. Acetylation of lysines within the hinge region of GR by Clock has been shown to result in normal ligand binding and nuclear translocation, but a complete loss of the ability of GR to both activate and repress transcription (Nader et al., 2009), very similar to what is seen in the female germ cells. Interestingly, our single cell RNA-seq data shows a strong enrichment for *Clock* expression in the germ cells in comparison to the soma (data not shown), further bolstering the idea that Clock could be acetylating and inactivating GR specifically in the germ cells.

Unfortunately, while our attempts to date to detect acetylation of GR in female germ cells have proven unsuccessful for a variety of technical reasons, and we hope to address this question with ongoing experiments in the near future. Lastly, it is also possible that GR binding sites in female germ cells are masked by regions of inaccessible chromatin. We find this possibility unlikely given the wide number of potential GR binding sites across the genome, although it cannot be ruled out without future profiling of chromatin accessibility at well characterized GR binding sites.

GR in the regulation of RNA splicing

In contrast to the lack of dex-induced transcriptional changes in the female germ cells, the male germline showed a considerable transcriptional response to dex treatment at PN1 (**Figure 2.12A**). While the somatic cells of the testis showed a more stereotyped glucocorticoid response (i.e. induction of canonical GR response genes such as *Tsc22d3*, *Klf9*, *Per1*, etc.), the germ cells did not show changes in canonical genes. Instead, to our surprise, the downregulated genes showed a strong enrichment for genes involved in RNA processing and RNA splicing (**Figure 2.12B**). Furthermore, we found this decrease in splice protein expression to be dex dose-dependent (**Figure 2.13A**), further suggesting GR-dependent suppression. To the best of our knowledge, this is the first time GR has been implicated in regulating the expression of genes involved in RNA splicing and transcript processing.

Unfortunately, when we extended our analysis to assess the effect of dex on splice factor expression at later stages of postnatal testis development (PN7 and PN21) following different dex-dosing regimens, we were unable to recapitulate the suppression of splice factor gene expression seen at PN1/PN2 (**Figure 2.14A**). We curated a list of target genes known to be differentially spliced during the transition from mitosis to meiosis (Schmid et al., 2013) between

PN7 and PN21, and used qRT-PCR to quantify precise changes in the isoforms of these targets. Consistent with lack of changes in splice factor expression, we saw no changes in transcript splicing and isoform usage at PN7 or PN21 in response to two different dex treatment regimens (**Figure 2.14D,E**). One possible biological explanation for these contradictory results could be that GR is regulating the expression of splicing genes during a narrow time window shortly after birth (up to at least PN2), and that expression of these genes is no longer GR-dependent as postnatal development continues. Another possible technical explanation could be that bulk testis tissue was utilized for all PN7 and PN21 qRT-PCR expression and splicing assays, making it extremely difficult to draw definitive conclusions about the effects of dex on the germ cells specifically. Unfortunately, the Tg:Oct4-GFP reporter that we utilized at PN1 and PN2 to sort out pro-spermatogonia is turned off shortly after birth, and we did not at the time of this study have an alternative mechanism to purify the spermatogenic cells from the surrounding soma at PN7 or PN21. As splice factors are ubiquitously expressed at high levels throughout all cell types, and as the GR⁺ spermatogonia are only a small subset of the population by PN7/PN21 when the somatic compartment has grown substantially, it is entirely possible that any dex-dependent changes in splice factor expression or isoform splicing in the spermatogonia are drowned out by signal from other cells present. While Schmid and colleagues were able to detect changes in splicing in the spermatogonia using bulk testis tissue, they were comparing PN7 and PN21 testis tissue, where changes in isoform switching were quite dramatic between timepoints (Schmid et al., 2013). Dex treatment may simply elicit a more subtle phenotype that is difficult to detect without purifying the spermatogenic compartment. Future unbiased transcriptomic methods on purified spermatogonia will be more efficient and more sensitive for detecting any dex-dependent changes in splice factor expression or isoform splicing. While we employed a candidate-based approach to assess meiotic splicing events based on the work by Schmid and colleagues, it is entirely possible that GR is regulating splicing of other genes we did not query.

Difficulties in generating adult GR knockout mice

As alluded to above, we have had tremendous difficulties to date in generating adult mice with a genetic deletion of GR. Full body loss of GR results in lethality at birth due to severe defects in organogenesis, particularly in lung maturation (Cole et al., 1995), thus necessitating the creation of a conditional knockout model. At the time of this work, our lab had access to two mouse models that could be utilized to delete GR in the germline: a constitutive, transgenic *Blimp1-Cre*, and a tamoxifen inducible, endogenously targeted *Oct4-CreERT2*. Most of our work to date has been attempting to utilize the *Oct4-CreERT2* model, as *Blimp1-Cre* mice demonstrated exceptionally poor breeding efficiency, and extremely small litter sizes, even when outcrossed to a mixed genetic background. This *Oct4-CreERT2* line has proven very effective at excising GR from virtually every germ cell of both male and female when tamoxifen (125 µg / g) is administered during gestation (between E9.5 and E10.5). However, the high doses of tamoxifen required in order to induce recombination of the GR flox allele also led to high rates of dystocia in the dam, and overall inability to deliver pups (presumably due to adverse effects of tamoxifen on the uterus (Lizen et al., 2015; Nakamura et al., 2006)). While our lab has had some success with co-administration of progesterone to counteract the effects of tamoxifen (B. Soygur, personal communication), this is only efficient when low doses of tamoxifen are used (e.g. for sparse labeling) and thus not efficient for this system. While some groups we have spoken with have reported success with C-sections and fostering of pups, we have had extremely variable results - including high rates of cannibalism by foster mothers.

To circumvent this problem of fetal tamoxifen administration, we have recently begun attempts to administer tamoxifen to early postnatal pups immediately after birth. As GR expression is maintained in the spermatogonia into adulthood, and as the vast majority of pro-spermatogonia still express *Oct4* prior to PN2, we are hopeful that this will enable us to efficiently delete GR in

the majority of the germline while avoiding the problems of fetal tamoxifen administration as outlined above. While pups are able to survive two sequential days of tamoxifen treatment (PN1 and PN2; 125 µg / g) without any problems, we recently noticed that Oct4-CreERT2+ pups have selectively begun to die at approximately PN10 (in comparison to their CreERT2- littermates). This was an extremely surprising finding, given that Oct4 is believed to be expressed exclusively in the pro-spermatogonia at this time point. This result would suggest, however, that Oct4 is expressed elsewhere in the body, particularly in a cell type in which loss of GR is lethal. Experiments are ongoing to address whether this can be resolved. Furthermore, this system of postnatal administration of tamoxifen is unfortunately not useful for the female, as the peak in GR expression in the oocyte is E13.5/E14.5. Therefore, additional methods will need to be explored in order to generate female conditional knockout mice.

Lastly, current attempts to generate conditional knockout mice (both male and female) using the Blimp1-Cre model were unsuccessful. To date, we have not obtained any live mice with a Blimp1-Cre mediated excision of GR. While Blimp1 expression in the gonad is specifically limited to the germ cells, Blimp1 is also expressed in many other tissues, including the skin and a subset of T cells. It is unclear whether loss of GR in these or any other Blimp1+ tissues is lethal and thus could explain why we are not able to get any conditional knockout mice, or whether this is simply a result of the extremely small litters of 1-3 pups.

The generation of a conditional knockout model of GR in the germline is crucial for answering many outstanding questions in the field of transgenerational epigenetic inheritance of stress-induced phenotypes. While there is a vast body of literature demonstrating that stress models and direct glucocorticoid administration can dramatically impact the cells of the germline, it remains difficult to disentangle the direct effects of stress/glucocorticoids on the germ cells from the various other somatic cell alterations and/or hormonal dysregulation that

accompany these phenotypes. Therefore, there is a crucial need to generate germ cell conditional knockouts of GR in order to determine the germ cell intrinsic roles, if any, that GR might be playing in both the male and female germline. This is particularly important for the female, as the effects of GR perturbations may not become apparent until later in life. It was recently demonstrated in zebrafish that while deletion of GR resulted in no fertility problems early in life, fish eventually developed a phenotype of accelerated ovarian aging and decline in fertility (Facchinello et al., 2017; Faught et al., 2020; Maradonna et al., 2020). It is very possible that the same could hold true for mice, and we have thus far been unable to detect any phenotypic consequences of disrupted GR signaling in the female as we are limited to observing fetal samples. Similar questions exist in the male, where the stage-specific expression of GR in the spermatogonia suggests a functional role for GR in maintaining the spermatogonia fate. The effects of loss of GR in the spermatogonia might not be immediately apparent, and thus may also require longer-term fertility studies following loss of GR. Overall, the germ cell intrinsic role of GR in both the male and the female remains perhaps one of most important unanswered questions regarding whether the direct effects of stress and glucocorticoids on the germ cells can lead to heritable phenotypic changes. I urge anyone following up on my work to consider this question carefully.

2.16 - Materials and Methods

Mouse husbandry. All animal work was performed under strict adherence to the guidelines and protocols set forth by the University of California San Francisco's Institutional Animal Care and Use Committee (IACUC), and all experiments were performed in an animal facility approved by the Association for the Assessment and Accreditation of Laboratory Animal Care International (AAALAC). All mice were maintained in a temperature-controlled animal facility with 12 hour light dark cycles, and were given access to food and water ad libitum.

Mouse timed pregnancies. All matings were set in the evenings (15:00 or after), and the presence of a vaginal plug the morning after mating (08:00 – 11:00) was denoted embryonic day 0.5 (E0.5). Pregnant females were dissected at various timepoints, the uterine horns removed into ice-cold 0.4% BSA in PBS, and embryos dissected and staged based on canonical morphologic features. For all postnatal timepoints, postnatal day 0 (PN0) was assigned as the morning a litter was first seen (where litters were dropped the night of E18.5).

Genotyping. Total genomic DNA was extracted from ear punches or tail tips by boiling in alkaline lysis buffer (25 mM NaOH ; 0.2 mM EDTA) for 45 minutes at 95°C, cooling to 4°C, and then neutralizing with an equal volume of 40 mM Tris-HCl. All genotyping reactions were performed with KAPA HotStart Mouse Genotyping Kit (Roche, 07961316001) with 1 µL of gDNA and a final primer concentration of 5 µM each. Cyclor conditions are listed below each table. All PCR products were separated by electrophoresis on a 2% agarose gel in TBS stained with ethidium bromide (VWR, E3050), and genotypes determined based on sizes of DNA products.

Table 2.1: Mouse lines used, genotyping primers, and genotyping reactions

Allele	Primer Sequences	Expected Sizes	MGI#	Rxn
<i>Nr3c1</i> ^{tm1.1Jda}	5'-CAGGTATTGGTGCTTGTAGCACTT-3'	WT: 155 bp	5447468	A
	5'-GCCTGCATCTTTTACATGTGTTGTTTCC-3'	KO: 208 bp		
	5'-CAGCTTACAGGATAGCCAGTGATATCTGT-3'	Flox: 318 bp		
<i>Pou5f1</i> ^{tm1.1(cre/Esr1*)Yseg}	5'-GCTTTCTCCAACCGCAGGCTCTC-3'	WT: 234 bp	5049897	A
	5'-CCAAGGCAAGGGAGGTAGACAAG-3'	Cre: 169 bp		
	5'-GCCCTCACATTGCCAAAAGACGG-3'			
<i>Tmem163</i> ^{Tg(ACTB-cre)2Mrt}	5'-TGCAATCCCTTGACACAGA-3'	WT: 241 bp	2176050	A
	5'-ACCAGTTTCCAGTCCTTCTGG-3'	Cre: 187 bp		
	5'-GTCCTTACCCAGAGTGCAGGT-3'			
<i>Tg(Pou5f1-EGFP)2Mnn</i>	5'-GCACGACTTCTTCAAGTCCGCCATGC-3'	Tg: 270 bp	3057158	B
	5'-GCGGATCTTGAAGTTCACCTTGATGCC-3'			
<i>Tg(Prdm1-cre)1Masu</i>	5'-GCCGAGGTGCGCGTCAGTAC-3'	Tg: 200 bp Ctrl: 324 bp	3586890	C
	5'-CTGAACATGTCCATCAGGTTCTTG-3'			
	5'-CTAGGCCACAGAATTGAAAGATCT-3'			
	5'-GTAGGTGGAAATTCTAGCATCATCC-3'			
Cycler conditions: (A) 94°C, 30 sec – 1 cycle // (94°C, 15 sec ; 60°C, 15 sec ; 72°C, 30 sec) – 35 cycles // (72°C, 10 min) – 1 cycle // 4°C hold. (B) 93°C, 1 min – 1 cycle // (93°C, 20 sec ; 68°C, 3 min) – 30 cycles // (72°C, 10 min) – 1 cycle // 4°C hold. (C) 94°C, 30 sec – 1 cycle // (94°C, 15 sec ; 66°C, 15 sec ; 72°C, 30 sec) – 35 cycles // (72°C, 10 min) – 1 cycle // 4°C hold.				

Embryonic gonad digestion. Fetal gonads were dissected into ice cold 0.4% BSA in PBS, washed once, and maintained on ice until ready for digestion. 0.4% BSA solution was removed and replaced with 100 µL of 0.25% Trypsin-EDTA (Fisher Sci, 25200056) per ovary pair, or 150 µL per testis pair. Samples were incubated in a 37°C water bath for 30 minutes, with gentle pipetting every 10-15 minutes to facilitate the dissociation. After 30 minutes, DNase I (1 mg /

mL) was added at a 1:10 dilution, and samples were incubated another 10 minutes at 37°C. Samples were pipetted to ensure complete digestion, and then an equal volume of ice-cold FBS (Gibco, 10437028) was added to inactivate trypsin. To prepare for FACS sorting, Sytox Blue viability dye (Invitrogen, S34857) was added to samples at 1:1000 dilution, and then samples were filtered through a 35 µm filter into FACS tubes (Falcon, 352235).

Tissue Fixation. All mouse gonad tissue was fixed with fresh 4% paraformaldehyde (PFA) in PBS at 4°C with rocking. Fixation times were as follows:

Table 2.2: Tissue fixation parameters

Sex	Stage	Vol 4% PFA	Fixation Time	PBS Washes
XY	E12.5 - E14.5	1 mL / litter	30 min	3 x 10 min
	E15.5 - E16.5	1 mL / litter	45 min	3 x 10 min
	E17.5 - E18.5	1 mL / litter	1 hr	3 x 10 min
	PN0 - PN2	1 mL / pair	2 hr	4 x 10 min
	PN3 - PN5	1 mL / pair	4 hr	4 x 10 min
	PN6 - PN10	1 mL / testis	6 hr	4 x 15 min
	PN11 - PN14	4 mL / testis	12 hr	4 x 15 min
	PN15 - PN17	4 mL / testis	15 hr	4 x 15 min
	PN18 - PN21	4 mL / testis	18 hr	4 x 15 min
	Adult	4 mL / testis	O/N	4 x 15 min
XX	E12.5 - E15.5	1 mL / litter	30 min	3 x 10 min
	E16.5 - E18.5	1 mL / litter	45 min	3 x 10 min
	PN0 - PN7	1 mL / pair	2 hr	4 x 10 min
	PN21 - Adult	4 mL / ovary	O/N	4 x 15 min

Tissue Embedding and Sectioning. Following PFA fixation and PBS washes, embryonic gonads were incubated overnight in 30% sucrose (in PBS) at 4°C. The following day, the tissue was embedded in OCT (Tissue-Tek, 4583) and blocks stored at -80°C until ready for sectioning. For all postnatal and adult tissues, gonads were first incubated in 10% sucrose (in PBS) for about 1-2 hours at 4°C until the tissue sank to the bottom of the tube. Gonads were then transferred to incubate overnight in 30% sucrose (in PBS) at 4°C. The following day, the tissue was transferred to 50/50 OCT / 30% sucrose and allowed to equilibrate for 6 hours at 4°C prior to embedding in 100% OCT. Blocks were similarly stored at -80°C until ready for sectioning. All blocks were sectioned on a Leica 3050S Cryostat at a thickness of 5 – 10 µm depending on the tissue.

Section Immunofluorescence. For all cryosectioned slides, slides were thawed to room temperature and then washed three times (5 min each) with 1X PBS to remove residual OCT. Slides were blocked for one hour at room temperature in 10% heat inactivated donkey serum + 0.1% Triton X-100 in PBS. All primary antibody incubations were performed at 4°C overnight in a humidified chamber, with primary antibodies diluted accordingly in blocking buffer. The next day, slides were washed three times with 1X PBS (5 min each), followed by a one hour incubation at RT with secondary antibodies diluted in blocking buffer. Samples were washed three times with 1X PBS (5 min each), mounted in VECTASHIELD Antifade Mounting Medium (Vector Laboratories, H-1000), and sealed with a coverslip.

Wholemout Immunofluorescence. Mouse fetal gonads for wholemount immunofluorescence staining were dissected at E18.5 into 0.2% bovine serum albumin (BSA) in 1X phosphate-buffered saline (PBS) then transferred into 1.5mL Eppendorf tubes. Subsequent fixation and staining steps were carried out on a rocking shaker. Fetal gonads were fixed with 4% paraformaldehyde (PFA) in PBS for 2 hours at 4°C. After fixation, the samples were washed

3 times for 10 minutes each in 0.2% BSA in PBS at room temperature. The fetal gonads were then blocked with 2% BSA and 0.1% Triton X-100 in PBS overnight at 4°C. Primary antibodies were diluted in 0.2% BSA and 0.1% Triton X-100 in PBS and fetal gonads were incubated in primary antibody for 5 nights at 4°C. The samples were then washed 4 times for 15 minutes each in 0.1% Triton X-100 in PBS at room temperature. Alexa Fluor-conjugated secondary antibodies were diluted in 0.2% BSA and 0.1% Triton X-100 in PBS and fetal gonads were incubated in secondary antibody for 5 nights at 4°C. The samples were then washed 3 times for 30 minutes each in 0.2% BSA and 0.1% Triton X-100 in PBS at room temperature. Fetal gonads were dehydrated using a methanol:PBS series (25% to 50% to 75% to 100%) for 10 minutes each, incubating in 100% methanol twice, at room temperature. To remove autofluorescence from blood cells, dehydrated gonads were then incubated in 3% H₂O₂ in methanol overnight at 4°C. Fetal gonads were washed 2 times for 30 minutes each in 100% methanol at room temperature then transferred into 10mm long glass cylinders (ACE Glass 3865-10) mounted on coverslips (Fisherfinest Premium Cover Glass 12-548-5P) and incubated in benzyl alcohol:benzyl benzoate (1:2) overnight at 4°C. Fetal gonads were imaged using a white-light Leica TCS SP8 inverted confocal microscope with an HC PL APO CS 10X/0.40 dry objective and 1024x1024 pixel resolution. Fetal ovaries were imaged with 1X optic zoom and 2 µm z stacks. Fetal testes were imaged with 0.75X optic zoom, 3 µm z stacks, and using tile scans which were merged using Leica software.

Confocal Microscopy. All imaging was performed on a white-light Leica TCS SP8 inverted confocal microscope (both section IF and wholemount IF) using either an HC FLUOTAR L 25x/0.95 VISIR water objective (Leica) or an HC PL APO 63x/1.40 CS2 oil objective (Leica). All images were taken at 1024 x 1024 pixel resolution, and any tile scan images were merged using Leica software.

Quantitative Image Analysis using Imaris. All analyses described below were performed using Imaris Microscopy Image Analysis Software v8.3.1 (Oxford Instruments).

Cellular segmentation with WGA: In order to segment individual cells within a tissue section, we utilized fluorophore-conjugated forms of the lectin wheat germ agglutinin (WGA) (Biotium, 29022-1, 29062-1, 29025-1) to outline all cellular membranes. Slides were stained overnight with WGA (1:50) using the standard section immunofluorescence protocol outlined above. Confocal .lif files were imported into Imaris, and individual cells were computationally segmented using the “Cell” module with the following settings: { Detection Type: “Detect Cell Only” // Region: “Whole Image” // Cell Type: “Cell Membrane” // Cell Smallest Diameter: “7 μm ” // Cell Membrane Detail: “0.75 μm ” // Cell Filter Type: “Smooth” // Quality Threshold: “Manual” // Number of voxels: >20.0 }. The resulting segmented regions were then filtered to remove “empty” (non-cell-containing) regions by applying the following filters: { Size Filter: “25 – 400 μm^2 ” // Cell Intensity Mean (DAPI channel): >20.0 }. Lastly, regions containing doublet cells (based on DAPI), were manually removed. To further subset out germ cells, an additional filter was applied based on the germ cell marker used: { Cell Intensity Mean (Germ cell marker channel): *manually determined* }.

Calculating normalized GR protein levels: After performing cellular segmentation with WGA as described above, the mean fluorescence intensity values of all channels were exported for each individual cell. Mean fluorescence intensity values for the GR channel were normalized to those of the DAPI channel on a per cell basis, and the resulting normalized values were plotted.

RNA isolation. For bulk gonad tissue (both freshly isolated and *ex vivo* cultured), gonads were first homogenized in a 1.5 mL centrifuge tube in 100 μL TRIzol (Invitrogen 15596026) using a motorized pestle. After bringing the final volume to 1 mL with TRIzol, samples were vortexed on

high for 30 seconds before storing at -80°C. To extract total RNA from TRIzol samples, 200 µL of chloroform was added per sample. Samples were vortexed vigorously for 30 seconds and then centrifuged at 12,000xg for 15 min at 4°C. The upper aqueous layer was carefully extracted, mixed 1:1 with an equal volume of fresh 70% ethanol, and loaded onto a QIAgen RNeasy Micro spin column for further cleanup and elution. The QIAgen RNeasy Micro Kit (cat. no. 74004) protocol was followed exactly, including the on-column DNase digestion for 15 min. For FACS-sorted cell samples that were sorted into QIAgen RLT Plus Buffer, samples were mixed with equal volume of 70% ethanol and loaded onto column without TRIzol homogenization and chloroform extraction. RNA concentrations were quantified using the Qubit RNA HS Assay Kit (ThermoFisher cat. no. Q32852) following the manufacturer's protocol.

Quantitative RT-PCR. Prior to qRT-PCR, 100 – 1000 ng of RNA per sample was reverse transcribed using the qScript cDNA SuperMix (QuantaBio cat. no. 95048-100). qRT-PCR was performed using PowerUp SYBR Green Master Mix (Thermo A25776), as per manufacturer's instructions. For each individual reaction, 1 ng total cDNA was used, with a final primer concentration of 0.5 µM each, and all reactions were performed in technical triplicate. All experiments were run on a ThermoFisher QuantStudio 5 with the following cycler conditions: (50°C, 2 min) – 1 cycle // (95°C, 2 min) – 1 cycle // (95°C, 30 sec ; 60°C, 1 min) – 40 cycles. For all experiments, qRT-PCR analysis was performed using standard $\Delta\Delta C_T$ method. Briefly, ΔC_T values were calculated by normalizing C_T values for individual target probes to the average C_T value of a standard housekeeping gene (typically 18S ribosomal RNA); $\Delta\Delta C_T$ values were calculated by normalizing sample ΔC_T values to the reference sample of choice (here usually "WT" or dex untreated); Fold change values were calculated by taking $2^{-\Delta\Delta C_T}$.

SYBR Green qRT-PCR Primer Design. All primer sets used for qRT-PCR were designed from scratch. For each gene of interest, the mouse cDNA sequence of the predominant, full-length

isoform was downloaded from the Ensembl database (<https://www.ensembl.org>). To identify potential primers with minimal off-target amplification across the mouse transcriptome, cDNA sequences were uploaded to NCBI's Primer BLAST tool (<https://www.ncbi.nlm.nih.gov/tools/primer-blast>), and primer searches were run with the following modified search parameters: PCR product size: 70-200 bp; Primer melting temperatures: Min: 60°C, Opt: 62°C, Max: 64°C, Max T_m diff: 1°C ; Database: Refseq mRNA ; Organism: Mus musculus ; Primer specificity stringency: "Ignore targets that have more than 4 or more mismatches to the primer" ; Primer GC content: 30-70% ; Max self complementarity: 3.00 ; Max pair complementarity: 3.00 ; Concentration of divalent cations: 3 ; Concentration of dNTPs: 0.2. Resulting putative primer pairs were screen manually for minimal self/pair complementarity scores, and then checked using the Beacon Designer tool (<http://www.premierbiosoft.com/qOligo/Oligo.jsp?PID=1>) for any potential primer-dimer events by selecting for primer pairs that had ΔG values closest to zero for Cross Dimer, Self Dimer and Hairpin scores. Lastly, the expected PCR product of any putative primer pairs was checked for potential secondary structure formation using IDT's UNAFold program (<https://www.idtdna.com/unafold>). As no primer pairs were completely without potential secondary structure formation, primer pairs were deemed acceptable so long as none of the predicted secondary structures had an anticipated T_m value at or above the annealing temperature of our cycler reaction (60°C). Whenever possible, primer pairs that spanned an intron were selected to minimize any amplification from contaminating genomic DNA. All primers used were validated through a standard melt curve analysis following qRT-PCR reactions (95°C, 30 sec // 60°C, 1 min // 95°C then dec by 0.15°C every sec) to ensure the amplification of a single PCR product as anticipated, and any primer pairs that failed melt curve analysis were discarded and redesigned.

Qualitative RT-PCR. Prior to RT-PCR, 100 – 1000 ng of RNA per sample was reverse transcribed using the qScript cDNA SuperMix (QuantaBio, 95048-100). All PCR reactions were performed using GoTaq Green Master Mix (Promega, M7123) with 0.25 ng total cDNA per reaction, with a final primer concentration of 0.5 μ M each. Cyclor conditions: { 95°C, 3 min – 1 cycle // (95°C, 15 sec ; (55-60)°C, 15 sec ; 72°C, 30 sec) – 35 cycles // (72°C, 10 min) – 1 cycle // 4°C hold }. For each primer pair, a temperature gradient PCR was used to determine the optimal annealing temperature. Products were electrophoresed on a 2% agarose gel at 150V for 30 minutes, and then visualized using a Bio-Rad GelDoc imager. Mouse XpressRef Universal Total RNA (QIAGEN, 338114) was reverse transcribed and used at a concentration of 250 ng cDNA per reaction as a positive control for each primer set. Nuclease free water (Thermo Fisher, AM9937) was used as a negative control.

Fluorescence Activated Cell Sorting (FACS). To isolate germ cells expressing the Pou5f1- Δ PE-eGFP transgene from the GFP⁻ somatic compartment, we utilized either a BD FACSAria II or III system. Briefly, cells were gated to remove doublets/multiplets via FSC height vs area comparison, and then dead cells were gated out based on uptake of the Sytox Blue viability dye. GFP⁺ germ cells and GFP⁻ somatic cells were sorted directly into 300 μ L of QIAGEN RLT Plus Buffer (with β ME). Upon completion of the sort, samples were immediately vortexed for 30 sec and flash frozen.

Dex *in vivo* dosing. For all *in vivo* dex dosing experiments, a water-soluble form of dex (Sigma, D2915) was utilized to allow for delivery in a saline vehicle (0.9% NaCl w/v in ddH₂O). The developmental time windows of dex administration were determined based on GR's germline expression profile, and differed for the male and female germline. Dex dose and time windows varied between experiments, and are carefully outlined for each experiment in the Results section. For all injections, the volume given to both saline and dex treated animals was fixed,

where the concentration of dex in the injected solution was scaled to ensure precise dose delivery (normalized to body weight) in the fixed volume. For gestational timepoints (E12.5 - E18.5), pregnant dams were injected via IP injection at approximately 09:00 with 100 μ L saline/dex. For postnatal timepoints (PN0 - PN21), pups were weighed and injected subcutaneously (in the back flank) with 20 μ L of saline or dex. See experimental schematics for exact doses and timing.

Ex vivo gonad culture. Fetal ovaries were dissected at E14.5 and pooled into ice cold 0.4% BSA in PBS as described above. Ovaries were cultured in Millicell 24-well hanging inserts, 1.0 μ m PET (Millipore, MCRP24H48) at 37°C, 5% CO₂. Ovaries were cultured in DMEM / F12 base medium (Gibco, 11330-032) supplemented with 10% charcoal-stripped FBS (Sigma, F6765), 1 mM sodium pyruvate (Gibco, 11360070), 0.5X MEM Nonessential Amino Acids (Corning, 25-025-CI), and 100 U/mL pen/strep (Gibco, 15140-122). Bottom chambers were filled with 1.3 mL of media, top inserts with 200 μ L of media, and the media was changed daily. For experimental conditions, dex (Sigma, D1756) dissolved in DMSO was added to cultures at a final concentration of 1.0 μ M.

Preparation of Meiotic Spreads from Embryonic Ovaries. After dissection, ovary pairs were transferred to 1 mL centrifuge tubes containing 100 μ L of dissociation buffer (0.025% Trypsin, 2.5 mg/mL collagenase, and 0.1mg/mL DNase). Samples were incubated in a 37°C water bath for 30 minutes, and were pipetted vigorously every 10 minutes using a P-200 pipette to facilitate digestion. After 30 minutes, trypsin activity was stopped by adding an equal volume of FBS and mixing well. Next, an equal volume of hypotonic buffer (30 mM Tris pH 8.2, 50 mM sucrose, 17 mM sodium citrate, 5 mM EDTA, 0.5 mM DTT, 0.5 mM PMSF, at a final pH of 8.2) was added per sample, and samples were incubated for 30 minutes at room temperature. Samples were centrifuged for 10 min at 1000 rpm at room temperature, the supernatant removed, and then

resuspended in 100 mM sucrose (+ 7.5 mM Boric acid, final pH 8.2). Samples were typically resuspended in 60 μ L per ovary, which usually made three slides per ovary. Positively charged slides were pre-cleaned with 70% ethanol, and then dried gently with a Kimwipe. Using a hydrophobic pen, a small (~2cm x 2cm) square was drawn on each slide, and the squares were each coated with approximately 20 μ L of fixative solution (1% PFA, 0.15% Triton X-100, 3 mM DTT, 7.5 mM Boric acid, final pH 9.2). Using a P-20 pipette, 20 μ L of the cell suspension was dropped onto the square from approximately one foot above. Slides were incubated for 1 hour in a covered humidified chamber at room temperature to allow fixation of nuclei to slide, and then incubated uncovered for approximately three hours to allow slides to fully dry. Once dry, slides were washed twice with 0.4% Photoflo in H₂O (Kodak, 146 4510) by fully submerging slides for two minutes each. Finally, slides were allowed to fully dry, then stored at -80°C until ready to stain.

Staining of Meiotic Spreads – Sycp1, Sycp3 and γ H2AX co-stain. Slides were warmed to room temperature, and then immediately incubated with 0.1% Triton X-100 in PBS for 10 minutes to permeabilize. Slides were washed three times with 1X PBS for five minutes each, and then blocked for 1 hour at room temp in 5% BSA in PBS. Slides were incubated overnight at 4°C with primary antibodies diluted in 5% BSA: rabbit α -Sycp1 (abcam, ab15090; 1:200) and mouse α - γ H2AX (Millipore Sigma, 05-636-I; 1:200). The following day, slides were washed three times, ten minutes each, with 1X PBS, and then incubated for 1 hour at room temp with secondaries in 5% BSA: donkey α -mouse 555 (1:200), donkey α -rabbit 647 (1:200), and DAPI (1:1000). Next, slides were washed three times, ten minutes each, with 1X PBS, and then incubated for 1 hour at room temp with pre-conjugated mouse α -Sycp3 (abcam, ab205846; 1:50). Slides were washed again three times, and then mounted with VECTASHIELD Antifade Mounting Medium (Vector Laboratories, H-1000).

Protein Extraction and Quantification. Proteins were extracted from either whole-gonad tissue or FACS-sorted cells using Pierce RIPA Buffer (Thermo Fisher, 89900) as per the manufacturer's protocol. For FACS-sorted, frozen cell pellets (100-300k cells), pellets were thawed on ice and resuspended in 100 μ L of RIPA buffer. Suspension was incubated on ice for 15 minutes, with vortexing every three minutes. Suspension was spun at 16,000xg for 15 min at 4°C to pellet non-soluble cellular debris, and then supernatant transferred to a fresh tube. For whole-gonad tissue, dissected gonads were washed once with 1X PBS (without BSA), and then resuspended in 100-200 μ L of RIPA buffer (depending on stage / number of gonads). Tissue was homogenized using a motorized pestle, on ice, until no visible tissue pieces remained. The suspension was then incubated on ice for 15 minutes (with vortexing every three minutes), and spun at 16,000xg for 15 min at 4°C as described above. Total amount of protein was quantified using a Pierce BCA Protein Assay Kit (Thermo Fisher, 23227) with BSA protein standards, following the manufacturer protocol exactly.

Western Blotting. Prior to loading, protein samples were diluted with sample buffer (4X Laemmli Buffer (Bio-Rad, #1610747) supplemented with 10% β -mercaptoethanol) and water to reach a final sample buffer concentration of 1X. Samples were boiled in microcentrifuge tubes in a thermocycler for 5 minutes at 95°C to denature proteins. For all blots, samples were run on Tris/Glycine Mini-PROTEAN TGX Precast SDS-PAGE gels, 4-15% (Bio-Rad #4561085), with 1X Tris/Glycine/SDS Buffer (Bio-Rad #1610732). 5 μ L of either WesternSure Pre-stained Chemiluminescent Protein Ladder (LI-COR #926-98000) or Chameleon Duo Pre-stained Protein Ladder (LI-COR #928-60000) were used depending on the downstream imaging system. All gels were electrophoresed at 50V for 10 minutes, and then 100V for 50-60 minutes. All gels were transferred to Immobilon-FL PVDF Membrane (Millipore #IPFL10100) (pre-activated with 100% methanol) using the Bio-Rad Trans-Blot SD semi-dry transfer cell (Bio-Rad # 1703940) at 15V for 60 min at 4°C. Transfer buffer was prepared as a 1X final solution by mixing 7:2:1 of

ddH₂O : methanol : 10X Tris/Glycine Transfer Buffer (Bio-Rad #1610734). Following transfer, membranes were blocked for 60 min with 5% non-fat milk (Bio-Rad #1706404) prepared in 1X TBST (TBS + 0.1% Tween 20 ; Bioworld #42020084-1) on a rotator at RT. Primary antibodies were diluted in 5% non-fat milk and membranes incubated at 4°C overnight with gentle rotation. The following day, membranes were washed three times with 1X TBST for 5 min at RT with gentle rotation. Secondary antibodies, HRP-conjugated goat α-rabbit IgG (Abcam #ab205718) or HRP-conjugated goat α-mouse IgG (Abcam #ab205719) were diluted 1:5000 in 5% non-fat milk and incubated with membranes for 1 hr at RT with gentle rotation, and then washed three times with 1X TBST for 5 min at RT with gentle rotation. Membranes were imaged using the Pierce ECL Western Blotting Substrate (Thermo #32109) and developed on autoradiography film.

Single cell RNA sequencing.

Sample preparation: To generate embryos homozygous for the GR knockout allele (GR^{KO/KO}), heterozygous females (GR^{KO/+}) were crossed to heterozygous males also carrying an Oct4-GFP transgene (GR^{KO/+} ; Tg:Oct4^{GFP/GFP}) to facilitate FACS sorting of germ cells. Pregnant dams were dissected the morning of E15.5, and tail clips were taken from each embryo to determine GR genotype. Fetal ovaries were dissected on ice, the mesonephroi removed, and the ovaries were digested for FACS sorting as described above. Fetal ovaries were pooled based on genotype (n=4 ovary pairs for WT GR^{+/+}, and n=2 ovary pairs for GR^{KO/KO}). In order to enrich for germ cells (relative to the predominant somatic cells), live germ cells were FACS sorted based on Tg:Oct4^{GFP} expression, and somatic cells spiked back into the germ cell population at a ratio of 60 : 40, germ : soma. The final cell suspension was resuspended in 0.04% BSA at a concentration of 1000 cells / μL, and was used for 10X single cell capture as described below.

10X Capture, Library Preparation, and Sequencing: The following sample preparation and sequencing was all performed by the UCSF CoLabs Initiative. All samples were processed with the standard Chromium 10X Single Cell 3' Reagent Kit v3 workflow. In summary, final cell suspensions were loaded onto the 10X Chromium microfluidics chip along with reaction master mix, partitioning oil, and Single Cell 3' v3 Gel Beads in order to generate Gel Beads-in-emulsion (GEMs) containing individual cells. RT reactions were performed within individual GEMs to generate cell-barcoded full-length cDNA, followed by GEM breakdown, cDNA pooling, cDNA PCR amplification, cleanup, and QC. Amplified cDNA was enzymatically fragmented, end repaired, A-tailed, size selected, and ligated with adapters. Following a sample indexing PCR reaction and final size selection, sample libraries were pooled, QC'ed, and sequenced on an Illumina NovoSeq 6000 platform. Resulting paired-end sequencing reads were processed using the 10X Cell Ranger software to generate feature-barcode matrices.

Data Analysis: All single cell RNA-seq data processing was performed in house using Seurat(Satija et al., 2015) v3.2.3. Count matrices for both WT and KO conditions were read into Seurat to create Seurat Objects, and were then filtered as follows: WT: { nFeature_RNA: 1500 – 6500 // nCount_RNA: 5500 – 40000 // % mitochondria: < 10% }; KO: { nFeature_RNA: 1200 – 5500 // nCount_RNA: 3000 – 30000 // % mitochondria: < 10% }. Both WT and KO Seurat objects were combined using the “merge” function, and the resulting objects were processed for dimensional reduction using the standard Seurat workflow using the following functions: NormalizeData, FindVariableFeatures, ScaleData, RunPCA, RunUMAP, FindNeighbors, and FindClusters. During ScaleData, the following variables were regressed out: nFeature_RNA, nCount_RNA, percent.mito, and percent.ribo. The cell type identities of each cluster were determined by comparing top cluster markers to a previously annotated list E16.5 ovarian cell type specific markers(Niu and Spradling, 2020). Pairwise differential gene expression analyses were performed between WT and KO cells independently for each of the main cell type clusters

(germ, theca, granulosa, and epithelia) using the FindMarkers function using the default Wilcoxon Rank Sum test. Genes with an adjusted p-value less than 0.05 and a log fold change greater than 0.25 were considered significant.

3' Tag-Seq

Sample preparation: To generate embryos homozygous for the GR knockout allele ($GR^{KO/KO}$), heterozygous females ($GR^{KO/+}$) were crossed to heterozygous males also carrying an Oct4-GFP transgene ($GR^{KO/+}$; $Tg:Oct4^{GFP/GFP}$) to facilitate FACS sorting of germ cells. Pregnant dams were dissected the morning of E17.5, and tail clips were taken from each embryo to determine GR genotype. Fetal ovaries were dissected on ice, the mesonephroi removed, and the ovaries were digested for FACS sorting as described above. $Tg:Oct4-GFP^+$ germ cells from individual embryo ovary pairs were FACS sorted directly in QIAgen RLT+ buffer and stored at -80 until ready for RNA extractions as outlined above. To generate embryos with a conditional deletion of GR ($GR^{cKO/cKO}$), females homozygous for an exon 3 floxed GR allele ($GR^{flox/flox}$) were crossed to similar males that were also heterozygous for the germ cell specific Oct4^{CreERT2} allele ($GR^{flox/flox}$; $Oct4^{CreERT2/+}$; $Tg:Oct4^{GFP/GFP}$). Pregnant dams were injected at E10.5 with 125 μ g / g tamoxifen to induce recombination and deletion of GR exon 3 specifically in the germ cells. Pregnant dams were dissected the morning of E17.5 and processed for FACS sorting as described for $GR^{KO/KO}$ females above.

Library Preparation and Sequencing: All library preparations and sequencing were performed by the University of California, Davis DNA Technologies & Expression Analysis Core. Gene expression profiling was carried out using a 3' Tag-RNA-Seq protocol. Barcoded sequencing libraries were prepared using the QuantSeq 3' mRNA-Seq Library Prep FWD kit (Lexogen) for multiplexed sequencing according to the manufacturer recommendations. The library fragment

size distribution was determined using microcapillary gel electrophoresis on a Bioanalyzer 2100 (Agilent), and libraries were quantified using a Qubit fluorometer (LifeTechnologies). Final libraries were pooled in equimolar ratios and sequenced on an Illumina HiSeq 4000.

Data Analysis: Data analysis of 3' Tag-Seq data was performed in house. Illumina universal adapters (AGATCGGAAGAG) were trimmed from fastq files using cutadapt(Martin, 2011). Paired-end reads were aligned to the mm10 genome using STAR(Dobin et al., 2013) v2.6.0, and counts files were generated using featureCounts(Liao et al., 2014) v1.6.3. Differential expression analysis was performed using edgeR(Robinson et al., 2010) v3.28.1 and limma(Ritchie et al., 2015) v3.42.2. The resulting p-values were adjusted using the Benjamini and Hochberg's approach for controlling the false discovery rate. Genes with an adjusted p-value ≤ 0.05 were assigned as differentially expressed.

Bulk RNA-seq on *in vivo* dex-dosed gonads.

Sample preparation: For analysis of female germ cells by RNA-seq, pregnant dams were injected by IP at approximately 09:00 with either saline or 10 mg dex / kg weight daily at E12.5, E13.5, E14.5 and E15.5. Embryos were dissected at E15.5 at approximately 15:00, and fetal ovaries placed in ice-cold 0.4% BSA in PBS. Mesonephroi were carefully microdissected away from the ovary, and ovaries were then digested for FACS sorting as described above. For analysis of male germ cells by RNA-seq, pregnant dams were injected via IP at approximately 09:00 with either saline or 10 mg dex / kg weight daily at E17.5 and E18.5. Following delivery the evening of E18.5, PN0 pups were injected the following morning subcutaneously with either saline or 10 mg dex / kg bodyweight. Pups were then sacrificed at approximately 11:00 on PN1, and testes placed in ice-cold 0.4% BSA in PBS. The tunica vaginalis was carefully

microdissected away from each testis, and testes were then digested for FACS-sorting as described above.

Library Preparation and Sequencing: All library preparations and sequencing were performed by the company Novogene. mRNA was purified from total RNA using poly-dT magnetic beads. Following mRNA fragmentation, first strand cDNA synthesis was carried out using random hexamer primers, followed by second strand cDNA synthesis. Fragment ends were repaired, A-tailed, and ligated with sequencing adapters, followed by size selection, PCR amplification, and purification. Final libraries were quantified using Qubit and run on an Agilent Bioanalyzer system to ensure proper size distribution. Quantified libraries were pooled and sequenced on an Illumina platform. Clustering of the index-coded samples was performed according to the manufacturer's instructions, and library preparations were subsequently sequenced to generate paired-end reads.

Data Analysis: Initial data QC, genome alignment, and differential expression analysis was all carried out by Novogene.

Data QC: Raw fastq reads were processed using custom perl scripts to remove reads containing adapter sequences, reads containing poly-N, and low quality reads (based on Q20, Q30 and %GC scores).

Alignment: The mm10 reference genome was indexed using Hisat2 (Pertea et al., 2016) v2.0.5. Cleaned, paired-end reads were aligned to the mm10 genome using the splice-aware aligner Hisat2 v2.0.5.

Expression Quantification: Counts of reads mapping to each gene were determined using featureCounts (Liao et al., 2014) v1.5.0-p3. FPKM values were calculated for each gene based on the length of the gene, sequencing depth, and read counts mapping to the gene.

Differential Expression Analysis: Differential expression analysis of pairwise conditions was performed using DESeq2 (Love et al., 2014) (v1.20.0). The resulting p-values were adjusted using the Benjamini and Hochberg's approach for controlling the false discovery rate. Genes with an adjusted p-value ≤ 0.05 were assigned as differentially expressed.

Gene Ontology Enrichment Analysis. GO Term enrichment analysis was performed using the GO Consortium's online tool at: <http://geneontology.org/>. A list of significant genes (adjusted p-value ≤ 0.05) was uploaded and used to look for enriched biological processes, utilizing a Fisher's Exact test followed by Bonferroni correction for multiple testing. Lists for upregulated and downregulated genes were run independently. The results were sorted based on highest fold enrichment scores, and the top ten processes for each category plotted.

Differential splicing analysis using rMATS: Differential transcript splicing analysis was performed using rMATS (Shen et al., 2012) version 4.1.2, with genome-aligned BAM files generated from paired end RNA-seq reads used as input. Comparisons were made between saline treated and dex treated germ cells from PN1 testes (Figure 2.12A), using the rMATS settings: -t paired ; --readLength 150. Results were visualized as sashimi plots, generated with the program rmats2sashimipLOT.

Table 2.3: Antibodies Used

Target	Company	Product #	Dilution	Host Species	Clonality
GR (<i>Nr3c1</i>)	Cell Signaling	12041S	1:200 (IF)	Rabbit, IgG	mono
GFP	Aves	GFP-1020	1:200 (IF)	Chicken, IgY	poly
Tra98 (<i>Gcna1</i>)	Abcam	ab82527	1:300 (IF)	Rat, IgG2a	mono
Nobox	N/A*	N/A	1:400 (IF)	Goat	unknown
Sycp3-488	Abcam	ab205846	1:50 (spreads)	Mouse, IgG1	mono
γ H2AX (Ser139)	Millipore Sigma	05-636-I	1:200 (spreads)	Mouse, IgG1 κ	mono
Sycp1	Abcam	ab15090	1:200 (spreads)	Rabbit, IgG	poly
Fkbp5	ThermoFisher	711292	1:200 (IF)	Rabbit, IgG	poly
PLZF (<i>Zbtb16</i>)	R&D	AF2944	1:200 (IF)	Goat, IgG	poly
c-Kit (<i>CD117</i>)	R&D	AF1356	1:200 (IF)	Goat, IgG	poly
VASA/MVH (<i>Ddx4</i>)	Abcam	ab13840	1:500 (IF)	Rabbit, IgG	poly

*Not commercially available

Table 2.4: RT-PCR Primers Used

Target	Forward Primer	Reverse Primer
<i>Actb</i>	5'-ACTCTGTGTGGATCGGTGGC-3'	5'-AGCTCAGTAACAGTCCGCCTAGAA-3'
<i>Ddx4</i>	5'-AGGCCCGTTTCTGCTAGAGGGG-3'	5'-GCCTGAATCACTTGCTGCTGGT-3'
<i>Nr3c1</i> - exon 1A	5'-GCCCCGGCCTTATCTGCTAGAAAGTGG-3'	5'-ACAAGTCCATCACGCTTCCCCTCC-3'
<i>Nr3c1</i> - exon 1B	5'-TATCTGGCTGCGGTGGGAGCC-3'	5'-ACAAGTCCATCACGCTTCCCCTCC-3'
<i>Nr3c1</i> - exon 1C	5'-GGAGCCAGGGAGAAGAGAACTAAAG-3'	5'-ACAAGTCCATCACGCTTCCCCTCC-3'
<i>Nr3c1</i> - exon 1D	5'-GACCTGGCAGCACGCGAGT-3'	5'-ACAAGTCCATCACGCTTCCCCTCC-3'
<i>Nr3c1</i> - exon 1E	5'-TTCGCCGTGCAACTTCTCCGAAT-3'	5'-ACAAGTCCATCACGCTTCCCCTCC-3'
<i>Nr3c1</i> - exon 1F	5'-CACTGAGCCTGGAGCAGCAAATG-3'	5'-ACAAGTCCATCACGCTTCCCCTCC-3'
<i>Nr3c1</i> - exon 1G	5'-GAGGGCAGGCTTCCGTGACAAC-3'	5'-ACAAGTCCATCACGCTTCCCCTCC-3'
<i>Nr3c1</i> - exon 1α	5'-CCTTGCACTTGCCGACAGTCG-3'	5'-ACAAGTCCATCACGCTTCCCCTCC-3'
<i>Nr3c1</i> - exon 1β	5'-CATAACACCTTACTCCCCAACCCCC-3'	5'-ACAAGTCCATCACGCTTCCCCTCC-3'
<i>Nr3c1</i> - exon 1γ	5'-GAGCACCTCTGCCAAATGGTGAC-3'	5'-ACAAGTCCATCACGCTTCCCCTCC-3'
<i>Nr3c1</i> - exon 2-3	5'-CAGTCCTCCACAGCAACGG-3'	5'-TGCTGTCCTTCCACTGCTCTTT-3'

Table 2.5: Splice Junction Primers Used (qRT-PCR)

Target	Forward Primer	Reverse Primer
<i>Ezh2</i>	5'-GACAGTTCGTGCCCTTGTG-3'	5'-CTCGGACAGCCAGGTAGC-3'
<i>Epb41l4b</i>	5'-GCCTTCTTCCGTCTGCG-3'	5'-TTGCTTTAGAGCTGAACCG-3'
<i>Plag1</i>	5'-GCCAAAATGGGAAGGACTGG-3'	5'-TAGCCATGTGCCTGATTGGTGA-3'
<i>Ralgps2</i>	5'-ACAAGAGTGCCGCGAAATGG-3'	5'-CACCGCCAAATCTTCCGACT-3'
<i>Usp14</i>	5'-GGGGAAACATCAAAATGAAAAATATGGAATTGC-3'	5'-CAGGCACAGAACGAATACACTGA-3'
<i>Vapa</i>	5'-AGGGAACATAAAGAGGTGAAGCA-3'	5'-TTGGCAGGGGTCCGTCT-3'

Table 2.6: qRT-PCR Primers Used

Target	Forward Primer	Reverse Primer
<i>Dmc1</i>	5'-CGGCTACTCAGGTGGAAAGA-3'	5'-GTTGAAGCGGTCAGCAATGT-3'
<i>Epb41l4b</i>	5'-GCCCAGGTCACGCACT-3'	5'-CATAGGCAGGTCCCACCTTTCA-3'
<i>Fkbp5</i>	5'-ATGCTTATGGCTCGGCTGG-3'	5'-AGTATCCCTCGCCTTTCCGT-3'
<i>Fus</i>	5'-GGACAGACCCAAAACACAGG-3'	5'-GAACTGCCACCATAACTTCCT-3'
<i>Gapdh</i>	5'-ACTTTGGCATTGTGGAAGGG-3'	5'-AGGGATGATGTTCTGGGCA-3'
<i>Hnrnpa2b1</i>	5'-CTTTCTCATCTCGCTCGGCT-3'	5'-GTTCCTTTTCTCTCTCCATCGC-3'
<i>Hnrnp3</i>	5'-AGGATACGGGTCTGTTGGGA-3'	5'-TCCACTCATTCCACCTTGCC-3'
<i>Map3k6</i>	5'-TGTAAGTGGTGCTGGAGGTG-3'	5'-ACACAATCCGAGTTCTTCTGG-3'
<i>Nr3c1</i>	5'-CAGCTCCTCCACAGCAACGG-3'	5'-TGCTGTCCTTCCACTGCTCTTT-3'
<i>Plag1</i>	5'-ACAATGGCTGCTGGAAAGAG-3'	5'-CAATACCACCCAGGCAGCAC-3'
<i>Prdm9</i>	5'-GCAGAGATGGGAGAGTGGGA-3'	5'-TGGGGTTTCATTGCTTGCCT-3'
<i>Prpf31</i>	5'-ACCCTGTCTGGCTTCTCTTC-3'	5'-CACCTTCCCTTCTGTGCTCT-3'
<i>Rn18S</i>	5'-TGCATGTCTAAGTACGCACGGC-3'	5'-AGCGAGCGACCAAAGGAACC-3'
<i>Slc25a34</i>	5'-GACTCAACCCTCATCCCACC-3'	5'-TGTTCCCTTGCCCTTCTCCTCC-3'
<i>Smc1b</i>	5'-GCCCACCTTACACTCCTTCT-3'	5'-TCTGGCTTCCCTTCTGCTGG-3'
<i>Srsf7</i>	5'-GAGGATTGGATGGGAAAGTGAT-3'	5'-CGTGACCTGCTTCTTCTTCG-3'
<i>Sycp1</i>	5'-GAGGGGAAGCTCACGGTTC-3'	5'-CAGTGTGAAGGGCTTTTGCT-3'
<i>Sycp3</i>	5'-ATCTGGGAAGCCACCTTTGG-3'	5'-GAGCCTTTTCATCAGCAACATCT-3'
<i>Tra2b</i>	5'-GCTCCTCGCAAAAGTGTGG-3'	5'-GATTCCCCTCGCCGT-3'
<i>U2af2</i>	5'-AAACAAGAGCGGGACAAGGA-3'	5'-CGGGGAGAACGAATCAATCCA-3'
<i>Usp14</i>	5'-CGCCTTTTCTTCCTTCTGCT-3'	5'-CTTTTTGTCTGGCTGGCTGG-3'
<i>Zbtb16</i>	5'-GGTGCCCAAGTTCTCAAAGGA-3'	5'-TTTCCCACACAGCAGACAGA-3'

Chapter 3 - Heterogeneity of transposon expression and activation of the repressive network in human fetal germ cells

3.1 - Introduction

Tasked with the vital role of species propagation, germ cells must be able to faithfully transmit heritable units of information between generations. A potential risk to genome integrity during this transmission arises in the developing embryo as the primordial germ cells (PGCs) undergo epigenetic reprogramming, characterized by both DNA demethylation and global resetting of histone marks (Gkountela et al., 2015; Guo et al., 2015; Tang et al., 2015; Tang et al., 2016). This rearrangement of the epigenetic landscape primes germ cells for meiotic entry in fetal ovaries, and mitotic arrest and differentiation in the fetal testis (Messerschmidt et al., 2014), yet comes at the risk of reactivating transposable elements (TEs), which are normally silenced by repressive epigenetic marks. The greatest threat comes from retrotransposons, which comprise ~40% of the human genome (Kazazian and Moran, 2017). Although most TEs are mutated and inactive, some remain capable of retrotransposition in the human genome, mostly stemming from the evolutionarily young long interspersed element type 1 (L1), SVA and Alu families (Kazazian and Moran, 2017). L1-mediated integration of active TEs at random genomic sites is potentially dangerous, and has been associated with over 100 disease mutations in humans (Hancks and Kazazian, 2016). Their activity in humans is high, with new L1 and Alu integrations observed in ~1/100 and 1/20 human births, respectively (Hancks and Kazazian, 2012), although not as high as other mammalian species such as mice, where new L1 insertions occur in 1/8 births (Richardson et al., 2017).

In germ cells, the activity of TEs is mollified by an evolutionarily conserved genome defense system made up of PIWI proteins and PIWI-interacting RNAs (piRNAs) collectively called the PIWI/piRNA pathway. piRNAs that are 26-32 nt complex with PIWI family proteins to directly

target retrotransposons for mRNA degradation in the cytoplasm, while also leading to nuclear silencing at endogenous genomic loci through the deposition of DNA methylation and histone modifications (Ernst et al., 2017; Iwasaki et al., 2015). The PIWI-piRNA pathway is required for male fertility, and genetic mutations in this pathway invariably lead to meiotic catastrophe and failure to make mature sperm, while displaying increased expression of TEs along with decreased DNA methylation and loss of the repressive Histone 3 lysine 9 trimethyl (H3K9me3) mark at TE genomic loci (Aravin et al., 2007; Aravin et al., 2009; Carmell et al., 2007; Pezic et al., 2014). Elevated retrotransposition has also been observed in piRNA-deficient mice using a transgenic model for L1 mobilization (Newkirk et al., 2017). Germ cells deploy the PIWI-piRNA pathway at two stages during development: in pre-pachytene fetal germ cells and postnatally in pachytene stage germ cells (Czech and Hannon, 2016; Iwasaki et al., 2015). In mice, expression of the effector proteins PIWIL2 (MILI) and PIWIL4 (MIWI2) in fetal germ cells regulates transposons at multiple levels. TE transcripts are processed into primary piRNAs, which are subjected to MILI-mediated amplification, generating antisense secondary piRNAs. The latter are loaded onto MIWI2, resulting in their nuclear localization and the subsequent epigenetic silencing of TEs (Aravin et al., 2008; Fazio et al., 2011; Kuramochi-Miyagawa et al., 2008; Manakov et al., 2015; Pezic et al., 2014). An array of co-factors is involved in the PIWI-piRNA pathway, including the inducible chaperone Hsp90 (HSP90AA1/HSP90 α in mammals), which assists in piRNA biogenesis, loading of piRNAs onto PIWI-family proteins and transposon repression (Gangaraju et al., 2011; Ichiyanagi et al., 2014; Izumi et al., 2013; Specchia et al., 2010; Xiol et al., 2012).

Most studies of TE repression in developing mammalian germ cells have been conducted in mice due to the limited availability and ethical considerations of studying human fetal gonads. However, it was recently shown that epigenetic reprogramming via global DNA demethylation and histone modification is conserved in human fetal cells (Gkountela et al., 2013; Guo et al.,

2015; Tang et al., 2015; Tang et al., 2016), as is the accompanying activation of retrotransposon transcript expression (Gkountela et al., 2015; Guo et al., 2015; Tang et al., 2015) and upregulation of PIWI-piRNA pathway genes (Tang et al., 2015). The expression of PIWI proteins and piRNAs has furnished evidence of an active piRNA pathway in adult human testis and in fetal human ovaries (Ha et al., 2014; Roovers et al., 2015; Williams et al., 2015). Notably, the human piRNAs identified are derived from piRNA clusters and resemble the composition of mouse pachytene piRNAs rather than fetal pre-pachytene piRNAs, which are largely transposon-derived (Aravin et al., 2007; Aravin et al., 2008; Kuramochi-Miyagawa et al., 2008). In the human fetal testis, piRNA expression has been difficult to detect due to low abundance (Gainetdinov et al., 2017; Williams et al., 2015), and reported localization of PIWIL2 (HILI) and PIWIL4 (HIWI2) in the cytoplasm does not support nuclear silencing by this pathway (Fernandes et al., 2018).

In this study, we generate the most comprehensive picture to date of the dynamic expression of transposons, their derivative piRNAs and PIWI family proteins in humans. This constitutes the first evidence for activity of the PIWI-piRNA pathway in the human fetal testis. We identify pre-pachytene TE-derived piRNAs that contain the signature of secondary biogenesis. L1 expression increases concomitantly with L1-derived piRNAs and PIWI-piRNA machinery in fetal germ cells during mid-gestation; conversely, we find that L1 levels decline during development, as levels of the repressive histone mark H3K9me3 increase. However, we observe surprising heterogeneity at the single cell level that suggests only a subset of human fetal germ cells express L1 and deploy the PIWI-piRNA pathway to repress TEs via H3K9me3-mediated silencing, whereas other germ cells remain resistant.

3.2 - Dynamic expression and subcellular localization of PIWI homologs in male fetal germ cells

The piRNA pathway is regulated by the PIWI family of conserved RNA-binding proteins, which is expressed almost exclusively in germ cells. In mouse fetal testis, biogenesis as well as secondary amplification of pre-pachytene piRNAs depends upon MILI, which turns on at approximately embryonic day (E) 12.5, shortly after the onset of sex differentiation (Aravin et al., 2008). In human fetal testis, we detected protein expression of HILI from gestational week (GW) 11 to 22, which corresponds to the period of sex-specific differentiation. HILI was found in the more differentiated population termed advanced germ cells (AGCs) (Gkoutela et al., 2013) marked by VASA (**Figure 3.1A**) as well as in the co-existing more primitive population of PGCs defined by the pluripotency marker OCT4 (**Figure 3.2A**). Initially low levels of HILI at GW11 progressively increased through development, and protein was distributed throughout the cytoplasm as well as in puncta beginning at GW13, consistent with reported localization of MILI to pi-bodies, or the intermitochondrial cement, in mice (Aravin et al., 2009). HIWI (PIWIL1) protein expression was not observed in fetal testes from GW10 to GW22 (**Figure 3.2B**), as expected based on its known adult-specific expression pattern in human (Fernandes et al., 2018) and mouse (Deng and Lin, 2002) (**Figure 3.2C**). HIWI2 was first detected in a small subset of VASA⁺ AGCs at GW14, and in an increased proportion of AGCs from GW18 onwards (**Figure 3.1B**). The subcellular localization of HIWI2 underwent a dramatic shift from predominantly cytoplasmic before GW18 to nuclear in most AGCs by GW21-22 (**Figure 3.1C**). In mice, MIWI2 is predominantly nuclear by E16.5-E17.5 (Aravin et al., 2008; Aravin et al., 2009; Kuramochi-Miyagawa et al., 2010; Shoji et al., 2009), but remains cytoplasmic in fetal germ cells of piRNA pathway mutants, including Mili (Piwil2) Mael and Mov10l1 (Aravin et al., 2009; Shoji et al., 2009; Zheng et al., 2010). Indeed, we observed a cytoplasmic to nuclear progression of MIWI2 from E16.5 to E17.5 in mouse fetal testes (**Figure 3.2D**). Nuclear localization of PIWIL4

homologs in other species requires piRNAs and co-factors such as HSP90 α , and leads to transcriptional silencing of transposons at endogenous genomic loci (Fu and Wang, 2014; Ichiyanagi et al., 2014; Iwasaki et al., 2015). Accordingly, the dynamic localization of HIWI2 from the cytoplasm to the nucleus between GW18 and 21 suggests that piRNAs are produced and transported to the nucleus for similar epigenetic functions in male fetal germ cells of humans.

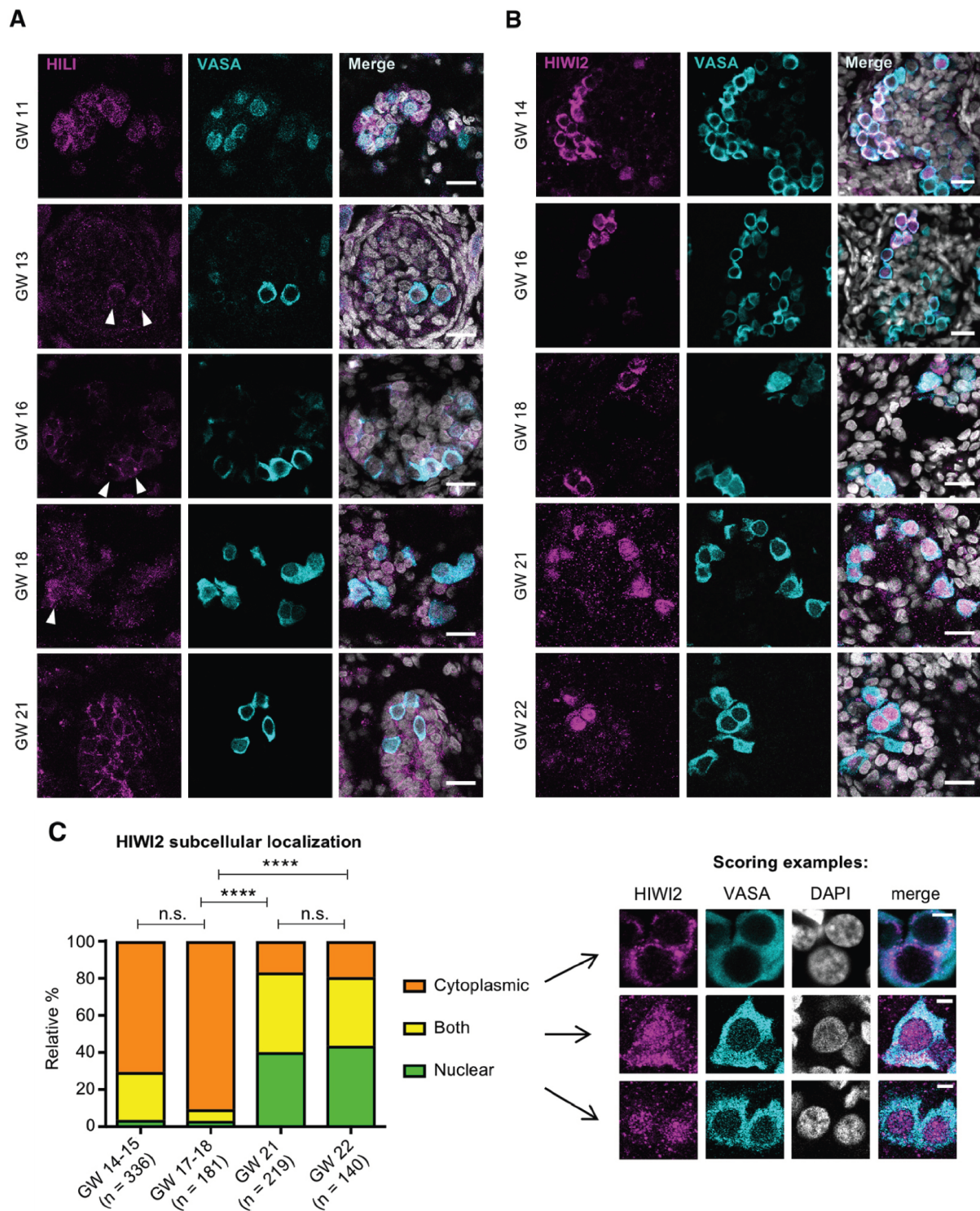


Figure 3.1 - Expression of PIWI proteins in human fetal testis across development.

(A) Expression of HILI and VASA at gestational week (GW) 11, 13, 16, 18 and 21, counterstained with DAPI (white, in merge images). Scale bars: 20 μ m. Arrowheads indicate germ cells with HILI foci. A total of 12 embryos were analyzed across all time points.

(B) Expression of HIWI2 and VASA at GW14, 16, 18, 21 and 22, counterstained with DAPI. Scale bars: 20 μm . A total of 11 embryos were analyzed across all time points.

(C) Relative percentages of VASA⁺ germ cells with HIWI2 localization in cytoplasm or nucleus, or both, at indicated time points, with scoring examples on the right. Two-tailed Fisher's exact test was performed on 'nuclear' and grouped 'non-nuclear' categories across two time points; ****P<0.0001, n.s., not significant. Scale bars: 5 μm .

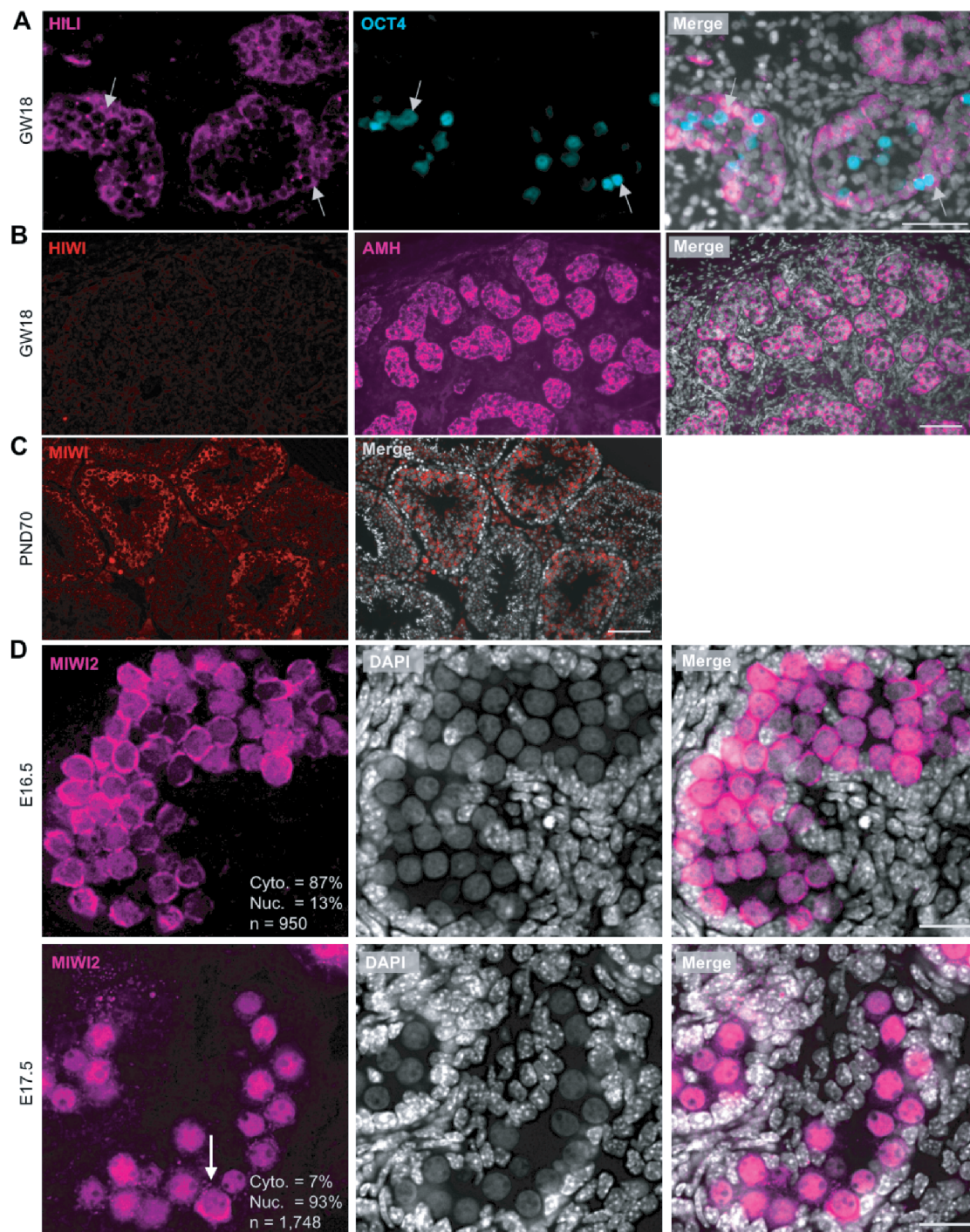


Figure 3.2 - Expression of PIWI proteins in human and mouse fetal testis.

(A) Immunofluorescence of GW18 human fetal testis to detect HILI and OCT4 expression. Merge is shown with DAPI co-stain. Arrows indicate HILI⁺/OCT⁺ germ cells. Scale bar: 50 μ m. (B) Expression of HIWI in GW18 human fetal testis. Also shown is staining for AMH as a positive control (middle panel), and merged staining with DAPI (right panel). Scale bar: 100 μ m.

(C) MIWI staining of spermatogonia in adult mouse testis PND70. Similar staining and microscope acquisition settings were used as for the human sample in (B). Scale bar: 100 μ m. **(D)** MIWI2 localization in murine fetal testis at E16.5 (top panel) and E17.5 (bottom panel) with subcellular localization of MIWI2 indicated. n = number of cells counted in four fetal testes across both timepoints. Arrow indicates a rare cytoplasmic MIWI2 germ cell at E17.5. Scale bars: 20 μ m.

3.3 - Evidence of transposon-derived primary and secondary piRNAs in fetal testis

We next looked for evidence of piRNAs across developmental timepoints spanning GW13-22. Small RNA sequencing was performed on bulk fetal testis tissue from eight samples at a depth of 35-40 million reads and processed according to our custom pipeline (**Figure 3.4**). Trimmed 18-40 nt reads were first aligned to a curated list of human TE consensus sequences obtained from the GIRI Repbase database (Bao et al., 2015), and the remainder were aligned to the human genome (hg38). An overall alignment rate of >97% was obtained across all samples (**Table 3.1**). At all timepoints, the majority of reads (~75%) corresponded to miRNAs, with smaller fractions derived from tRNAs, snoRNAs and protein coding transcripts (**Figure 3.3A**, left panel; **Figure 3.5A**; **Table 3.1**). Strikingly, fewer than 1% of reads for all samples mapped to Repbase, and these resolved into two size classes: 27 nt and 22 nt (**Figure 3.5B**). Reads comprising the 22 nt peak showed extremely low sequence diversity, with the vast majority mapping to the L2C retrotransposon (data not shown). The 27 nt peak was highest at GW20, and likely corresponds to putative TE-derived piRNAs, which range from 26-32 nt in other species. As our small RNA populations were derived from bulk fetal testis tissue without cell type or biochemical enrichment, we focused on the 26-32 nt small reads for the remainder of the analysis (**Figure 3.4**). This increased the fraction of Repbase-mapping reads to ~6% in the 26-32 nt RNAs but not in 18-22 nt small RNAs, which were mostly miRNAs (**Figure 3.3A**, middle and right panels). The number of Repbase mapping reads was dynamic over

development, with a maximum at GW20-21 (**Figure 3.3B**, **Table 3.1**), corresponding to the window of HIWI2 nuclear translocation. Hallmarks of pre-pachytene piRNAs were identified in these 26-32 nt Repbase-mapping reads, including a bias toward 1st position uridine (**Figure 3.3C**, **Figure 3.5C**) – a key signature of primary piRNA biogenesis (Iwasaki et al., 2015). Additionally, an adenine bias at the 10th position of mapped 26-32 nt reads at all timepoints with the exception of the earliest, GW13A (**Figure 3.3C**, **Figure 3.5D**), suggests active secondary piRNA biogenesis, also known as ‘ping-pong’ amplification (Czech and Hannon, 2016). Corroborating the specificity of Repbase-mapping reads, nucleotide distribution analysis on miRNA-annotated reads demonstrated a reduced, yet still apparent, 5' U bias (**Figure 3.5E**), similar to miRNAs in fetal ovary and adult testis (Williams et al., 2015), and no adenine bias at position 10 (**Figure 3.5F**). Another signature of ping-pong biogenesis, ten nucleotide overlaps between reverse complementary piRNAs, was detected in all samples to varying extents, with the exception of GW13A, and most strongly at GW20 (**Figure 3.3D**). Together, these analyses identify small RNAs in human fetal testes with defining characteristics of pre-pachytene piRNAs, although at much lower abundance than found in mice or human fetal ovaries (Roovers et al., 2015; Vasiliauskaite et al., 2018; Williams et al., 2015).

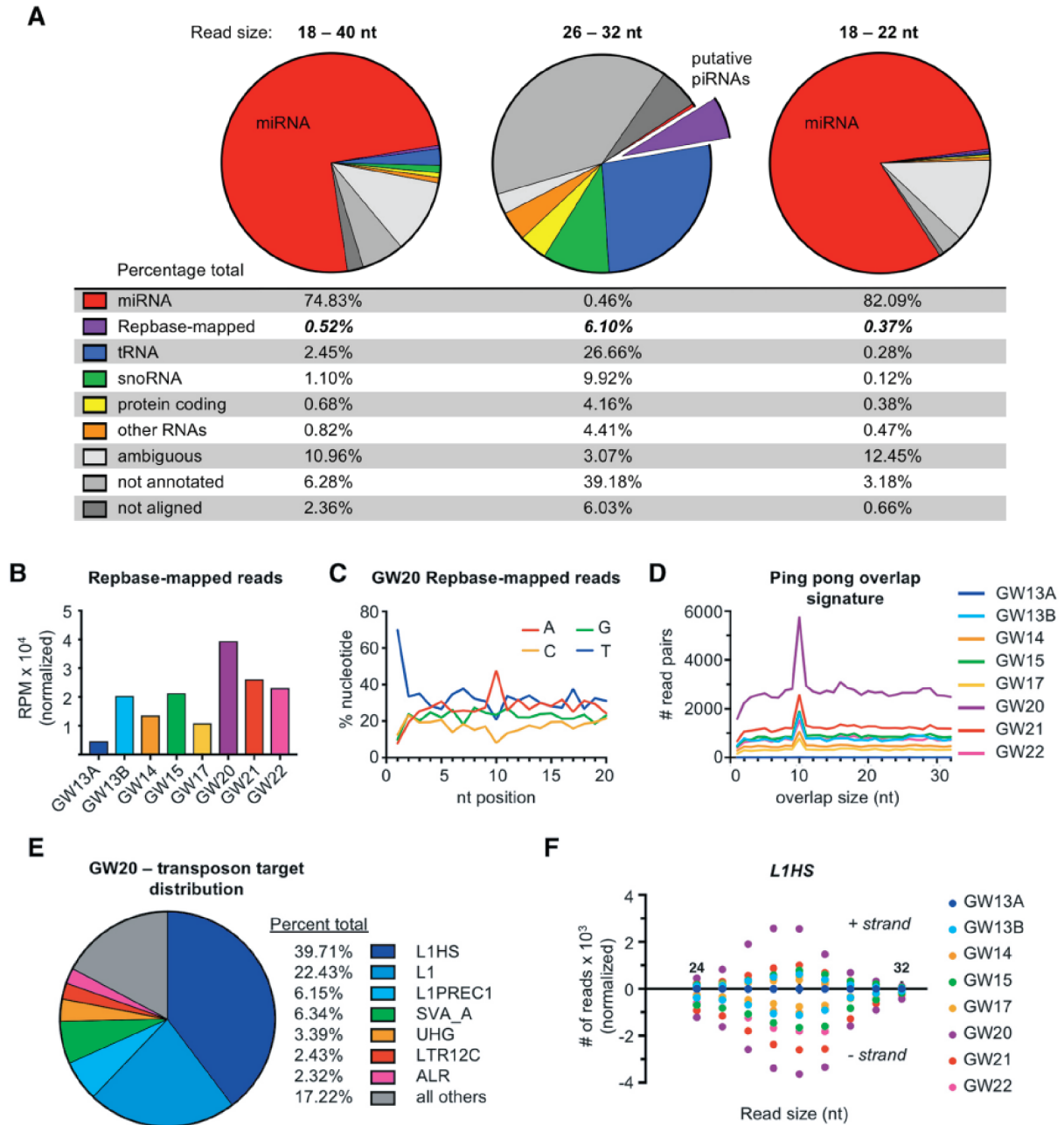


Figure 3.3 - Identification of transposon derived piRNAs in the human fetal testis.

(A) Relative percentages of different RNA subtypes present in gestational week (GW) 20 sample after size filtering for 18-40 nt, 26-32 nt and 18-22 nt small RNAs. Values in bold italic highlight Repbase-mapped reads, which include putative piRNAs.

(B) Normalized number of reads (26-32 nt) mapped to human transposon consensus sequences in Repbase database across all samples.

(C) Relative nucleotide distribution at a given read position of pooled Repbase-mapping reads (26-32 nt) at GW20.

(D) Ping-pong overlap signatures calculated on pooled Repbase-mapping reads (26-32 nt).

(E) Top transposable elements mapped to by Repbase-mapping reads (26-32 nt) at GW20.

(F) Distribution of read sizes mapping to the L1HS transposon across all samples. Positive and negative values represent reads that map to the positive and negative strand, respectively.

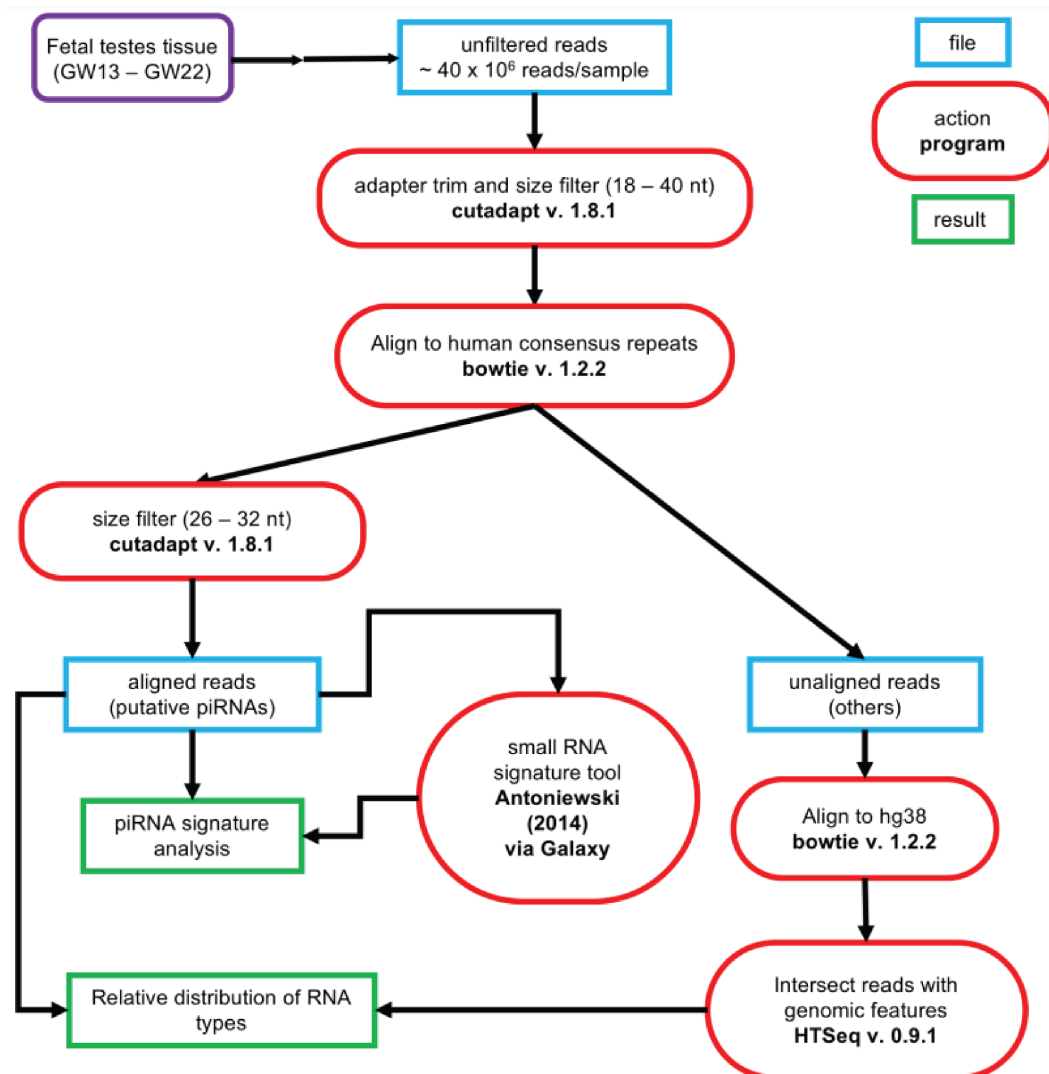


Figure 3.4 - Schematic of small RNA-seq data analysis pipeline.

Analysis pipeline used to interrogate small RNA species from eight fetal testes tissue samples from GW13 – GW22.

Table 3.1 - Relative percentage of all RNA subtypes across all samples

	miRNA	tRNA	snoRNA	protein coding	other RNAs	Repbse-mapping	ambiguous annotation (all)	not annotated	not aligned
GW13A	78.16%	2.31%	0.76%	0.38%	0.66%	0.20%	11.55%	4.09%	1.89%
GW13B	78.36%	1.29%	0.88%	0.50%	0.74%	0.39%	11.25%	4.68%	1.91%
GW14	74.55%	1.57%	1.04%	1.40%	1.14%	0.45%	10.49%	7.22%	2.14%
GW15	77.05%	1.40%	0.74%	0.53%	0.68%	0.35%	11.78%	5.59%	1.89%
GW17	77.86%	2.04%	0.84%	0.49%	0.68%	0.25%	11.38%	4.37%	2.08%
GW20	74.83%	2.45%	1.10%	0.68%	0.82%	0.52%	10.96%	6.28%	2.36%
GW21	77.32%	2.36%	0.82%	0.64%	0.72%	0.42%	10.96%	4.72%	2.04%
GW22	78.19%	0.94%	1.06%	0.53%	0.61%	0.37%	11.43%	4.70%	2.17%

Among the Repbase-mapping reads, the L1 family was the most abundantly represented class of repeat elements at GW20 (**Figure 3.3E**). This result is consistent with the derivation of piRNAs from actively transcribed TEs, given that L1 elements are known to be active in humans (Hancks and Kazazian, 2012). The evolutionarily youngest L1 family (Smit et al., 1995), L1HS, was the most highly represented element in all samples (with the exception of GW13A), followed by 'L1' elements, which here represent the broad primate-specific L1PA clade (Kojima, 2018) (**Table 3.2**). Reads were mapped to both the forward and reverse strand of L1HS, particularly at later stages (**Figure 3.3F**), consistent with a progressive ping-pong amplification process. Analysis of other highly represented classes of TEs revealed different strand-specific biases, yet consistently showed GW20 as the sample with the largest number of relative mapping reads (**Figure 3.5G-I**). We conclude that pre-pachytene piRNAs are produced and amplified in the human fetal testes, with a large fraction derived from TEs, which is similar to the developing mouse testis (Aravin et al., 2007; Aravin et al., 2008).

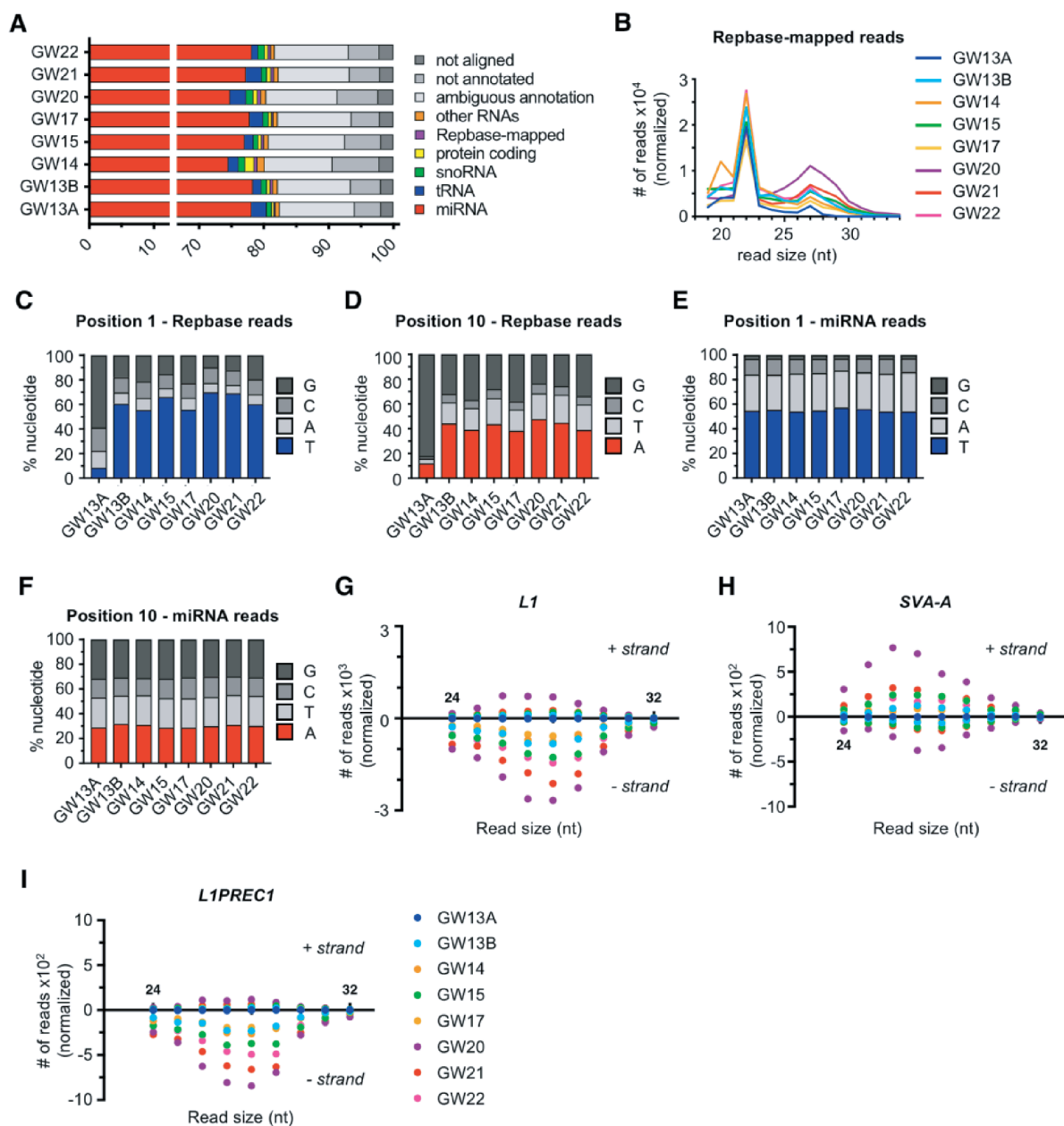


Figure 3.5 - Small RNA-seq analysis of human fetal testis.

(A) Relative percentages of different RNA subtypes present across all samples.

(B) Size distribution of reads mapping to the Repbase database across all samples.

(C-D) Relative nucleotide distribution at read position 1 (C) and read position 10 (D) for all samples, calculated on pooled Repbase-mapping reads (26-32 nt).

(E-F) Controls showing relative nucleotide distribution at read position 1 (E) and read position 10 (F) for all samples, for 18-22 nt size reads only.

(G-I) Distribution of Repbase-mapped read sizes mapping to the L1 (G), SVA-A (H), and L1PREC1 (I) elements across all samples, normalized to number of input reads. Positive and negative values represent reads mapping to the positive and negative strand, respectively.

Table 3.2 - Top ten transposable elements mapped to by Repbase-mapping reads across all samples

GW13A (AC126)	GW13B (AC598)	GW14 (AC560)	GW15 (AC423)	GW17 (AC422)	GW20 (AC157)	GW21 (AC182)	GW22 (AC565)
70.18% UHG	28.53% L1HS	31.83% L1HS	34.69% L1HS	31.06% L1HS	39.71% L1HS	37.72% L1HS	32.18% L1HS
FORDPREF							
10.05% ECT	16.30% L1	18.12% L1	21.13% L1	19.30% L1	22.43% L1	23.89% L1	20.70% L1
3.80% ALU	13.01% UHG	13.28% UHG	8.29% UHG	15.20% UHG	6.34% SVA_A	7.63% L1PREC1	11.38% UHG
2.98% L1HS	12.19% ALR	5.88% L1PREC1	6.43% L1PREC1	6.57% L1PREC1	6.15% L1PREC1	5.88% UHG	7.02% L1PREC1
2.23% L1	6.38% ALR1	5.33% ALR	5.35% SVA_A	FORDPREF	3.39% UHG	4.59% SVA_A	3.91% SVA_A
				ECT			
1.84% ALR	4.38% L1PREC1	FORDPREF	2.78% ALR	3.44% SVA_A	2.43% LTR12C	1.83% ALR	FORDPREF
		ECT					ECT
0.97% HERV49I	2.99% SVA_A	3.35% SVA_A	FORDPREF	1.61% ALR	2.32% ALR	1.40% L1PREC2	1.31% HERV9
			ECT				
0.94% L1PREC1	FORDPREF	2.76% ALR1	1.57% ALR1	1.15% LTR12C	1.26% ALR1	1.24% LTR12C	1.17% HERV17
	ECT						
0.77% ALR1	2.14% ALR_	1.28% L1PREC2	1.39% ALR_	1.07% ALR1	1.25% L1PA7_5	1.15% L1PA7_5	1.13% LTR12C
0.36% SVA_A	2.13% ALRb	1.15% ALR_	1.20% L1PREC2	1.04% L1PA7_5	FORDPREF	1.09% ALR1	1.11% L1PREC2
					ECT		
5.88% all others	9.32% all others	13.28% all others	15.50% all others	15.90% all others	13.68% all others	13.58% all others	18.23% all others

3.4 - L1 transposons are expressed in AGCs coordinately with the transposon repression network at the single cell level

The prevalence of L1-derived piRNAs and the possibility of piRNA-mediated nuclear silencing prompted a closer examination of the relationship between transposons and the transposon-repression network in an unbiased, population-wide manner. We took advantage of a recently published single cell RNA-seq dataset from human fetal testis tissue (Li et al., 2017) to assess the heterogeneity of transposon-derived and gene-coding transcripts. By mapping to repeat elements (based on RepeatMasker annotations) as well as the genome, we obtained profiles for expression of TEs as well as genes for each cell (**Figure 3.7**). We focused on GW19 in light of the high level of piRNA expression and dynamic HIWI2 localization. t-distributed stochastic neighbor embedding (t-SNE) analysis based on gene expression profiles identified

three distinct clusters corresponding to PGCs, AGCs and somatic support cells based on known lineage- and stage-specific markers (**Figure 3.6A,B, Figure 3.8A-C**). As anticipated, PGC and AGC clusters were distinguished by high expression of OCT4 (POU5F1) and VASA (DDX4), respectively (**Figure 3.6B**). The machinery of primary piRNA biogenesis [MAEL and HILI (PIWIL2)] was expressed in both PGCs and AGCs, though higher in the latter, whereas HIWI2 mRNA was largely limited to AGCs (**Figure 3.6B,C**). This developmental delay in transcription of HIWI2 as compared with HILI recapitulates the sequential expression of the proteins observed in the fetal testis tissues (**Figure 3.1A,B**). With a few exceptions, TE expression was dramatically elevated in AGCs compared with PGCs, and absent in the soma (**Figure 3.6B,C**). The most highly expressed TEs in AGCs belong to the L1 clade, specifically L1HS, L1PA2 and L1PA3. This corresponds well with the abundance of piRNAs derived from the L1 clade (**Figure 3.3E**). Other highly expressed TEs include members of the Alu family, especially the evolutionarily young AluYa5 and AluYb8 subfamilies, which are known to be active in humans (Batzer and Deininger, 2002). Paired correlation analyses between L1HS, and either HILI or HIWI2 both yielded positive correlations (**Figure 3.6D,E**). Together, this analysis shows that at the single cell level, the expression of genes of the transposon repression network is upregulated during germ cell development in concert with the expression of transposons (**Figure 3.6C**).

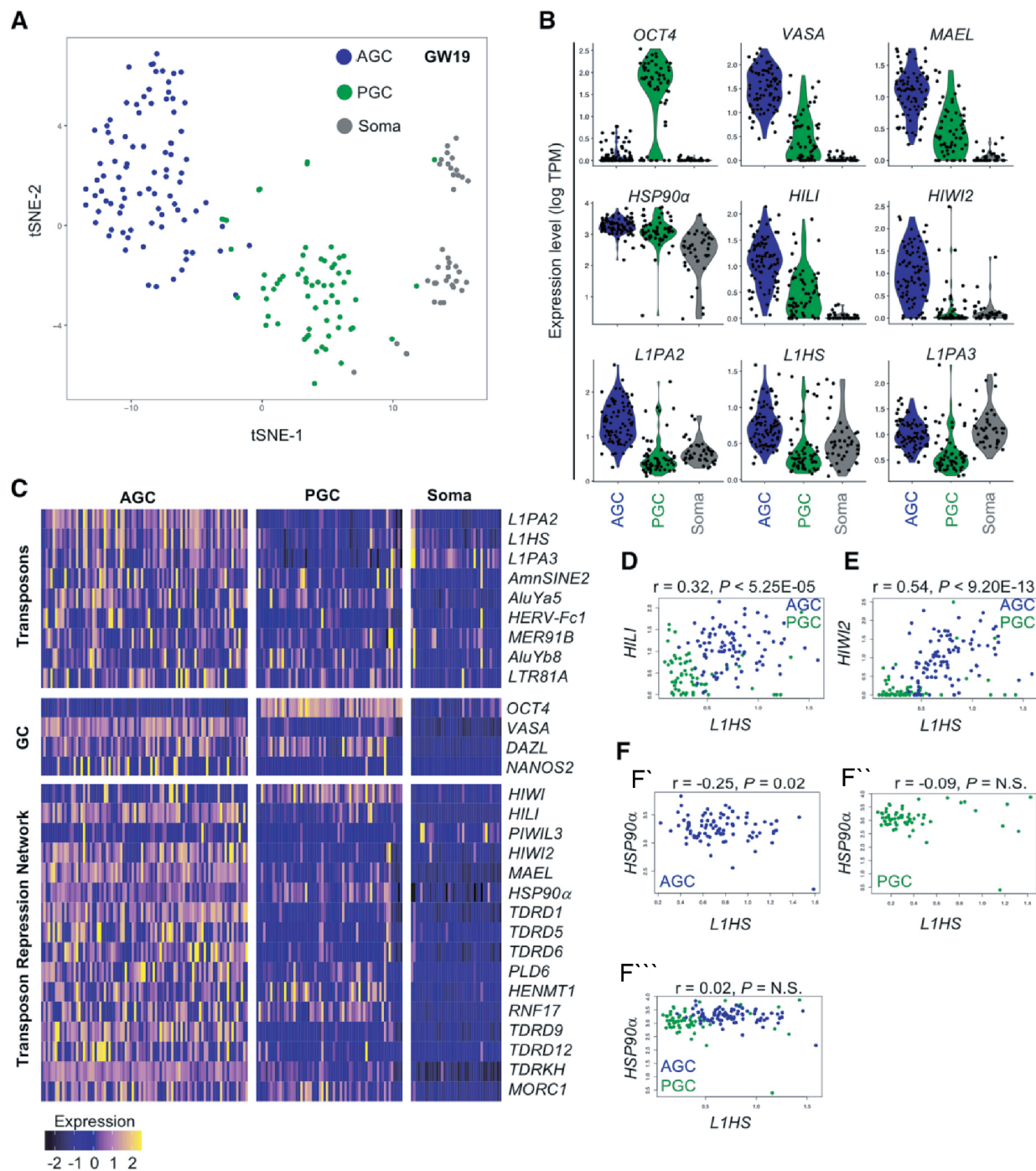


Figure 3.6 - Single cell sequencing reveals dramatic upregulation of L1 family retrotransposons in advanced germ cells.

(A) tSNE clustering on transcriptome reference was used to generate three distinct cell populations in the GW19 dataset.

(B) Violin plots showing expression of germ cell markers (top), transposon repression genes (middle) and L1 family retrotransposons (bottom) in AGCs, PGCs and soma.

(C) Heatmap displaying the most differentially expressed transposons sorted by myAUC score (top), and expression of germ cell markers (middle) and transposon repression genes (bottom). (D-F) Pairwise correlation analysis between L1HS and HILI (D) and HIWI2 (E) in GCs; and HSP90 α (F) in AGCs (F'), PGCs (F'') and combined GCs (F'''). Pearson's correlation coefficient scores and P-values are listed above graph.

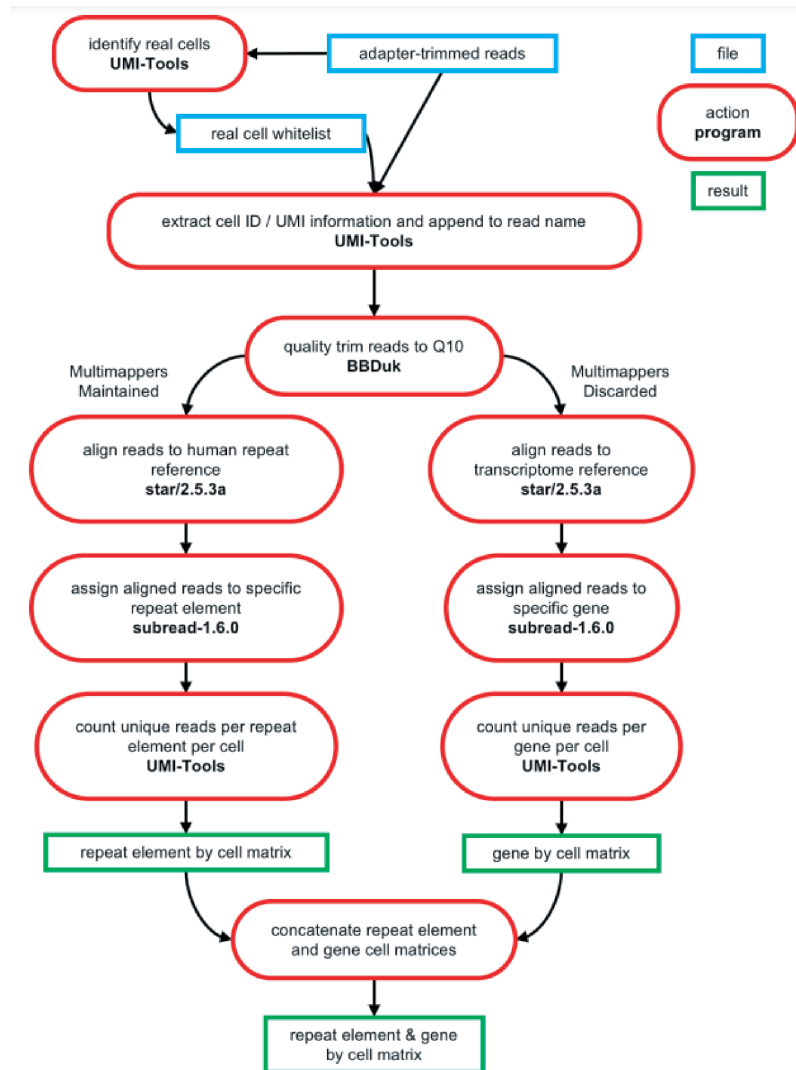


Figure 3.7 - Schematic of single cell RNA-seq data analysis pipeline.

Single cell RNA-seq analysis pipeline to interrogate GW 19 male human germ cell sample for gene and transposon expression.

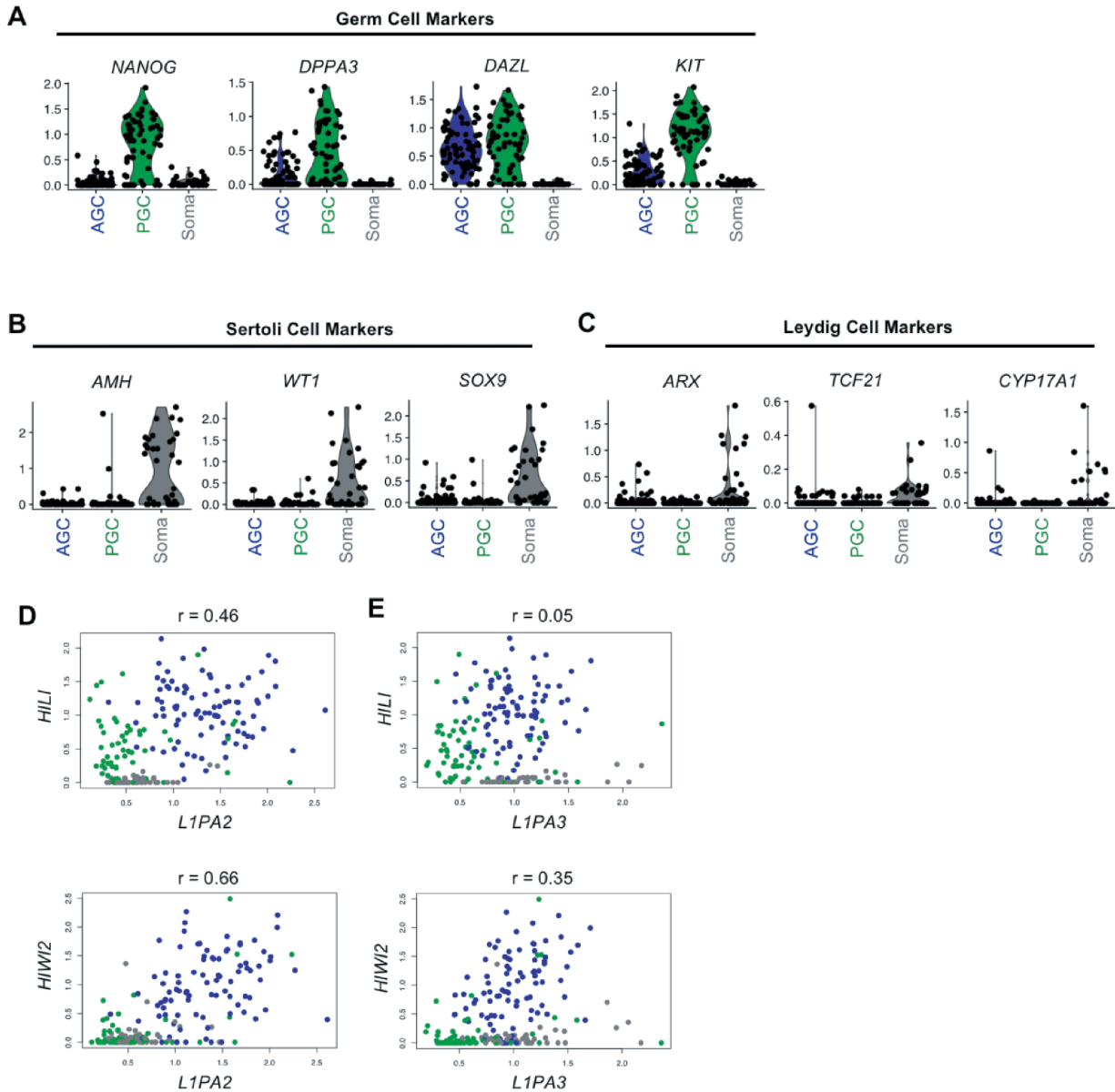


Figure 3.8 - Validation of cluster identities in analysis of human fetal testis single cell RNA-seq.

(A-C) Violin plots validating expression of additional germ cell markers (A), as well as somatic cell markers of Sertoli cells (B) and Leydig cells (C).

(D-E) Pairwise correlation analysis between L1PA2 (E), and L1PA3 (F) against HILI and HIWI2 in the total population. Pearson's correlation coefficient scores are listed above each graph.

3.5 - Dynamic relationships between L1 and the repression pathway at transcript and protein level

To confirm the correlation between L1 transcripts and the transposon repression network, we performed immunostaining. Using a previously validated antibody against the L1-ORF1p RNA-binding protein (Rodić et al., 2014), we detected expression primarily in VASA⁺ AGCs starting at GW16, whereas earlier it was found very sparsely and at low levels (**Figure 3.10**). L1-ORF1p was restricted to the cytoplasm and concentrated in granules, some of which colocalized with HILI foci (**Figure 3.9A**). However, L1-ORF1p granules were distinct from those containing HIWI2 (**Figure 3.9B**). As suggested by the heatmap in Figure 3.6C, a small subset of PGCs express high levels of L1 transcript but not the transposon repression network. We similarly observed rare instances of robust L1-ORF1p expression in OCT4⁺ PGCs (**Figure 3.9C**, top panel) and in cells lacking VASA and harboring low levels of OCT4 (**Figure 3.9C**, bottom panel). It is not clear whether these cells are transitioning between PGCs and AGCs or whether they will successfully turn on the repression machinery, but this observation raises the issue of whether transposon protein expression precedes that of HIWI2 and piRNA biogenesis.

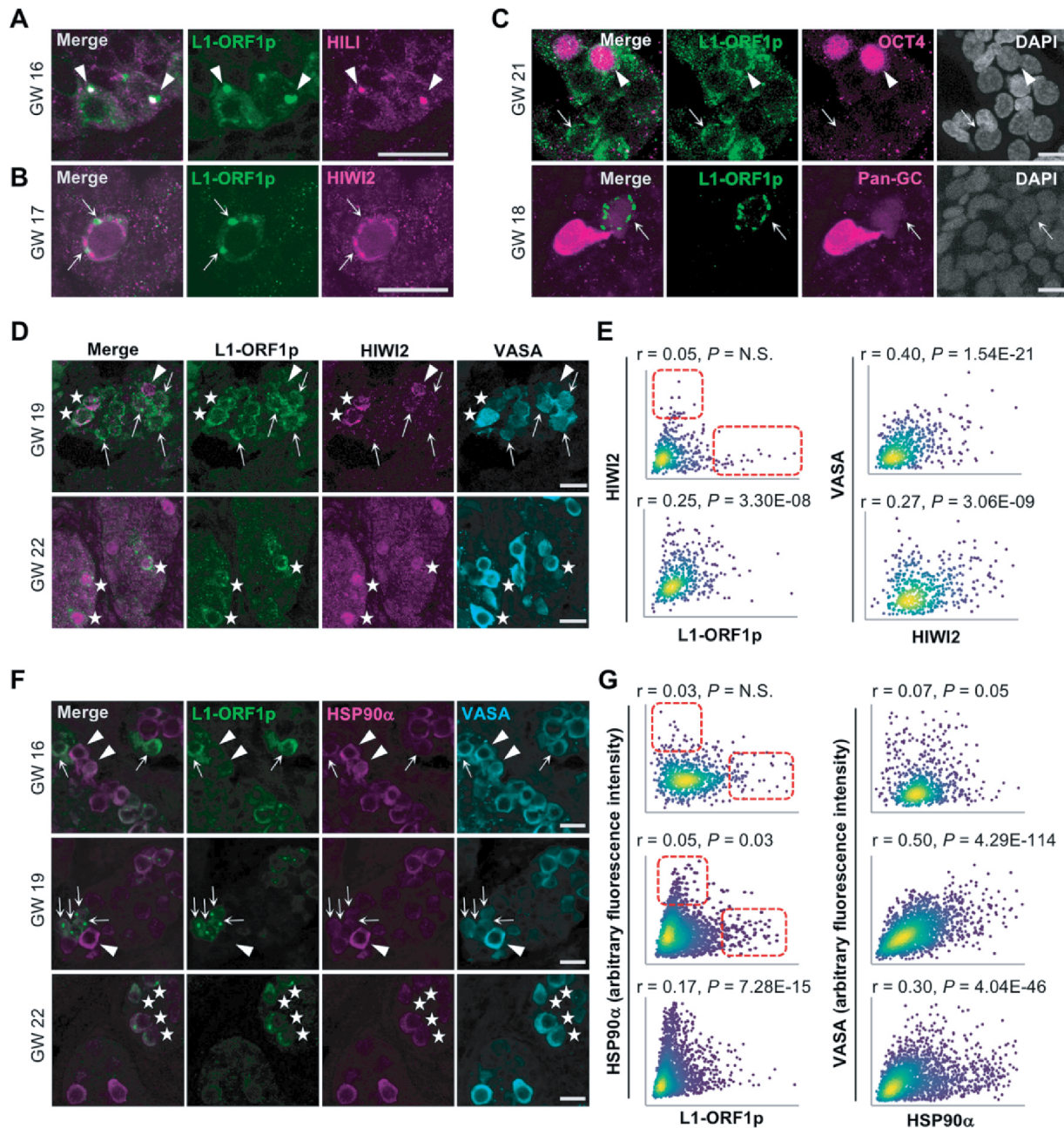


Figure 3.9 - L1 expression in advanced germ cells.

(A) L1 and HILI immunofluorescence in a GW16 human testis. Arrowheads indicate puncta of L1/HILI colocalization.

(B) Expression of L1 and HIWI2 at GW17. Scale bars: 20 μm . Arrows indicate regions of mutually exclusive staining between L1 and HIWI2 puncta.

(C) L1 expression at GW21 (top panel) and GW18 (bottom panel), co-stained with OCT4 or a pan-GC marker (OCT4 and VASA), respectively. (Top) Arrowheads indicate an L1⁺, OCT4⁺ germ cell; arrows highlight a L1⁺, OCT4⁻ cell. (Bottom) Arrows indicate L1⁺ and pan-GC negative cell.

(D) L1⁺ / HIWI2^{low} germ cells (arrows), a HIWI2^{high} / L1^{low} germ cell (arrowheads) and double-positive AGCs (stars) in human fetal testis at GW19 and GW22.

(E) xy scatter plots of HIWI2 versus L1 fluorescence intensities (left panels) and HIWI2 versus VASA (right panels), with Pearson's correlation coefficients and corresponding P values. For GW19 (top), n=526 VASA⁺ objects, counted from three stitched xy sections. For GW22 (bottom), n=472 VASA⁺ objects, from two stitched xy sections.

(F) L1^{high} / HSP90α^{low} cells (arrows), HSP90α^{high} / L1^{low} cells (arrowheads) and double-positive cells (stars) in human fetal testis at GW16-22.

(G) xy scatter plots of HSP90α versus L1 fluorescence intensities (left) and HSP90α versus VASA fluorescence intensities (right). Pearson's correlation coefficients and corresponding P values are indicated. For GW16 (top), n=768 VASA⁺ objects, counted from three stitched xy sections. For GW19 (middle), n=1809 VASA⁺ objects, counted from four stitched xy sections. For GW22 (bottom), n=2098 VASA⁺ objects, counted from three stitched xy sections.

Scale bars: 20 μm in A,B,D,F; 10 μm in C. Dashed red boxes in E and G indicate the 'arms' of single-positive cell populations.

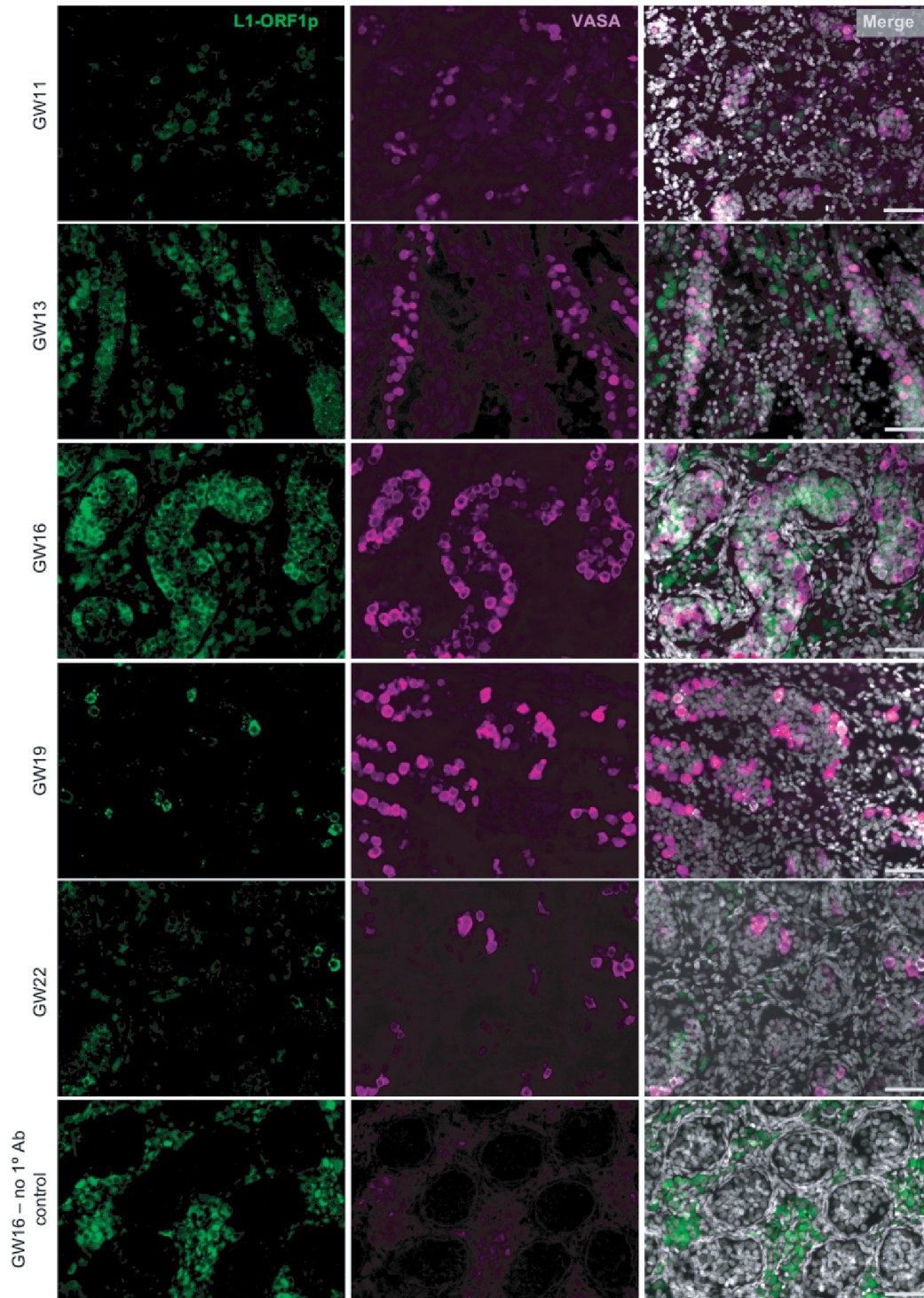


Figure 3.10 - Developmental time course of L1 expression in human fetal testis

L1 and VASA immunofluorescence in GW11 - 22 human fetal testis, counterstained with DAPI (shown in merge). A total of 12 embryos were analyzed across all time points. Bottom panel shows no primary antibody control and background fluorescence in corresponding channels. Scale bars: 20 μ m.

Examination of the relative expression of L1-ORF1p, HIWI2 and VASA in AGCs revealed a more dynamic relationship during fetal development than previously identified in the single cell RNA-seq analysis. The majority of L1-ORF1p expressing AGCs at GW22 coexpressed HIWI2 with significant correlation that approached the r value between HIWI2 and VASA (**Figure 3.9D,E**). Earlier, however, at GW19, we observed VASA⁺ cells with exclusive expression of either L1-ORF1p or HIWI2 and within the AGC population, the correlation between the two proteins was lacking at this timepoint (**Figure 3.9D,E**). Compared with the high correlation between L1 and HIWI2 transcripts in single cell RNA-seq at GW19 (**Figure 3.6E, Figure 3.8D,E**), these results indicate a delay in the coordinated expression of HIWI2 and L1-ORF1p proteins during fetal development. It is likely that the VASA single-positive cells at GW22 (**Figure 3.9E**, right) represent newly differentiating PGCs that have not yet turned on HIWI2.

HSP90 α is a chaperone protein, with an inducible isoform enriched in germ cells, which has been implicated in transposon repression and piRNA biogenesis in flies and mice (Gangaraju et al., 2011; Ichiyanagi et al., 2014; Izumi et al., 2013; Specchia et al., 2010; Xiol et al., 2012). Levels of HSP90 α transcript were high but variable in AGCs and PGCs (**Figure 3.6B,C**), with a negative correlation observed between HSP90 α and L1HS in AGCs but not PGCs (**Figure 3.6F**). Consistent with this, immunofluorescence revealed that a significant number of AGCs at GW16 and GW19 expressed exclusively L1-ORF1p or HSP90 α proteins but not both (**Figure 3.9F**, top and middle panels); accordingly, the XY scatter plots for L1-ORF1p and HSP90 α intensities displayed ‘arms’ at the extreme end of each axis of AGCs with mutually exclusive expression (dashed red boxes in **Figure 3.9G**). This relationship changed by GW22, when most AGCs expressing L1-ORF1p also expressed HSP90 α (**Figure 3.9F**, bottom panel), and a highly significant correlation was found (**Figure 3.9G**). Together, these observations suggest that three AGC subpopulations co-exist at GW16 – L1-high, HSP90 α -high and those low for both – and by

GW22 a subpopulation of HSP90 α single positive AGCs persist, but the majority of L1⁺ cells also express moderate to high levels of HSP90 α .

3.6 - Declining L1 expression and increasing H3K9me3 during fetal development

Thus far, we have characterized expression of key proteins of the PIWI-piRNA pathway (HILI and HIWI2) and confirmed expression of piRNAs and retrotransposons, yet it remains unclear whether the PIWI-piRNA pathway represses retrotransposons in human fetal testis. Although we observed increasing cytoplasmic to nuclear relocalization of HIWI2 by GW21 (**Figure 3.1C**), examination of subsequent events is limited by the availability of samples after GW22. We returned to the published single cell RNA-seq dataset of human fetal germ cells (Li et al., 2017) to examine the expression of TEs at GW25, again mapping reads to repeats as well as the genome. Distinct populations of somatic cells, PGCs and AGCs persisted at GW25, and TEs were largely absent from somatic cells and PGCs, but highly expressed in AGCs (**Figure 3.12**). Comparing the scaled expression of L1 family transposons in AGCs between GW19 and GW25 revealed a modest but statistically significant decrease (**Figure 3.11, Table 3.3**). This decline in L1 transcript at GW25 follows the upregulation of the transposon repression network, increased piRNA expression and nuclear translocation of HIWI2, suggesting that the PIWI-piRNA pathway may play an active role to silence TEs in developing AGCs.

Table 3.3 - L1 transcript expression from the single cell dataset in Figure 3.11. Data are mean \pm s.d. Student's t-test with two-tailed distribution and two-sample unequal variance was used to determine P values.

	TE	GW19	GW25	p-value
AGC	L1HS	0.75 \pm 0.27	0.59 \pm 0.27	4.84E-05
	L1PA2	1.33 \pm 0.43	1.07 \pm 0.43	3.70E-05
	L1PA3	1.01 \pm 0.27	0.88 \pm 0.35	<0.003
PGC	L1HS	0.39 \pm 0.31	0.35 \pm 0.31	N.S.
	L1PA2	0.55 \pm 0.41	0.52 \pm 0.22	N.S.
	L1PA3	0.63 \pm 0.38	0.57 \pm 0.29	N.S.

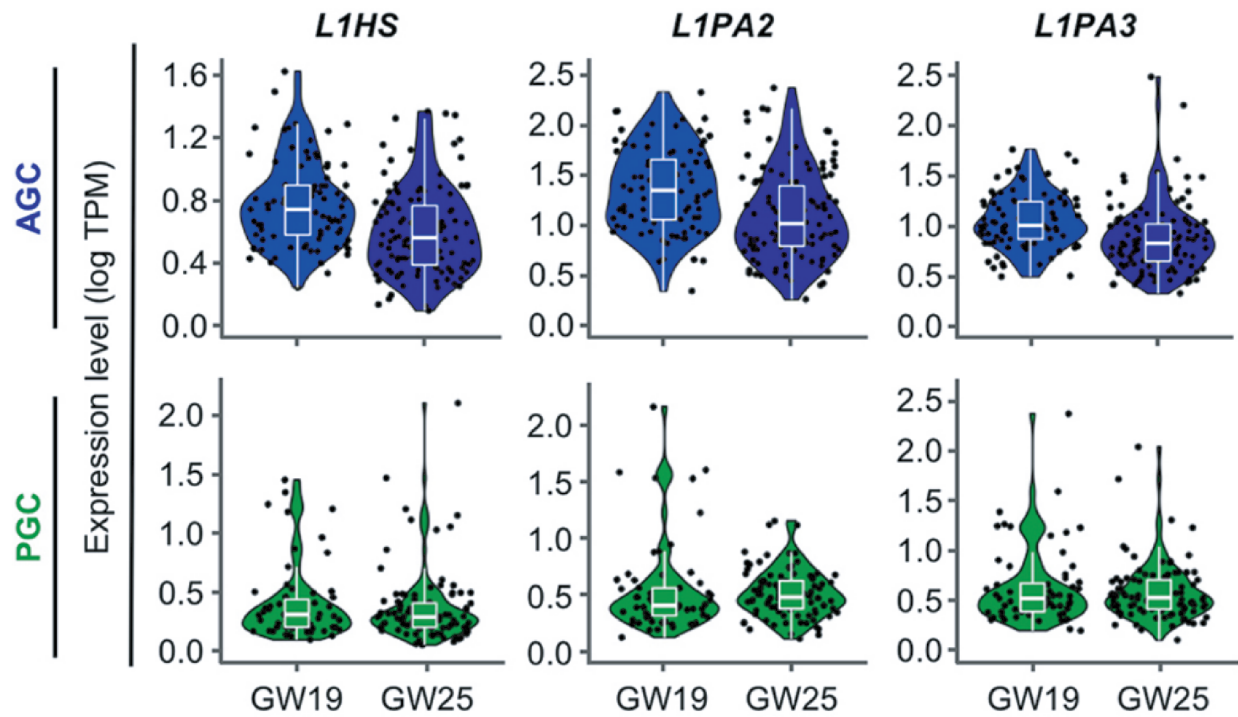


Figure 3.11 - Decrease in L1 transcript levels as development progresses.

Expression of L1 transcripts from the single cell RNA-sequencing dataset at GW19 and GW25. Violin plots showing expression of L1 family retrotransposons in AGCs (top) and PGCs (bottom), with median and quartile levels displayed in the box plots.

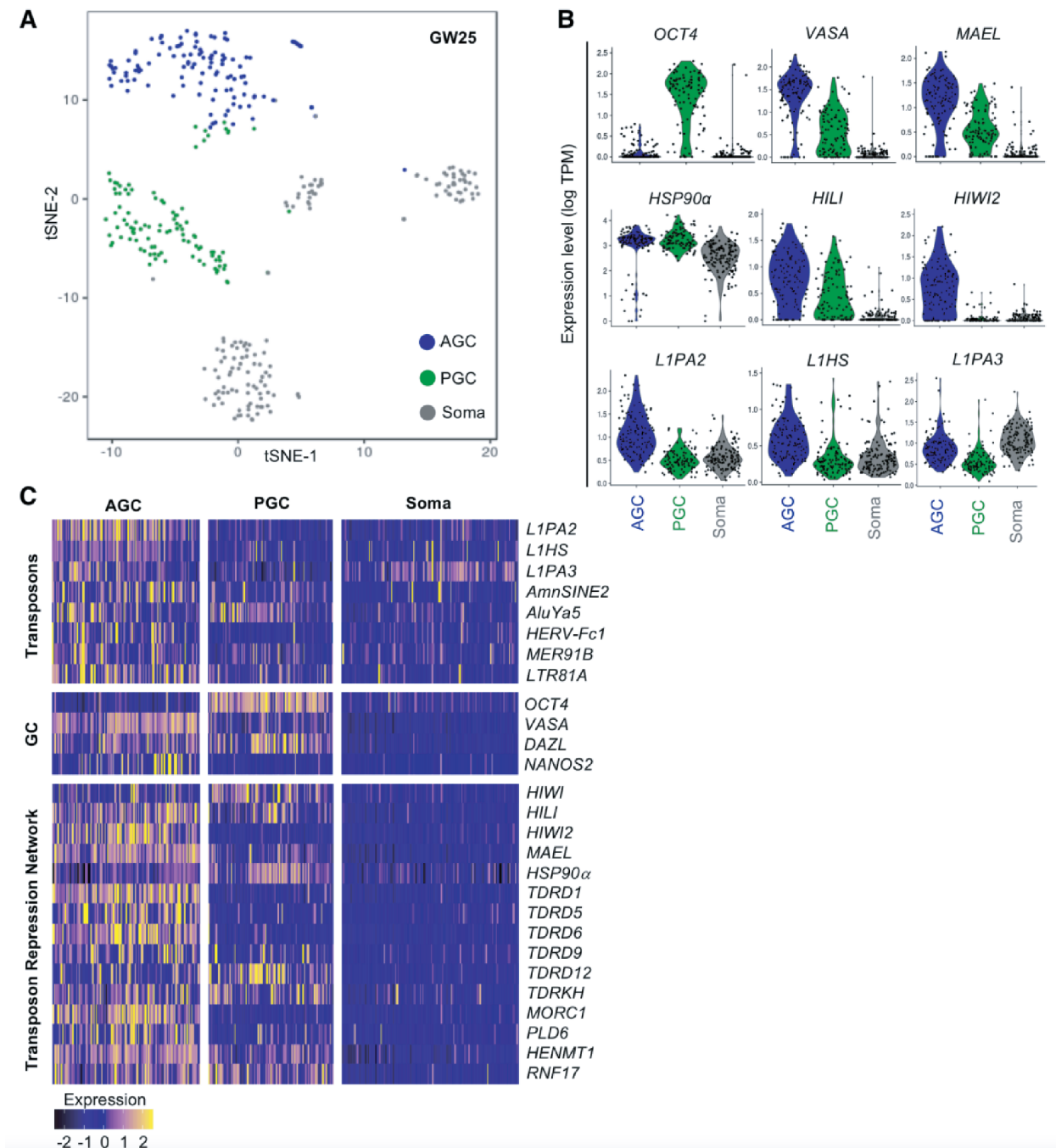


Figure 3.12 - Single cell sequencing of GW25 human fetal germ cells.

(A) tSNE clustering on transcriptome reference was used to generate five distinct cell populations, including AGCs, PGCs, and three somatic cell types grouped as one.

(B) Violin plots showing expression of germ cell markers (top), transposon repression genes (mid), and L1 family retrotransposons (bottom) in AGCs, PGCs, and soma.

(C) Heatmap displaying TE expression (top), and expression of germ cell markers (mid) and transposon repression genes (bottom).

To further examine the relationship between the PIWI-piRNA pathway and L1 by immunostaining, we turned to a xenograft model (Mitchell et al., 2010; Tharmalingam et al., 2018), in which human fetal testis implanted under the kidney capsule of immunocompromised mice will vascularize and continue to grow. Fragments of two testes, GW16 and GW17, were grafted into separate mice and allowed to grow from 1 to 4 months (**Figure 3.13A, Figure 3.14A**). We confirmed the continued development of fetal germ cells in grafts by examining HIWI2 localization. For both testes, there was a notable shift in HIWI2 localization. Although nontransplanted GW17 samples showed predominantly cytoplasmic localization of HIWI2 (~88% of cells), this frequency decreased in xenotransplanted samples after 4 or 8 weeks (41% and 60%; **Figure 3.13B,C**). Similarly, the non-transplanted GW16 sample was enriched for cytoplasmic rather than nuclear HIWI2 in AGCs (~70% versus 7%, respectively), but nuclear localization greatly increased after 5 and 16 weeks engraftment up to 41% and 55% of AGCs (**Figure 3.14B,C**). This change in HIWI2 distribution suggests that grafted tissues continue to develop to an equivalent of GW22 given the similar frequency of HIWI2 distribution, or that HIWI2 does not egress from the cytoplasm in all germ cells.

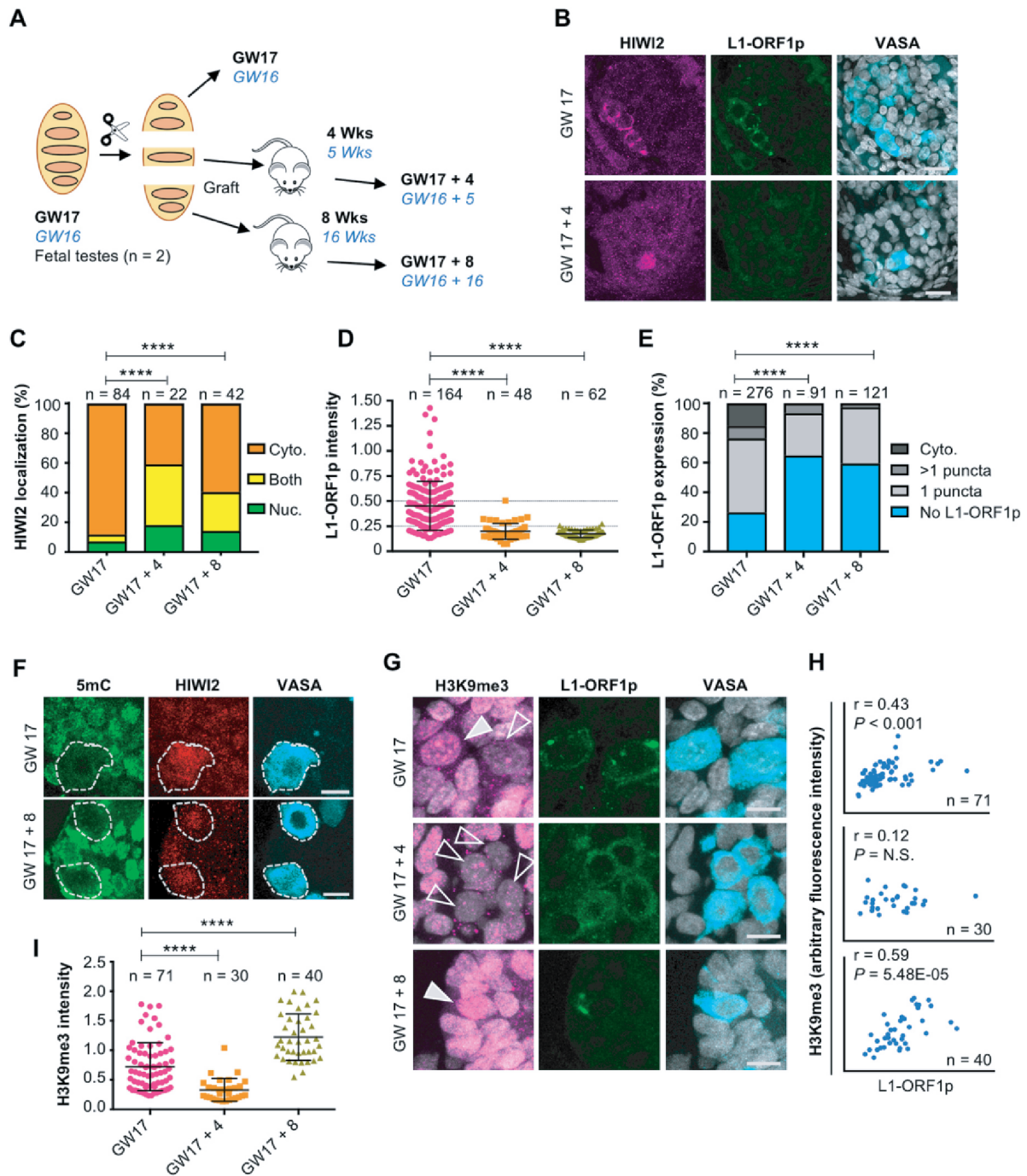


Figure 3.13 - Evidence for PIWI-piRNA pathway activity in fetal testis.

(A) Schematic of xenotransplant model with timepoints examined for n=2 biological repeats. The GW17 sample is shown, whereas the GW16 sample (blue italic text) is depicted in Fig. S8.

(B) Immunostaining for HIWI2, L1-ORF1p and VASA (shown in merge with DAPI) at GW17 (no xenograft; top) and GW17+4 weeks xenograft (bottom). Scale bars: 20 μ m.

- (C) Quantification of HIW12 subcellular localization in VASA⁺ cells of xenografted testes. Two-tailed Fisher's exact test was performed on 'nuclear' and grouped 'non-nuclear' categories across two time points.
- (D) Quantification of L1-ORF1p intensity normalized to VASA; Mann-Whitney U-tests were used to test significance.
- (E) Manual scoring of L1-ORF1p expression in VASA⁺ cells grouped into one of four categories: cytoplasmic staining; punctate cytoplasmic staining (either one puncta or multiple puncta); or no L1-ORF1p expression. Two-tailed Fisher's exact test was performed on the categories 'no L1-ORF1p' versus all grouped 'L1-ORF1p-expressing' cells across two time points to determine significance.
- (F) Immunostaining for 5mC, HIW12 and VASA in fetal testis at GW17 and xenografts. VASA⁺ cells are outlined. Scale bars: 10 μ m.
- (G) Immunostaining for H3K9me3, L1-ORF1p and VASA (shown in merge with DAPI) at GW17 and xenografts. Filled and empty arrowheads indicate high and low H3K9me3, respectively. Scale bars: 10 μ m.
- (H) xy scatter plots of H3K9me3 and L1-ORF1p fluorescence intensities with Pearson's correlation coefficients, P values and number of cells counted.
- (I) Quantification of H3K9me3 intensity normalized to VASA, measured in Volocity. Mann-Whitney U-tests were used to test significance. For all graphs, ****P<0.0001; n.s., not significant; n represents number of individual cells counted per time point.

We next examined the persistence of L1 expression in germ cells of xenografted testes. Similar to the decline observed in vivo from GW16 to GW22 (**Figure 3.10**), L1-ORF1p attenuated significantly over the first 4 weeks following transplant, with levels decreased by ~50% in individual AGCs (**Figure 3.13D**) and ~2/3 of VASA⁺ cells devoid of L1-ORF1p (**Figure 3.13E**). A similar decline was observed in the GW16 xenograft sample after 16 but not 5 weeks (**Figure 3.14B,D,E**). As the vast majority of AGCs at this timepoint have entered mitotic arrest (Li et al., 2017; Mitchell et al., 2010) (data not shown), a decrease in the frequency of L1-ORF1p⁺ cells must arise through degradation of protein, in addition to locus-specific silencing or transcript degradation. To determine whether the decrease in L1-ORF1p levels correlates with an increase in DNA methylation over time, we performed immunostaining for 5-methylcytosine (5mC). While robust methylation was detected in surrounding somatic cells, we were unable to detect 5mC in VASA⁺ AGCs at GW17-22 or in xenografted tissues (**Figure 3.13F**, **Figure 3.14F**, **Figure 3.15**).

This is consistent with previous reports of low global DNA methylation levels at GW26 (Guo et al., 2017b), suggesting that DNA remethylation occurs at later timepoints.

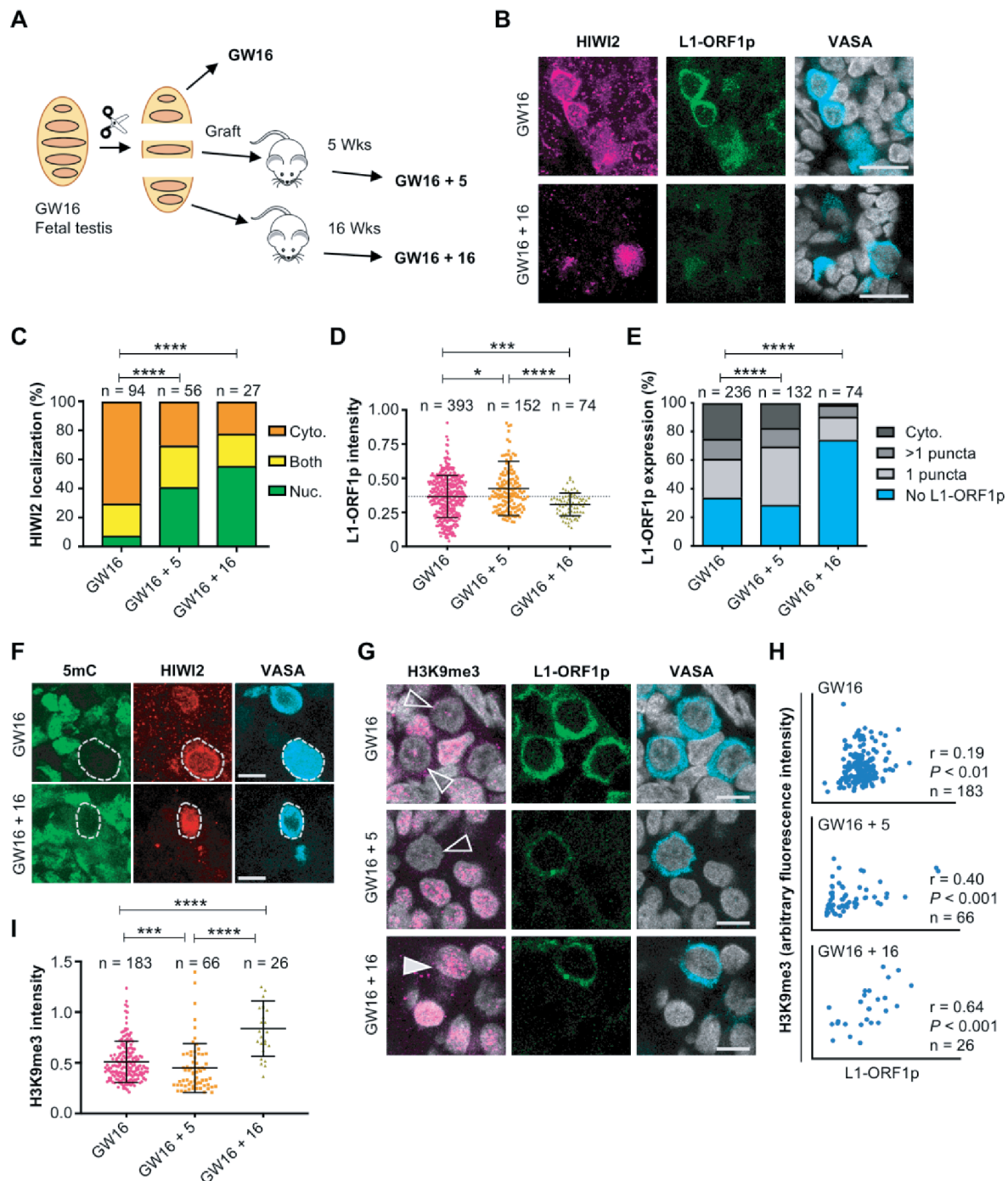


Figure 3.14 - Evidence for PIWI-piRNA pathway activity in fetal testis.

(A) Schematic of the xenotransplant model for the GW16 sample.

(B) Immunostaining for HIWI2, L1-ORF1p, and VASA (shown in merge with DAPI) at GW16 (no xenograft; top) and GW16 + 16 weeks xenograft (bottom). Scale bars: 20 μ m.

- (C) Quantification of HIWI2 subcellular localization in VASA⁺ cells of xenografted testes, with scoring and statistics as in Fig. 1C.
- (D) Quantification of L1-ORF1p intensity normalized to VASA; Mann-Whiney U tests were used to test significance.
- (E) Manual scoring of L1-ORF1p expression in VASA⁺ cells grouped into one of four categories: cytoplasmic staining, punctate cytoplasmic staining (either one puncta, or multiple puncta), or no L1- ORF1p expression. Two-tailed Fisher's exact test was performed on the categories "no L1-ORF1p" vs all grouped "L1-ORF1p-expressing" cells across two time points to determine significance.
- (F) Immunostaining for H3K9me3, L1-ORF1p, and VASA (with H3K9me3 and VASA shown in merge with DAPI) at GW 16 and xenografts. Filled and empty arrowheads denote high and low H3K9me3, respectively. Scale bars: 10 μ m.
- (G) XY scatter plots of H3K9me3 and L1-ORF1p fluorescence intensities with Pearson's correlation coefficients, p-values, and number of cells counted.
- (H) Quantification of H3K9me3 intensity normalized to VASA, measured in Volocity. Mann-Whiney U tests were used to test significance. For all graphs, **** = $p < 0.0001$; *** = $p < 0.001$; * = $p < 0.05$; "n" represents number of individual cells counted per time point.

The piRNA-guided deposition of H3K9me3 marks has emerged as an additional mechanism for transcriptional silencing of retrotransposons (Pezic et al., 2014). Thus, we examined this repressive histone modification by immunofluorescence. Many VASA⁺ cells harbored few or no H3K9me3 puncta at GW16/17 or in the xenografts aged 4 or 5 weeks (**Figure 3.13G, Figure 3.14G**). Following prolonged engraftment, we observed a significant increase in the levels in AGCs by GW17+8 and GW16+16 (**Figure 3.13G,I; Figure 3.14G,I**). The parallel trends of decreasing L1-ORF1p and rising H3K9me3 repressive mark would seem to be functionally related. However, unexpectedly, on a per cell basis, we observed that high levels of H3K9me3 were associated with high levels of L1-ORF1p (**Figure 3.13H, Figure 3.14H**). Thus, we conclude that the developmental trends of L1-ORF1p and H3K9me3 in human AGCs parallel those described in mouse at the population level, but that our analysis of single cells opens up the possibilities that either nuclear silencing operates independently of L1 protein degradation, or that some level of L1 protein will persist in human AGCs. Our results also raise the possibility that the TE nuclear silencing mechanism via H3K9me3 is exclusively activated in the subset of AGCs that initially express high levels of L1 protein.

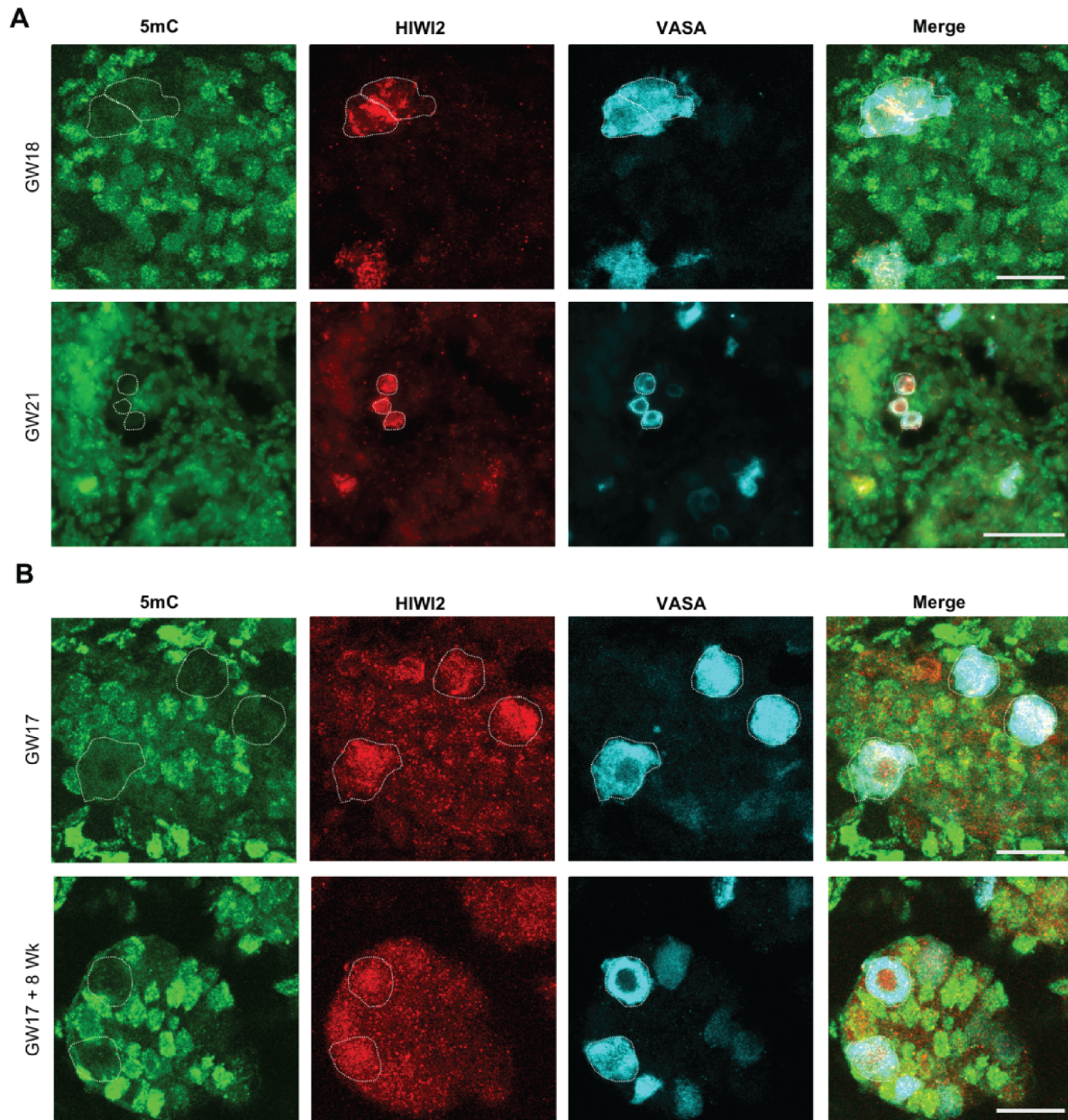


Figure 3.15 - No evidence for global DNA remethylation in AGCs

Immunostaining for 5mC, HIWI2, and VASA in fetal testis at indicated gestational ages (A) and in xenotransplant samples (B). All scale bars indicate 20 μ m except for bottom panel in (A) which is 50 μ m.

Our observations raise the possibility that expression of L1 precedes that of the repressive pathway. Unresolved issues include the means by which the PIWI-piRNA network becomes activated as well as how TEs remain adequately repressed in PGCs given their demethylated

state. The arginine methyltransferase PRMT5 has been implicated in TE repression in mouse PGCs by depositing repressive H2A/H4R3me2 marks on retrotransposons (Kim et al., 2014) and subsequent modification/activation of PIWI-family proteins (Vagin et al., 2009). We detected PRMT5 expression in fetal testes across development. Intriguingly, at GW13, when PGCs outnumber AGCs, PRMT5 could be detected in the cytoplasm and the nucleus, whereas it was exclusively cytoplasmic by GW17 (**Figure 3.16**). In mouse male germ cells, such a nuclear to cytoplasmic translocation is observed by E11.5, signifying the transition from the role of PRMT5 in histone modification to methylation of PIWI proteins (Kim et al., 2014; Vagin et al., 2009). Together, these results indicate that conserved mammalian mechanisms regulate TEs in the human testes. However, our analysis at the single cell level suggests that TE expression, and the resulting activation of the PIWI-piRNA pathway, occur in a subset of germ cells, whereas others are resistant.

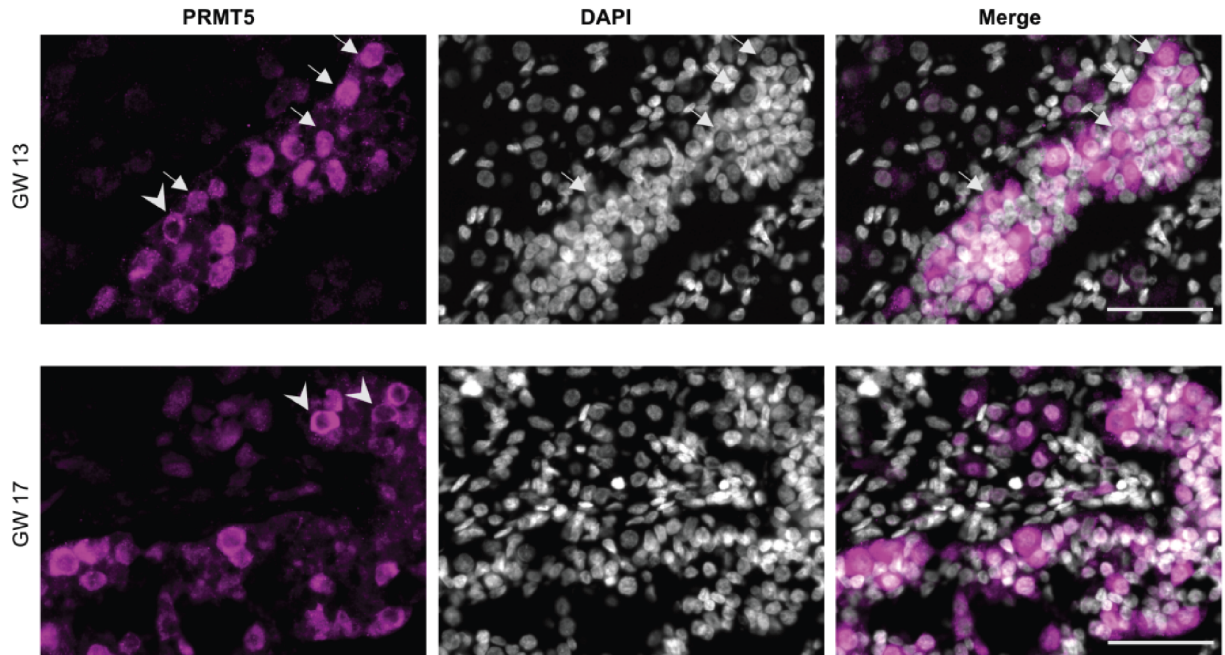


Figure 3.16 - PRMT5 expression in human fetal testis

Immunostaining for PRMT5 in fetal testis at indicated gestational ages. Arrows indicate germ cells with nuclear accumulation while arrowheads indicate cells with cytoplasmic PRMT5. Scale bar: 50 μ m.

3.7 - Discussion

In preparation for gametogenesis, PGCs undergo genome-wide epigenetic reprogramming; the removal of silencing marks that normally suppress TEs leaves the germline vulnerable to DNA breaks or transposition. Our characterization of L1 expression in human fetal germ cell development (**Figures 3.6, 3.8, 3.10, 3.11, 3.13**) underscores the need for the PIWI-piRNA pathway to protect germ cells from TE activity and maintain germline integrity. In this study, we describe the rise and fall of L1 expression in germ cells of the human fetal testis and provide evidence in support of an active TE repression network, including key PIWI proteins, pre-pachytene piRNAs and crucial co-factors, such as HSP90 α .

The fetal PIWI-piRNA pathway in mice is defined by PIWI family protein expression, TE-derived piRNAs and piRNA-dependent deposition of repressive epigenetic marks (Ernst et al., 2017). We show that these features are conserved in the human fetal testis by characterizing: (1) the composition, temporal expression pattern and sub-cellular localization of PIWI-family proteins (**Figure 3.1**); and (2) the presence of transposon-derived piRNAs that feature a secondary amplification signature (**Figure 3.3**). In mouse germ cells, MIWI2 is expressed from E15 to P3 (Aravin et al., 2008), during which time it is required for deposition of the epigenetic silencing marks 5mC (Aravin et al., 2008; Kuramochi-Miyagawa et al., 2008) and H3K9me3 (Pezic et al., 2014) in order to fully deplete L1-ORF1p by P2 (Aravin et al., 2009). Similarly, we observed a decline in the expression of L1 transcripts (**Figure 3.11, Table 3.4**) and L1-ORF1p that coincided with rising levels of H3K9me3 in AGCs from GW17 onwards (**Figure 3.10, 3.13, 3.14**). Given the limitations of working with human clinical samples, we could not test whether this was directly attributable to the PIWI-piRNA pathway or to the specific sites of H3K9me3 acquisition in the genome. However, our cumulative results suggest that the fetal PIWI-piRNA pathway restricts TE expression in human fetal germ cells.

Table 3.4 - Samples used for small RNA analysis

Sample ID	Exact Sample Age	RNA QC (RIN score)
GW13A	13 weeks	6.3
GW13B	13 weeks	6.3
GW14	14 weeks	6.9
GW15	15 weeks	6.6
GW17	17 weeks	5.9
GW20	19 weeks, 4 days	5.8
GW21	20 weeks, 5 days	5.2
GW22	21 weeks, 5 days	4.1

Our study provides the most comprehensive characterization of the PIWI-piRNA pathway in the human fetal testis to date. In addition to confirming and expanding upon the reported expression of HILI and HIWI2 in the human fetal testis (Fernandes et al., 2018), we observed dynamic localization of HIWI2 during human development, with transition from the cytoplasm to the nucleus occurring between GW18 and GW21 (**Figure 3.1**). Recent studies in human fetal ovary and adult testis showed that piRNAs were derived from genomic piRNA clusters (Ha et al., 2014; Roovers et al., 2015; Williams et al., 2015). Previous efforts to identify piRNAs from fetal testis were confounded by low abundance, dearth of samples and conflicting analyses (Gainetdinov et al., 2017; Williams et al., 2015). Here, we characterized piRNAs from eight fetal testes samples across a wide developmental range (GW13-22) and identified TE-derived piRNAs with a peak expression at GW20, which corresponds with the timing of nuclear HIWI2 translocation and further supports an active PIWI-piRNA pathway that represses TEs. This notion is corroborated by the finding that high L1 transcript correlates with lower expression of

PIWI-piRNA pathway genes, including HIWI2, in boys at risk of infertility (Hadziselimovic et al., 2015). Additionally, mechanistic studies in human iPS cells showed that HILI can directly modulate L1 activity (Marchetto et al., 2013).

Human fetal germ cell development is marked by heterogeneity at the level of transcript, protein and cell state. For example, whereas PGCs in mice acquire markers of male differentiation and undergo mitotic arrest from E13.5 to E14.5 (Western et al., 2008), in humans the transition from PGC to AGC is spread across weeks and results in both populations within the same gonad (Gkoutela et al., 2013). We observed heterogeneity between cells in the expression of transcripts for TEs and the TE repression network (**Figure 3.6, 3.11 3.12**). Similarly, we observed heterogeneity in the levels of L1- ORF1p, HIWI2 and HSP90 α proteins (**Figure 3.9**). Notably, heterogenous L1-ORF1p expression was previously observed in fetal oocytes in mice (Malki et al., 2014). HSP90 is a highly expressed molecular chaperone, constituting ~1% of soluble cytoplasmic protein content (Buchner, 1999). A germ cell specific inducible isoform, HSP90 α , has been implicated in regulating the abundance of L1-ORF1p in mouse, most likely at the translational or post-translational stage (Ichiyanagi et al., 2014). A physical interaction between HSP90 α and the second open reading frame of L1 (ORF2p) was recently revealed by proteomics (Taylor et al., 2018). In the fetal testes at GW16-19, we observed a pattern of reciprocal expression between HSP90 α and L1-ORF1p, with AGCs positive for one or the other, but not both proteins (**Figure 3.9F**); however, by GW22 and later, the expression of L1- ORF1p was diminished overall (**Figure 3.13D, Figure 3.14D**) and cells retaining L1-ORF1p now simultaneously expressed HSP90 α (**Figure 3.9F**). A similar trajectory was found with HIWI2 and L1- ORF1p, in which AGCs at GW19 were primarily single positive, but express both proteins at similar levels by GW22 (**Figure 3.9E**). Based on these observations, we propose a model whereby a subset of early AGCs marked by high levels of HSP90 α at ~GW16 is resistant to the expression of transposons (**Figure 3.17**). After this point, we propose that AGC development

diverges and HSP90 α low AGCs become susceptible to expression of L1-ORF1p, which leads to the upregulation of the PIWI-piRNA pathway and transposon silencing. Based on the coincidence of sustained L1-ORF1p and high levels of HIWI2 and H3K9me3 in later AGCs, we suggest that silencing occurs through piRNA-guided deposition of H3K9me3 in the nucleus (**Figure 3.13G**, **Figure 3.14G**). Although we did not detect 5mC in AGCs in xenografted testes after 2-4 months (**Figure 3.13F**, **Figure 3.14F**), DNA remethylation at TE loci could be undetectable by immunofluorescence or else could occur later in development. By contrast, we propose that HSP90 α high AGCs are protected from initial transposon expression and it remains to be determined if they ever express transposons or upregulate the transposon repression/ PIWI-piRNA pathway. Our data suggest that suppression of TEs earlier in development in PGCs, prior to the expression of PIWI genes, could occur via other mechanisms such as PRMT5-mediated nuclear silencing (**Figure 3.16**), as previously shown in the mouse (Kim et al., 2014).

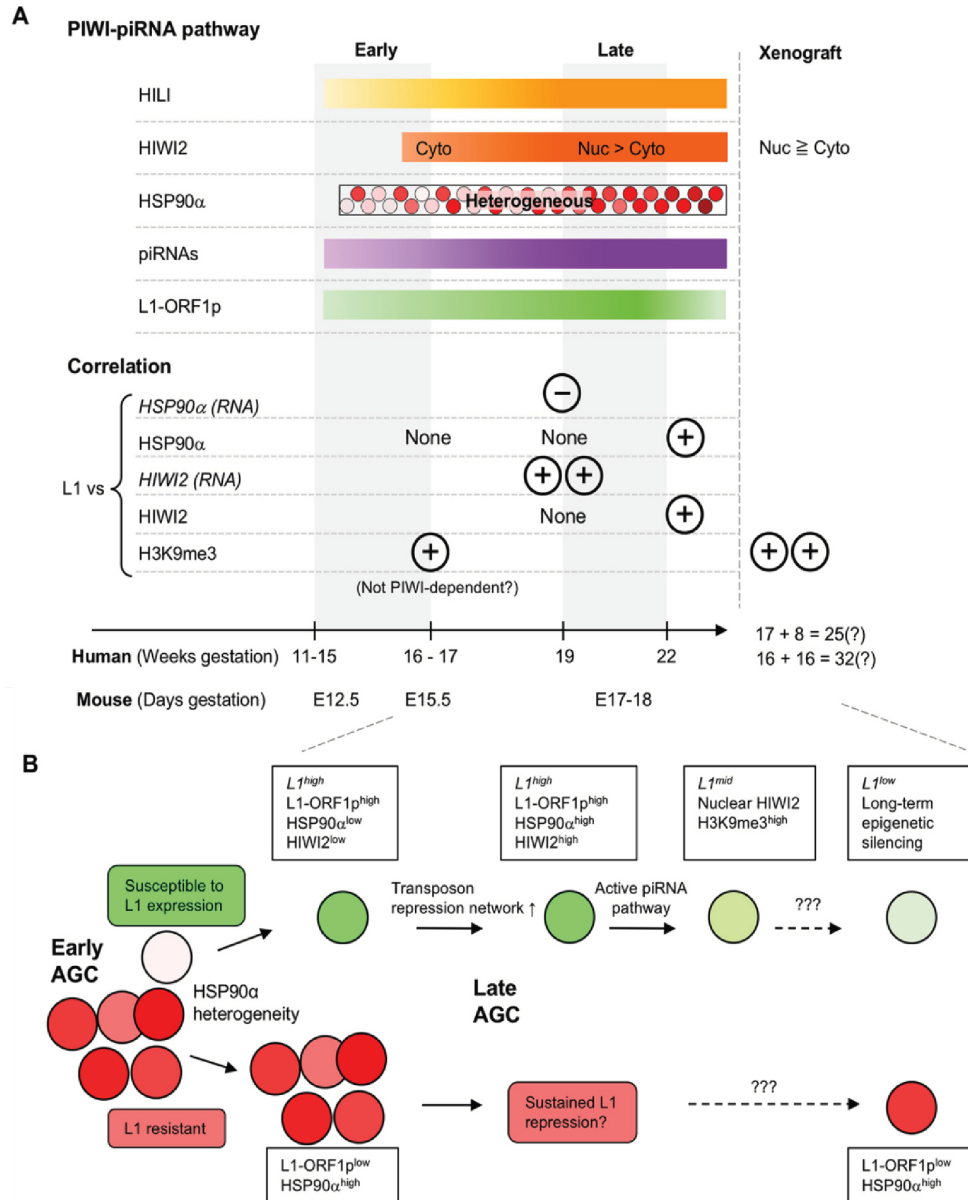


Figure 3.17 - Coordinated transposon repression in GCs of the human fetal testis.

(A) (Top) Summary of the expression pattern of PIWIpiRNA pathway components and L1 protein in developing germ cells in the human fetal testis at indicated timepoints and in aged xenograft samples. (Bottom) Relationships between L1 expression (protein, except where indicated) and expression of PIWI-piRNA pathway factors and H3K9me3 at indicated developmental stages. By GW22, many L1-expressing AGCs also express components of the repression network.

(B) Model for transposon expression and repression in developing AGCs. See Discussion for details.

The PIWI-piRNA pathway is often considered the immune system of the germline. In this paradigm, TEs are viewed as a threat to developing germ cells that must be immediately silenced by the PIWI-piRNA pathway to prevent their mobilization and subsequent genome disruption. However, our single cell analyses reveal that the expression of TEs (**Figure 3.6, 3.9, 3.12**) precedes that of the transposon repression network, and thus cells experience a window of TE expression prior to repression. This observation is consistent with previous studies that have shown consistent L1 transcript expression from GW4-19 (Guo et al., 2015), where the earliest timepoint, GW4, substantially predates the onset of the repression pathway. Could this early expression of TEs play a functional role during germ cell development? Recent studies argue in favor of this idea, by providing evidence that the L1 transcript is essential for early embryonic development in mice and may function in the remodeling of the epigenetic landscape (Jachowicz et al., 2017; Percharde et al., 2018). In addition, both L1-ORF1p and L1-ORF2p were previously observed in a single GW18 testis (Ergün et al., 2004). As we observe the onset of HIWI2 and HSP90 α ~1 month later than the first L1-ORF1p (**Figure 3.17**), it is tempting to speculate that initial expression of TEs is required to 'prime' the activation of the repression network. This issue, and whether L1 plays any other functional roles during germ cell development will be the subject of future investigations.

3.8 - Materials and Methods

Human sample collection and processing

Human fetal specimens were collected free of patient identifiers after elective termination of pregnancy (Committee on Human Research, University of California, San Francisco, IRB# 12-08813 and 16-11909). All fetal samples were transported on ice for gonad microdissection. Age of specimen (referred to as GW – gestational week in text) was determined by heel-toe measurement. Gonads were left in RPMI 1640 media supplemented with L-glutamine at 4°C from a few hours to overnight, and for up to two nights for some samples. Specimens were either flash frozen for molecular biology analysis or fixed for immunofluorescent staining. For staining, tissues were fixed overnight in 2% PFA in PBS solution at 4°C with gentle agitation. Tissues were then washed, incubated overnight in 30% sucrose at 4°C, embedded and frozen in OCT solution (Tissue-Tek). Embedded tissues were cryosectioned at 8 µm.

Animals and xenograft model

Wild-type embryos were generated by mating CD1 females with homozygous Oct4-ΔPE-GFP males (MGI:3057158, multiple-copy transgene insertion (Anderson et al., 1999)). Embryos were dissected from timed matings and staged using anatomical landmarks from E16.5 to E18.5. Immunodeficient CD1 nud/nud homozygous (Charles River) mice were used as host for the xenograft. Prior to surgery, human fetal testes were cut into four fragments and held in ice-cold RPMI 1640 medium until xenografting, with one fragment set aside for fixation. Hosts were anesthetized, a 2 cm back midline incision was made to exteriorize each kidney and a 2 mm opening was made in the renal capsule. One fetal testis fragment was xenografted into the left

kidney capsule of each host. The peritoneum was closed with c-9 silk surgical sutures (Henry Schein), and the incision was stapled closed with stainless steel wound clips (MikRon). Following surgery, animals were monitored daily for food and water intake, and any obvious signs of stress. All mouse work was carried out under the University of California, San Francisco, Institutional Animal Care and Use Committee guidelines in an approved facility of the Association for Assessment and Accreditation of Laboratory Animal Care International.

Immunofluorescence

We performed immunofluorescent staining on sectioned slides using our general staining protocol. Slides were washed three times with 1× PBS for 5 min at room temperature to dissolve OCT. Samples were permeabilized with PBT (1× PBS+0.5% Triton X -100) for 10 min at room temperature, followed by three short rinses with 1× PBS, and then blocked for 1 h at room temperature with fresh blocking buffer (10% heat inactivated donkey serum in 1× PBS+0.1% Triton X-100). Subsequent primary antibody incubations were performed in humidified chambers at 4°C overnight, with primary antibodies (see **Table 3.5**) diluted appropriately in blocking buffer. The next day, slides were washed three times in 1× PBS for 5 min at room temperature, and then treated with secondary antibodies (1:200) and DAPI nuclear counterstain (1:1000) for 1 h at room temperature. Slides were washed three times in 1× PBS, and then mounted with Vectashield Antifade Mounting Medium (Vector Laboratories, H-1000). Some antibodies required antigen retrieval with either sodium citrate buffer (pH 6.0) or Tris-EDTA buffer (pH 8.8) (see Table S3). Antigen retrieval conditions consisted of boiling slides in appropriate solution for 10 min, followed by washes in 1× PBS and processing according to the general staining protocol. 5meC antibody staining required Tris-EDTA (pH 8.8) antigen retrieval followed by PBT permeabilization and incubation in 3.5 N HCl for 1 h prior to the general staining protocol. Xenograft samples incubated with a primary antibody from a mouse host required antigen

retrieval and blocking with Mouse on Mouse blocking reagent (Vector Laboratories, MKB-2213). Following our staining protocols, images were acquired from a Keyence fluorescence microscope and/or Leica Sp5 upright confocal microscope w/AOBS.

Table 3.5 - Antibodies used

Antibody	Company	Catalog #	Lot #	Concentration	Antigen retrieval?
VASA	R&D	AF2030		1:100	
HIWI2	abcam	ab180867	GR3177109-1	1:400	Tris-EdDTA pH8.8
HILI	Origene	TA319952		1:500	Tris-EdDTA pH8.8
MIWI	Cell Signaling	2079	1	1:200	
HSP90AA1	Life technologies	PA3013	PL210596	1:1500	
L1-ORF1p	Millipore	MABC1152	2881932	1:200	
OCT4	Abcam	ab27985	GR3183882-1	1:100	
5mC	Eurogentec	BI-MECY-0100	vt15210d	1:100	Tris-EDTA pH 8.8 -> 3.5 N HCl
PRMT5	Millipore	07-405	2716186	1:500	
H3K9me3	Abcam	Ab8898	GR3207391-1	1:400	Tris-EdDTA pH8.8

Automated fluorescence intensity quantification

Images were obtained from Keyence microscope (model BZ-X710) using a 20× objective and stitched with Keyence imaging software. Background was subtracted on FIJI software (Schindelin et al., 2012) using a rolling ball radius of 25 pixels and disabled smoothing. VASA⁺ objects corresponding to single cells were identified using Volocity version 6.3. Our VASA⁺ object detection protocol included the following modules: ‘Find objects’ in the VASA channel, ‘Close’ objects for two iterations, followed by ‘Fill holes in objects’ and separate touching objects at a size of 600 μm^2 . Next, VASA objects were excluded below and above size thresholds (<599 μm^2 and >2405 μm^2). Finally, VASA⁺ objects were filtered for mean VASA channel

intensity >45 and shape factor >0.413. Identified objects were manually inspected and non-cellular objects were manually deleted. A variation of this protocol was used to find VASA⁺ objects from images acquired from the Leica Sp5 confocal microscope using a 63× oil objective.

Manual scoring for HIWI2 localization

Z-stack images through the entire section width (8 μm) were obtained on a Leica Sp5 confocal microscope using a 63× oil objective. Z-stacks were opened on FIJI imaging software and VASA⁺ cells were manually scored for HIWI2 subcellular localization. HIWI2 localization was compared with VASA (cytoplasmic marker) and DAPI (nuclear marker) and assigned to either of three categories – nuclear (where the majority of HIWI2 appeared overlapped with DAPI staining), cytoplasmic (where HIWI2 staining was excluded from DAPI and overlapped with VASA) or both (where HIWI2 staining appeared equally distributed between the compartments). See Figure 3.1C for representative examples of cells scored for each localization phenotype.

Small RNA-sequencing of human fetal testis

All samples were processed and sequenced by Quick Biology. Total RNA extractions were performed on bulk fetal testis tissue using Trizol, and quality control was performed on total RNA using the Agilent Total RNA Nano Bioanalyzer kit. Resulting RNA integrity number (RIN) scores, are provided in **Table 3.4**. Libraries were prepared using the QIAseq miRNA Library Kit, and library quality was assessed using the Agilent Bioanalyzer High Sensitivity DNA assay. Paired-end sequencing was performed on an Illumina HiSeq 4000.

Small RNA-sequencing data analysis

All samples were sequenced to a depth of approximately 35-40 million reads in order to meet the minimum read requirement for small RNA-seq data of 30 million as outlined by the ENCODE consortium (www.encodeproject.org/rna-seq/small-rnas/#restrictions). Raw reads in fastq files were trimmed to remove the adapter sequence (AACTGTAGGCACCATCAAT) using cutadapt version 1.8.1 (Martin, 2011), and reads were subsequently size filtered to 18-40 nt using cutadapt. FastQC (version 0.11.5) was utilized to broadly assess read quality. Trimmed reads were aligned to Repbase (version 22.11), a collection of consensus sequences of known human transposons, curated by GIRI: the Genetic Information Research Institute (Bao et al., 2015). Alignments were performed with bowtie (Langmead et al., 2009) version 1.2.2 using the following options: -v 1, -M 1, -best, -strata, signifying a maximum of one mismatch between the read and reference sequence, with multimappers being randomly assigned to only one location. All reads that did not align to Repbase were subsequently aligned (with bowtie version 1.2.2 and same options) to the human genome (GRCh38) in order to determine the contribution of other RNA types to the total small RNA pool. Aligned reads were intersected with genomic features and counted using the htseq-count function of HTSeq (Anders et al., 2015) version 0.9.1, with the following parameters: -f sam -t exon -s yes -i gene_type -m intersection-nonempty -nonunique all -a 0. The reference file containing genomic feature coordinates was a custom GTF file generated by merging the GENCODE 28 comprehensive gene annotation list with GENCODE 28 predicted tRNA genes. Feature counts for miRNAs, tRNAs, snoRNAs and protein-coding transcripts were combined with the number of Repbase-mapping reads to generate a breakdown of RNA subtypes. For a comprehensive explanation of RNA subtypes and relative percentages, see Table S1. Repbase-mapped reads were further analyzed for known piRNA signatures, including a 5' uridine bias and 10th position adenine bias, by calculating the nucleotide frequency distribution per base position along the read for all pooled

Rebase-mapped reads of a given sample. Read overlap signatures, which are characteristic of the piRNA ping-pong biogenesis cycle, were calculated on the MISSISSIPPI Galaxy server (mississippi.snv.jussieu.fr) using the 'Small RNA Signatures' tool (Galaxy Version 3.1.0), developed by Antoniewski (2014). Transposable element annotations and transposable element-specific read size distributions were calculated directly from alignment files post Rebase mapping.

Bioinformatic pipeline for single-cell RNA-seq data analysis

Adapter trimmed reads were downloaded from Gene Expression Omnibus (GEO). FastQC (Conesa et al., 2016) was used initially for a broad quality control check. Using UMI-Tools (Smith et al., 2017), we determined real cells from background noise using the cell ID/UMI information in read 2. Cell IDs/ UMI information from read 2 was extracted and appended to the read name. Using BBduk (Mbandi et al., 2014; Mills, 2014) (sourceforge.net/projects/bbmap/), reads were quality trimmed to Q10. For our transcriptome alignment, we used the default STAR/2.9.3a parameters (Dobin et al., 2013) to align to reference genome GRCh38.91 human transcriptome (Ensembl) with mitochondrial annotations added. To maintain the presence of multimappers in our human repeat reference alignment, the following STAR parameters were used: `--outFilterMultimapNmax 100`, `--winAnchorMultimapNmax 100`, `--outSAMmultNmax 100` and `--outFilterMismatchNmax 3` (Ge, 2017). After specific gene or repeat element annotations were respectively assigned to the aligned files using Subread (Liao et al., 2014), UMI-Tools was used to count the unique reads per annotated gene/repeat element per cell. Finally, count matrices of the human repeat reference alignment and transcriptome were concatenated, providing standard single cell RNA-sequencing data on the transcriptome in conjunction with novel count data of repeat elements at a single cell level.

Clustering and differential gene expression analysis

Briefly, the concatenated count matrix was read into R/3.4.4 for analysis with the Seurat/2.1 suite of tools (Satija et al., 2015). Beginning with 196 cells from GW19 and 389 cells from GW25, we filtered on a 0.06% mitochondrial gene expression threshold and an nGene value of 3000. We were left with 191 cells from GW19 and 363 cells from GW25. 24,432 genes and 1225 repeat elements were expressed across all 191 cells from GW19. 24,507 genes and 1320 repeat elements were expressed across all 363 cells from GW19. Using Seurat, 782 and 637 variable genes were identified from the three defined clusters of somatic cells, primordial germ cells and advanced germ cells in GW19 and GW25, respectively. Transcriptome markers for the primordial and advanced germ cell populations were determined using the FindMarkers Seurat function and the 'roc' test with a minimum cellular detection threshold of 0.25 for each population. Additionally, transposon expression data alone were appended as an assay to the Seurat object, enabling us to ascertain which repeat elements were markers for each germ cell population.

Statistics

Experimental data were compared using Student's t-test and Fisher's exact test as noted in the figure legends. The significance of Pearson's correlation coefficient was determined with regression analysis.

Chapter 4 - Future Directions and Concluding Remarks

4.1 - Fertility studies in GR conditional knockout mice

An open question in the field is whether the negative effects of glucocorticoid treatment and stress on fertility are acting solely at the level of hormonal regulation, or if there is a direct impact of GR signaling on the germline. Fertility studies using conditional knockout mice will be the most conclusive way to prove whether there is a cell-intrinsic role of GR in either the male or female germline, and thus should be prioritized very highly. Therefore, a pressing piece of follow up work for this project is the generation of a conditional knockout model of GR in both the male and female germline. The perinatal lethality of homozygous loss of GR has thus far made it impossible to study the effect of loss of germ cell GR on adult fertility, and efforts to date have proven unsuccessful in generating a conditional knockout model for both the male and female as described extensively in Chapter 2.

In moving forward, one potential Cre driver to consider is the Ddx4-Cre (also known as Vasa-Cre or MVH-Cre), which would allow for GR excision specifically in the germline in both the male and female starting at ~E15.5. This system doesn't utilize tamoxifen, and thus will allow for successful delivery of pups without needed c-sections/fostering. This system will be ideal for studies in the male, as GR does not come on until E17.5 at the earliest, thus ensuring that GR is never expressed in the germline. In the female, GR is already on by E13.5, and thus this line may not be ideal for the female. For the male, utilizing the spermatogonial PLZF-Cre could also work well. PLZF expression in the male comes on just before birth, at about the same time as GR, and is maintained into the spermatogonia into adulthood. Unfortunately, this line has proven a bit difficult to procure. For the female, considerably less options exist given that we effectively need to excise GR before E13.5. At the time of writing this, the only two options are

Blimp1-Cre and Oct4-CreERT2, both of which have considerable limitations as described. Oocyte Cre lines such as Zp3-Cre likely won't be helpful as we have seen no GR expression in the adult oocyte thus far. Although current options are limited, designing other (non-inducible) Cre models in the future for early germ cell markers (e.g. Tra98) may be the most useful way to overcome these limitations.

While we have not seen any transcriptional or obvious phenotypic defects in embryonic female germ cells following perturbations to GR, it is possible that the functional consequences of fetal disruption to GR may not manifest until adulthood. In fact, in zebrafish where deletion of GR is not lethal, females don't show any germ cell defects until later in their reproductive lifespan. This highlights to us the importance of extending our initial analysis of GR knockout embryos into adulthood, thus further emphasizing the importance of generating a conditional knockout model moving forward.

4.2 - Mechanistic analysis of GR signaling resistance in female germ cells

An additional facet of this work that potentially warrants further follow up is trying to elucidate the underlying reason as to why female germ cells are resistant to changes in GR signaling. Our work has suggested that something inherent to the female germ cells is buffering these cells from changes to GR activity, although the mechanism behind why this is occurring is unclear. While we have already ruled out the presence of different dominant negative isoforms, we have faced considerable technical limitations for additional mechanistic experiments. Two of the (non-mutually exclusive) hypotheses that we have are that either (a) some post translational modification is added to GR specifically in the germ cells that renders it inactive, or (b)

something is interfering with GR's ability to bind DNA, thus preventing downstream transcriptional changes.

Unfortunately, the most definitive experiments to test these two hypotheses, mass spectrometry and ChIP-seq (respectively), require very high numbers of cells. We have been very limited thus far, as FACS sorts typically yield only 10-20,000 germ cells per embryo. Considering mass spec and ChIP-seq experiments typically require millions of cells (an absolute *minimum* of one million, or 50-100 embryos of sorted germ cells), and need to be performed in biological replicates to gain sufficient statistical power, the sample collection becomes exponentially time consuming and costly. As we have not optimized mass spec or ChIP-seq protocols on germ cells specifically, this will also require considerable time and large numbers of cells. While not impossible, these limitations are substantial, and should be considered very carefully before moving forward with employing these techniques. While we have considered targeted mass spec to look for specific PTMs of GR, we would be limited to looking for known PTM events/sites, which may or may not be driving the phenotype seen. An alternative strategy to ChIP-seq for assessing DNA binding of a transcription factor that utilizes far fewer cells is CUT&RUN (Skene and Henikoff, 2017). While we have been successful in employing this technique to measure genome wide histone modifications in germ cells, we have been unsuccessful thus far in profiling transcription factor binding (a problem many other groups have been facing based on personal communication). The final technique that could be employed fairly successfully given our cell number limitation is ATAC-seq for profiling chromatin accessibility. While it may be possible through transcription factor footprinting analysis to get an idea for whether GR binding sites are occluded by condensed chromatin in the female germ cells, this technique is far less direct than measuring direct GR binding to DNA. It may also prove difficult to interpret the results due to the fact that GR can also be tethered to DNA indirectly through protein-protein interactions.

Despite some of these alternative strategies to explore the mechanism of GR resistance in female germ cells, we also recognize the potential difficulty in validating any of these mechanisms further. If any potential inhibitory PTMs are found on GR, validation would require introducing point mutations in GR and generating a novel mouse model(s), which is not trivial. As GR is expressed and required ubiquitously throughout the body, any modifications to GR at potentially important sites of post-translational modifications may be lethal, and thus impossible to validate further. Similarly, any impaired DNA binding ability of GR would be difficult to perturb or validate further in our *in vivo* system. Therefore, it will be extremely important to prioritize fertility studies in cKO females before exploring any of this mechanism of GR resistance. If loss of GR in the oocytes does not impair fertility in any way, the effort to explore this resistance mechanism may not be worth the time and cost.

4.3 - Further analysis to confirm GR regulation of RNA splicing in spermatogonia

As explained extensively in Chapter 2, our initial RNA-seq data of dex-dosed germ cells at PN1 implicated GR in the regulation of RNA splicing. This was a very exciting result as (a) GR had not previously been implicated in regulating the expression of splicing machinery, and (b) proper splicing is known to be crucial for proper meiotic progression, implicating GR as a potential regulator of this process. However attempts to validate this link between GR and splicing at later time points yielded conflicting results, which may have been due to a variety of technical reasons including performing qPCR analyses on bulk testis tissue. At the time when experiments were being performed, we did not have a protocol in the lab for isolating spermatogenic cells of the testis away from the soma, and thus decided to perform a bulk tissue analysis. Therefore, a simple initial follow up experiment would be to repeat these dex dosing

experiments to look for changes in splice factor gene expression and isoform splicing (by similar qPCR experiments), but in sorted populations to remove the potential ambiguity introduced by the somatic cells. Differential sedimentation protocols exist for roughly isolating spermatogenic cell types, although cleaner genetic systems (such as a Ddx4-Cre crossed to a recombination reporter such as Ai14) could also be feasibly employed. Furthermore, based on the highly restricted expression pattern of GR in the spermatogonia, it might also be beneficial to further isolate spermatogonia from the total spermatogenic cell population to further drill down on the role of GR in splicing in this specific cell type.

It is also still unclear whether GR regulation of splicing may be time point dependent. Our initial RNA-seq analysis was performed at PN1, as we initially believed that GR was turning off in the pro-spermatogonia between PN2 and PN5. As we refined our tissue processing protocol for cryo-embedding and sectioning of postnatal and adult testis tissue, we then realized that GR expression dips between PN7 and PN14, but increases again and becomes restricted to spermatogonia by PN21. This spermatogonia-specific expression pattern is maintained into adulthood, and therefore it would be logical to now test whether dex treatment of adult males leads to any impairments in splicing within adult spermatogonia. Perhaps the most unbiased method to do this would be to utilize RNA-seq on purified spermatogonia from dex-dosed males, in order to capture both changes in splice factor expression, as well as differential splicing events within the global transcriptome. A single cell RNA-seq approach could also be considered to avoid the need for cell type specific isolation, while also having the added benefit of capturing all spermatogenic stages to query any effects of GR perturbation on downstream spermatogenic differentiation. If a conditional knockout model can be successfully implemented, including spermatogonia with a GR cKO in this transcriptomic analysis would prove invaluable as a complementary group in which GR signaling is lost in comparison to activation by dex.

Lastly, if we can confirm that GR is regulating splicing in the adult spermatogonia, we would then need to characterize the downstream effect of GR perturbation on meiosis. As described more extensively in Chapter 2, proper transcript splicing in the testis is crucial for the proper progression of meiosis and spermatogenesis. If perturbations to GR signaling can disrupt proper meiotic progression through the dysregulation of RNA splicing, this would have tremendous implications for the field regarding the effects of stress hormones on the overall integrity of the germline.

4.4 - Concluding Remarks

For any of you who have made it this far, I thank you for taking the time to read through my thesis work. To any of my future colleagues who may be following up on this work in the near or distant future, I hope that I have been able to provide a sufficient foundation off which your work can be built. This project has yielded many unexpected and confounding results, and I hope that you take the time to carefully read through this chapter in particular before following up on any of the pieces of this work. I have done my best to present my results clearly, and I have done my best to provide my best interpretation of the data I have collected. Lastly, I hope I have clearly outlined the caveats of both the experiments conducted and the future experiments proposed so that you are aware and prepared for these limitations before moving forward.

References

- Adashi, E. Y., Jones, P. B. C. And Hsueh, A. J. W. (1981). Synergistic Effect of Glucocorticoids on the Stimulation of Progesterone Production by Follicle-Stimulating Hormone in Cultured Rat Granulosa Cells. *Endocrinology* 109, 1888–1894.
- Almeida, S. A., Petenusci, S. O., Anselmo-Franci, J. A., Rosa-e-Silva, A. A. M. and Lamano-Carvalho, T. L. (1998). Decreased spermatogenic and androgenic testicular functions in adult rats submitted to immobilization-induced stress from prepuberty. *Braz J Med Biol Res* 31, 1443–1448.
- Amweg, A. N., Rodríguez, F. M., Huber, E., Marelli, B. E., Salvetti, N. R., Rey, F. and Ortega, H. H. (2016). Role of Glucocorticoids in Cystic Ovarian Disease: Expression of Glucocorticoid Receptor in the Bovine Ovary. *Cells Tissues Organs* 201, 138–147.
- Anders, S., Pyl, P. T. and Huber, W. (2015). HTSeq—a Python framework to work with high-throughput sequencing data. *Bioinformatics* 31, 166–169.
- Andersen, C. Y. (2003). Effect of glucocorticoids on spontaneous and follicle-stimulating hormone induced oocyte maturation in mouse oocytes during culture. *J Steroid Biochem Mol Biology* 85, 423–427.
- Anderson, R., Fässler, R., Georges-Labouesse, E., Hynes, R. O., Bader, B. L., Kreidberg, J. A., Schaible, K., Heasman, J. and Wylie, C. (1999). Mouse primordial germ cells lacking beta1 integrins enter the germline but fail to migrate normally to the gonads. *Dev Camb Engl* 126, 1655–64.
- Aravin, A. A., Sachidanandam, R., Girard, A., Fejes-Toth, K. and Hannon, G. J. (2007). Developmentally regulated piRNA clusters implicate MILI in transposon control. *Science*

316, 744–747.

Aravin, A. A., Sachidanandam, R., Bourc'his, D., Schaefer, C., Pezic, D., Toth, K. F., Bestor, T. and Hannon, G. J. (2008). A piRNA pathway primed by individual transposons is linked to de novo DNA methylation in mice. *Mol Cell* 31, 785–799.

Aravin, A. A., Heijden, G. W. van der, Castañeda, J., Vagin, V. V., Hannon, G. J. and Bortvin, A. (2009). Cytoplasmic compartmentalization of the fetal piRNA pathway in mice. *PLoS Genet* 5, e1000764.

Babb, J. A., Carini, L. M., Spears, S. L. and Nephew, B. C. (2014). Transgenerational effects of social stress on social behavior, corticosterone, oxytocin, and prolactin in rats. *Horm Behav* 65, 386–393.

Badrinarayanan, R., Rengarajan, S., Nithya, P. and Balasubramanian, K. (2006). Corticosterone impairs the mRNA expression and activity of 3 β - and 17 β -hydroxysteroid dehydrogenases in adult rat Leydig cells. *Biochem Cell Biology Biochimie Et Biologie Cell* 84, 745–754.

Ballard, P. L., Baxter, J. D., Higgins, S. J., Rousseau, G. G. And Tomkins, G. M. (1974). General Presence of Glucocorticoid Receptors in Mammalian Tissues 1. *Endocrinology* 94, 998–1002.

Bamberger, C. M., Bamberger, A. M., Castro, M. de and Chrousos, G. P. (1995). Glucocorticoid receptor beta, a potential endogenous inhibitor of glucocorticoid action in humans. *J Clin Invest* 95, 2435–2441.

Bambino, T. H. and Hsueh, A. J. (1981). Direct inhibitory effect of glucocorticoids upon testicular luteinizing hormone receptor and steroidogenesis in vivo and in vitro. *Endocrinology* 108, 2142–8.

- Bao, W., Kojima, K. K. and Kohany, O. (2015). Repbase Update, a database of repetitive elements in eukaryotic genomes. *Mobile Dna-uk* 6, 11.
- Barros, J. W. F. de, Borges, C. dos S., Missassi, G., Pacheco, T. L. and Kempinas, W. D. G. (2018). Impact of intrauterine exposure to betamethasone on the testes and epididymides of prepubertal rats. *Chem-biol Interact* 291, 202–211.
- Batzer, M. A. and Deininger, P. L. (2002). Alu repeats and human genomic diversity. *Nat Rev Genet* 3, 370–379.
- Biagini, G. and Pich, E. M. (2002). Corticosterone administration to rat pups, but not maternal separation, affects sexual maturation and glucocorticoid receptor immunoreactivity in the testis. *Pharmacol Biochem Be* 73, 95–103.
- Bohacek, J., Farinelli, M., Mirante, O., Steiner, G., Gapp, K., Coiret, G., Ebeling, M., Durán-Pacheco, G., Iniguez, A. L., Manuella, F., et al. (2015). Pathological brain plasticity and cognition in the offspring of males subjected to postnatal traumatic stress. *Mol Psychiatr* 20, 621–631.
- Borges, C. S., Dias, A. F. M. G., Rosa, J. L., Silva, P. V., Silva, R. F., Barros, A. L., Sanabria, M., Guerra, M. T., Gregory, M., Cyr, D. G., et al. (2016). Alterations in male rats following in utero exposure to betamethasone suggests changes in reproductive programming. *Reprod Toxicol* 63, 125–134.
- Borges, C. dos S., Dias, A. F. M. G., Silva, P. V., Rosa, J. L., Guerra, M. T., Silva, R. F., Kiguti, L. R. A., Pupo, A. S. and Kempinas, W. D. G. (2017a). Long-term adverse effects on reproductive function in male rats exposed prenatally to the glucocorticoid betamethasone. *Toxicology* 376, 15–22.
- Borges, C. dos S., Pacheco, T. L., Silva, K. P. da, Fernandes, F. H., Gregory, M., Pupo, A. S.,

- Salvadori, D. M. F., Cyr, D. G. and Kempinas, W. D. G. (2017b). Betamethasone causes intergenerational reproductive impairment in male rats. *Reprod Toxicol* 71, 108–117.
- Borges, C. S., Pacheco, T. L., Guerra, M. T., Barros, A. L., Silva, P. V., Missassi, G., Silva, K. P. da, Anselmo-Franci, J. A., Pupo, A. S. and Kempinas, W. D. G. (2017c). Reproductive disorders in female rats after prenatal exposure to betamethasone: Prenatal betamethasone exposure and female reproductive disorders. *J Appl Toxicol* 37, 1065–1072.
- Brewer, J. A., Khor, B., Vogt, S. K., Muglia, L. M., Fujiwara, H., Haegele, K. E., Sleckman, B. P. and Muglia, L. J. (2003). T-cell glucocorticoid receptor is required to suppress COX-2-mediated lethal immune activation. *Nat Med* 9, 1318–1322.
- Buchner, J. (1999). Hsp90 & Co. – a holding for folding. *Trends Biochem Sci* 24, 136–141.
- Calogero, A. E., Burrello, N., Bosboom, A. M. J., Garofalo, M. R., Weber, R. F. A. and D'Agata, R. (1999). Glucocorticoids inhibit gonadotropin-releasing hormone by acting directly at the hypothalamic level. *J Endocrinol Invest* 22, 666–670.
- Carmell, M. A., Girard, A., Kant, H. J. G. van de, Bourc'his, D., Bestor, T. H., Rooij, D. G. de and Hannon, G. J. (2007). MIWI2 Is Essential for Spermatogenesis and Repression of Transposons in the Mouse Male Germline. *Dev Cell* 12, 503–514.
- Cartier, J., Smith, T., Thomson, J. P., Rose, C. M., Khulan, B., Heger, A., Meehan, R. R. and Drake, A. J. (2018). Investigation into the role of the germline epigenome in the transmission of glucocorticoid-programmed effects across generations. *Genome Biol* 19, 50.
- Casillas, F., Betancourt, M., Juárez-Rojas, L., Duclomb, Y., López, A., Ávila-Quintero, A., Zamora, J., Ommati, M. M. and Retana-Márquez, S. (2021). Chronic Stress

- Detrimentially Affects In Vivo Maturation in Rat Oocytes and Oocyte Viability at All Phases of the Estrous Cycle. *Animals Open Access J Mdpi* 11, 2478.
- Chan, J. C., Morgan, C. P., Leu, N. A., Shetty, A., Cisse, Y. M., Nugent, B. M., Morrison, K. E., Jašarević, E., Huang, W., Kanyuch, N., et al. (2020). Reproductive tract extracellular vesicles are sufficient to transmit intergenerational stress and program neurodevelopment. *Nat Commun* 11, 1499.
- Chandran, U. R., Attardi, B., Friedman, R., Dong, K. W., Roberts, J. L. and DeFranco, D. B. (1994). Glucocorticoid receptor-mediated repression of gonadotropin-releasing hormone promoter activity in GT1 hypothalamic cell lines. *Endocrinology* 134, 1467–1474.
- Charpenet, G., Tache, Y., Forest, M. G., Haour, F., Saez, J. M., Bernier, M., Ducharme, J. R. and Collu, R. (1981). Effects of chronic intermittent immobilization stress on rat testicular androgenic function. *Endocrinology* 109, 1254–8.
- Chen, Y., Wang, Q., Wang, F.-F., Gao, H.-B. and Zhang, P. (2011). Stress induces glucocorticoid-mediated apoptosis of rat Leydig cells in vivo. *Ann Ny Acad Sci* 15, 74–84.
- Chen, L.-Y., Brown, P. R., Willis, W. B. and Eddy, E. M. (2014). Peritubular Myoid Cells Participate in Male Mouse Spermatogonial Stem Cell Maintenance. *Endocrinology* 155, 4964–4974.
- Chen, X., Luan, X., Zheng, Q., Qiao, C., Chen, W., Wang, M., Yan, Y., Xie, B., Shen, C., He, Z., et al. (2019). Precursor RNA processing 3 is required for male fertility, and germline stem cell self-renewal and differentiation via regulating spliceosome function in *Drosophila* testes. *Sci Rep-uk* 9, 9988.
- Cole, T. J., Blendy, J. A., Monaghan, A. P., Kriegstein, K., Schmid, W., Aguzzi, A., Fantuzzi, G.,

- Hummler, E., Unsicker, K. and Schütz, G. (1995). Targeted disruption of the glucocorticoid receptor gene blocks adrenergic chromaffin cell development and severely retards lung maturation. *Gene Dev* 9, 1608–1621.
- Conesa, A., Madrigal, P., Tarazona, S., Gomez-Cabrero, D., Cervera, A., McPherson, A., Szczesniak, M. W., Gaffney, D. J., Elo, L. L., Zhang, X., et al. (2016). A survey of best practices for RNA-seq data analysis. *Genome Biol* 17, 13.
- Constantinof, A., Moisiadis, V. G., Kostaki, A., Szyf, M. and Matthews, S. G. (2019a). Antenatal Glucocorticoid Exposure Results in Sex-Specific and Transgenerational Changes in Prefrontal Cortex Gene Transcription that Relate to Behavioural Outcomes. *Scientific Reports* 9, 764.
- Constantinof, A., Boureau, L., Moisiadis, V. G., Kostaki, A., Szyf, M. and Matthews, S. G. (2019b). Prenatal Glucocorticoid Exposure Results in Changes in Gene Transcription and DNA Methylation in the Female Juvenile Guinea Pig Hippocampus Across Three Generations. *Sci Rep-uk* 9, 18211.
- Cumming, D. C., Quigley, M. E. And Yen, S. S. C. (1983). Acute Suppression of Circulating Testosterone Levels by Cortisol in Men*. *J Clin Endocrinol Metabolism* 57, 671–673.
- Czech, B. and Hannon, G. J. (2016). One Loop to Rule Them All: The Ping-Pong Cycle and piRNA-Guided Silencing. *Trends Biochem Sci* 41, 324–337.
- Deng, W. and Lin, H. (2002). miwi, a Murine Homolog of piwi, Encodes a Cytoplasmic Protein Essential for Spermatogenesis. *Dev Cell* 2, 819–830.
- Dobin, A., Davis, C. A., Schlesinger, F., Drenkow, J., Zaleski, C., Jha, S., Batut, P., Chaisson, M. and Gingeras, T. R. (2013). STAR: ultrafast universal RNA-seq aligner. *Bioinformatics* 29, 15–21.

- Ehrmann, I., Crichton, J. H., Gazzara, M. R., James, K., Liu, Y., Grellscheid, S. N., Curk, T., Rooij, D. de, Steyn, J. S., Cockell, S., et al. (2019). An ancient germ cell-specific RNA-binding protein protects the germline from cryptic splice site poisoning. *Elife* 8, e39304.
- Encío, I. J. and Detera-Wadleigh, S. D. (1991). The genomic structure of the human glucocorticoid receptor. *J Biol Chem* 266, 7182–7188.
- Ergün, S., Buschmann, C., Heukeshoven, J., Dammann, K., Schnieders, F., Lauke, H., Chalajour, F., Kilic, N., Strätling, W. H. and Schumann, G. G. (2004). Cell Type-specific Expression of LINE-1 Open Reading Frames 1 and 2 in Fetal and Adult Human Tissues. *J Biol Chem* 279, 27753–27763.
- Ernst, C., Odom, D. T. and Kutter, C. (2017). The emergence of piRNAs against transposon invasion to preserve mammalian genome integrity. *Nat Commun* 8, 1411.
- Evain, D., Morera, A. M. and Saez, J. M. (1976). Glucocorticoid receptors in interstitial cells of the rat testis. *J Steroid Biochem* 7, 1135–1139.
- Facchinello, N., Skobo, T., Meneghetti, G., Colletti, E., Dinarello, A., Tiso, N., Costa, R., Gioacchini, G., Carnevali, O., Argenton, F., et al. (2017). nr3c1 null mutant zebrafish are viable and reveal DNA-binding-independent activities of the glucocorticoid receptor. *Sci Rep-uk* 7, 4371.
- Fahim, A. T., El-Fattah, A. A. A., Sadik, N. A. H. and Ali, B. M. (2019). Resveratrol and dimethyl fumarate ameliorate testicular dysfunction caused by chronic unpredictable mild stress-induced depression in rats. *Arch Biochem Biophys* 665, 152–165.
- Faught, E. and Vijayan, M. M. (2018). The mineralocorticoid receptor is essential for stress axis regulation in zebrafish larvae. *Sci Rep-uk* 8, 18081.

- Faught, E., Santos, H. B. and Vijayan, M. M. (2020). Loss of the glucocorticoid receptor causes accelerated ovarian ageing in zebrafish. *Proc Royal Soc B* 287, 20202190.
- Fazio, S. D., Bartonicek, N., Giacomo, M. D., Abreu-Goodger, C., Sankar, A., Funaya, C., Antony, C., Moreira, P. N., Enright, A. J. and O'Carroll, D. (2011). The endonuclease activity of Mili fuels piRNA amplification that silences LINE1 elements. *Nature* 480, 259–263.
- Fernandes, M. G., He, N., Wang, F., Iperen, L. van, Eguizabal, C., Matorras, R., Roelen, B. A. J. and Lopes, S. M. C. de S. (2018). Human-specific subcellular compartmentalization of P-element induced wimpy testis-like (PIWIL) granules during germ cell development and spermatogenesis. *Hum Reprod* 33, 258–269.
- Franklin, T. B., Russig, H., Weiss, I. C., Gräff, J., Linder, N., Michalon, A., Vizi, S. and Mansuy, I. M. (2010). Epigenetic transmission of the impact of early stress across generations. *Biol Psychiat* 68, 408–415.
- Franklin, T. B., Linder, N., Russig, H., Thöny, B. and Mansuy, I. M. (2011). Influence of early stress on social abilities and serotonergic functions across generations in mice. *Plos One* 6, e21842.
- Fu, Q. and Wang, P. J. (2014). Mammalian piRNAs: Biogenesis, function, and mysteries. *Spermatogenesis* 4, e27889.
- Fu, X.-Y., Chen, H.-H., Zhang, N., Ding, M.-X., Qiu, Y.-E., Pan, X.-M., Fang, Y.-S., Lin, Y.-P., Zheng, Q. and Wang, W.-Q. (2018). Effects of chronic unpredictable mild stress on ovarian reserve in female rats: Feasibility analysis of a rat model of premature ovarian failure. *Mol Med Rep* 18, 532–540.
- Gagnon, S., Atmodjo, W., Humes, D., McKerlie, C., Kaplan, F. and Sweezey, N. B. (2006).

- Transgenic Glucocorticoid Receptor Expression Driven by the SP-C Promoter Reduces Neonatal Lung Cellularity and Midkine Expression in GRhypo Mice. *Neonatology* 90, 46–57.
- Gainetdinov, I., Skvortsova, Y., Kondratieva, S., Funikov, S. and Azhikina, T. (2017). Two modes of targeting transposable elements by piRNA pathway in human testis. *Rna* 23, 1614–1625.
- Gangaraju, V. K., Yin, H., Weiner, M. M., Wang, J., Huang, X. A. and Lin, H. (2011). Drosophila Piwi functions in Hsp90-mediated suppression of phenotypic variation. *Nat Genet* 43, 153 U107.
- Gao, H.-B., Tong, M.-H., Hu, Y.-Q., Guo, Q.-S., Ge, R. and Hardy, M. P. (2002). Glucocorticoid Induces Apoptosis in Rat Leydig Cells. *Endocrinology* 143, 130–138.
- Gao, H.-B., Tong, M.-H., Hu, Y.-Q., You, H.-Y., Guo, Q.-S., Ge, R.-S. and Hardy, M. P. (2003). Mechanisms of glucocorticoid-induced Leydig cell apoptosis. *Mol Cell Endocrinol* 199, 153–163.
- Gao, Y., Chen, F., Kong, Q.-Q., Ning, S.-F., Yuan, H.-J., Lian, H.-Y., Luo, M.-J. and Tan, J.-H. (2016). Stresses on Female Mice Impair Oocyte Developmental Potential: Effects of Stress Severity and Duration on Oocytes at the Growing Follicle Stage. *Reproductive Sci Thousand Oaks Calif* 23, 1148–57.
- Gao, L., Zhao, F., Zhang, Y., Wang, W. and Cao, Q. (2019). Diminished ovarian reserve induced by chronic unpredictable stress in C57BL/6 mice. *Gynecol Endocrinol* 36, 1–6.
- Gapp, K., Jawaid, A., Sarkies, P., Bohacek, J., Pelczar, P., Prados, J., Farinelli, L., Miska, E. and Mansuy, I. M. (2014). Implication of sperm RNAs in transgenerational inheritance of the effects of early trauma in mice. *Nat Neurosci* 17, 667–669.

- Gapp, K., Corcoba, A., Steenwyk, G. van, Mansuy, I. M. and Duarte, J. M. (2016). Brain metabolic alterations in mice subjected to postnatal traumatic stress and in their offspring. *J Cereb Blood Flow Metabolism* 37, 2423–2432.
- Gapp, K., Steenwyk, G. van, Germain, P. L., Matsushima, W., Rudolph, K. L. M., Manuella, F., Roszkowski, M., Vernaz, G., Ghosh, T., Pelczar, P., et al. (2020). Alterations in sperm long RNA contribute to the epigenetic inheritance of the effects of postnatal trauma. *Mol Psychiatr* 25, 2162–2174.
- Gapp, K., Parada, G. E., Gross, F., Corcoba, A., Kaur, J., Grau, E., Hemberg, M., Bohacek, J. and Miska, E. A. (2021). Single paternal dexamethasone challenge programs offspring metabolism and reveals multiple candidates in RNA-mediated inheritance. *Iscience* 24, 102870.
- Ge, S. X. (2017). Exploratory bioinformatics investigation reveals importance of “junk” DNA in early embryo development. *Bmc Genomics* 18, 200.
- Ge, W., Wang, J.-J., Zhang, R.-Q., Tan, S.-J., Zhang, F.-L., Liu, W.-X., Li, L., Sun, X.-F., Cheng, S.-F., Dyce, P. W., et al. (2021). Dissecting the initiation of female meiosis in the mouse at single-cell resolution. *Cell Mol Life Sci* 78, 695–713.
- Geraghty, A. C. and Kaufer, D. (2015). Glucocorticoid Regulation of Reproduction. *Adv Exp Med Biol* 872, 253–78.
- Gkountela, S., Li, Z., Vincent, J. J., Zhang, K. X., Chen, A., Pellegrini, M. and Clark, A. T. (2013). The ontogeny of cKIT⁺ human primordial germ cells proves to be a resource for human germ line reprogramming, imprint erasure and in vitro differentiation. *Nat Cell Biol* 15, 113–122.
- Gkountela, S., Zhang, K. X., Shafiq, T. A., Liao, W.-W., Hargan-Calvopiña, J., Chen, P.-Y. and

- Clark, A. T. (2015). DNA Demethylation Dynamics in the Human Prenatal Germline. *Cell* 161, 1425–1436.
- Gong, S., Sun, G.-Y., Zhang, M., Yuan, H.-J., Zhu, S., Jiao, G.-Z., Luo, M.-J. and Tan, J.-H. (2017). Mechanisms for the species difference between mouse and pig oocytes in their sensitivity to glucocorticoids. *Biol Reprod* 96, 1019–1030.
- Gong, X., Dai, S., Wang, T., Zhang, J., Fan, G., Luo, M., Yi, Y., Wang, H., Lu, D. and Xu, D. (2021a). MiR-17-5p/FOXO2/CDKN1B signal programming in oocytes mediates transgenerational inheritance of diminished ovarian reserve in female offspring rats induced by prenatal dexamethasone exposure. *Cell Biol Toxicol* 1–17.
- Gong, X., Zhang, J., Ge, C., Yi, Y., Dai, S., Fan, G., Li, C., Zhang, Y., Wang, H. and Xu, D. (2021b). miRNA320a-3p/RUNX2 signal programming mediates the transgenerational inheritance of inhibited ovarian estrogen synthesis in female offspring rats induced by prenatal dexamethasone exposure. *Pharmacol Res* 165, 105435.
- González, R., Ruiz-León, Y., Gomendio, M. and Roldan, E. R. S. (2010a). The effect of glucocorticoids on mouse oocyte in vitro maturation and subsequent fertilization and embryo development. *Toxicol In Vitro* 24, 108–115.
- González, R., Ruiz-León, Y., Gomendio, M. and Roldan, E. R. S. (2010b). The effect of glucocorticoids on ERK-1/2 phosphorylation during maturation of lamb oocytes and their subsequent fertilization and cleavage ability in vitro. *Reprod Toxicol* 29, 198–205.
- Grellscheid, S., Dalglish, C., Storbeck, M., Best, A., Liu, Y., Jakubik, M., Mende, Y., Ehrmann, I., Curk, T., Rossbach, K., et al. (2011). Identification of Evolutionarily Conserved Exons as Regulated Targets for the Splicing Activator Tra2 β in Development. *Plos Genet* 7, e1002390.

- Guo, F., Yan, L., Guo, H., Li, L., Hu, B., Zhao, Y., Yong, J., Hu, Y., Wang, X., Wei, Y., et al. (2015). The Transcriptome and DNA Methylome Landscapes of Human Primordial Germ Cells. *Cell* 161, 1437–1452.
- Guo, Y., Sun, J., Li, T., Zhang, Q., Bu, S., Wang, Q. and Lai, D. (2017a). Melatonin ameliorates restraint stress-induced oxidative stress and apoptosis in testicular cells via NF- κ B/iNOS and Nrf2/HO-1 signaling pathway. *Sci Rep-uk* 7, 9599.
- Guo, H., Hu, B., Yan, L., Yong, J., Wu, Y., Gao, Y., Guo, F., Hou, Y., Fan, X., Dong, J., et al. (2017b). DNA methylation and chromatin accessibility profiling of mouse and human fetal germ cells. *Cell Res* 27, 165–183.
- Guo, Y., Du, X., Bian, Y. and Wang, S. (2020). Chronic unpredictable stress-induced reproductive deficits were prevented by probiotics. *Reprod Biology* 20, 175–183.
- Ha, H., Song, J., Wang, S., Kapusta, A., Feschotte, C., Chen, K. C. and Xing, J. (2014). A comprehensive analysis of piRNAs from adult human testis and their relationship with genes and mobile elements. *Bmc Genomics* 15, 545.
- Hadziselimovic, F., Hadziselimovic, N. O., Demougin, P., Krey, G. and Oakeley, E. (2015). Piwi-Pathway Alteration Induces LINE-1 Transposon Derepression and Infertility Development in Cryptorchidism. *Sex Dev* 9, 98–104.
- Hales, D. B. and Payne, A. H. (1989). Glucocorticoid-mediated repression of P450scc mRNA and de novo synthesis in cultured Leydig cells. *Endocrinology* 124, 2099–104.
- Hancks, D. C. and Kazazian, H. H. (2012). Active human retrotransposons: variation and disease. *Curr Opin Genet Dev* 22, 191–203.
- Hancks, D. C. and Kazazian, H. H. (2016). Roles for retrotransposon insertions in human

disease. *Mobile Dna-uk* 7, 9.

Hazra, R., Upton, D., Jimenez, M., Desai, R., Handelsman, D. J. and Allan, C. M. (2014). In vivo actions of the Sertoli cell glucocorticoid receptor. *Endocrinology* 155, 1120–1130.

He, N., Kong, Q.-Q., Wang, J.-Z., Ning, S.-F., Miao, Y.-L., Yuan, H.-J., Gong, S., Cui, X.-Z., Li, C.-Y. and Tan, J.-H. (2016). Parental life events cause behavioral difference among offspring: Adult pre-gestational restraint stress reduces anxiety across generations. *Sci Rep-uk* 6, srep39497.

Hinds, T. D., Ramakrishnan, S., Cash, H. A., Stechschulte, L. A., Heinrich, G., Najjar, S. M. and Sánchez, E. R. (2010). Discovery of glucocorticoid receptor-beta in mice with a role in metabolism. *Mol Endocrinol* 24, 1715–1727.

Hollenberg, S. M., Weinberger, C., Ong, E. S., Cerelli, G., Oro, A., Lebo, R., Thompson, E. B., Rosenfeld, M. G. and Evans, R. M. (1985). Primary structure and expression of a functional human glucocorticoid receptor cDNA. *Nature* 318, 635–641.

Horiuchi, K., Perez-Cerezales, S., Papasaikas, P., Ramos-Ibeas, P., López-Cardona, A. P., Laguna-Barraza, R., Balvís, N. F., Pericuesta, E., Fernández-González, R., Planells, B., et al. (2018). Impaired Spermatogenesis, Muscle, and Erythrocyte Function in U12 Intron Splicing-Defective Zrsr1 Mutant Mice. *Cell Reports* 23, 143–155.

Hou, G., Xiong, W., Wang, M., Chen, X. and Yuan, T. (2014). Chronic Stress Influences Sexual Motivation and Causes Damage to Testicular Cells in Male Rats. *J Sex Medicine* 11, 653–663.

Hsueh, A. J. W. and Erickson, G. F. (1978). Glucocorticoid inhibition of fsh-induced estrogen production in cultured rat granulosa cells. *Steroids* 32, 639–648.

- Hu, G.-X., Lian, Q.-Q., Lin, H., Latif, S. A., Morris, D. J., Hardy, M. P. and Ge, R.-S. (2008). Rapid mechanisms of glucocorticoid signaling in the Leydig cell. *Steroids* 73, 1018–1024.
- Hułas-Stasiak, M., Dobrowolski, P. and Tomaszewska, E. (2015). Prenatally administered dexamethasone impairs folliculogenesis in spiny mouse offspring. *Reproduction Fertility Dev* 28, 1038–1048.
- Hułas-Stasiak, M., Dobrowolski, P., Pawlikowska-Pawlęga, B., Tomaszewska, E. and Muszyński, S. (2017). The effects of dexamethasone administered during pregnancy on the postpartum spiny mouse ovary. *Plos One* 12, e0183528.
- Ichianagi, T., Ichianagi, K., Ogawa, A., Kuramochi-Miyagawa, S., Nakano, T., Chuma, S., Sasaki, H. and Udono, H. (2014). HSP90 α plays an important role in piRNA biogenesis and retrotransposon repression in mouse. *Nucleic Acids Res* 42, 11903–11911.
- Iwasaki, Y. W., Siomi, M. C. and Siomi, H. (2015). PIWI-Interacting RNA: Its Biogenesis and Functions. *Annu Rev Biochem* 84, 1–29.
- Izumi, N., Kawaoka, S., Yasuhara, S., Suzuki, Y., Sugano, S., Katsuma, S. and Tomari, Y. (2013). Hsp90 facilitates accurate loading of precursor piRNAs into PIWI proteins. *Rna* 19, 896–901.
- Jachowicz, J. W., Bing, X., Pontabry, J., Bošković, A., Rando, O. J. and Torres-Padilla, M.-E. (2017). LINE-1 activation after fertilization regulates global chromatin accessibility in the early mouse embryo. *Nat Genet* 49, 1502–1510.
- Jeanneteau, F. D., Lambert, W. M., Ismaili, N., Bath, K. G., Lee, F. S., Garabedian, M. J. and Chao, M. V. (2012). BDNF and glucocorticoids regulate corticotrophin-releasing hormone (CRH) homeostasis in the hypothalamus. *Proc National Acad Sci* 109, 1305–1310.

- Jeje, S. O. and Raji, Y. (2017). Maternal treatment with dexamethasone during gestation alters sexual development markers in the F1 and F2 male offspring of Wistar rats. *J Dev Orig Hlth Dis* 8, 101–112.
- Jeje, S. O., Akindele, O. O., Balogun, M. E. and Raji, Y. (2016). Maternal treatment with dexamethasone during lactation delays male puberty and disrupts reproductive functions via hypothalamic–pituitary–gonadal axis alterations. *Pathophysiol* 23, 43–49.
- Juma, A. R., Grommen, S. V. H., O'Bryan, M. K., O'Connor, A. E., Merriner, D. J., Hall, N. E., Doyle, S. R., Damdimopoulou, P. E., Barriga, D., Hart, A. H., et al. (2017). PLAG1 deficiency impairs spermatogenesis and sperm motility in mice. *Sci Rep-uk* 7, 5317.
- Kalinyak, J. E., Dorin, R. I., Hoffman, A. R. and Perlman, A. J. (1987). Tissue-specific regulation of glucocorticoid receptor mRNA by dexamethasone. *J Biol Chem* 262, 10441–10444.
- Kashino, C., Hasegawa, T., Nakano, Y., Iwata, N., Yamamoto, K., Kamada, Y., Masuyama, H. and Otsuka, F. (2021). Involvement of BMP-15 in glucocorticoid actions on ovarian steroidogenesis by rat granulosa cells. *Biochem Bioph Res Co* 559, 56–61.
- Kavitha, T. S., Parthasarathy, C., Sivakumar, R., Badrinarayanan, R. and Balasubramanian, K. (2006). Effects of excess corticosterone on NADPH generating enzymes and glucose oxidation in Leydig cells of adult rats. *Hum Exp Toxicol* 25, 119–125.
- Kazazian, H. H. and Moran, J. V. (2017). Mobile DNA in Health and Disease. *New Engl J Medicine* 377, 361–370.
- Kempinas, W. G., Borges, C. S., Leite, G. A. A., Figueiredo, T. M., Gregory, M. and Cyr, D. G. (2019). Prenatal exposure to betamethasone causes intergenerational impairment of epididymal development in the rat. *Andrology-us* 7, 719–729.

- Kim, S., Günesdogan, U., Zylitz, J. J., Hackett, J. A., Cougot, D., Bao, S., Lee, C., Dietmann, S., Allen, G. E., Sengupta, R., et al. (2014). PRMT5 Protects Genomic Integrity during Global DNA Demethylation in Primordial Germ Cells and Preimplantation Embryos. *Mol Cell* 56, 564–579.
- Kojima, K. K. (2018). Human transposable elements in Repbase: genomic footprints from fish to humans. *Mobile Dna-uk* 9, 2.
- Kolbasi, B., Bulbul, M. V., Karabulut, S., Altun, C. E., Cakici, C., Ulfer, G., Mudok, T. and Keskin, I. (2021). Chronic unpredictable stress disturbs the blood–testis barrier affecting sperm parameters in mice. *Reprod Biomed Online* 42, 983–995.
- Kovács, L., Nagy, Á., Pál, M. and Deák, P. (2020). Usp14 is required for spermatogenesis and ubiquitin stress responses in *Drosophila melanogaster*. *J Cell Sci* 133, jcs237511.
- Kuramochi-Miyagawa, S., Watanabe, T., Gotoh, K., Totoki, Y., Toyoda, A., Ikawa, M., Asada, N., Kojima, K., Yamaguchi, Y., Ijiri, T. W., et al. (2008). DNA methylation of retrotransposon genes is regulated by Piwi family members MILI and MIWI2 in murine fetal testes. *Gene Dev* 22, 908–17.
- Kuramochi-Miyagawa, S., Watanabe, T., Gotoh, K., Takamatsu, K., Chuma, S., Kojima-Kita, K., Shiromoto, Y., Asada, N., Toyoda, A., Fujiyama, A., et al. (2010). MVH in piRNA processing and gene silencing of retrotransposons. *Gene Dev* 24, 887–892.
- Kuroda, M., Sok, J., Webb, L., Baechtold, H., Urano, F., Yin, Y., Chung, P., Rooij, D. G. de, Akhmedov, A., Ashley, T., et al. (2000). Male sterility and enhanced radiation sensitivity in TLS^{-/-} mice. *Embo J* 19, 453–462.
- Langmead, B., Trapnell, C., Pop, M. and Salzberg, S. L. (2009). Ultrafast and memory-efficient alignment of short DNA sequences to the human genome. *Genome Biol* 10, R25.

- Laryea, G., Schütz, G. and Muglia, L. J. (2013). Disrupting hypothalamic glucocorticoid receptors causes HPA axis hyperactivity and excess adiposity. *Mol Endocrinol* 27, 1655–1665.
- Legrand, J. M. D., Chan, A.-L., La, H. M., Rossello, F. J., Änkö, M.-L., Fuller-Pace, F. V. and Hobbs, R. M. (2019). DDX5 plays essential transcriptional and post-transcriptional roles in the maintenance and function of spermatogonia. *Nat Commun* 10, 2278.
- Levy, F. O., Ree, A. H., Eikvar, L., Govindan, M. V., Jahnsen, T. And Hansson, V. (1989). Glucocorticoid Receptors and Glucocorticoid Effects in Rat Sertoli Cells*. *Endocrinology* 124, 430–436.
- Li, H., Watford, W., Li, C., Parmelee, A., Bryant, M. A., Deng, C., O'Shea, J. and Lee, S. B. (2007). Ewing sarcoma gene EWS is essential for meiosis and B lymphocyte development. *J Clin Invest* 117, 1314–1323.
- Li, L., Dong, J., Yan, L., Yong, J., Liu, X., Hu, Y., Fan, X., Wu, X., Guo, H., Wang, X., et al. (2017). Single-Cell RNA-Seq Analysis Maps Development of Human Germline Cells and Gonadal Niche Interactions. *Cell Stem Cell* 20, 858–873.e4.
- Li, C.-Y., Li, Z.-B., Kong, Q.-Q., Han, X., Xiao, B., Li, X., Chang, Z.-L. and Tan, J.-H. (2018a). Restraint-induced corticotrophin-releasing hormone elevation triggers apoptosis of ovarian cells and impairs oocyte competence via activation of the fas/fasL system. *Biol Reprod* 99, 828–837.
- Li, Q.-N., Li, L., Hou, G., Wang, Z.-B., Hou, Y., Liu, Z.-H., Schatten, H. and Sun, Q.-Y. (2018b). Glucocorticoid exposure affects female fertility by exerting its effect on the uterus but not on the oocyte: lessons from a hypercortisolism mouse model. *Hum Reprod* 33, 2285–2294.

- Lian, H.-Y., Gao, Y., Jiao, G.-Z., Sun, M.-J., Wu, X.-F., Wang, T.-Y., Li, H. and Tan, J.-H. (2013). Antioxidant supplementation overcomes the deleterious effects of maternal restraint stress-induced oxidative stress on mouse oocytes. *Reproduction* 146, 559–568.
- Liang, B., Wei, D.-L., Cheng, Y.-N., Yuan, H.-J., Lin, J., Cui, X.-Z., Luo, M.-J. and Tan, J.-H. (2013). Restraint Stress Impairs Oocyte Developmental Potential in Mice: Role of CRH-Induced Apoptosis of Ovarian Cells¹. *Biol Reprod* 89, Article 64, 1-12.
- Liao, Y., Smyth, G. K. and Shi, W. (2014). featureCounts: an efficient general purpose program for assigning sequence reads to genomic features. *Bioinformatics* 30, 923–930.
- Lin, H., Yuan, K., Zhou, H., Bu, T., Su, H., Liu, S., Zhu, Q., Wang, Y., Hu, Y., Shan, Y., et al. (2014). Time-Course Changes of Steroidogenic Gene Expression and Steroidogenesis of Rat Leydig Cells after Acute Immobilization Stress. *Int J Mol Sci* 15, 21028–21044.
- Liu, W., Wang, F., Xu, Q., Shi, J., Zhang, X., Lu, X., Zhao, Z.-A., Gao, Z., Ma, H., Duan, E., et al. (2017). BCAS2 is involved in alternative mRNA splicing in spermatogonia and the transition to meiosis. *Nat Commun* 8, 14182.
- Liu, M., Chen, B., Pei, L., Zhang, Q., Zou, Y., Xiao, H., Zhou, J., Chen, L. and Wang, H. (2018). Decreased H3K9ac level of StAR mediated testicular dysplasia induced by prenatal dexamethasone exposure in male offspring rats. *Toxicology* 408, 1–10.
- Lizen, B., Claus, M., Jeannotte, L., Rijli, F. M. and Gofflot, F. (2015). Perinatal induction of Cre recombination with tamoxifen. *Transgenic Res* 24, 1065–1077.
- Love, M. I., Huber, W. and Anders, S. (2014). Moderated estimation of fold change and dispersion for RNA-seq data with DESeq2. *Genome Biol* 15, 550.
- Lu, N. Z. and Cidlowski, J. A. (2005). Translational Regulatory Mechanisms Generate

- N-Terminal Glucocorticoid Receptor Isoforms with Unique Transcriptional Target Genes. *Mol Cell* 18, 331–342.
- Lv, F., Wan, Y., Chen, Y., Pei, L., Luo, D., Fan, G., Luo, M., Xu, D. and Wang, H. (2018). Prenatal Dexamethasone Exposure Induced Ovarian Developmental Toxicity and Transgenerational Effect in Rat Offspring. *Endocrinology* 159, 1401–1415.
- Maekawa, M., Kamimura, K. And Nagano, T. (1996). Peritubular Myoid Cells in the Testis: Their Structure and Function. *Arch Histol Cytol* 59, 1–13.
- Mahmoud, H., Mahmoud, O., Layasadat, K. and Naeim, A. (2009). Dexamethasone effects on Bax expression in the mouse testicular germ cells. *Folia Histochem Cyto* 47, 237–41.
- Malki, S., van der Heijden, G. W., O'Donnell, K. A., Martin, S. L. and Bortvin, A. (2014). A Role for Retrotransposon LINE-1 in Fetal Oocyte Attrition in Mice. *Dev Cell* 29, 521–33.
- Manakov, S. A., Pezic, D., Marinov, G. K., Pastor, W. A., Sachidanandam, R. and Aravin, A. A. (2015). MIWI2 and MILI Have Differential Effects on piRNA Biogenesis and DNA Methylation. *Cell Reports* 12, 1234 1243.
- Mancini, R. E., Laveri, J. C., Muller, F., Andrada, J. A. and Saraceni, D. J. (1966). Effect of Prednisolone upon Normal and Pathologic Human Spermatogenesis. *Fertil Steril* 17, 500–513.
- Manners, M. T., Yohn, N. L., Lahens, N. F., Grant, G. R., Bartolomei, M. S. and Blendy, J. A. (2019). Transgenerational inheritance of chronic adolescent stress: Effects of stress response and the amygdala transcriptome. *Genes Brain Behav* 18, e12493.
- Maradonna, F., Gioacchini, G., Notarstefano, V., Fontana, C. M., Citton, F., Valle, L. D., Giorgini, E. and Carnevali, O. (2020). Knockout of the Glucocorticoid Receptor Impairs

- Reproduction in Female Zebrafish. *Int J Mol Sci* 21, 9073.
- Marchetto, M. C. N., Narvaiza, I., Denli, A. M., Benner, C., Lazzarini, T. A., Nathanson, J. L., Paquola, A. C. M., Desai, K. N., Herai, R. H., Weitzman, M. D., et al. (2013). Differential L1 regulation in pluripotent stem cells of humans and apes. *Nature* 503, 525–529.
- Marić, D., Kostić, T. and Kovačević, R. (1996). Effects of acute and chronic immobilization stress on rat Leydig cell steroidogenesis. *J Steroid Biochem Mol Biology* 58, 351–355.
- Martin, M. (2011). Cutadapt removes adapter sequences from high-throughput sequencing reads. *Embnet J* 17, 10–12.
- Mattox, W. and Baker, B. S. (1991). Autoregulation of the splicing of transcripts from the transformer-2 gene of *Drosophila*. *Gene Dev* 5, 786–796.
- Mbandi, S. K., Hesse, U., Rees, D. J. G. and Christoffels, A. (2014). A glance at quality score: implication for de novo transcriptome reconstruction of Illumina reads. *Frontiers Genetics* 5, 17.
- McCormick, J. A., Lyons, V., Jacobson, M. D., Noble, J., Diorio, J., Nyirenda, M., Weaver, S., Ester, W., Yau, J. L. W., Meaney, M. J., et al. (2000). 5'-Heterogeneity of Glucocorticoid Receptor Messenger RNA Is Tissue Specific: Differential Regulation of Variant Transcripts by Early-Life Events. *Mol Endocrinol* 14, 506–517.
- Mehfooz, A., Wei, Q., Zheng, K., Fadlalla, M. B., Maltasic, G. and Shi, F. (2018). Protective roles of Rutin against restraint stress on spermatogenesis in testes of adult mice. *Tissue Cell* 50, 133–143.
- Merris, V. V., Wemmel, K. V. and Cortvrindt, R. (2007). In vitro effects of dexamethasone on mouse ovarian function and pre-implantation embryo development. *Reprod Toxicol* 23, 32–41.

- Messerschmidt, D. M., Knowles, B. B. and Solter, D. (2014). DNA methylation dynamics during epigenetic reprogramming in the germline and preimplantation embryos. *Gene Dev* 28, 812–828.
- Michael, A. E., Pester, L. A., Curtis, P., Shaw, R. W., Edwards, C. R. W. and Cooke, B. A. (1993). Direct inhibition of ovarian steroidogenesis by Cortisol and the modulatory role of 11 β -hydroxysteroid dehydrogenase. *Clin Endocrinol* 38, 641–644.
- Mills, L. (2014). Common File Formats. *Curr Protoc Bioinform* 45, A.1B.1-A.1B.18.
- Mitchell, R. T., Saunders, P. T. K., Childs, A. J., Cassidy-Kojima, C., Anderson, R. A., Wallace, W. H. B., Kelnar, C. J. H. and Sharpe, R. M. (2010). Xenografting of human fetal testis tissue: a new approach to study fetal testis development and germ cell differentiation. *Hum Reproduction Oxf Engl* 25, 2405–2414.
- Moisiadis, V. G., Constantinof, A., Kostaki, A., Szyf, M. and Matthews, S. G. (2017). Prenatal Glucocorticoid Exposure Modifies Endocrine Function and Behaviour for 3 Generations Following Maternal and Paternal Transmission. *Sci Rep-uk* 7, 11814.
- Nader, N., Chrousos, G. P. and Kino, T. (2009). Circadian rhythm transcription factor CLOCK regulates the transcriptional activity of the glucocorticoid receptor by acetylating its hinge region lysine cluster: potential physiological implications. *Faseb J* 23, 1572–1583.
- Nakamura, E., Nguyen, M. and Mackem, S. (2006). Kinetics of tamoxifen-regulated Cre activity in mice using a cartilage-specific CreERT to assay temporal activity windows along the proximodistal limb skeleton. *Dev Dynam* 235, 2603–2612.
- Naro, C., Jolly, A., Persio, S. D., Bielli, P., Setterblad, N., Alberdi, A. J., Vicini, E., Geremia, R., Grange, P. D. la and Sette, C. (2017). An Orchestrated Intron Retention Program in Meiosis Controls Timely Usage of Transcripts during Germ Cell Differentiation. *Dev Cell*

41, 82-93.e4.

- Natale, M. D., Soch, A., Ziko, I., Luca, S. D., Spencer, S. J. and Sominsky, L. (2019). Chronic predator stress in female mice reduces primordial follicle numbers: implications for the role of ghrelin. *J Endocrinol* 1, 201–219.
- Newkirk, S. J., Lee, S., Grandi, F. C., Gaysinskaya, V., Rosser, J. M., Berg, N. V., Hogarth, C. A., Marchetto, M. C. N., Muotri, A. R., Griswold, M. D., et al. (2017). Intact piRNA pathway prevents L1 mobilization in male meiosis. *Proc National Acad Sci* 114, E5635 E5644.
- Nilsson, E. E., Sadler-Riggleman, I., Skinner, M. K. and Mansuy, I. (2018). Environmentally induced epigenetic transgenerational inheritance of disease. *Environ Epigenetics* 4, dvy016.
- Nirupama, M., Devaki, M., Nirupama, R. and Yajurvedi, H. N. (2013). Chronic intermittent stress-induced alterations in the spermatogenesis and antioxidant status of the testis are irreversible in albino rat. *J Physiol Biochem* 69, 59–68.
- Niu, W. and Spradling, A. C. (2020). Two distinct pathways of pregranulosa cell differentiation support follicle formation in the mouse ovary. *Proc National Acad Sci* 117, 20015–20026.
- Nordkap, L., Almstrup, K., Nielsen, J. E., Bang, A. K., Priskorn, L., Krause, M., Holmboe, S. A., Winge, S. B., Palme, D. L. E., Mørup, N., et al. (2017). Possible involvement of the glucocorticoid receptor (NR3C1) and selected NR3C1 gene variants in regulation of human testicular function. *Andrology-us* 5, 1105–1114.
- Oakley, R. H., Sar, M. and Cidlowski, J. A. (1996). The Human Glucocorticoid Receptor β Isoform EXPRESSION, BIOCHEMICAL PROPERTIES, AND PUTATIVE FUNCTION (*). *J Biol Chem* 271, 9550–9559.

- Oakley, A. E., Breen, K. M., Clarke, I. J., Karsch, F. J., Wagenmaker, E. R. and Tilbrook, A. J. (2009). Cortisol Reduces Gonadotropin-Releasing Hormone Pulse Frequency in Follicular Phase Ewes: Influence of Ovarian Steroids. *Endocrinology* 150, 341–349.
- Oakley, R. H., Ren, R., Cruz-Topete, D., Bird, G. S., Myers, P. H., Boyle, M. C., Schneider, M. D., Willis, M. S. and Cidlowski, J. A. (2013). Essential role of stress hormone signaling in cardiomyocytes for the prevention of heart disease. *Proc National Acad Sci* 110, 17035–17040.
- O'Bryan, M. K., Clark, B. J., McLaughlin, E. A., D'Sylva, R. J., O'Donnell, L., Wilce, J. A., Sutherland, J., O'Connor, A. E., Whittle, B., Goodnow, C. C., et al. (2013). RBM5 Is a Male Germ Cell Splicing Factor and Is Required for Spermatid Differentiation and Male Fertility. *Plos Genet* 9, e1003628.
- Ong, M., Cheng, J., Jin, X., Lao, W., Johnson, M., Tan, Y. and Qu, X. (2019). Paeoniflorin extract reverses dexamethasone-induced testosterone over-secretion through downregulation of cytochrome P450 17A1 expression in primary murine theca cells. *J Ethnopharmacol* 229, 97–103.
- Orazizadeh, M., Khorsandi, L. S. and Hashemitabar, M. (2010). Toxic effects of dexamethasone on mouse testicular germ cells. *Andrologia* 42, 247–253.
- Orr, T. E. and Mann, D. R. (1990). Effects of restraint stress on plasma LH and testosterone concentrations, Leydig cell LH/HCG receptors, and in vitro testicular steroidogenesis in adult rats. *Horm Behav* 24, 324–341.
- Orr, T. E. and Mann, D. R. (1992). Role of glucocorticoids in the stress-induced suppression of testicular steroidogenesis in adult male rats. *Horm Behav* 26, 350–363.
- Otto, C., Reichardt, H. M. and Schütz, G. (1997). Absence of Glucocorticoid Receptor- β in

- Mice*. *J Biol Chem* 272, 26665–26668.
- Page, K. C., Sottas, C. M. And Hardy, M. P. (2001). Prenatal Exposure to Dexamethasone Alters Leydig Cell Steroidogenic Capacity in Immature and Adult Rats. *J Androl* 22, 973–980.
- Percharde, M., Lin, C.-J., Yin, Y., Guan, J., Peixoto, G. A., Bulut-Karslioglu, A., Biechele, S., Huang, B., Shen, X. and Ramalho-Santos, M. (2018). A LINE1-Nucleolin Partnership Regulates Early Development and ESC Identity. *Cell* 174, 391-405.e19.
- Pertea, M., Kim, D., Pertea, G. M., Leek, J. T. and Salzberg, S. L. (2016). Transcript-level expression analysis of RNA-seq experiments with HISAT, StringTie and Ballgown. *Nat Protoc* 11, 1650–1667.
- Petropoulos, S., Matthews, S. G. and Szyf, M. (2014). Adult glucocorticoid exposure leads to transcriptional and DNA methylation changes in nuclear steroid receptors in the hippocampus and kidney of mouse male offspring. *Biol Reprod* 90, 43.
- Pezic, D., Manakov, S. A., Sachidanandam, R. and Aravin, A. A. (2014). piRNA pathway targets active LINE1 elements to establish the repressive H3K9me3 mark in germ cells. *Gene Dev* 28, 1410–1428.
- Piffer, R. C., Garcia, P. C., Gerardin, D. C. C., Kempinas, W. G. and Pereira, O. C. M. (2009). Semen parameters, fertility and testosterone levels in male rats exposed prenatally to betamethasone. *Reproduction Fertility Dev* 21, 634–639.
- Pontes, J. T., Maside, C., Lima, L. F., Magalhães-Padilha, D. M., Padilha, R. T., Matos, M. H. T., Figueiredo, J. R. and Campello, C. C. (2019). Immunolocalization for glucocorticoid receptor and effect of cortisol on in vitro development of preantral follicles. *Vet Animal Sci* 7, 100060.

- Poulain, M., Frydman, N., Duquenne, C., N'Tumba-Byn, T., Benachi, A., Habert, R., Rouiller-Fabre, V. and Livera, G. (2012). Dexamethasone Induces Germ Cell Apoptosis in the Human Fetal Ovary. *J Clin Endocrinol Metabolism* 97, E1890–E1897.
- Razoux, F., Russig, H., Mueggler, T., Baltes, C., Dikaïou, K., Rudin, M. and Mansuy, I. M. (2017). Transgenerational disruption of functional 5-HT_{1A}R-induced connectivity in the adult mouse brain by traumatic stress in early life. *Mol Psychiatr* 22, 519–526.
- Ren, L., Zhang, Y., Xin, Y., Chen, G., Sun, X., Chen, Y. and He, B. (2021). Dysfunction in Sertoli cells participates in glucocorticoid-induced impairment of spermatogenesis. *Mol Reprod Dev* 88, 405–415.
- Rengarajan, S. and Balasubramanian, K. (2007). Corticosterone has direct inhibitory effect on the expression of peptide hormone receptors, 11 beta-HSD and glucose oxidation in cultured adult rat Leydig cells. *Mol Cell Endocrinol* 279, 52–62.
- Rengarajan, S. and Balasubramanian, K. (2008). Corticosterone induces steroidogenic lesion in cultured adult rat Leydig cells by reducing the expression of star protein and steroidogenic enzymes. *J Cell Biochem* 103, 1472–1487.
- Ribeiro, C. T., Souza, D. B. D., Costa, W. S., Sampaio, F. J. B. and Pereira-Sampaio, M. A. (2018). Immediate and late effects of chronic stress in the testes of prepubertal and adult rats. *Asian J Androl* 20, 385–390.
- Richardson, S. R., Gerdes, P., Gerhardt, D. J., Sanchez-Luque, F. J., Bodea, G.-O., Muñoz-Lopez, M., Jesuadian, J. S., Kempen, M.-J. H. C., Carreira, P. E., Jeddeloh, J. A., et al. (2017). Heritable L1 retrotransposition in the mouse primordial germline and early embryo. *Genome Res* 27, 1395–1405.
- Ristić, N., Nestorović, N., Manojlović-stojanoski, M., Filipović, B., Šošić-jurjević, B., Milošević,

- V. And Sekulić, M. (2008). Maternal dexamethasone treatment reduces ovarian follicle number in neonatal rat offspring. *J Microsc-oxford* 232, 549–557.
- Ristić, N., Nestorović, N., Manojlović-Stojanoski, M., Trifunović, S., Ajdžanović, V., Filipović, B., Pendovski, L. and Milošević, V. (2019). Adverse effect of dexamethasone on development of the fetal rat ovary. *Fundam Clin Pharm* 33, 199–207.
- Ritchie, M. E., Phipson, B., Wu, D., Hu, Y., Law, C. W., Shi, W. and Smyth, G. K. (2015). limma powers differential expression analyses for RNA-sequencing and microarray studies. *Nucleic Acids Res* 43, e47–e47.
- Robinson, M. D., McCarthy, D. J. and Smyth, G. K. (2010). edgeR: a Bioconductor package for differential expression analysis of digital gene expression data. *Bioinformatics* 26, 139–140.
- Rodgers, A. B., Morgan, C. P., Bronson, S. L., Revello, S. and Bale, T. L. (2013). Paternal Stress Exposure Alters Sperm MicroRNA Content and Reprograms Offspring HPA Stress Axis Regulation. *J Neurosci* 33, 9003–9012.
- Rodgers, A. B., Morgan, C. P., Leu, N. A. and Bale, T. L. (2015). Transgenerational epigenetic programming via sperm microRNA recapitulates effects of paternal stress. *Proc National Acad Sci* 112, 13699–13704.
- Rodić, N., Sharma, R., Sharma, R., Zampella, J., Dai, L., Taylor, M. S., Hruban, R. H., Iacobuzio-Donahue, C. A., Maitra, A., Torbenson, M. S., et al. (2014). Long Interspersed Element-1 Protein Expression Is a Hallmark of Many Human Cancers. *Am J Pathology* 184, 1280–1286.
- Roovers, E. F., Rosenkranz, D., Mahdipour, M., Han, C.-T., He, N., Chuva de Sousa Lopes, S. M., van der Westerlaken, L. A. J., Zischler, H., Butter, F., Roelen, B. A. J., et al. (2015).

- Piwi Proteins and piRNAs in Mammalian Oocytes and Early Embryos. *Cell Reports* 10, 2069–2082.
- Saavedra-Rodríguez, L. and Feig, L. A. (2013). Chronic social instability induces anxiety and defective social interactions across generations. *Biol Psychiat* 73, 44–53.
- Saez, J. M., Morera, A. M., Haour, F. And Evain, D. (1977). Effects of in Vivo Administration of Dexamethasone, Corticotropin and Human Chorionic Gonadotropin on Steroidogenesis and Protein and DNA Synthesis of Testicular Interstitial Cells in Prepuberal Rats. *Endocrinology* 101, 1256–1263.
- Sakr, H. F., Abbas, A. M., Elsamanoudy, A. Z. and Ghoneim, F. M. (2015). Effect of fluoxetine and resveratrol on testicular functions and oxidative stress in a rat model of chronic mild stress-induced depression. *J Physiology Pharmacol Official J Pol Physiological Soc* 66, 515–27.
- Sankar, B., Maran, R., Sudha, S., Govindarajulu, P. and Balasubramanian, K. (2000). Chronic Corticosterone Treatment Impairs Leydig Cell 11 β -Hydroxysteroid Dehydrogenase Activity and LH-Stimulated Testosterone Production. *Horm Metab Res* 32, 142–146.
- Sasson, R. and Amsterdam, A. (2003). Pleiotropic anti-apoptotic activity of glucocorticoids in ovarian follicular cells. *Biochem Pharmacol* 66, 1393–1401.
- Sasson, R., Tajima, K. and Amsterdam, A. (2001). Glucocorticoids protect against apoptosis induced by serum deprivation, cyclic adenosine 3',5'-monophosphate and p53 activation in immortalized human granulosa cells: involvement of Bcl-2. *Endocrinology* 142, 802–11.
- Satija, R., Farrell, J. A., Gennert, D., Schier, A. F. and Regev, A. (2015). Spatial reconstruction of single-cell gene expression data. *Nat Biotechnol* 33, 495–502.

- Scarlet, D., Ille, N., Ertl, R., Alves, B. G., Gastal, G. D. A., Paiva, S. O., Gastal, M. O., Gastal, E. L. and Aurich, C. (2017). Glucocorticoid metabolism in equine follicles and oocytes. *Domest Anim Endocrin* 59, 11–22.
- Schmid, R., Grellscheid, S. N., Ehrmann, I., Dalglish, C., Danilenko, M., Paronetto, M. P., Pedrotti, S., Grellscheid, D., Dixon, R. J., Sette, C., et al. (2013). The splicing landscape is globally reprogrammed during male meiosis. *Nucleic Acids Res* 41, 10170–10184.
- Schoonmaker, J. N. and Erickson, G. F. (1983). Glucocorticoid modulation of follicle-stimulating hormone-mediated granulosa cell differentiation. *Endocrinology* 113, 1356–63.
- Schreiber, J. R., Nakamura, K. and Erickson, G. F. (1982). Rat ovary glucocorticoid receptor: Identification and characterization. *Steroids* 39, 569–584.
- Schultz, R., Isola, J., Parvinen, M., Honkaniemi, J., Wikström, A.-C., Gustafsson, J.-Å. and Peltö-Huikko, M. (1993). Localization of the glucocorticoid receptor in testis and accessory sexual organs of male rat. *Mol Cell Endocrinol* 95, 115–120.
- Shen, S., Park, J. W., Huang, J., Dittmar, K. A., Lu, Z., Zhou, Q., Carstens, R. P. and Xing, Y. (2012). MATS: a Bayesian framework for flexible detection of differential alternative splicing from RNA-Seq data. *Nucleic Acids Res* 40, e61–e61.
- Shoji, M., Tanaka, T., Hosokawa, M., Reuter, M., Stark, A., Kato, Y., Kondoh, G., Okawa, K., Chujo, T., Suzuki, T., et al. (2009). The TDRD9-MIWI2 Complex Is Essential for piRNA-Mediated Retrotransposon Silencing in the Mouse Male Germline. *Dev Cell* 17, 775–787.
- Short, A. K., Fennell, K. A., Perreau, V. M., Fox, A., O'Bryan, M. K., Kim, J. H., Bredy, T. W., Pang, T. Y. and Hannan, A. J. (2016). Elevated paternal glucocorticoid exposure alters the small noncoding RNA profile in sperm and modifies anxiety and depressive

- phenotypes in the offspring. *Transl Psychiat* 6, e837.
- Skene, P. J. and Henikoff, S. (2017). An efficient targeted nuclease strategy for high-resolution mapping of DNA binding sites. *Elife* 6, e21856.
- Smit, A. F. A., Tóth, G., Riggs, A. D. and Jurka, J. (1995). Ancestral, Mammalian-wide Subfamilies of LINE-1 Repetitive Sequences. *J Mol Biol* 246, 401–417.
- Smith, L. B. and Walker, W. H. (2014). The regulation of spermatogenesis by androgens. *Semin Cell Dev Biol* 30, 2–13.
- Smith, T., Heger, A. and Sudbery, I. (2017). UMI-tools: modeling sequencing errors in Unique Molecular Identifiers to improve quantification accuracy. *Genome Res* 27, 491–499.
- Soygur, B., Jaszczak, R. G., Fries, A., Nguyen, D. H., Malki, S., Hu, G., Demir, N., Arora, R. and Laird, D. J. (2021). Intercellular bridges coordinate the transition from pluripotency to meiosis in mouse fetal oocytes. *Sci Adv* 7, eabc6747.
- Specchia, V., Piacentini, L., Tritto, P., Fanti, L., D'Alessandro, R., Palumbo, G., Pimpinelli, S. and Bozzetti, M. P. (2010). Hsp90 prevents phenotypic variation by suppressing the mutagenic activity of transposons. *Nature* 463, 662–665.
- Stalker, A., Hermo, L. and Antakly, T. (1989). Covalent affinity labeling, radioautography, and immunocytochemistry localize the glucocorticoid receptor in rat testicular leydig cells. *Am J Anat* 186, 369–377.
- Stocco, C., Telleria, C. and Gibori, G. (2007). The Molecular Control of Corpus Luteum Formation, Function, and Regression. *Endocr Rev* 28, 117–149.
- Sugino, N., Tamura, H., Nakamura, Y., Ueda, K. and Kato, H. (1991). Different mechanisms for the inhibition of progesterone secretion by ACTH and corticosterone in pregnant rats. *J*

Endocrinol 129, 405–10.

Sun, J., Guo, Y., Zhang, Q., Bu, S., Li, B., Wang, Q. and Lai, D. (2018). Chronic restraint stress disturbs meiotic resumption through APC/C-mediated cyclin B1 excessive degradation in mouse oocytes. *Cell Cycle* 17, 1591–1601.

Sun, J., Guo, Y., Fan, Y., Wang, Q., Zhang, Q. and Lai, D. (2021). Decreased expression of IDH1 by chronic unpredictable stress suppresses proliferation and accelerates senescence of granulosa cells through ROS activated MAPK signaling pathways. *Free Radical Bio Med* 169, 122–136.

Tang, W. W. C., Dietmann, S., Irie, N., Leitch, H. G., Floros, V. I., Bradshaw, C. R., Hackett, J. A., Chinnery, P. F. and Surani, M. A. (2015). A Unique Gene Regulatory Network Resets the Human Germline Epigenome for Development. *Cell* 161, 1453–1467.

Tang, W. W. C., Kobayashi, T., Irie, N., Dietmann, S. and Surani, M. A. (2016). Specification and epigenetic programming of the human germ line. *Nat Rev Genet* 17, 585–600.

Taylor, M. S., Altukhov, I., Molloy, K. R., Mita, P., Jiang, H., Adney, E. M., Wudzinska, A., Badri, S., Ischenko, D., Eng, G., et al. (2018). Dissection of affinity captured LINE-1 macromolecular complexes. *Elife* 7, e30094.

Tetsuka, M., Milne, M., Simpson, G. E. and Hillier, S. G. (1999). Expression of 11 β -Hydroxysteroid Dehydrogenase, Glucocorticoid Receptor, and Mineralocorticoid Receptor Genes in Rat Ovary1. *Biol Reprod* 60, 330–335.

Tetsuka, M., Nishimoto, H., Miyamoto, A., Okuda, K. And Hamano, S. (2010). Gene Expression of 11 β -HSD and Glucocorticoid Receptor in the Bovine (*Bos taurus*) Follicle During Follicular Maturation and Atresia: The Role of Follicular Stimulating Hormone. *J Reprod Develop* 56, 616–622.

- Tharmalingam, M. D., Jorgensen, A. and Mitchell, R. T. (2018). Experimental models of testicular development and function using human tissue and cells. *Mol Cell Endocrinol* 468, 95–110.
- Tohei, A., Sakamoto, S. and Kogo, H. (2001). Dexamethasone or Triamcinolone increases Follicular Development in Immature Female Rats. *Jpn J Pharmacol* 84, 281–286.
- Towns, R., Menon, K. M. J., Brabec, R. K., Silverstein, A. M., Cohen, J. M., Bowen, J. M. and Keyes, P. L. (1999). Glucocorticoids Stimulate the Accumulation of Lipids in the Rat Corpus Luteum. *Biol Reprod* 61, 416–421.
- Tronche, F., Kellendonk, C., Kretz, O., Gass, P., Anlag, K., Orban, P. C., Bock, R., Klein, R. and Schütz, G. (1999). Disruption of the glucocorticoid receptor gene in the nervous system results in reduced anxiety. *Nat Genet* 23, 99–103.
- Turner, J. D., Schote, A. B., Macedo, J. A., Pelascini, L. P. L. and Muller, C. P. (2006). Tissue specific glucocorticoid receptor expression, a role for alternative first exon usage? *Biochem Pharmacol* 72, 1529–1537.
- Uhlén, M., Fagerberg, L., Hallström, B. M., Lindskog, C., Oksvold, P., Mardinoglu, A., Sivertsson, Å., Kampf, C., Sjöstedt, E., Asplund, A., et al. (2015). Proteomics. Tissue-based map of the human proteome. *Sci New York N Y* 347, 1260419.
- Vagin, V. V., Wohlschlegel, J., Qu, J., Jonsson, Z., Huang, X., Chuma, S., Girard, A., Sachidanandam, R., Hannon, G. J. and Aravin, A. A. (2009). Proteomic analysis of murine Piwi proteins reveals a role for arginine methylation in specifying interaction with Tudor family members. *Gene Dev* 23, 1749–1762.
- Vasiliauskaite, L., Berrens, R. V., Ivanova, I., Carrieri, C., Reik, W., Enright, A. J. and O'Carroll, D. (2018). Defective germline reprogramming rewires the spermatogonial transcriptome.

Nat Struct Mol Biol 25, 394–404.

- Weber, M. -A., Groos, S., Höpfl, U., Spielmann, M., Aumüller, G. and Konrad, L. (2000). Glucocorticoid receptor distribution in rat testis during postnatal development and effects of dexamethasone on immature peritubular cells in vitro. *Andrologia* 32, 23–30.
- Wei, Y., Li, W., Meng, X., Zhang, L., Shen, M. and Liu, H. (2019). Corticosterone Injection Impairs Follicular Development, Ovulation and Steroidogenesis Capacity in Mice Ovary. *Animals Open Access J Mdpi* 9, 1047.
- Weikum, E. R., Knuesel, M. T., Ortlund, E. A. and Yamamoto, K. R. (2017). Glucocorticoid receptor control of transcription: precision and plasticity via allostery. *Nat Rev Mol Cell Bio* 18, 159–174.
- Weiss, I. C., Franklin, T. B., Vizi, S. and Mansuy, I. M. (2011). Inheritable Effect of Unpredictable Maternal Separation on Behavioral Responses in Mice. *Front Behav Neurosci* 5, 3.
- Welter, H., Herrmann, C., Dellweg, N., Missel, A., Thanisch, C., Urbanski, H. F., Köhn, F.-M., Schwarzer, J. U., Müller-Taubenberger, A. and Mayerhofer, A. (2020). The Glucocorticoid Receptor NR3C1 in Testicular Peritubular Cells is Developmentally Regulated and Linked to the Smooth Muscle-Like Cellular Phenotype. *J Clin Medicine* 9, 961.
- Western, P. S., Miles, D. C., Bergen, J. A. van den, Burton, M. and Sinclair, A. H. (2008). Dynamic Regulation of Mitotic Arrest in Fetal Male Germ Cells. *Stem Cells* 26, 339–347.
- Whirledge, S. and Cidlowski, J. A. (2010). Glucocorticoids, stress, and fertility. *Minerva Endocrinol* 35, 109–25.
- Whirledge, S. and DeFranco, D. B. (2018). Glucocorticoid Signaling in Health and Disease: Insights from Tissue-Specific GR Knockout Mice. *Endocrinology* 159, 46–64.

- Whirledge, S. D., Oakley, R. H., Myers, P. H., Lydon, J. P., DeMayo, F. and Cidlowski, J. A. (2015). Uterine glucocorticoid receptors are critical for fertility in mice through control of embryo implantation and decidualization. *Proc National Acad Sci* 112, 15166–15171.
- Williams, Z., Morozov, P., Mihailovic, A., Lin, C., Puvvula, P. K., Juranek, S., Rosenwaks, Z. and Tuschl, T. (2015). Discovery and Characterization of piRNAs in the Human Fetal Ovary. *Cell Reports* 13, 854–863.
- Wu, L.-M., Hu, M.-H., Tong, X.-H., Han, H., Shen, N., Jin, R.-T., Wang, W., Zhou, G.-X., He, G.-P. and Liu, Y.-S. (2012a). Chronic Unpredictable Stress Decreases Expression of Brain-Derived Neurotrophic Factor (BDNF) in Mouse Ovaries: Relationship to Oocytes Developmental Potential. *Plos One* 7, e52331.
- Wu, L.-M., Liu, Y.-S., Tong, X.-H., Shen, N., Jin, R.-T., Han, H., Hu, M.-H., Wang, W. and Zhou, G.-X. (2012b). Inhibition of Follicular Development Induced by Chronic Unpredictable Stress Is Associated with Growth and Differentiation Factor 9 and Gonadotropin in Mice¹. *Biol Reprod* 86, Article 121, 1-7.
- Wu, H., Sun, L., Wen, Y., Liu, Y., Yu, J., Mao, F., Wang, Y., Tong, C., Guo, X., Hu, Z., et al. (2016). Major spliceosome defects cause male infertility and are associated with nonobstructive azoospermia in humans. *Proc National Acad Sci* 113, 4134–4139.
- Wu, R., Zhang, H., Xue, W., Zou, Z., Lu, C., Xia, B., Wang, W. and Chen, G. (2017). Transgenerational impairment of hippocampal Akt-mTOR signaling and behavioral deficits in the offspring of mice that experience postpartum depression-like illness. *Prog Neuro-psychopharmacology Biological Psychiatry* 73, 11–18.
- Wu, R., Zhan, J., Zheng, B., Chen, Z., Li, J., Li, C., Liu, R., Zhang, X., Huang, X. and Luo, M. (2021). SYMPK Is Required for Meiosis and Involved in Alternative Splicing in Male

Germ Cells. *Frontiers Cell Dev Biology* 9, 715733.

- Xiao-Chi, J., Tor, N. and Hsueh, A. J. W. (1990). Synergistic effect of glucocorticoids and androgens on the hormonal induction of tissue plasminogen activator activity and messenger ribonucleic acid levels in granulosa cells. *Mol Cell Endocrinol* 68, 143–151.
- Xiol, J., Cora, E., Kogelgruber, R., Chuma, S., Subramanian, S., Hosokawa, M., Reuter, M., Yang, Z., Berninger, P., Palencia, A., et al. (2012). A Role for Fkbp6 and the Chaperone Machinery in piRNA Amplification and Transposon Silencing. *Mol Cell* 47, 970–979.
- Xu, K., Yang, Y., Feng, G.-H., Sun, B.-F., Chen, J.-Q., Li, Y.-F., Chen, Y.-S., Zhang, X.-X., Wang, C.-X., Jiang, L.-Y., et al. (2017). Mettl3-mediated m6A regulates spermatogonial differentiation and meiosis initiation. *Cell Res* 27, 1100–1114.
- Xu, M., Sun, J., Wang, Q., Zhang, Q., Wei, C. and Lai, D. (2018). Chronic restraint stress induces excessive activation of primordial follicles in mice ovaries. *Plos One* 13, e0194894.
- Xu, H.-X., Lin, S.-X., Gong, Y., Huo, Z.-X., Zhao, C.-Y., Zhu, H.-M. and Xi, S.-Y. (2020). Chaoyu-Dixian Formula Exerts Protective Effects on Ovarian Follicular Abnormal Development in Chronic Unpredictable Mild Stress (CUMS) Rat Model. *Front Pharmacol* 11, 245.
- Yang, J.-G., Chen, W.-Y. and Li, P. S. (1999). Effects of Glucocorticoids on Maturation of Pig Oocytes and Their Subsequent Fertilizing Capacity In Vitro. *Biol Reprod* 60, 929–936.
- Yazawa, H., Sasagawa, I., Ishigooka, M. and Nakada, T. (1999). Effect of immobilization stress on testicular germ cell apoptosis in rats. *Hum Reprod* 14, 1806–1810.
- Yazawa, H., Sasagawa, I. and Nakada, T. (2000). Apoptosis of testicular germ cells induced by

- exogenous glucocorticoid in rats. *Hum Reprod* 15, 1917–1920.
- Young, J. M. and McNeilly, A. S. (2010). Theca: the forgotten cell of the ovarian follicle. *Reproduction* 140, 489–504.
- Yuan, X.-H., Yang, B.-Q., Hu, Y., Fan, Y.-Y., Zhang, L.-X., Zhou, J.-C., Wang, Y.-Q., Lu, C.-L. and Ma, X. (2014). Dexamethasone altered steroidogenesis and changed redox status of granulosa cells. *Endocrine* 47, 639–647.
- Yuan, H.-J., Han, X., He, N., Wang, G.-L., Gong, S., Lin, J., Gao, M. and Tan, J.-H. (2016). Glucocorticoids impair oocyte developmental potential by triggering apoptosis of ovarian cells via activating the Fas system. *Sci Rep-uk* 6, 24036.
- Yuan, H.-J., Li, Z.-B., Zhao, X.-Y., Sun, G.-Y., Wang, G.-L., Zhao, Y.-Q., Zhang, M. and Tan, J.-H. (2020). Glucocorticoids impair oocyte competence and trigger apoptosis of ovarian cells via activating the TNF- α system. *Reproduction* 160, 129–140.
- Yuan, S., Feng, S., Li, J., Wen, H., Liu, K., Gui, Y., Wen, Y. and Wang, X. (2021). hnRNPH1 recruits PTBP2 and SRSF3 to cooperatively modulate alternative pre-mRNA splicing in germ cells and is essential for spermatogenesis and oogenesis.
- Zagore, L. L., Grabinski, S. E., Sweet, T. J., Hannigan, M. M., Sramkoski, R. M., Li, Q. and Licatalosi, D. D. (2015). RNA Binding Protein Ptbp2 Is Essential for Male Germ Cell Development. *Mol Cell Biol* 35, 4030–4042.
- Zhang, S.-Y., Wang, J.-Z., Li, J.-J., Wei, D.-L., Sui, H.-S., Zhang, Z.-H., Zhou, P. and Tan, J.-H. (2011). Maternal Restraint Stress Diminishes the Developmental Potential of Oocytes¹. *Biol Reprod* 84, 672–681.
- Zhao, X.-Y., Li, Z.-B., Yuan, H.-J., Han, X., Wu, J.-S., Feng, X.-Y., Zhang, M. and Tan, J.-H.


- (2020). Restraint stress and elevation of corticotrophin-releasing hormone in female mice impair oocyte competence through activation of the tumour necrosis factor α (TNF- α) system. *Reproduction Fertility Dev* 32, 862.
- Zheng, K., Xiol, J., Reuter, M., Eckardt, S., Leu, N. A., McLaughlin, K. J., Stark, A., Sachidanandam, R., Pillai, R. S. and Wang, P. J. (2010). Mouse MOV10L1 associates with Piwi proteins and is an essential component of the Piwi-interacting RNA (piRNA) pathway. *P Natl Acad Sci Usa* 107, 11841–6.
- Zhou, R., Wu, J., Liu, B., Jiang, Y., Chen, W., Li, J., He, Q. and He, Z. (2019). The roles and mechanisms of Leydig cells and myoid cells in regulating spermatogenesis. *Cell Mol Life Sci* 76, 2681–2695.
- Zou, P., Wang, X., Yang, W., Liu, C., Chen, Q., Yang, H., Zhou, N., Zeng, Y., Chen, H., Zhang, G., et al. (2019). Mechanisms of Stress-Induced Spermatogenesis Impairment in Male Rats Following Unpredictable Chronic Mild Stress (uCMS). *Int J Mol Sci* 20, 4470.

Publishing Agreement

It is the policy of the University to encourage open access and broad distribution of all theses, dissertations, and manuscripts. The Graduate Division will facilitate the distribution of UCSF theses, dissertations, and manuscripts to the UCSF Library for open access and distribution. UCSF will make such theses, dissertations, and manuscripts accessible to the public and will take reasonable steps to preserve these works in perpetuity.

I hereby grant the non-exclusive, perpetual right to The Regents of the University of California to reproduce, publicly display, distribute, preserve, and publish copies of my thesis, dissertation, or manuscript in any form or media, now existing or later derived, including access online for teaching, research, and public service purposes.

DocuSigned by:



380A34980CAE4C8...

Author Signature

5/18/2022

Date